

**MONOMER SYNTHESIS AND POLYMER PYROLYSIS**

by

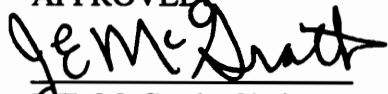
Harvey J. Grubbs

Dissertation submitted to the Faculty of the  
Virginia Polytechnic Institute and State University  
in partial fulfillment of the requirements for the degree of  
DOCTOR OF PHILOSOPHY

in

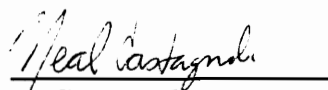
CHEMISTRY

APPROVED:

  
J. E. McGrath, Chairman

  
J. S. Riffle

  
J. Merola

  
N. Castagnoli

  
G. Long

  
H. Marand

December, 1993

Blacksburg, Virginia

# MONOMER SYNTHESIS AND POLYMER PYROLYSIS

by

Harvey J. Grubbs

Committee Chairman: James E. McGrath

Chemistry

(Abstract)

Methods for the large scale preparation and purification of bis(4-aminophenyl)-1-phenyl-2,2,2-trifluoroethane (3F-diamine) and bis(4-hydroxyphenyl)-1-phenyl-2,2,2-trifluoroethane (3F bis-phenol) have been developed. Spectroscopic characterization of by-products was used to develop a mechanistic understanding for synthetic design and to formulate purification techniques needed to produce monomer grade products. Utilizing the preparative methods represented in the present work, it was possible to obtain sufficiently pure 3F-diamine to allow the synthesis of soluble, end-capped, fully cyclized polyimides with glass transition temperatures greater than 430°C. The direct preparation of 3F bis-phenol from phenol and trifluoroacetophenone by trifluoromethanesulfonic acid catalyzed hydroxyalkylation was optimized to produce monomer grade 3F bis-phenol. Previously reported methods were less direct and produced lower purity product. Current research efforts are exploring the utility of this monomer system for the preparation of novel poly(arylene ethers), polycarbonates, and polyesters. Bis(4-hydroxy-3-aminophenyl)-1-phenyl-2,2,2-trifluoroethane [3F-bis(aminophenol)] has recently been successfully prepared from 3F-phenol. Soluble, high glass transition temperature, fully-cyclized polybenzoxazoles have been obtained from 3F-bis(aminophenol).

The synthesis and characterization of polymer systems containing the phosphine oxide unit as an integral part of the backbone continue to be areas of active research. To date the majority of research activity has centered on the synthesis and features of poly(arylene ether phosphine oxide) (PEPO). All PEPOs gave significant amounts of phosphorus-containing char at temperatures where other engineering polymers are completely volatilized. This behavior was related to the superior self-extinguishing behavior of all the phosphorus containing systems. A detailed pyrolytic degradation study of the phosphorus containing PEPO system was carried out. The study utilized analytical techniques such as pyrolysis-gas chromatography-mass spectroscopy and neutron activation analysis.

To continue the exploration of the phosphine oxide systems, the synthesis and characterization of a novel phosphorus containing diamine, bis(4-amino-phenyl)phenylphosphine oxide, has been completed. Further research is in progress preparing phosphine oxide based polyimides from this diamine. Synthesis of bis(4-hydroxyphenyl)phenylphosphine oxide and additional phosphine oxide intermediates are also reported.

## Acknowledgments

I would like first and foremost to thank Professor James E. McGrath for his guidance and kindness throughout my graduate education at Virginia Tech. Through the teaching and advice provided by Professor McGrath, I have grown greatly in two very important areas. He has taught a great deal of polymer science by exposure to both his teaching ability and a broad range of his academic and industrial colleagues. One learns very quickly in this teaching environment that learning only begins in the classroom and that accomplishment is only limited by personal initiative. A second and equally valuable area is in the much more complex arena of interpersonal relationships. The polymer research group is a very diverse group of individuals with varying ethnic and cultural backgrounds which functions as a well coordinated team. Lessons learned here will prove invaluable for the duration of my career.

Next, my wife Lynn must be thanked for her endless patience and tolerance for my strange living and working habits during the course of my graduate education. Without her love and support, none of this would have been possible.

The advice and comradery of my colleagues at Philip Morris U.S.A. has also been of extreme value. For the encouragement and support of Dr. Ken Houghton, Dr. A. C. Lilly and Dr. Edward B. Sanders, I am particularly grateful. To Dr. Ken Houghton for his long term support and faith in my ability to pursue this opportunity I am very grateful.

Additionally, the experiences with my fellow graduate students, both in and out of the polymer group, have been most rewarding. Especially worth mentioning are the contributions and suggestions from the following individuals: Dr. Carrington Smith, Mr. Martin Rodgers, Mr. Bill Joseph, and Mr. Greg Lyle.

## Table of Contents

	<u>Page</u>
1.0 INTRODUCTION.....	1
2.0 BACKGROUND.....	3
2.1 High Temperature Polymers.....	3
2.2 Flame Retardant Polymers.....	9
2.3 High Temperature Polymer Characterization.....	18
3.0 EXPERIMENTAL - GENERAL INFORMATION.....	27
4.0 TRIFLUOROMETHYL MONOMER INVESTIGATIONS.....	29
4.1 INTRODUCTION AND BACKGROUND.....	29
4.2 SYNTHESSES.....	35
4.2.1 2,2,2-Trifluoroacetophenone (Trifluoroacetyl Chloride Method).....	35
4.2.2 2,2,2-Trifluoroacetophenone (Trifluoroacetic Anhydride Method)...	35
4.2.3 2,2,2-Trifluoroacetophenone (Ethyl Trifluoroacetate, -85°C).....	40
4.2.4 2,2,2-Trifluoroacetophenone (Ethyl Trifluoroacetate, 20°C).....	40
4.2.5 2,2,2-Trifluoroacetophenone (Ethyl Trifluoroacetate, 20°C, Extended Hydrolysis).....	41
4.2.6 2,2,2-Trifluoroacetophenone (Ethyl Trifluoroacetate, -40°C).....	41
4.2.7 2,2,2-Trifluoroacetophenone (Ethyl Trifluoroacetate, Room Temperature, Extended Hydrolysis).....	42
4.2.8 2,2,2-Trifluoroacetophenone (Ethyl Trifluoroacetate, 20°C).....	42
4.2.9 2,2,2-Trifluoroacetophenone (Trifluoroacetic Acid Route).....	42
4.2.10 1,1-Bis(4-aminophenyl)-1-phenyl-2,2,2-trifluoroethane (Aniline Hydrochloride Method).....	43
4.2.11 1,1-Bis(4-aminophenyl)-1-phenyl-2,2,2-trifluoroethane (Trifluoro- methane Sulfonic Acid Method).....	49
4.2.12 1,1-Bis(4-hydroxyphenyl)-1-phenyl-2,2,2-trifluoroethane (No Solvent).....	50
4.2.13 1,1-Bis(4-hydroxyphenyl)-1-phenyl-2,2,2-trifluoroethane (Tetrachloroethylene Solvent).....	56
4.2.14 1,1-Bis(4-hydroxyphenyl)-1-phenyl-2,2,2-trifluoroethane.....	56
4.2.15 1,1-Bis(4-methylphenyl)-1-phenyl-2,2,2-trifluoroethane.....	57
4.2.16 1,1-Bis(4-ethylphenyl)-1-phenyl-2,2,2-trifluoroethane.....	63
4.2.17 1,1-Bis(4-fluorophenyl)-1-phenyl-2,2,2-trifluoroethane.....	63
4.2.18 1,1-Bis(4-bromo-4-phenoxyphenyl)-1-phenyl-2,2,2-trifluoroethane..	68
4.2.19 1,1-Bis(4-phenoxyphenyl)-1-phenyl-2,2,2-trifluoroethane.....	68
4.2.20 Perfluoroacetophenone.....	77
4.2.21 1,1-Bis(4-hydroxyphenyl)-1-pentafluorophenyl-2,2,2-trifluoroethane	82

## Table of Contents

	<u>Page</u>
4.3 RESULTS AND DISCUSSION.....	84
4.3.1 Survey of the Properties and Preparative Techniques of Trifluoromethyl Ketones.....	89
4.3.2 Preparation and Characterization of 1,1-Bis(4-aminophenyl)-1- phenyl-2,2,2-trifluoroethane.....	94
4.3.3 Mass Spectrometric Investigations.....	100
4.3.4 Liquid Chromatographic - Mass Spectrometric Investigations.....	126
4.3.5 Conclusions from the Preparation and Purification of 1,1-Bis(4- amino-phenyl)-1-phenyl-2,2,2-trifluoroethane.....	134
4.3.6 Preparation and Characterization of 1,1-Bis(4-hydroxyphenyl)- 1-phenyl-2,2,2-trifluoroethane.....	136
4.3.7 Mass Spectrometric Investigations.....	139
4.3.8 Conclusions from the Preparation and Purification of 1,1-Bis(4- hydroxyphenyl)-1-phenyl-2,2,2-trifluoroethane.....	149
4.3.9 Additional Trifluoromethyl Monomers Produced by the Hydroxy-alkylation Reaction.....	151
4.3.10 CONCLUSIONS.....	153
5.0 PHOSPHINE OXIDE MONOMER INVESTIGATION.....	155
5.1 INTRODUCTION AND BACKGROUND.....	155
5.2 SYNTHESSES.....	167
5.2.1 Bis(4-methylphenyl)phenylphosphine Sulfide.....	167
5.2.2 Bis(4-carboxyphenyl)phenylphosphine Oxide.....	167
5.2.3 Bis(4-isopropylphenyl)phenylphosphine Sulfide.....	177
5.2.4 Bis(4-phenoxyphenyl)phenylphosphine Sulfide.....	177
5.2.5 Bis(4-fluorophenyl)phenylphosphine Oxide.....	182
5.2.6 Bis(4-hydroxyphenyl)phenylphosphine Oxide.....	187
5.2.7 N,N-Bis(trimethylsilyl)-4-bromoaniline.....	187
5.2.8 Bis(4-aminophenyl)phenylphosphine Oxide.....	199
5.2.9 Bis(4-aminophenyl)phenylphosphine Oxide.....	201
5.2.10 Attempted Preparation of Bis(4-nitrophenyl)phenylphosphine Oxide.....	207
5.2.11 Attempted Preparation of Bis(4-acetaminophenyl)phenyl- phosphine Oxide.....	207
5.3 RESULTS AND DISCUSSION.....	208
5.3.1 Liquid Chromatographic - Mass Spectrometric Investigations.....	218
6.0 PYROLYSIS OF POLY(ARYLENE ETHERS).....	224
6.1 INTRODUCTION AND BACKGROUND.....	224

## Table of Contents

	<u>Page</u>
6.2 EXPERIMENTAL.....	230
6.2.1 Pyrolysis Unit Construction.....	230
6.2.2 Neutron Activation Analysis.....	230
6.2.3 Polymer Pyrolysis.....	234
6.3 Results and Discussion.....	236
7.0 SUMMARY.....	249
8.0 REFERENCES.....	250
9.0 VITA.....	269

## List of Figures

		<u>Page</u>
Figure 1	Structure of 1,1,1,3,3,3-hexafluoroisopropylidene-2,2-bis(phthalic anhydride).....	31
Figure 2	Substituted 1,1,1-triaryl-2,2,2-trifluoroethanes.....	32
Figure 3	CF <sub>3</sub> -damine and CF <sub>3</sub> -bis-phenol.....	33
Figure 4	<sup>1</sup> H NMR spectrum of 2,2,2-trifluoroacetophenone.....	36
Figure 5	<sup>13</sup> C NMR spectrum of 2,2,2-trifluoroacetophenone.....	37
Figure 6	Mass spectrum (EI) of 2,2,2-trifluoroacetophenone.....	38
Figure 7	IR spectrum of 2,2,2-trifluoroacetophenone.....	39
Figure 8	<sup>1</sup> H NMR spectrum of 1,1-bis(4-aminophenyl)-1-phenyl-2,2,2-trifluoroethane.....	44
Figure 9	<sup>13</sup> C NMR spectrum of 1,1-bis(4-aminophenyl)-1-phenyl-2,2,2-trifluoroethane.....	45
Figure 10	2D HETCOR NMR spectrum of 1,1-bis(4-aminophenyl)-1-phenyl-2,2,2-trifluoroethane.....	46
Figure 11	Mass spectrum (EI) of 1,1-bis(4-aminophenyl)-1-phenyl-2,2,2-trifluoroethane.....	47
Figure 12	IR spectrum of 1,1-bis(4-aminophenyl)-1-phenyl-2,2,2-trifluoroethane.....	48
Figure 13	<sup>1</sup> H NMR spectrum of 1,1-bis(4-hydroxyphenyl)-1-phenyl-2,2,2-trifluoroethane.....	51
Figure 14	<sup>13</sup> C NMR spectrum of 1,1-bis(4-hydroxyphenyl)-1-phenyl-2,2,2-trifluoroethane.....	52
Figure 15	2D HETCOR NMR spectrum of 1,1-bis(4-hydroxyphenyl)-1-phenyl-2,2,2-trifluoroethane.....	53



## List of Figures (continued)

		<u>Page</u>
Figure 16	Mass spectrum of 1,1-bis(4-hydroxyphenyl)-1-phenyl-2,2,2-trifluoroethane.....	54
Figure 17	IR spectrum of 1,1-bis(4-hydroxyphenyl)-1-phenyl-2,2,2-trifluoroethane.....	55
Figure 18	<sup>1</sup> H NMR spectrum of 1,1-bis(4-methylphenyl)-1-phenyl-2,2,2-trifluoroethane.....	58
Figure 19	<sup>13</sup> C NMR spectrum of 1,1-bis(4-methylphenyl)-1-phenyl-2,2,2-trifluoroethane.....	59
Figure 20	2D HETCOR NMR spectrum of 1,1-bis(4-methylphenyl)-1-phenyl-2,2,2-trifluoroethane.....	60
Figure 21	Mass spectrum (EI) of 1,1-bis(4-methylphenyl)-1-phenyl-2,2,2-trifluoroethane.....	61
Figure 22	IR spectrum of 1,1-bis(4-methylphenyl)-1-phenyl-2,2,2-trifluoroethane.....	62
Figure 23	<sup>1</sup> H NMR spectrum of 1,1-bis(4-ethylphenyl)-1-phenyl-2,2,2-trifluoroethane.....	64
Figure 24	<sup>13</sup> C NMR spectrum of 1,1-bis(4-ethylphenyl)-1-phenyl-2,2,2-trifluoroethane.....	65
Figure 25	Mass spectrum (EI) of 1,1-bis(4-ethylphenyl)-1-phenyl-2,2,2-trifluoroethane.....	66
Figure 26	IR spectrum of 1,1-bis(4-ethylphenyl)-1-phenyl-2,2,2-trifluoroethane.....	67
Figure 27	<sup>1</sup> H NMR spectrum of 1,1-bis(4-fluorophenyl)-1-phenyl-2,2,2-trifluoroethane.....	69
Figure 28	<sup>13</sup> C NMR spectrum of 1,1-bis(4-fluorophenyl)-1-phenyl-2,2,2-trifluoroethane.....	70

## List of Figures (continued)

		<u>Page</u>
Figure 29	Mass spectrum (EI) of 1,1-bis(4-fluorophenyl)-1-phenyl-2,2,2-trifluoroethane.....	71
Figure 30	IR spectrum of 1,1-bis(4-fluorophenyl)-1-phenyl-2,2,2-trifluoroethane.....	72
Figure 31	<sup>1</sup> H NMR spectrum of 1,1-bis[4-(4-bromophenoxy)-phenyl]-1-phenyl-2,2,2-trifluoroethane.....	73
Figure 32	<sup>13</sup> C NMR spectrum of 1,1-bis[4-(4-bromophenoxy)-phenyl]-1-phenyl-2,2,2-trifluoroethane.....	74
Figure 33	Mass spectrum (EI) of 1,1-bis[4-(4-bromophenoxy)-phenyl]-1-phenyl-2,2,2-trifluoroethane.....	75
Figure 34	IR spectrum of 1,1-bis[4-(4-bromophenoxy)phenyl]-1-phenyl-2,2,2-trifluoroethane.....	76
Figure 35	<sup>1</sup> H NMR spectrum of 1,1-bis(4-phenoxyphenyl)-1-phenyl-2,2,2-trifluoroethane.....	78
Figure 36	<sup>13</sup> C NMR spectrum of 1,1-bis(4-phenoxyphenyl)-1-phenyl-2,2,2-trifluoroethane.....	79
Figure 37	Mass spectrum (EI) of 1,1-bis(4-phenoxyphenyl)-1-phenyl-2,2,2-trifluoroethane.....	80
Figure 38	IR spectrum of 1,1-bis(4-phenoxyphenyl)-1-phenyl-2,2,2-trifluoroethane.....	81
Figure 39	<sup>13</sup> C NMR spectrum of perfluoroacetophenone.....	83
Figure 40	<sup>1</sup> H NMR spectrum of 1,1-bis(4-hydroxyphenyl)-1-pentafluorophenyl-2,2,2-trifluoroethane.....	85
Figure 41	<sup>13</sup> C NMR spectrum of 1,1-bis(4-hydroxyphenyl)-1-pentafluorophenyl-2,2,2-trifluoroethane.....	86

## List of Figures (continued)

		<u>Page</u>
Figure 42	Mass spectrum (EI) of 1,1-bis(4-hydroxyphenyl)-1-pentafluorophenyl-2,2,2-trifluoroethane.....	87
Figure 43	IR spectrum of 1,1-bis(4-hydroxyphenyl)-1-pentafluorophenyl-2,2,2-trifluoroethane.....	88
Figure 44	Stable tetrahedral intermediate.....	90
Figure 45	Trapping of stable intermediate.....	91
Figure 46	Routes explored to trifluoroacetophenone.....	94
Figure 47	Mass spectrum (EI) of crude 1,1-bis(4-aminophenyl)-1-phenyl-2,2,2-trifluoroethane.....	103
Figure 48	Mass spectrum (EI) of sublimate from crude 1,1-bis(4-aminophenyl)-1-phenyl-2,2,2-trifluoroethane....	104
Figure 49	Mass spectrum (EI) of purified 1,1-bis(4-aminophenyl)-1-phenyl-2,2,2-trifluoroethane.....	105
Figure 50	Mass spectrum (FAB, glycerol matrix) of crude 1,1-bis(4-aminophenyl)-1-phenyl-2,2,2-trifluoroethane....	106
Figure 51	Mass spectrum (FAB, glycerol matrix) of purified 1,1-bis(4-aminophenyl)-1-phenyl-2,2,2-trifluoroethane...	107
Figure 52	MS/MS of m/z 354 from the FAB mass spectrum (glycerol matrix) of crude 1,1-bis(4-aminophenyl)-1-phenyl-2,2,2-trifluoroethane.....	108
Figure 53	MS/MS of m/z 343 from the FAB mass spectrum (glycerol matrix) of crude 1,1-bis(4-aminophenyl)-1-phenyl-2,2,2-trifluoroethane.....	109
Figure 54	MS/MS of m/z 268 from the FAB mass spectrum of sublimate shown in Figure 48.....	111

**List of Figures (continued)**

		<u>Page</u>
Figure 55	MS/MS of m/z 250 from the FAB mass spectrum of sublimate from crude 1,1-bis(4-aminophenyl)-1-phenyl-2,2,2-trifluoroethane.....	112
Figure 56	MS/MS of m/z 342 from the mass spectrum of purified 1,1-bis(4-aminophenyl)-1-phenyl-2,2,2-trifluoroethane.....	113
Figure 57	MS/MS of m/z 423 from the mass spectrum of sublimate shown in Figure 48.....	115
Figure 58	MS/MS of m/z 354 from the mass spectrum of sublimate shown in Figure 48.....	116
Figure 59	MS/MS of m/z 267 from the mass spectrum of sublimate shown in Figure 48.....	118
Figure 60	MS/MS of m/z 251 from the mass spectrum of sublimate shown in Figure 48.....	120
Figure 61	MS/MS of m/z 248 from the mass spectrum of sublimate shown in Figure 48.....	121
Figure 62	FAB MS <sup>3</sup> of m/z 423 to 354 to second generation products	123
Figure 63	FAB MS <sup>3</sup> of m/z 267 to 248 to second generation products	124
Figure 64	FAB MS <sup>3</sup> of m/z 267 to 180 to second generation products	125
Figure 65	Liquid chromatogram of sublimate.....	127
Figure 66	Total ion current plot of the chromatogram shown in Figure 65.....	128
Figure 67	Mass spectrum (FAB) of component 1 of Figure 65.....	129
Figure 68	Mass spectrum (FAB) of component 2 of Figure 65.....	131
Figure 69	Mass spectrum (FAB) of component 3 of Figure 65.....	132

## List of Figures (continued)

		<u>Page</u>
Figure 70	Mass spectrum (FAB) of component 4 of Figure 65.....	133
Figure 71	Mechanism for multiple product formation in the synthesis of 1,1-bis(4-aminophenyl)-1-phenyl-2,2,2-trifluoroethane.....	135
Figure 72	Mass spectrum (EI) of 1,1-bis(4-hydroxyphenyl)-1-phenyl-2,2,2-trifluoroethane.....	141
Figure 73	Mass spectrum (EI) of crude 1,1-bis(4-hydroxyphenyl)-1-phenyl-2,2,2-trifluoroethane.....	142
Figure 74	Mass spectrum (EI) of the methylene chloride residue from the isolation of 1,1-bis(4-hydroxyphenyl)-1-phenyl-2,2,2-trifluoroethane.....	143
Figure 75	MS/MS of m/z 344 of the spectrum shown in Figure 74.....	144
Figure 76	MS/MS of m/z 268 of the spectrum shown in Figure 74.....	146
Figure 77	MS/MS of m/z 249 of the spectrum shown in Figure 74.....	147
Figure 78	MS/MS of m/z 250 of the spectrum shown in Figure 74.....	148
Figure 79	Phosphine oxide monomers.....	158
Figure 80	<sup>13</sup> C NMR spectrum of bis(4-methylphenyl)phenylphosphine sulfide.....	168
Figure 81	<sup>1</sup> H NMR spectrum of bis(4-methylphenyl)phenylphosphine sulfide.....	169
Figure 82	IR spectrum of bis(4-methylphenyl)phenylphosphine sulfide	170
Figure 83	Mass spectrum of bis(4-methylphenyl)phenylphosphine sulfide.....	171
Figure 84	<sup>13</sup> C NMR spectrum of bis(4-carboxyphenyl)phenylphosphine oxide.....	172

**List of Figures (continued)**

		<u>Page</u>
Figure 84a	Expansion of the aromatic region of the $^{13}\text{C}$ NMR spectrum of bis(4-carboxyphenyl)phenylphosphine oxide.....	173
Figure 85	$^1\text{H}$ NMR spectrum of bis(4-carboxyphenyl)phenylphosphine oxide.....	174
Figure 86	IR spectrum of bis(4-carboxyphenyl)phenylphosphine oxide	175
Figure 87	Mass spectrum of bis(4-carboxyphenyl)phenylphosphine oxide.....	176
Figure 88	$^{13}\text{C}$ NMR spectrum of bis(4-isopropylphenyl)phenylphosphine sulfide.....	178
Figure 89	$^1\text{H}$ NMR spectrum of bis(4-isopropylphenyl)phenylphosphine sulfide.....	179
Figure 90	IR spectrum of bis(4-isopropylphenyl)phenylphosphine sulfide.....	180
Figure 91	Mass spectrum of bis(4-isopropylphenyl)phenylphosphine sulfide.....	181
Figure 92	$^{13}\text{C}$ NMR spectrum of bis(4-phenoxyphenyl)phenylphosphine sulfide.....	183
Figure 93	$^1\text{H}$ NMR spectrum of bis(4-phenoxyphenyl)phenylphosphine sulfide.....	184
Figure 94	IR spectrum of bis(4-phenoxyphenyl)phenylphosphine sulfide.....	185
Figure 95	Mass spectrum of bis(4-phenoxyphenyl)phenylphosphine sulfide.....	186
Figure 96	$^{13}\text{C}$ NMR spectrum of bis(4-fluorophenyl)phenylphosphine oxide.....	188

## List of Figures (continued)

		<u>Page</u>
Figure 96a	Expansion of the aromatic region of the $^{13}\text{C}$ NMR spectrum of bis(4-fluorophenyl)phenylphosphine oxide.....	189
Figure 97	$^1\text{H}$ NMR spectrum of bis(4-fluorophenyl)phenylphosphine oxide.....	190
Figure 97a	Expansion of the aromatic region of the $^1\text{H}$ NMR spectrum of bis(4-fluorophenyl)phenylphosphine oxide.....	191
Figure 98	IR spectrum of bis(4-fluorophenyl)phenylphosphine oxide..	192
Figure 99	Mass spectrum of bis(4-fluorophenyl)phenylphosphine oxide.....	193
Figure 100	$^{13}\text{C}$ NMR spectrum of bis(4-hydroxyphenyl)phenylphosphine oxide.....	194
Figure 101	$^1\text{H}$ NMR spectrum of bis(4-hydroxyphenyl)phenylphosphine oxide.....	195
Figure 102	2D NMR spectrum of bis(4-hydroxyphenyl)phenylphosphine oxide.....	196
Figure 103	IR spectrum of bis(4-hydroxyphenyl)phenylphosphine oxide.....	197
Figure 104	Mass spectrum of bis(4-hydroxyphenyl)phenylphosphine oxide.....	198
Figure 105	$^{13}\text{C}$ NMR spectrum of bis(4-aminophenyl)phenylphosphine oxide.....	202
Figure 106	$^1\text{H}$ NMR spectrum of bis(4-aminophenyl)phenylphosphine oxide.....	203
Figure 107	2D NMR spectrum of bis(4-aminophenyl)phenylphosphine oxide.....	204

## List of Figures (continued)

		<u>Page</u>
Figure 108	IR spectrum of bis(4-aminophenyl)phenylphosphine oxide..	205
Figure 109	Mass spectrum of bis(4-aminophenyl)phenylphosphine oxide.....	206
Figure 110	Preparation of bis(4-carboxyphenyl)phenylphosphine oxide by Grignard and Friedel-Crafts routes.....	211
Figure 111	Grignard mediated preparation of bis(4-hydroxyphenyl)phenylphosphine oxide.....	213
Figure 112	Friedel-Crafts mediated preparation of bis(4-hydroxyphenyl)phenylphosphine oxide.....	214
Figure 113	Proposed alternate synthesis of bis(4-hydroxyphenyl)phenylphosphine oxide.....	216
Figure 114	FAB mass spectrum of component 1 from the direct ammonolysis of 1,1-bis(4-fluorophenyl)phenylphosphine oxide.....	220
Figure 115	FAB mass spectrum of component 2 from the direct ammonolysis of 1,1-bis(4-fluorophenyl)phenylphosphine oxide.....	221
Figure 116	Polymer burning mechanisms.....	227
Figure 117	Chemical structures of pyrolysed engineering thermoplastics	231
Figure 118	Pyrolysis unit construction.....	232
Figure 119	Off-line pyrolysis unit.....	235
Figure 120	TGA thermogram of PEEK, UDEL, PSF and BP PEPO.....	237
Figure 121	600°C Pyrogram of PEEK.....	239
Figure 122	600°C Pyrogram of UDEL.....	240



### List of Figures (continued)

		<u>Page</u>
Figure 123	600°C Pyrogram of ULTEM.....	241
Figure 124	600°C Pyrogram of Bis A PEPO.....	242
Figure 125	600°C Pyrogram of BP PEPO.....	243
Figure 126	600°C Pyrogram of HQ PEPO.....	244
Figure 127	NAA phosphorous determination of Bis A PEPO.....	246
Figure 128	NAA phosphorous determination of BQ PEPO.....	247
Figure 129	NAA phosphorous determination of HQ PEPO.....	248

## List of Schemes

		<u>Page</u>
Scheme 1	Hydroxylation mechanism.....	34
Scheme 2	Preparation of 1,1-bis(4-aminophenyl)-1-phenyl- 2,2,2-trifluoroethane.....	95
Scheme 3	Mechanism of formation of 1,1-bis(4-aminophenyl)- 1-phenyl-2,2,2-trifluoroethane.....	97
Scheme 4	Purification of 1,1-bis(4-aminophenyl)-1-phenyl- 2,2,2-trifluoroethane.....	99
Scheme 5	Hydrogen fluoride mediated preparation of 1,1- bis(4-hydroxyphenyl)-1-phenyl-2,2,2-trifluoroethane	137
Scheme 6	Preparation of 1,1-bis(4-hydroxyphenyl)-1-phenyl- 2,2,2-trifluoroethane by the Frosh method.....	137
Scheme 7	Direct preparation of 1,1-bis(4-hydroxyphenyl)- 1-phenyl-2,2,2-trifluoroethane.....	138
Scheme 8	Alternate product formation from 1-(4-hydroxy- phenyl)-1-phenyl-2,2,2-trifluoroethan-1-ol.....	150
Scheme 9	Polyphosphonate synthesis.....	157
Scheme 10	Polyester formation from bis(4-carboxyphenyl)- phenylphosphine oxide.....	159
Scheme 11	Preparation of polybenzimidazoles containing phosphine oxide moieties.....	160
Scheme 12	Preparation of phosphine oxide diamine by nitration and reduction.....	162
Scheme 13	Alleged preparation of bis(4-aminophenyl)phenyl- phosphine oxide.....	163
Scheme 14	Preparation of bis(4-halophenyl)phenylphosphine oxides.....	166

### List of Schemes (continued)

	<u>Page</u>
Scheme 15	Preparation of N,N-bis(trimethylsilyl)-4-bromoaniline..... 217
Scheme 16	Preparation of bis(4-aminophenyl)phenylphosphine oxide... 217
Scheme 17	Preparation of bis(4-nitrophenyl)phenylphosphine oxide..... 222
Scheme 18	Attempted preparation of bis(4-acetamidophenyl)- phenylphosphine oxide..... 223
Scheme 19	PEPO synthetic scheme..... 225

## List of Tables

		<u>Page</u>
Table 1	Step Growth Polymers.....	10
Table 2	Heterocyclic Polymers.....	11
Table 3	Step Growth/Heterocyclic Polymers.....	12
Table 4	Ladder and Spiro Polymers.....	13
Table 5	Thermosetting End-Groups.....	14
Table 6	Exploration of Phenyllithium Route to Trifluoroacetophenone	92
Table 7	Types of Organophosphorus Linkages.....	156

## 1.0 INTRODUCTION

High temperature organic polymers are frequently defined as materials that perform for long time duration at 200°C or above without regard for environmental conditions. This definition is somewhat misleading and is not used uniformly among researchers and end users. High temperature polymers may include systems that survive high temperature fabrication cycles but are used at temperatures less than 200°C. As an example, polymers used in certain microelectronic components are exposed to high temperature soldering steps (greater than 300°C) but see routine use at much lower temperatures. Other systems may be used to construct polymer composite panels with processing at temperatures above 350°C and then see service temperatures of less than 200°C. Extensive work in the area of high temperature polymer systems began in the 1950's to supply the needs of the aerospace and the electronic industries. While many new systems were discovered and explored extensively, only a few are commercially available today. These polymers are used in such varied applications as coatings, composites, foams, films, fibers, membranes, and moldings.

Many significant advances have been made in the field of high temperature polymers within the last thirty years. A basic understanding at a fundamental level permits the synthesis of polymers with tailored properties. Within limits, many properties of polymer systems may be controlled by careful design of the polymer chemical structure. Properties such as coefficients of thermal expansion, glass transition temperatures, color, dielectric constants, toughness, solubility, and flammability may be tailored by careful chemical design of the monomer/polymer systems. Molecular weight, molecular weight distribution control, and end-capping may be used to further alter certain properties.

The design of monomers synthesized to deliver high temperature polymers in this dissertation refer to materials designed to yield polymers with glass transition temperatures greater than 200°C. They also exhibit chemical structures that should provide high thermooxidative stability.

In modern life, polymers have become versatile and widely accepted materials for many everyday applications. High performance engineering thermoplastics are becoming increasingly important in applications traditionally filled by metallic materials. Their use in the field of high strength lightweight composite resins has already found many applications in the aerospace, automotive and related industries. Many of these applications may involve exposure to fire hazards. Serious fire hazards in homes, commercial buildings, ships, and aircraft have created the need for the investigation of the possible role that polymeric materials contribute to this hazard. Since polymers containing phosphorus as an integral part of the backbone are known to be thermally stable and flame-retardant, synthesis and characterization of these monomer/polymer systems is an attractive area for research efforts.

The synthesis of high performance monomers based on the precursor trifluoroacetophenone and phenylphosphine oxide systems is the subject of this dissertation. The resulting monomers are designed to be important intermediates for a variety of thermally stable polymers such as polyimides, poly(arylene ether)s, and polybenzoxazoles. Pyrolysis studies are reported which characterize in detail the unique properties of poly(arylene ether phosphine oxide) systems. These systems gave significant amounts of phosphorus-containing char at temperatures where many available engineering polymers were completely volatilized. This behavior has been related to the superior self-extinguishing behavior of all of the phosphorus containing poly(arylene ether)s examined.

## 2.0 BACKGROUND

### 2.1 HIGH TEMPERATURE POLYMERS

The quest for high temperature polymeric materials has been continuous for the last forty years. One of the largest and long term forces in this quest has been the aerospace industry. Perhaps the oldest and most prevalent class of heat-resistant polymers is the polyimide. This class of polymer, first reported by Bogert and Renshaw in 1908 (1), remains to date one of the most interesting and widely explored heat-resistant polymeric materials. Advancement of interest in these materials accelerated with the discovery of high temperature resistant materials containing aromatic and heterocyclic amide linkages (2). The demand for structural heat-resistant polymers for aerospace and military application was a primary focus of polymer research in the 1950's. These investigations were primarily focused on the thermooxidative stability of the finished product polymer and were less concerned with the practical limits of applicability that are of crucial importance today. Application temperature, processability, and the cost are critical driving forces in current research designed to deliver high performance thermooxidatively stable polymer systems. Examples of current commercial materials which exhibit this blend of properties are the E. I. du Pont de Nemours and Company Kapton® polyimide and the aromatic polyamide fiber Nomex®.

Perhaps the single largest concern in the continuing advancement of heat-resistant polymers has been the need to produce thermally stable materials that are also amenable to conventional processing procedures. Desirable properties include tractability, solubility, and good moldability. These properties must be balanced against the inherent properties of good thermooxidative stability which includes higher softening point, rigidity, strength, and modulus. A careful balance of these enhanced properties is critical in the production of a commercially viable polymeric system. As a consequence of the

varied and difficult criteria, only a small number of the many reported examples of high temperature thermooxidatively stable polymeric systems are commercial realities today.

High performance high temperature polymeric materials have found many applications today that are not related to high thermal stability. Some of these applications include: membrane application for gaseous and liquid separations (polyimides) (3); high-modulus fibers for use in bullet proof clothing and automobile tire cords (aromatic polyamides) (4); and adhesives for aerospace applications (polyphenylquinoxalines) (5).

Heat-resistant polymer systems are frequently defined by applications of thermal stress over specified time and temperature. The expected useful lifetime of the polymer decreases with increases in exposure temperature or exposure time. As a guideline, heat-resistant thermooxidatively stable polymers have a useful lifetime (retain mechanical properties) for thousands of hours at 230°C, hundreds of hours at 300°C, minutes at 540°C, or seconds at 760°C (6). A summary of the polymer property requirements for heat resistant polymers is as follows (7):

1. high resistance to thermal breakdown
2. high glass transition temperature
3. retention of mechanical properties
4. high resistance to oxidation
5. high resistance to hydrolysis.

One of the most important measures of thermal resistance is the retention of physical properties at a stated exposure to temperature over a set period of time (8). After considerations of many mechanisms of polymer degradation, these generalizations are cited as valuable for attaining high thermal stability (9):

1. low energy degradation pathways must be avoided
2. high energy bonding must be optimized



3. normal bond angles must be utilized
4. resonance stabilization must be optimized
5. poly bonding should be utilized.

Thermal stability mandates the use of the highest energy bonding systems available. Increasing temperatures cause increased vibrational energy which in turn causes bond rupture. The weakest structural bond will rupture at the lowest temperature which represents the minimum energy needed for bond rupture. With a rupture of only one percent of the main chain bond "architecture," useful physical properties are completely lost.

High heat-resistant polymers must be constructed using high bond dissociation energy linkages. This provides the foundation for high thermal stability. High bond dissociation energy "architecture" does not by itself guarantee high thermal stability. Structural features must avoid alternative low-energy processes of chain scission. The carbon-carbon single bond and the carbon-carbon double bond have dissociation energies of 348 kJ/mole and 682 kJ/mole respectively (9-11). This may be supplemented by an additional 167-290 kJ/mole by resonance stabilization in aromatic systems. An extremely attractive system is the phosphorus-carbon bonding system with a dissociation energy of 580 kJ/mole.

Secondary bonding interactions frequently are relied upon to further induce desirable thermal stability properties in polymeric systems. Solubility, melting point, and glass transition temperature are affected directly by these interactions. The summation of these interactions produces an electrostatic attraction which assists in holding chains together. These stabilizing forces increase with increasing polarity. Hydrogen bonding also adds to increasing stability due to secondary bonding interactions.

The use of aromatic and heterocyclic rings in the construction of high temperature resistant polymer main chains has been explored extensively. These rings contribute to thermal stability as a consequence of their crystallinity, rigidity, and the extended resonance configuration that their structure permits.

The highest heat-resistance structures generally contain phenylene rings that are para-linked in the main chains. This system is the standard by which most polymer systems are compared to as it produces a very high softening point. The example most often cited is poly(p-phenylene) which melts above 530°C (12) and is stable up to 800°C (13). These highly desired physical properties are unfortunately balanced by low solubility and generally intractable behavior which prevents processing.

Processability can be greatly improved by incorporating bridging groups (flexible linking) between aromatic or heterocyclic rings in polymer main chain structure. This produces additional rotational freedom which also generally increases solubility. The use of non-aromatic bridging linkages reduces thermooxidative stability as compared to a totally aromatic or heterocyclic main chain structure. The choice of bridging linkages group must be made such that it avoids offering a low energy degradation pathway while maintaining the highest resistance to hydrolytic, oxidative, and thermal attack. Methylene or aliphatic chains may be incorporated between heterocyclic and aromatic main groups to produce a polymer system that has improved processing characteristics. This modification will markedly reduce thermal stability. The effects of linking or bridging groups on polymer thermal stability has been studied extensively (7,14). Those linkages that reduce thermal stability the least are the carbonyl, amide, ether, sulfide, and various fluorinated alkyl groups (7).

Generally, the use of electron-donating groups, such as the ether linkage, are less thermally stable than the electron withdrawing groups such as the carbonyl and amide

linkages (6,15). The use of an aliphatic pendant, as well as aliphatic chain linkages, reduces both thermal and thermooxidative stability. The Tg-structure relationship of semi-rigid polymers (polyquinoxalines, polyquinolines, and polyimides) has been reviewed by Lee (15). The conclusions reported two general observations. There was observed an isomerization effect for a given ring-linking repeat unit and a universal relative linking effect. This implies that regardless of the type of semi-rigid polymer system, the incorporation of a flexible linking group will produce the same set of altered physical properties. Lee concludes that a rotational barrier energy can be correlated directly to a given flexible linking group. This allows the relative bridging effect to be considered as a rigidity index of the repeat unit.

The synthesis of thermally stable polymers is driven by two major strategies. Monomer systems must be designed such that polymer structures have high bonding energy and restrictive bond rotation.

High bonding energy may be obtained by utilizing aromatic ring structures to maximize the advantage of resonance stabilization. An excellent example of this is one of the first completely aromatic polymers, poly(p-phenylene) as reported by Marvel (12). Aromatic systems with C-S, C-N, and C-O bonding in the chain, as in the heterocyclic systems, are very thermally stable. An early example of such a system is the polybenzimidazole as reported by Marvel (16).

Either rigid or crosslinked structures can lead to restricting the motions of bonds in polymers. The linear bonding between aromatic and heterocyclic structures results in rigid polymer systems with high glass transition temperatures and/or crystalline melting points. Heat-resistant systems have limited need for crystalline properties due to the more strenuous processing conditions and lowered solubilities that crystallinity imparts. Ring systems may be immobilized into planar structures that result in restriction of the

confirmation or hindrance to the rotation of the ring around the main chain of the polymer. Planar rings may be obtained by the incorporation of C=O groups as in polyimides or by C=N units as in polyimidazoles and polybenzoxazoles.

Double-stranded (ordered linear networks) polymers that possess increased heat-resistance are referred to as ladder and spiro polymers. Their increased heat-resistance is attributed to the stiffness imparted by restrictive bond rotation. A single bond cleavage in a system of this type does not result in a reduction in the polymer molecular weight. A loss of polymer properties would require two or more bonds to break in the same ring (17).

Three dimensional infusible networks can be incorporated into aromatic and heteroaromatic systems by the utilization of pendant or terminal reactive groups that undergo addition crosslinking reactions. Functional end-groups utilized for the preparation of thermally crosslinkable systems include acetylenics, nadimides, maleimides and styrls. These functional groups allow crosslinking without the evolution of volatile by-products.

In summary, high heat-resistant polymers can be represented by five general (18) categories.

1. Step-growth Polymers - systems prepared by polymerizing aromatic rings either directly or by use of linking groups via condensation reactions (Table 1).
2. Heterocyclic Polymers - systems prepared by combining aromatic rings with heterocyclic systems (Table 2).
3. Step-growth/Heterocyclic Copolymers - systems prepared by condensation linkages in combination with aromatic and heterocyclic rings (Table 3).
4. Ladder and Spiro Polymers - systems prepared from heterocyclic linkages which are based on double strands (Table 4).

5. Thermosetting Polymers - prepared by the introduction of crosslinks in the previously defined (1-4) systems (Table 5).

## **2.2 FLAME RETARDANT POLYMERS**

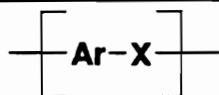
In modern life, polymers have become versatile and widely accepted materials for many everyday applications. Many of these applications may involve exposure to fire hazards. Most of the combustible materials found in fatal fires are natural or synthetic polymers (61). Serious fire hazards in homes, commercial buildings, ships, and aircraft have created need for the investigation of the possible role that polymeric materials contribute to this hazard. From a safety standpoint, the amount of smoke and toxic gases produced during the combustion of polymeric materials is of key importance (62-64).

With many polymers possessing outstanding fuel value (heats of combustion are similar to many fuels), it is quite easy to understand the polymer combustion process in a typical fire. In the presence of oxygen and adequate heat, a series of chemical and physical changes takes place during the combustion of a polymeric substrate. These changes are best described as two consecutive chemical processes: the first being decomposition and the second being combustion. The processes are linked by ignition and thermal feedback. Three pyrolysis products control the ignition and thermal feedback process. These pyrolysis products are nonflammable gases, flammable gases, and char materials. Nonflammable gases serve to dilute flammable volatile products and provide an inert zone separating oxygen from the combustion zone. In a similar fashion, char produced acts as an insulator separating the underlying polymer from combustion generated heat. The charring process usually generates very little heat.

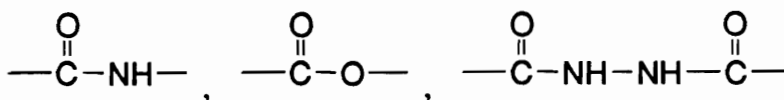
The flammability of polymers has been described by Hilado (65). Two different levels at which Hilado describes polymer combustion are the microscale and the macro

Table 1 (18, 19)

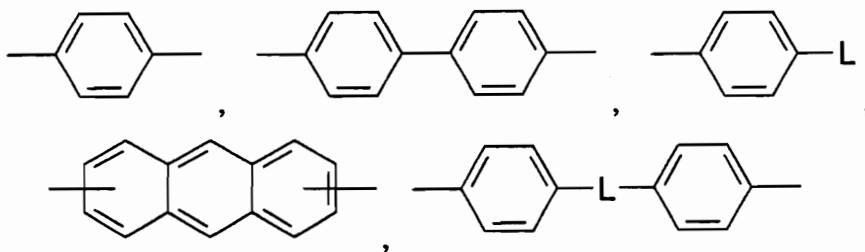
Step-Growth Polymers



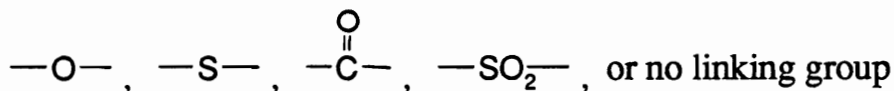
X =



Ar =



L =



**Polymers: (Reference)**

Poly(amide)s (20)

Poly(ester)s (21)

Poly(benzyl)s (22)

Poly(hydrazide)s (23)

Poly(phenylene)s (24)

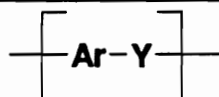
Poly(phenylene ether sulfone)s (25, 26)

Poly(phenylene ether ketone)s (27)

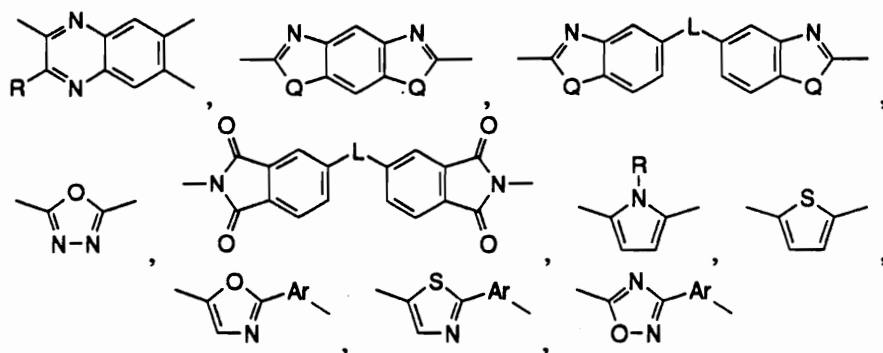
Poly(phenylene oxides, sulfides)s (28)

Table 2 (18, 19)

Heterocyclic Polymers



Y =



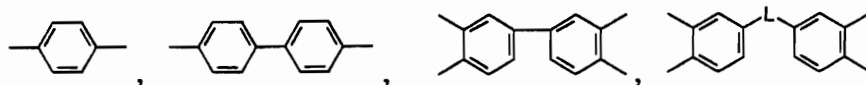
Q =  $-\text{O}-$ ,  $-\text{S}-$ ,  $-\text{NR}-$

R =  $\text{H}-$ ,  $\text{C}_6\text{H}_5-$

L =

$-\text{O}-$ ,  $-\text{S}-$ ,  $-\overset{\text{O}}{\parallel}{\text{C}}-$ ,  $-\text{SO}_2-$ ,  $-\text{C}(\text{CF}_3)_2-$ , or no linking group

Ar =



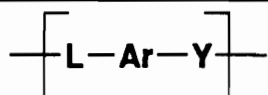
Polymers: (Reference)

Poly(imides)s (29)  
 Poly(oxazole)s (30)  
 Poly(thiazole)s (31)  
 Poly(quinoxaline)s (32)  
 Poly(benzoxazole)s (33)

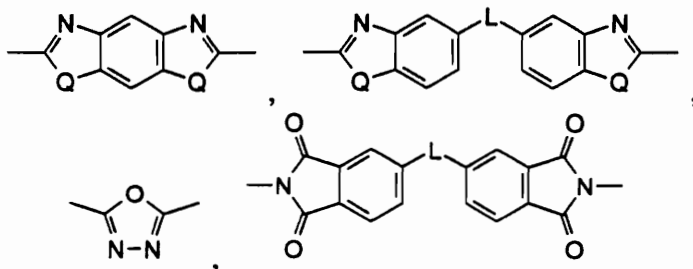
Poly(benzimidazole)s (34)  
 Poly(1,3,4-oxadiazole)s (35)  
 Poly(1,2,4-oxadiazole)s (36)  
 Poly(phenylenepyrrole)s (37)  
 Poly(phenylenethiophene)s (38)

Table 3 (18, 19)

Step-Growth / Heterocyclic Polymers



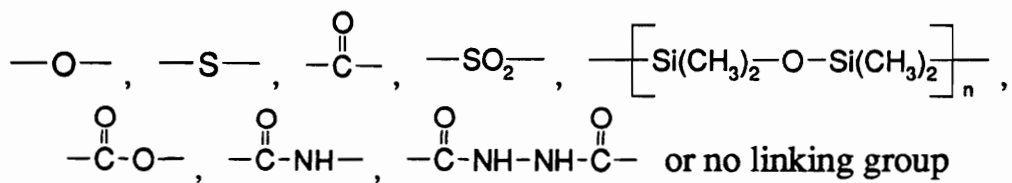
Y =



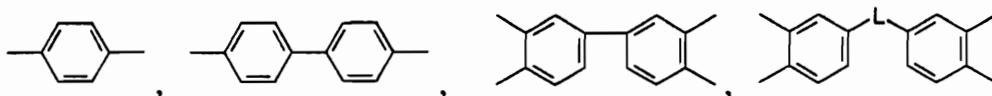
Q =  $-\text{O}-$ ,  $-\text{S}-$ ,  $-\text{NR}-$

R =  $\text{H}-$ ,  $\text{C}_6\text{H}_5-$

L =



Ar =



**Polymers: (Reference)**

Poly(ester-imides)s (39)

Poly(amide-imides)s (40)

Poly(siloxane-imide)s (41, 42)

Poly(amide-hydrazide)s (43)



**Table 4 (18, 19)**

**Ladder and Spiro Polymers**

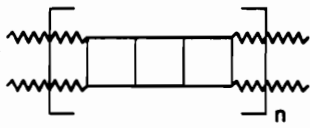
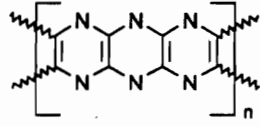
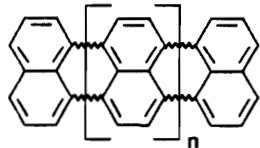
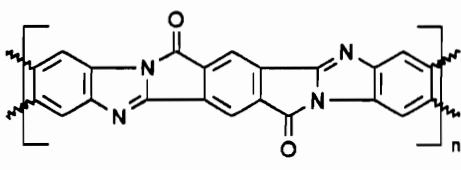
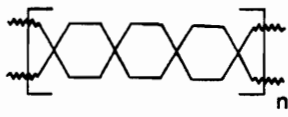
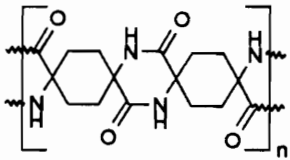
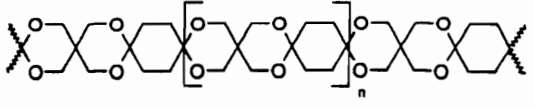
	
<b>Ladder</b>	
Function (Ref.)	X, Reactive End-Group
Poly(pyrazinopyrazine) (44)	
Poly(perinaphthalene) (45)	
Poly(imidazopyrrolone) (46)	
	
<b>Spiro</b>	
Poly(spiroamide) (47)	
Poly(spiroketal) (48)	

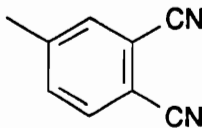
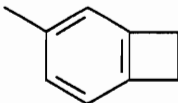
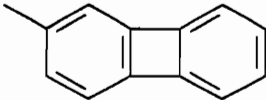
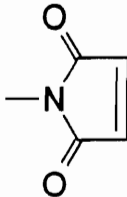
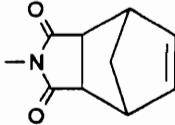
Table 5 (18, 19)

Thermosetting End-Groups

$\text{X} - \left[ \text{Ar} \right] - \text{X}$	
Function (Ref.)	X, Reactive End-Group
Styrl (49)	$-\text{CH}=\text{CH}_2$
Ethynyl (50)	$-\text{C}\equiv\text{CH}$
Nitrile (51)	$-\text{C}\equiv\text{N}$
Cyanate (52)	$-\text{O}-\text{C}\equiv\text{N}$
Cyanamide (53)	$-\text{NH}-\text{C}\equiv\text{N}$
N-Cyanourea (54)	$-\text{NH}-\text{CO}-\text{NH}-\text{C}\equiv\text{N}$
Phenylethynyl (55)	$-\text{C}\equiv\text{C}-\text{C}_6\text{H}_5$
Phenylbutadiynyl (56)	$-\text{C}\equiv\text{C}-\text{C}\equiv\text{C}-\text{C}_6\text{H}_5$
Phenylbutenyryl (56)	$-\text{C}\equiv\text{C}-\text{C}=\text{C}-\text{C}_6\text{H}_5$

**Table 5 (18, 19)**

**Thermosetting End-Groups (con't)**

$\text{X}-\left[ \text{Ar} \right]-\text{X}$	
Function (Ref.)	X, Reactive End-Group
Phthalonitrile (56)	
Benzocyclobutene (57)	
Biphenylene (58)	
Maleimide (59)	
Nadimide (60)	

scale. The microscale describes the behavior of the polymer itself while the macroscale is intended to describe the behavior of the unit mass of the polymeric substrate. At the microscale level, the solid polymer becomes a viscous liquid with extreme loss of the physical properties of the polymer. At appropriate elevated temperature in the presence of oxygen, oxidation occurs with heat and flame in the gaseous state. At the macroscale level, polymer combustion consists of several complex stages. These occur in the order of initial heating, decomposition and ignition. The ignition phase is best described by the flash-ignition temperature, the self-ignition temperature, and the oxygen index value. The flash ignition temperature is the temperature where gaseous materials evolved during heating reach the flash point and are ignited by the flame. The self-ignition or auto-ignition temperature is the temperature where the polymer substrate becomes self-sustaining to the point of ignition. The oxygen index is the oxygen level needed to sustain the ignition and combustion processes.

After ignition, the next stage is the combustion process, which serves to generate the heat needed to sustain the overall process. With sufficient combustion heat generated, the overall process is propagated. The propagation process is usually described as a surface phenomenon. With the removal of the ignition source, the combustion process becomes self-propagating if sufficient heat is present to generate and ignite fuel gases generated during the decomposition process. The overall process can best be described as controlled by the variables of heat generation, heat transfer to the polymer surface, and the rate at which the polymer surface decomposes.

To achieve a reduction in flammability, the general strategy involves the use of flame-retardant chemicals as additives or a modification of the polymer structure to produce an inherent resistance to ignition and combustion. Flame retardants are described as chemical compounds used to formulate polymer systems to meet specifications for fire

resistance. There are a large number of studies published on the subject of reducing polymer flammability (66-72). These studies teach three general methods of reducing the fire hazard of polymer substrates. The first, and most often encountered, is the use of compounded systems which contain flame retardant chemicals. The second approach involves producing polymers with structures that are stable to oxygen and heat and resist decomposition and subsequent combustion. The third method is chemical modification of the polymer surface to reduce flammability properties.

Flame retardant additives are the most common approach to imparting resistance to combustion. The requirements for success in the search for these compounds are numerous. They must be compatible with the polymer structure and produce no loss of desirable polymer physical properties. The compound must be stable to polymer processing temperature and solvent treatments. The additive must retain its properties for the life of the article made of the polymer substrate; it must not be susceptible to conditions that reduce the flame retardant property. Last, and of great importance, the additive should not be toxic or be capable of generating toxic products by decomposition if exposed to combustion products. It can be readily appreciated that to meet these rigorous requirements, presently available flame retardant materials are at best a compromise of these properties.

Fire retardant chemicals are widely used in the polymer industry. Most of these additives contain phosphorus, bromine or chlorines, or phosphorous/halogen structures. There has been extensive review (73) of the use of phosphorus compounds as flame retardant additives in polymer systems. The effect of phosphorus additives with cellulosic systems is to dramatically increase the amount of char produced and reduce the quantity of flammable gases obtained. Many of the phosphorous systems that degrade to produce acid fragments at moderate temperature are effective as flame retardants. The

glow that is often observed on the surface of combusting polymers is reported to be a solid-phase oxidation of carbon-to-carbon oxides. Phosphorous compounds are believed to produce a viscous surface coating that may be a viscous polymeric phosphoric acid or phosphate coating. This contributes to char formation and acts as a barrier to prevent further oxidation.

It is evident from the literature (66-72) that the non-burning, self-extinguishing, and flame retardant polymer structures currently under study, contain halogen or phosphorous atoms in the systems most often encountered. Phosphate esters are frequently used as flame retardant additives and more recent developments include the phosphorous/halogen additives such as tris-(dibromopropyl) phosphate. The most recent trend has been the development of systems that incorporate halogen and phosphorous atoms in the polymer backbone (74). It becomes apparent that to minimize polymer combustion, it is necessary to design polymer structures that are thermally stable, have demonstrated flame resistance, and do not possess low energy pathways for decomposition. Triphenylphosphine oxide is a very effective flame retardant which is not used in commercial application (75). The preparation of monomers which yield polymers with this inherent flame retardant structure and the pyrolysis characterization of representative aromatic ether phosphine oxide polymers are subjects reported in this dissertation.

### **2.3 HIGH TEMPERATURE POLYMER CHARACTERIZATION**

The rapid growth and development of high performance thermooxidatively stable polymers has produced a need for analytical characterization of these systems. An extrapolation may be made from the stability of smaller analogous molecules, however, polymer characterization will usually require broader considerations. The properties exhibited by polymer systems are a consequence of structure, conformation, and interac-

tions inherent in high molecular weight polymeric systems. The chain network of the backbone may be cyclic, branched, or linear in structure. These features will relate and contribute to many physical properties relating to processability. Properties such as glass transition temperature and solubility are among the most important of these features. The stereoregularity and the chemical functionality of these groups contribute to specific structural properties of a polymer system. To understand the complex behavior of polymer systems, analytical techniques have been developed. These systems have frequently involved thermal methods of analysis.

The classical thermal techniques such as thermogravimetric analysis (TGA), differential scanning calorimetry (DSC) and differential thermal analysis (DTA) have been used routinely for the study of polymer thermal stability. These methods focus primarily on changes in the sample substrate such as mass loss (TGA) and transitions (physical or chemical) which consume or liberate energy (DTA and DSC) as the substrate is heated under controlled conditions. In the last twenty years, new techniques have expanded the knowledge available from thermal analysis methodology. Among these techniques are pyrolysis gas chromatography, pyrolysis mass spectrometry, and combinations of these systems with the classical thermal methods. With these techniques, the emphasis is shifted from monitoring a property of the sample to separating, identifying, and quantitating the decomposition products produced as a function of heating.

TGA is a technique that measures the change in the mass of a sample as a function of temperature. This technique can be carried out under isothermal or non-isothermal conditions. Some examples of areas in which TGA has been used include determination of thermal and oxidative stability, quantitation of copolymer systems, and estimation of degradation kinetics.

Wendlandt and Brakson (76) compared the thermal stabilities for several polymer systems by TGA. Poly(vinyl chloride) was found to have the lowest decomposition temperature (270°C) within the series studied while polymellitimide remained stable to approximately 550°C. These studies were carried out to determine the influence of polymer structure on polymer properties. By carrying out this type of analysis in air and comparing the results to an inert atmosphere, the oxidative stability may also be examined (77).

The sensitivity of TGA to structural differences has routinely been used in the study of copolymers. The mass loss/temperature curve of copolymer systems generally will fall between the curves produced by the corresponding homopolymers. Based upon this change, the composition of copolymer systems can be determined (78).

Upon heating, many polymeric materials undergo a variety of transitions which consume or liberate energy but do not involve a change in mass. Phase and crystallinity transitions (physical changes in state) represent this type of transition. Alternative methods to TGA must be used to measure these transitions. Two thermal techniques that are primarily used to make these observations are differential thermal analysis (DTA) and differential scanning calorimetry (DSC). These techniques detect exothermic and endothermic transitions by comparison of the sample temperature with the temperature of a reference material. DTA is the more simplistic of the methods and records  $\Delta T$  (sample-reference) as a function of sample, reference, or furnace temperature. In the use of DSC analysis, a zero  $\Delta T$  condition is maintained by the application of heat to either the sample or the reference material as the furnace temperature is increased at a constant rate. In this case, heat flow becomes the quantity measured. Mathematically, the area of both DTA and DSC peaks can be equated to the enthalpy change of the transition. DSC is usually considered the more quantitative of the techniques. The determination of glass



transition temperature and melting point temperature are routinely determined using DTA and DSC techniques. The glass transition temperature is the characteristic of the onset of motion of chain segments in the amorphous regions of a polymer. Polymeric materials becomes flexible and rubber-like near this temperature. The melting point is characteristic of the melting of the crystalline portion of the polymer. Many polymers contain both amorphous and crystalline regions and will show both glass transition temperature and a melting temperature. The use of DTA and DSC to examine these properties has been extensively reviewed (79-81). DTA and DSC are often used to study thermal stability and to determine kinetic parameters of decomposition.

In contrast to the classical thermal methods which monitor sample changes, thermal decomposition analysis by gas chromatography and mass spectrometry allows the detection of decomposition products. In general, mass spectrometry has been underutilized in the past for the study of polymeric systems. The lack of suitable volatility has been the principal problem. To analyze by conventional mass spectrometry, the sample must be vaporized and ionized into the instrument vacuum system. This severe constraint requires the degradation of the polymer system to volatile fragments prior to analysis. Degradation methods, primarily pyrolysis (thermal degradation), are the most often used method to obtain a volatile sample for subsequent analysis.

Pyrolysis - gas chromatography - mass spectrometry (Py-GC-MS) and direct probe pyrolysis - mass spectrometry (Py-MS) are the most frequently observed pyrolysis techniques. For Py-GC-MS the mass spectrometer is used to identify peaks which have been separated and eluted by the gas chromatograph. Most often this type of analysis is qualitative only. Py-GC-MS is extremely useful for carrying out isotopic labeling experiments. The individual pyrolyzates obtained are separated by gas chromatography and the isotopic distributions are obtained by mass spectrometry.

Using Py-MS, pyrolyzates can be examined to identify components obtained or used to obtain "fingerprint" spectra. With both Py-MS and Py-GC-MS a wide variety of ionization techniques are used. Electron ionization (EI), at either normal or low voltage, is used most often. Chemical ionization (CI), field ionization (FI), and fast atom bombardment (FAB) are also used. These three techniques are particularly useful as they are capable of producing high molecular ion abundances.

The most frequently encountered types of pyrolyzers are the pulse mode and continuous mode systems (82-84). Resistively heated filament or Curie point systems are the most prevalent types of pulse-mode pyrolyzers. This type of unit consists of a platinum or platinum-rhodium ribbon or wire. Pyrolysis temperatures are controlled by passing a current through the wire element. These systems can be connected to the inlet port of a gas chromatograph or directly to the inlet of a mass spectrometer. In the Curie point pyrolyzer, a ferromagnetic wire is heated by radio frequency to its Curie point. The final temperature obtained in this system is obtained as a function of the alloy used to produce the wire (85-86).

The sample is applied to the filament from solution to obtain a thin film. Insoluble samples may be crimped in place on the filament or placed in a small thin-walled quartz tube which is then placed in a coil formed with the filament.

Tubular furnaces are generally used for the continuous-mode pyrolyzers (87). A low dead volume, uniformly heated pyrolysis zone, and a means of quickly inserting or removing the sample container are the essential features. This type of system offers rugged, reliable, and flexible operation.

A pyrolysis unit, regardless of type, must be capable of generating reproducibly the qualitative and quantitative release of pyrolyzate components. There are two basic considerations for obtaining this type of performance (88). First, the bond scission

decomposition pathways in polymer systems are time and temperature dependent. Decomposition pathways are competitive and many degradation pathways may be completed before the equilibrium pyrolysis temperature is obtained. The temperature rise time and the total heat content (mass) of the system are quite important. A second major factor in the design of pyrolysis instrumentation is the fate of primary degradation products. Excessively long residence time in the heated zone allows secondary reaction products and/or wall collisions to take place.

In summary, there are four guidelines that must be followed to obtain reproducible pyrolysis results (88):

1. The use of rapid temperature rise to reduce competitive degradation reactions.
2. A reasonable pyrolysis equilibrium temperature (500-600°C) should be used. Too low a temperature may not induce complete degradation and too high a temperature may yield only low molecular weight non-characteristic fragments.
3. The smallest sample size that produces sufficient degradation products for analysis helps to minimize secondary reactions.
4. Rapid transport of degradation products out of the pyrolysis zone reduces production of secondary reaction products. The use of an inert (or air) gas flow and low-dead-volume pyrolysis zones will facilitate rapid transport.

The molecular structure of the macromolecular system determines the mechanism(s) of degradation. Thermal input in a polymer system results in excitation in all vibrational modes and the weakest bond present ruptures first. Bond scission results in the production of macroradicals which by intra- and/or intermolecular reactions produce secondary products. The usual principles of free radical chemistry determine which free radical products are formed. Tertiary carbons form radical sites in preference to secon-

dary carbons; secondary carbons form radical sites in preference to primary carbons. If aromatic groups are present and benzylic sites are available, benzylic radicals are produced readily. If double bonds are present and an allylic site is available, allylic radical sites are formed.

The most prevalent macroradical reactions observed under pyrolysis conditions are  $\alpha$  cleavage, hydrogen-elimination, and hydrogen abstraction (89). Other observed free radical reactions are free radical addition and recombination.

Free radical generation and reaction are not the only type of polymeric degradation obtained during pyrolysis. Other common types of reaction observed are concerted cleavages, condensation reactions, various rearrangements, elimination reactions, and Diels-Alder cyclizations. The overall degradation process under pyrolytic conditions for any polymeric system is usually quite complex.

Random chain scission is the most prevalent pyrolysis reaction mechanism for most hydrocarbon polymers. It is observed with polyethylene, polyisoprene, polypropylene and polystyrene. The pyrolysis products consist of  $\alpha,\omega$ -dienes, and n-alkanes (89). Linear polyethylene yields pyrolyzate products that have been measured out to a carbon number of at least 55 (89).

Vinyl polymers frequently degrade to yield monomer and small amounts of oligomers. This "unzipping" mechanism is observed in the thermal degradation of polytetrafluoroethylene. A nearly quantitative yield of monomer (88) is obtained. In this system, hydrogen elimination and abstraction are not possible. This leaves only "retropolymerization" by  $\alpha$  cleavage as the dominant decomposition mechanism. The thermal decomposition of polystyrene (90) is more complex since abstractable hydrogen is present. In addition to small yields of toluene,  $\alpha$ -methyl styrene and other hydrocarbons, styrene is the main high yield component.

Concerted reactions involving hydrogen rearrangement are characteristic for certain polymer systems. As compared to the random nature of a free radical process, the concerted reaction pathways are normally very systematic. Voorhees *et al.* (91-92) have conducted extensive pyrolysis studies on polyurethanes and reported concerted degradation mechanisms.

Vinyl polymers ( $\text{CH}_2\text{-CHX}$ ) having polar side groups often pyrolyze to yield HX by elimination followed by aromatization. Ballistseri and co-workers (93-94) have studied poly(vinyl chloride), poly(vinyl bromide), poly(vinyl alcohol), and poly(vinylidene chloride). In the case of poly(vinylidene chloride), HCl is eliminated first, followed by the generation of vinylidene chloride, 1,3,5-trichlorobenzene and 1,3,5,8-tetrachloronaphthalene.

Poly(vinyl chloride) is the most studied polymer in this class. A large number of aliphatic and aromatic hydrocarbons are produced with benzene and toluene being the most abundant aromatics. The thermal degradation (90,95) process proceeds in a two step sequence. In a low temperature step hydrogen chloride, benzene, and naphthalene are produced. In a higher temperature step toluene and cyclohexadiene are produced. Extensive deuterium and  $^{13}\text{C}$ -labeling experiments for the elucidation of the thermal decomposition of poly(vinyl chloride) have been carried out (96-100).

Acrylic polymers are also known to pyrolyze to yield small molecules ( $\text{CO}_2$  and  $\text{H}_2\text{O}$ ), but the mechanism is different from that for vinyl halides. The pyrolysis of poly(methacrylic acid) has been studied extensively (101). Pyrolysis proceeds by anhydride formation and that is followed by decarboxylation. The unsaturated polymer backbone produced subsequently yields a large number of hydrocarbon pyrolysis products.

The most extensive use of Py-MS is the study of polymer decomposition mechanisms. In addition to these studies, Py-MS has application in the qualitative characteri-

zation of unknown polymer systems as well as the study of polymer microstructure. Commercial polymer systems are often polymer blends and/or copolymer systems. Frequently, compounding ingredients are added to provide particular physical properties. These ingredients include plasticizers, antioxidants, pigments, extenders, flame retardants, crosslinking agents, and light stabilizers. Pyrolysis patterns of polymer systems with these and other additives are often quite complex. Each component in the system will produce a set of pyrolyzates that often react with each other.

Both Py-GC-MS and direct Py-MS have been used extensively for the qualitative identification of polymer systems. Py-GC-MS has proven more useful for these studies as a consequence of the separating capability of the gas chromatograph.

Wuepper (102) has reported a large number of "diagnostic" pyrograms for the characterization of several commercial rubbers. Pyrolysis studies reported by Mol (103) characterized several commercial polystyrene-polyphenylene oxide blends. The fire retardant additive, triphenylphosphate, was readily identified by Py-GC-MS.

Quantitative pyrolysis analysis results have been reported. It is of critical importance in quantitative polymer analysis by Py-GC that pyrolysis conditions be precisely specified such that pyrograms are reproducible. Evans (104) has reported the compositions of styrene-methyl methacrylate and styrene butylmethacrylate copolymers by three methods - elemental carbon analysis, proton NMR, and Py-GC-MS. These polymer systems gave high yields of monomer when pyrolyzed. This allowed the integration of peak areas obtained in the gas chromatogram to be correlated with the weight percent composition. With the styrene/n-butyl methacrylate copolymer system, a plot of NMR versus Py-GC results was linear and had a high correlation coefficient.

It is possible to obtain sequence distribution information by Py-GC if sufficiently large fragments are observed in the pyrograms. Nagaya (105) reported the sequence

distributions in a series of acrylonitrile-styrene copolymers. Using capillary gas chromatographic capabilities, peaks were reported as monomers, dimers, and trimers. The determination of formation probability constants by use of the boundary effect theory (105-106) allowed the calculation of diad and triad concentrations. Using similar experimental technique, Tsuge (107) reported the sequence distributions in a methyl methacrylate-styrene series of polymers.

### 3.0 EXPERIMENTAL - GENERAL INFORMATION

NMR spectra were recorded on a Varian XL-300 Spectrometer fitted with a 5-mm  $^{13}\text{C}/^1\text{H}$  dual probe operating at 75.42 MHz for  $^{13}\text{C}$  and 299.92 MHz for  $^1\text{H}$ . Measurements were taken in solutions containing ca. 40-50 mg of compound in .5 mL of  $\text{CDCl}_3$  or  $\text{DMSO-d}_6$  at ambient temperature. Chemical shifts were measured relative to tetramethylsilane (TMS) in the chloroform solutions and usually to the solvent peaks in DMSO solutions. Homonuclear (1D) spectra were typically 32k and 16k data points for  $^{13}\text{C}$  and  $^1\text{H}$ , respectively.

Heteronuclear (2D) correlation ( $^{13}\text{C}-^1\text{H}$ ) spectra (HETCOR) were recorded using standard Varian software in the absolute value mode and typically using a 1k x 1k data matrix.

Infrared spectra were obtained using a Nicolet 740 FTIR Spectrometer. Liquids were analyzed as thin films between potassium chloride plates. Solid samples were placed on a diamond window, and measured in a Spectra Tech IR-PLAN Infrared Microscope.

Mass spectra were determined on a JEOL SX 102/SX 102 Tandem Mass Spectrometer using a DA6000 system to acquire and process data. Electron impact (EI) spectra were determined with the source heated to 200°C, 70 eV electron impact ioniza-

tion, 300 mA emission and 10 Kev acceleration potential. Samples were admitted directly to the probe, which was heated as needed. Fast atom bombardment (FAB) spectra were determined using xenon, the source at ambient temperature, 10 mA FAB emission, and 10 KeV acceleration potential. Samples were dissolved in either nitrobenzyl alcohol (NBA) or glycerol as the matrix, and admitted directly to the probe.

Gas chromatography was carried out on a Varian 3400 gas chromatograph using a 300 m X 0.53 mm DBS column. Specific conditions are given in pertinent experimental descriptions.

Reactants were either synthesized in house, or were obtained from Aldrich Chemical Co., Milwaukee, WI, or Fisher Scientific, Pittsburgh, PA. Solvents and reagents were obtained from the same companies, and from J. T. Baker, Phillipsburg, NJ, and Mallinckrodt, Inc., St. Louis, MO. Commercial reagents and solvents were used as supplied by the manufacturer unless otherwise indicated. Dimethyl sulfoxide was dried over molecular sieves.

Melting points were determined using a Mel-Temp, capillary heating block equipped with a Fluke 51 Digital Thermometer.

Reactions were normally run under nitrogen (99.998% pure).

Thin layer chromatography (TLC) was carried out on silica gel plates purchased from EM Science (Gibbstown, N.J.), the American subsidiary of E. M. Merck (Darmstadt, Germany). The most common solvent systems used were:

85/14/1	Chloroform/ethanol/ammonium hydroxide
5/1	Chloroform/ethanol
2/1	Ethyl Acetate/Hexane
1/2	Ethyl Acetate/Hexane



## 4.0 TRIFLUOROMETHYL MONOMER INVESTIGATIONS

### 4.1 INTRODUCTION AND BACKGROUND

Aromatic polyimides and polybenzoxazoles are well known for their thermo-oxidative stability and after more than twenty-five years of sustained research and development, polyimides remain the most important class of commercially available high temperature stable polymers. This situation is due primarily to the availability and low cost of available polyimide monomers and the ease of polymerization. Techniques exist to provide polyimide resins in a wide variety of useful forms such as moldings, coatings, films, and binder solutions.

The continuing demand for polymeric materials with these highly desired features has produced a large volume of research effort in exploration of the properties obtained from trifluoromethyl substituents. Most of this work has been concentrated on the 1,1,1,3,3,3-hexafluoroisopropylidene (HFIP) moiety which is formed from hexafluoroacetone. This work was initiated approximately twenty-five years ago when Rogers first reported the preparation of polyimides from a hexafluoroisopropylidene bridged diamine (108,109). Since this beginning, there have been numerous investigations reported on the synthesis, characterization, and evaluation of HFIP containing polymers (110). Much of the available information is found in the patent literature with disclosures of film formers, gas separation membranes, seals, coatings, and numerous high temperature applications. The desirable properties imparted by incorporation of the HFIP structural unit include increased solubility, glass transition temperature and thermal stability with decreased crystallinity, dielectric constant, and water absorption.

There is a continuing search in this field for precursor monomers and resultant high temperature resins which may be processed under favorable conditions. Current state of the art systems are not quite capable of meeting the demanding needs of 700°F

(371°C) service requirements for many aerospace applications. Polyimides and polybenzoxazoles continue to be suitable families for study to meet this high performance demand. Recent advances in this area include the incorporation of the trifluoromethyl group as a substituent in polyimides and polybenzoxazoles (110-112). As seen with HFIP substituent incorporation, inclusion of the trifluoromethyl group results in lower dielectric constant, lower moisture pickup and better solubility. A polyimide has been prepared by reaction of 3,6-bis(trifluoromethyl)pyromellitic dianhydride and 2,2'-bis(trifluoromethyl)-4,4'-diaminobiphenyl (113), and a dielectric constant of 2.6 was obtained. In other work, a series of polyimides was prepared from 2,2'-bis(trifluoromethyl)-4,4'-diaminobiphenyl and various dianhydrides in m-cresol (114). Polyimides with glass transitions as high as 320°C and having very good thermal oxidative stability (as measured by 5% weight loss in air) were reported.

1,3-Diamino-5-trifluoromethylbenzene has been polymerized with several dianhydrides (115,116) to provide polyimides with low moisture pickup, low dielectric constants, and Tg's up to 300°C.

Polyimides have in recent years become much more prevalent in the micro-electronic industry. High speed signal propagation (117) requires low interlayer dielectric constants. To prevent corrosion and to maintain electric stability, low water absorption is needed (118). For application with aluminum, silicon, or silicon dioxide, low thermal expansion is needed.

For optical use, polymers must have a low refractive index. Recent work (119) has reported a series of polyimides containing fluorinated alkoxy side chains. The dielectric constant, the refractive index, and the water absorption rate in this series of polyimides all decreased with increasing fluorine content.

Matsuura *et. al.* (120) recently reported investigations of the use of 2,2'-bis(trifluoromethyl)-4,4'-diaminobiphenyl for the synthesis of low thermal expansion and high optically transparent polyimides. In addition to these properties, low water absorption, low refractive index, and low dielectric constant were observed.

Fluorinated moieties in polyimides impart valuable properties. Fluorine containing substituents may be located in either the diamine monomer or the carboxyl containing monomer or in both monomers. As previously noted, much of the work to date has centered on use of the commercially available hexafluoroisopropylidene-2,2-bis(phthalic anhydride) [6F-DA] to prepare high performance polyimides.

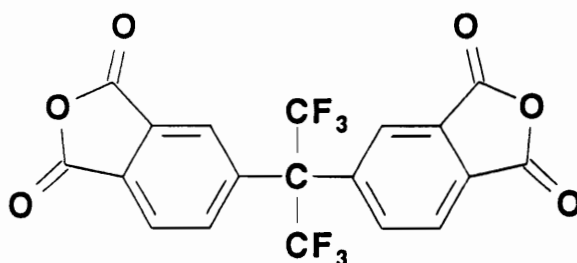


Figure 1. Structure of 1,1,1,3,3,3-hexafluoroisopropylidene-2,2-bis (phthalic anhydride)

The use of substituted 1,1,1-triaryl-2,2,2-trifluoroethane (3F) systems have been relatively overlooked for serious use for high performance applications in polyimide systems. The 3F monomer systems have several advantages over hexafluoroisopropylidene (6F) based systems. Added synthetic versatility is obtained with the capability of locating functional groups on the 3F phenyl ring. As in the 6F system, 3F moieties also restrict rotation at the quaternary carbon and raise T<sub>g</sub> when compared to smaller substituents. The 3F-diamine monomer should be less expensive than the 6F diamine due to a simpler synthetic route. The presence of two strong electron withdraw-

ing trifluoromethyl groups in the 6F diamine monomer greatly reduces the nucleophilicity of the diamine, decreasing greatly the reactivity with dianhydrides. This should allow the preparation of higher molecular weight polyimides with the corresponding 3F-diamine. Much of the pioneering effort in this area has been carried out by Alston and co-workers (121-135).

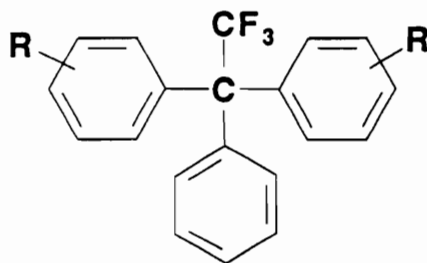
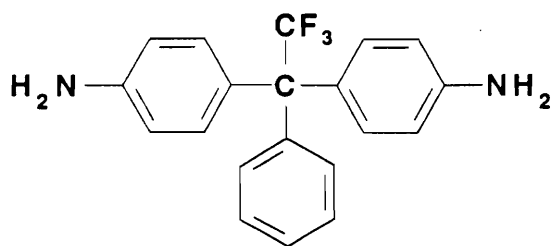
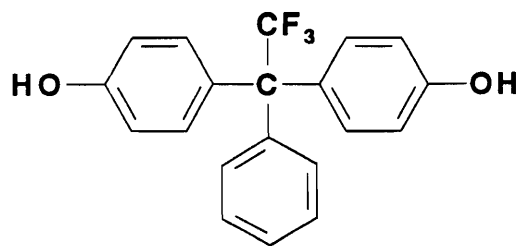


Figure 2. Substituted 1,1,1-triaryl-2,2,2-trifluoroethanes.

The main focus of research in this thesis section will center on the efficient synthesis of the intermediates and monomers of high performance organic materials. Synthetic methodology and mechanistic considerations of the synthesis of 1,1-bis(4-aminophenyl)-1-phenyl-2,2,2-trifluoroethane (3F-diamine) and 1,1-bis(4-hydroxyphenyl)-1-phenyl-2,2,2-trifluoroethane (3F bis-phenol) will be presented. Recent work in our laboratories has produced soluble, end-capped, fully cyclized polyimides, with glass transition temperatures above 430°C formed by the reaction of pyromellitic dianhydride (PMDA) and 3F-diamine (136). Comparable polybenzoxazoles using 3F bis-phenol based monomeric systems have also been prepared (137).



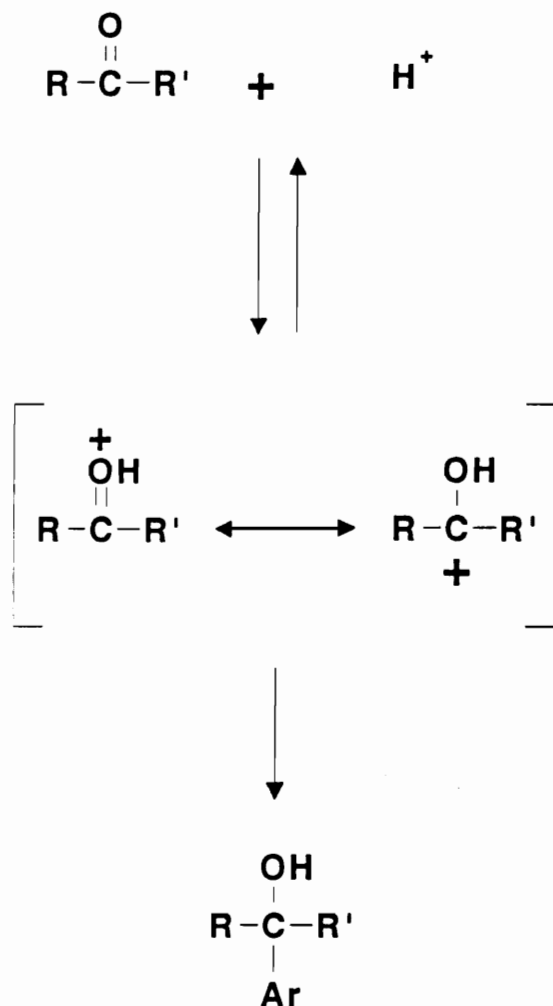
CF<sub>3</sub> - Diamine



CF<sub>3</sub> - bis-Phenol

Figure 3. CF<sub>3</sub> -Diamine and CF<sub>3</sub> bis Phenol.

The first reported preparation of 3F-diamine was that of Kray and Rosser (15) in 1977. The procedure, with modifications, is general for the preparation of 1,1,1-triaryl-2,2,2-trifluoroethanes. This method involved a modified hydroxyalkylation which utilized an appropriate 2,2,2-trifluoroacetophenone as the key starting material. There are numerous literature citations of hydroxyalkylation (138-140). In each case, aromatic substitution takes place as a consequence of the protonation of an aldehyde or ketone and the generation of an ion which acts as an electrophile as seen in Scheme 1.



Scheme 1. Hydroxyalkylation mechanism.

The reaction of fluoro ketones with aromatic substrates has been reported (141-143). In most cases, the reaction stopped at the carbinol stage as shown in Scheme 1 or further reacted only when a perfluoroalkyl ketone or an aldehyde was used. This general method of preparation is a modification of the procedures of Patai and Dayagi (144) and of Baeyer and Villiger (145) which were used to prepare 1,1,1-tris(4-amino-phenyl) methane derivatives from aldehydes.

## 4.2 SYNTHESIS

### 4.2.1 2,2,2-Trifluoroacetophenone (Trifluoroacetyl Chloride Method)

This procedure uses trifluoroacetyl chloride, and is a modification of the similar procedure of Simons and Ramler (146).

A 500 mL three-necked flask equipped with an overhead stirrer, condenser, thermometer, and gas inlet tube, and containing 39 g (0.50 mol) of benzene, 100 mL of carbon disulfide and 66 g of aluminum chloride (0.50 mol) was cooled to  $-15^{\circ}\text{C}$  under an atmosphere of dry argon. The condenser temperature was maintained at  $-50^{\circ}\text{C}$  by use of a circulating cooling bath. Trifluoroacetyl chloride (68.4 g, 0.52 mol) was added over a period of 8 hours. The temperature of the reaction mixture was not allowed to exceed  $-10^{\circ}\text{C}$ . After addition, the flask was allowed to warm to room temperature with stirring for 16 hours. The reaction mixture was poured into a mixture of three hundred grams of ice and 300 mL of concentrated hydrochloric acid. The mixture was extracted with three 300 mL portions of ether. The combined ether extracts were dried over anhydrous magnesium sulfate, filtered, and the ether removed by distillation. Careful distillation of the residue gave a fraction, bp  $153^{\circ}\text{C}/735$  torr, weighing 27 g (42%).

The proton and carbon NMR spectra, mass spectrum and infrared spectrum are shown in Figures 4-7.

### 4.2.2 Trifluoroacetophenone (Trifluoroacetic Anhydride Method)

To a mixture of 7.86 g (0.101 mol) of benzene and 30.60 g (0.225 mol) of aluminum chloride in 250 mL of carbon disulfide cooled to  $-10^{\circ}\text{C}$  was added dropwise 22.03 g (0.105 mol) of trifluoroacetic anhydride over a period of one hour. The mixture was allowed to warm slowly with stirring to  $25^{\circ}\text{C}$  over thirteen hours, during which time the mixture turned black. The mixture was added to 100 g of ice to which 100 g of water

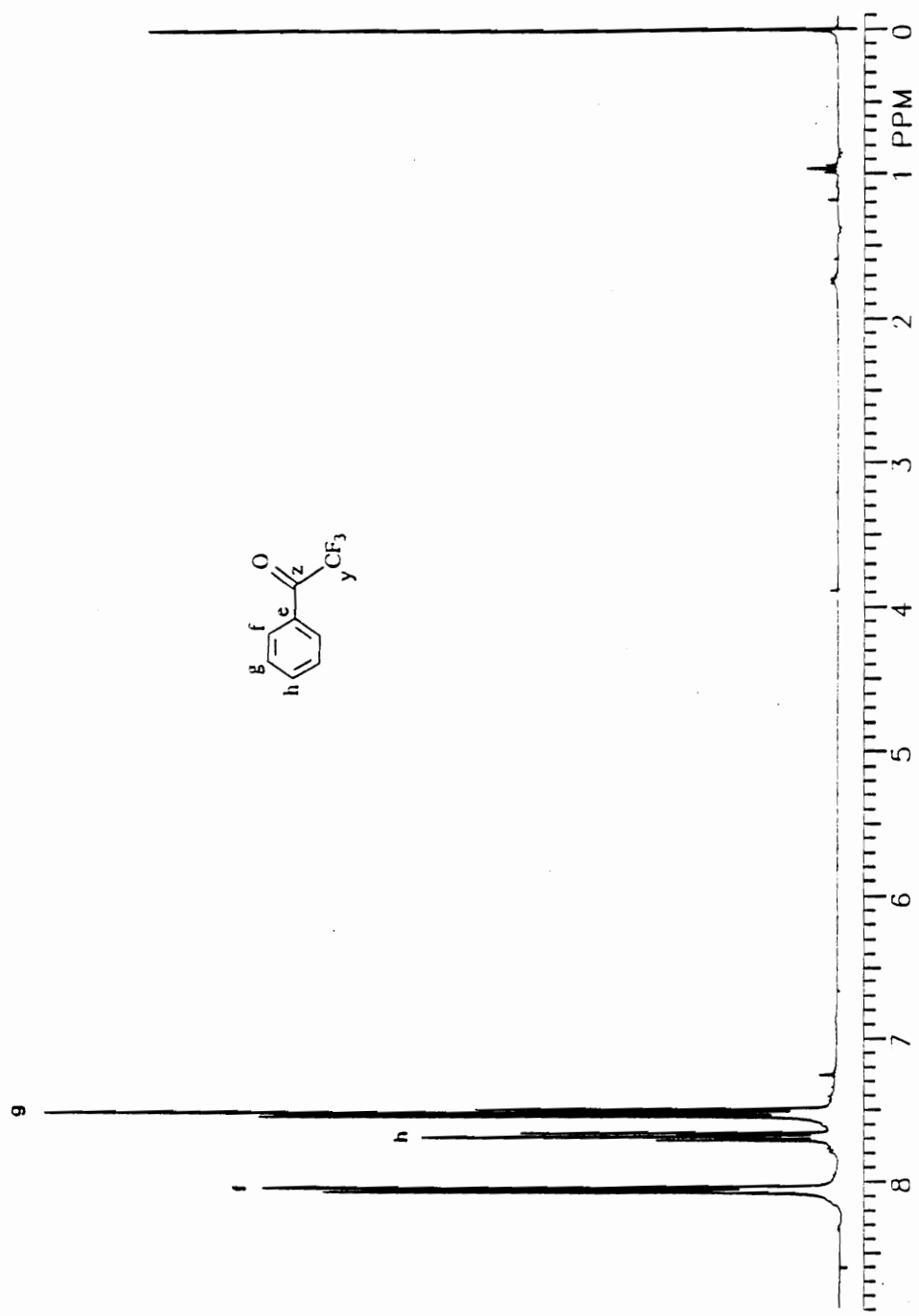


Figure 4. <sup>1</sup>H NMR spectrum of 2,2,2-trifluoroacetophenone.



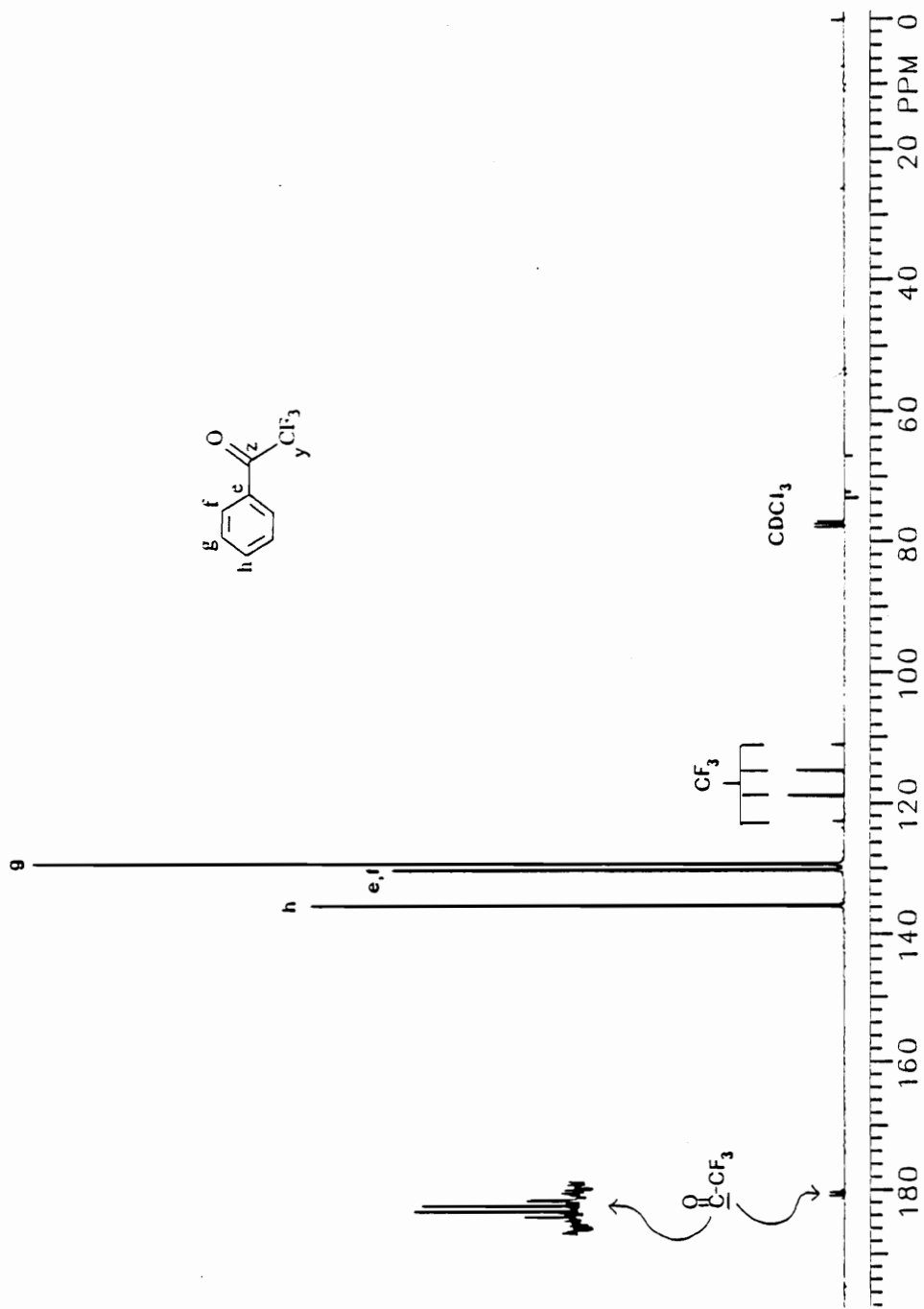


Figure 5.  $^{13}\text{C}$  NMR spectrum of 2,2,2-trifluoroacetophenone.

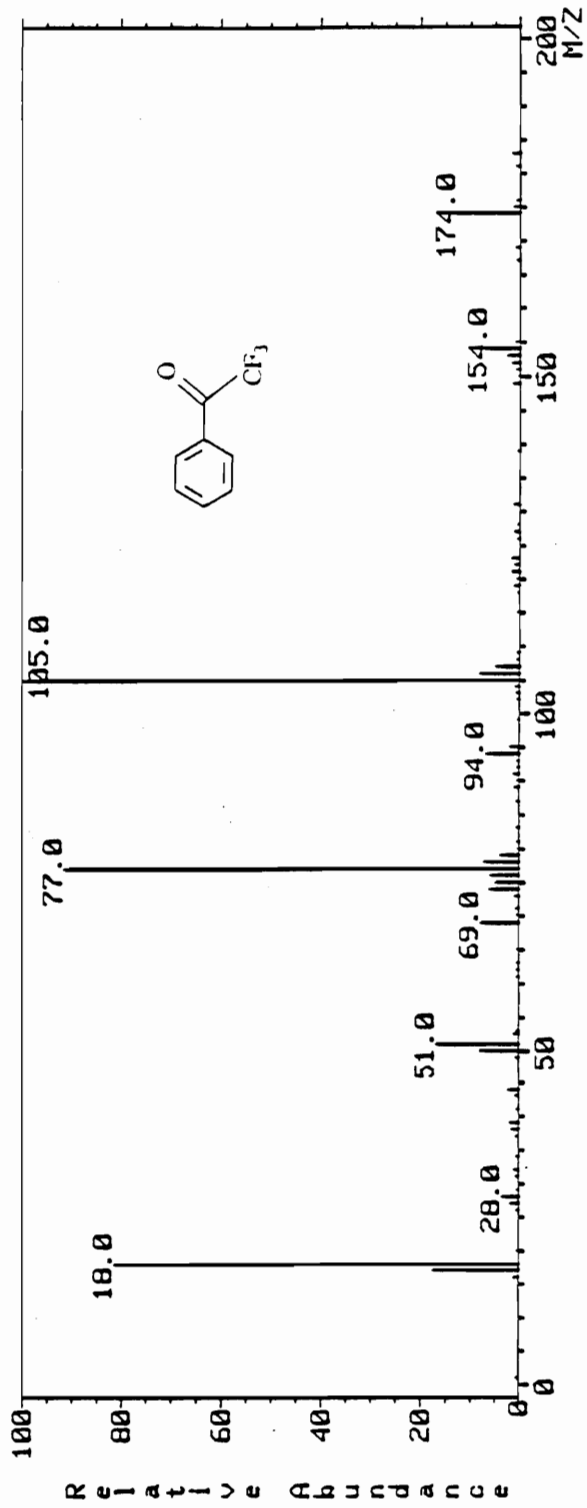


Figure 6. Mass spectrum (EI) of 2,2,2-trifluoroacetophenone.

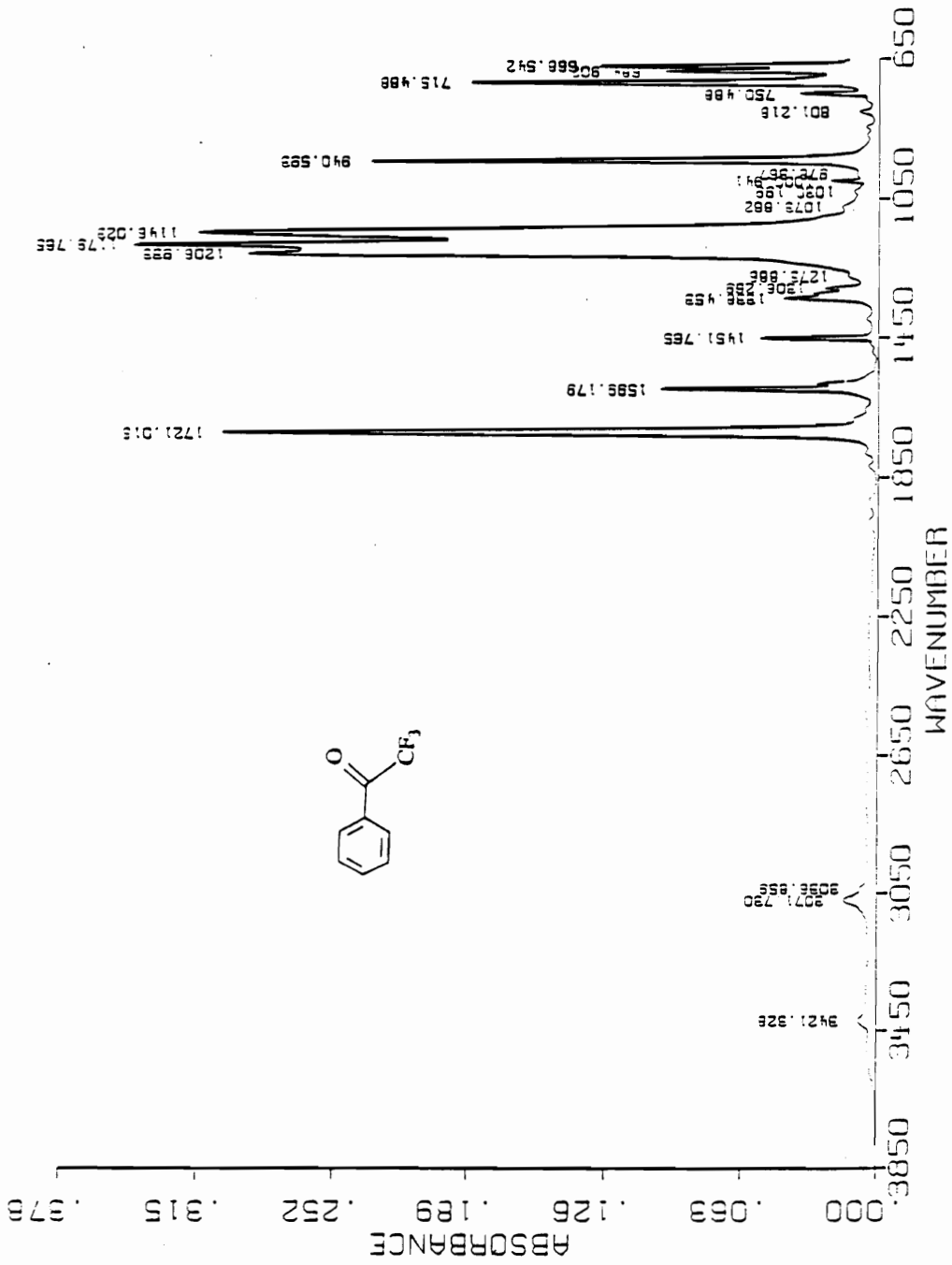


Figure 7. IR spectrum of 2,2,2-trifluoroacetophenone.

was added. Four hundred mL of ether was then added with stirring and the organic phase was separated and washed successively with two 200 mL portions of water, one 200 mL portions each of 10% sodium hydroxide, water, and 10% hydrochloric acid. A final wash of 100 mL of water was followed by drying over anhydrous magnesium sulfate. Distillation through a short path still gave 3.70 g (21.1%) of trifluoroacetophenone (bp 153-154°C/37 torr). The carbon NMR spectrum was identical with that shown in Figure 5.

#### 4.2.3 2,2,2-Trifluoroacetophenone (Ethyl Trifluoroacetate, -85°C)

Into a 250 mL three-necked flask fitted with an alcohol thermometer, a magnetic stirrer, and under an atmosphere of dry argon, was placed 90 mL of anhydrous ether and 3.75g of ethyl trifluoroacetate (0.026 mol). The mixture was cooled to -85°C with stirring. Phenyllithium (23.6 mL of 1.10 molar ether solution, 0.026 mol) was added over a period of 30 minutes such that the temperature did not rise above -78°C. After addition, the solution was stirred for 10 minutes at -78 to -80°C. A cooled solution (approximately -65°C) of 2.5 mL of concentrated hydrochloric acid and 5.0 mL of methanol was added over 15 minutes. After warming to room temperature, the mixture was added to 150 mL of 2 molar hydrochloric acid with stirring. Phases were separated and the organic phase was dried over anhydrous magnesium sulfate. Ether was removed under reduced pressure. Fractional distillation of the crude product gave 4.16 g (92%) bp 152-155°C/ 740 torr. The carbon NMR of this fraction was identical with that of Figure 5.

#### 4.2.4 2,2,2-Trifluoroacetophenone (Ethyl Trifluoroacetate, 20°)

Using the same procedure as example 3, a reaction temperature of 20°C was utilized for the addition of phenyllithium and the subsequent period prior to hydrolysis.

From 0.032 mol of ethyl trifluoroacetate, a 68% yield was isolated. The carbon NMR of the product was identical with that of Figure 5.

#### 4.2.5 2,2,2-Trifluoroacetophenone (Ethyl Trifluoroacetate, 20°, Extended Hydrolysis)

Using the same procedure as example 3, a reaction temperature of 20°C was utilized for the addition of phenyllithium and the subsequent period prior to hydrolysis. The hydrolysis period was extended from 10 minutes to 48 hours at 20°C. From 0.035 mol of ethyl trifluoroacetate, a 58% yield was isolated. The carbon NMR of the fraction obtained was identical with that of Figure 5.

#### 4.2.6 2,2,2-Trifluoroacetophenone (Ethyl Trifluoroacetate, -40°)

In a 250 mL three-necked flask fitted with an alcohol thermometer, a magnetic stirrer, and under an atmosphere of dry argon, 90 mL of anhydrous ether and 24.4 mL of a 1.10 molar ether solution of phenyllithium (0.027 mol) were stirred at -45°C. Over a period of 30 minutes, 3.84 g (0.027 mol) of ethyl trifluoroacetate in 20 mL of ether was added such that the temperature of the reaction did not exceed -40°C. After addition, the reaction was stirred for an additional 10 minutes at -40°C. A cooled solution (approximately -40°C) of 2.5 mL of concentrated hydrochloric acid and 5.0 mL of methanol was added over a period of 15 minutes. The reaction mixture was allowed to warm to room temperature and was added to 150 mL of 2 molar aqueous hydrochloric acid with stirring. Phases were separated and the organic phase was washed with three 100 mL portions of water. The organic phase was separated and dried over anhydrous magnesium sulfate. The ether was removed under reduced pressure. Distillation of the crude product through a short path still gave 4.32 g (92%), bp 152-156°C/745 torr. The carbon NMR spectrum of the fraction obtained was identical with that of Figure 5.

#### 4.2.7 2,2,2-Trifluoroacetophenone (Ethyl Trifluoroacetate, Room Temperature, Extended Hydrolysis)

This example was carried out the same way as example 6 except that 0.030 mol of ethyl trifluoroacetate was used. Hydrolysis was carried out 48 hours at room temperature. The yield was 90%. The carbon NMR spectrum was identical with that of Figure 5.

#### 4.2.8 2,2,2-Trifluoroacetophenone (Ethyl Trifluoroacetate, 20°)

Using the same procedure as example 6, the addition temperature of the ethyl trifluoroacetate and subsequent hydrolysis was +20°C. No trifluoroacetophenone was obtained.

#### 4.2.9 2,2,2-Trifluoroacetophenone

At room temperature, 228 g (2.0 mol) of trifluoroacetic acid was added over 4 hours to a stirred suspension of 52 g (.25 mol) of phosphorus pentachloride in 900 mL of 1,2-dichloroethane in a three-necked 5-L flask. The trifluoroacetyl chloride formed was condensed in a Dry ice/2-propanol cooled trap. The trifluoroacetyl chloride was distilled into a 5-L three-necked flask fitted with a Dry ice/2-propanol condenser and was cooled with a cooling bath to -50°C. The reaction vessel contained 270 g (2.0 mol) of finely ground aluminum chloride which was suspended with stirring in a mixture of 600 mL benzene and 450 mL of carbon disulfide. After completion of addition of the trifluoroacetyl chloride, the mixture was stirred for an additional 6 hours at -40°C. The reaction mixture was added (maintained at -40°C) to a mixture of 750 mL of concentrated hydrochloric acid and 750 g of ice. The phases were separated and the aqueous phase was extracted with one 500 mL portion of benzene and one 500 mL portion of

ether. The combined organic phases were washed with three 500 mL portions of saturated aqueous sodium bicarbonate. The organic phase was dried over anhydrous magnesium sulfate and filtered. Distillation gave 226 g (65%) of trifluoroacetophenone, bp 153 °C - 155°/750 torr. A carbon NMR spectrum of the fraction obtained was identical with that of Figure 5.

#### 4.2.10 1,1-Bis(4-aminophenyl)-1-phenyl-2,2,2-trifluoroethane (Aniline Hydrochloride Method)

Seventy-five grams (0.43 mol) of 2,2,2-trifluoroacetophenone and 300 mL of aniline were placed in a 1-L round bottomed flask equipped with a magnetic stirrer and reflux condenser. Addition of 75 g (0.58 mol) of aniline hydrochloride gave a solid cake which dissolved on warming to 60°C. The mixture was then heated at 160°C with stirring for 24 hours. It was allowed to cool to 100°C and 75 g (0.88 mol) of sodium carbonate stirred in 200 mL of water was added in small portions. The resulting purple solution was steam distilled until the distillate was clear. The aqueous solution of reaction product was cooled and the solid purple residue was collected by filtration. The residue was washed with four 200 mL portions of water. Drying in air gave 143 g of crude solid (98%). Column chromatography of the crude solid (5g of silica gel/g of crude product) using benzene (50 mL/g of crude product) as eluant, followed by crystallization from benzene/petroleum ether produced a rose-colored product, mp 202° - 206 °C (Lit. mp 201° - 204°C (15)), weighing 126 g (82% based on trifluoroacetophenone). Four recrystallizations from 95% ethanol (15 mL of ethanol per gram of product) gave 79.1 g of product (54%, mp 217°C (Lit. mp 217.0° - 217.5°C (122))) as a fine white powder.

The proton, carbon, and 2D NMR spectra, the mass spectrum, and infrared spectrum are shown in Figures 8-12.

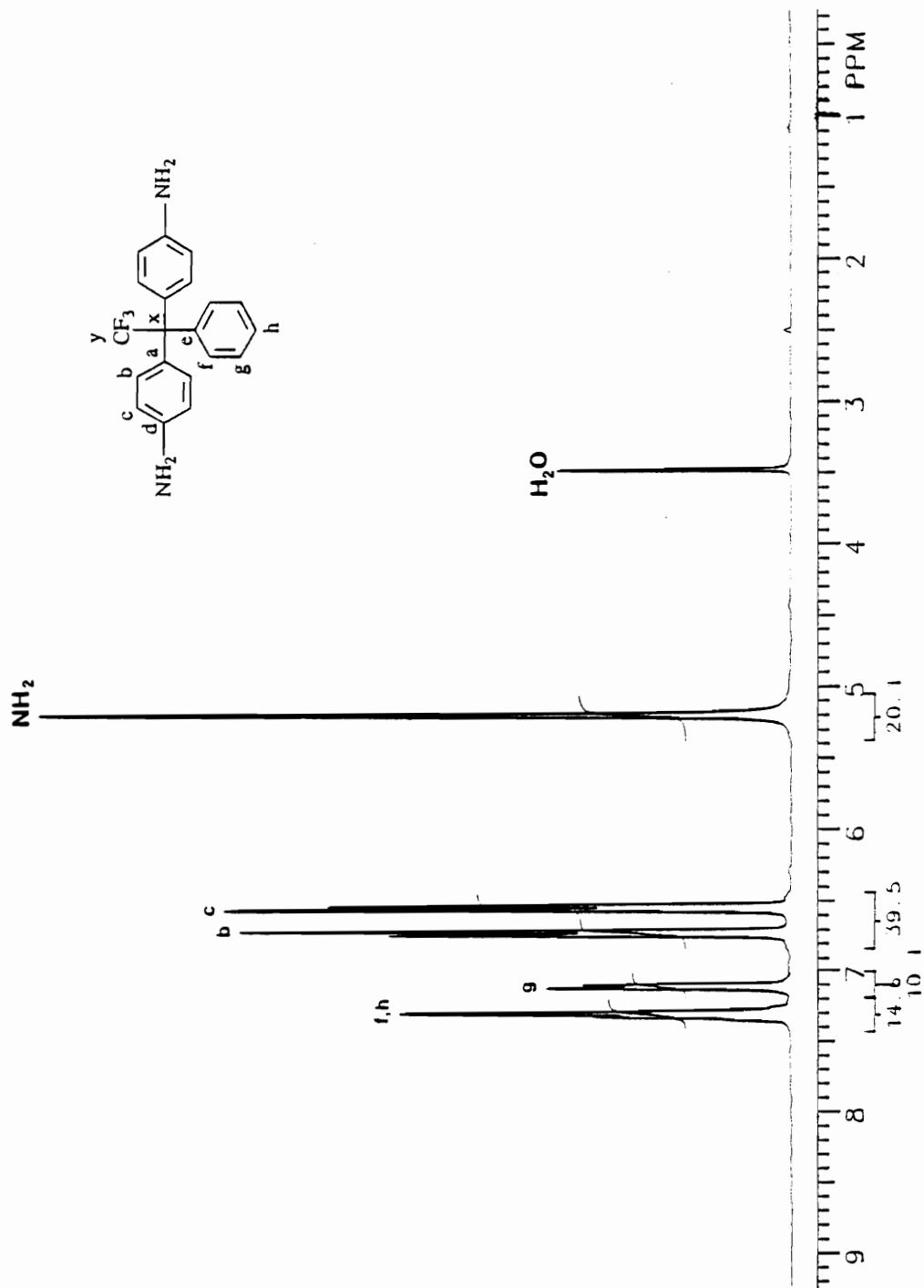


Figure 8.  $^1\text{H}$  NMR spectrum of 1,1-bis(4-aminophenyl)-1-phenyl-2,2,2-trifluoroethane.



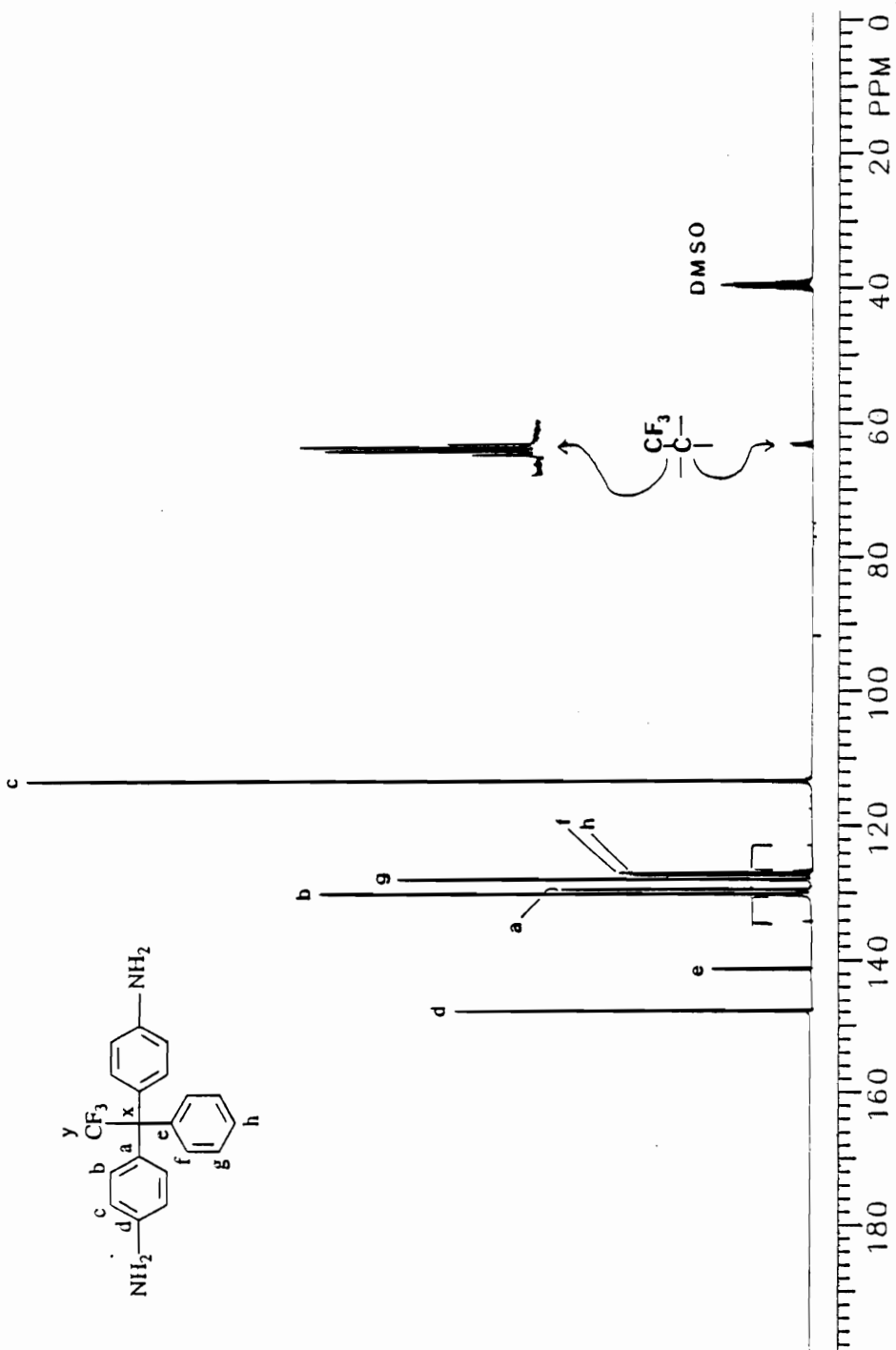


Figure 9.  $^{13}\text{C}$  NMR spectrum of 1,1-bis(4-aminophenyl)-1-phenyl-2,2,2-trifluoroethane.

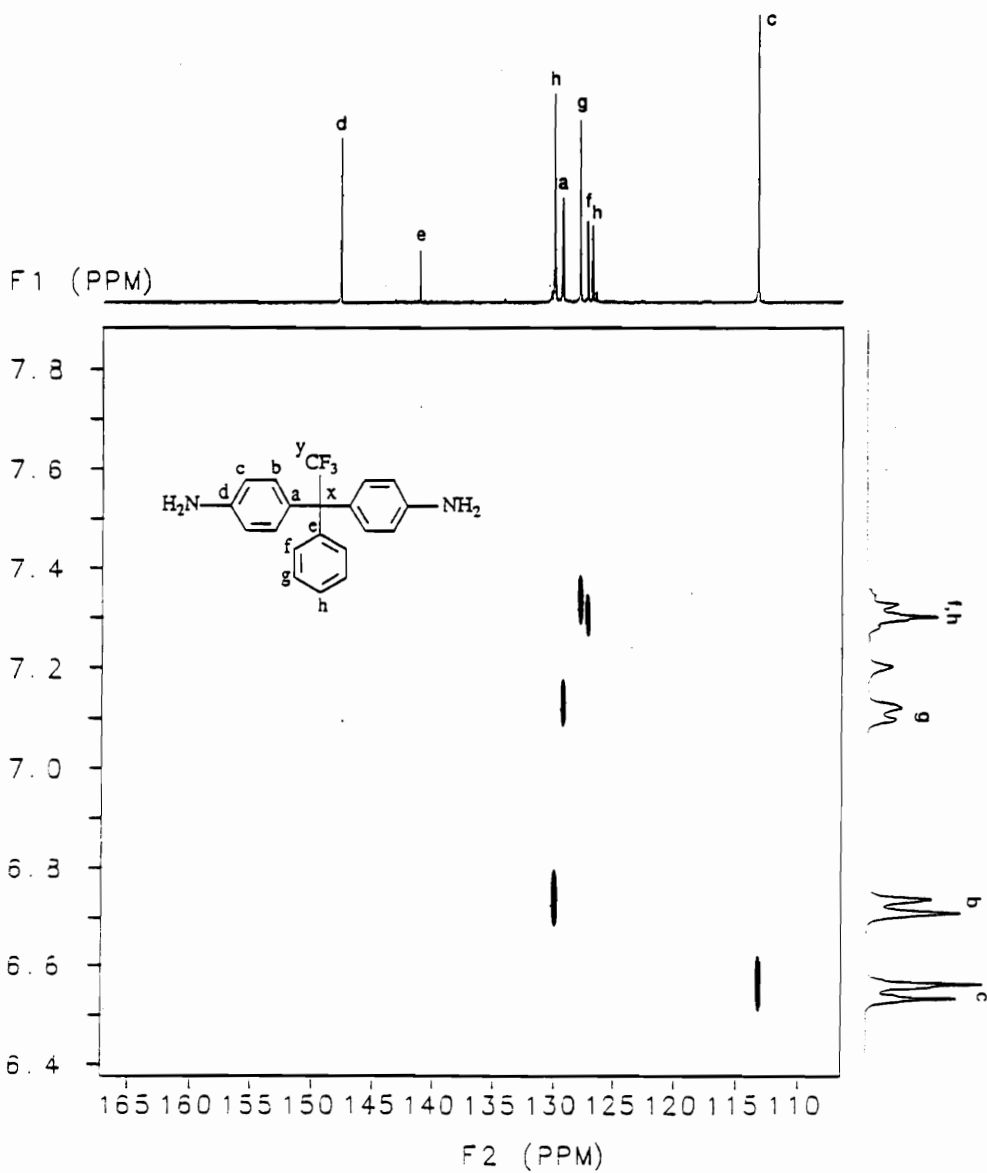


Figure 10. 2D HETCOR NMR spectrum of 1,1-bis(4-aminophenyl)-1-phenyl-2,2,2-trifluoroethane.

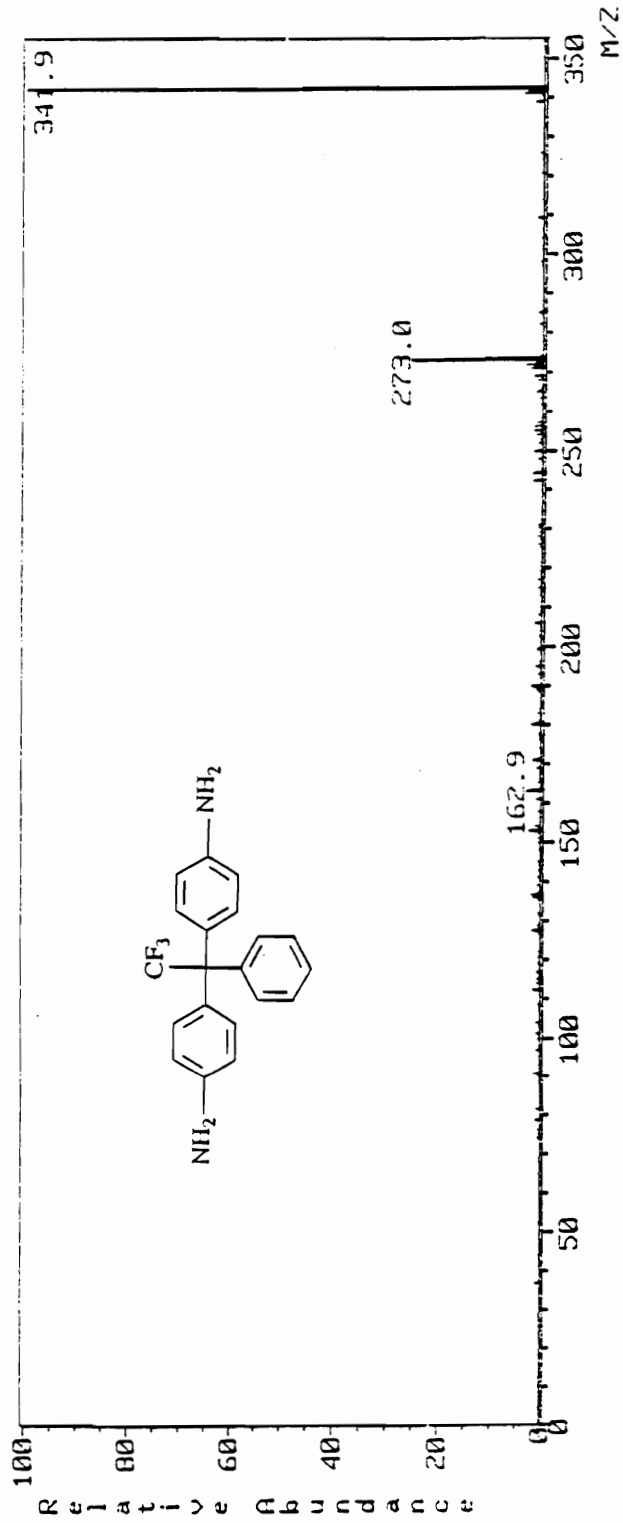


Figure 11. Mass spectrum (EI) of 1,1-bis(4-aminophenyl)-1-phenyl-2,2,2-trifluoroethane.

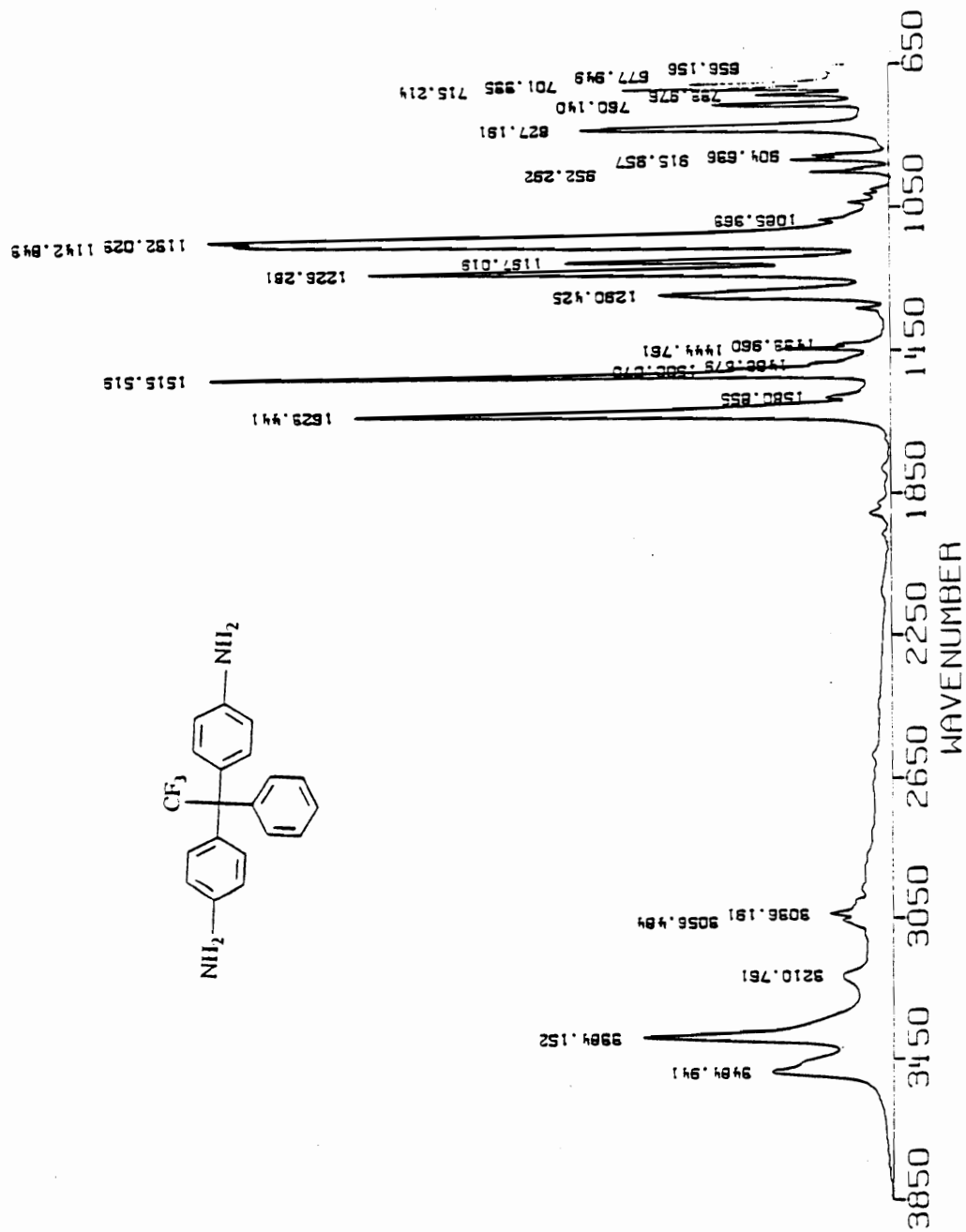


Figure 12. IR spectrum of 1,1-bis(4-aminophenyl)-1-phenyl-2,2,2-trifluoroethane.

#### 4.2.11 1,1-Bis(4-aminophenyl)-1-phenyl-2,2,2-trifluoroethane (Trifluoromethane Sulfonic Acid Method)

To a 2-L four-necked flask equipped with a mechanical stirrer, thermometer, condenser, gas inlet, and dropping funnel, 326.0 g of aniline (4.0 mol) was added under dry nitrogen. Trifluoromethanesulfonic acid (37), (100 g, 0.67 mol) was added over a two hour period. After addition, trifluoroacetophenone (70.8 mL, 87.1 g, 0.5 mol) was added over one hour. The mixture was then heated at 150°C for 15 hours with stirring. The reaction mixture was allowed to cool to approximately 100°C, and then heated under vacuum (110°C/25 torr) for 2 hours. The purple, slush-like residue was dried under vacuum (100°C/5 torr) for 16 hours.

Twenty-gram portions of the crude solid were purified by addition to 700 mL of 95% ethanol and the solution obtained was treated with 400 mL of 17% aqueous hydrochloric acid to obtain a pH of 2. Eight grams of activated carbon was added and the mixture was heated to reflux for five minutes. The solution was gravity filtered through paper and the procedure repeated twice. Aqueous sodium hydroxide (50%) was added with stirring to give a pH of 8 or greater and the formation of a second phase. The layers were separated and to the top layer 600 mL of toluene was added. After extraction and separation of layers, a tan colored top layer was obtained. The aqueous layer was extracted with three additional 300 mL toluene portions and all of the organic layers were combined. Removal of toluene under reduced pressure produced a tan solid. The tan solid was slurried with 500 mL portions of water and filtered until the filtrate obtained was neutral. The solid was dried for 24 hours at 100°C and 5 torr to yield a tan solid with a melting point of 218°C (217.0 - 217.5) (123). The total yield of product obtained was 187.9 g (82%).

Recrystallization from 95% ethanol (one gram of product per 10 mL of ethanol) produced a white product of melting point 218.0 - 218.5°C (yield from recrystallization: 179.6 g, 78.3%).

The NMR spectra, mass spectrum, and infrared spectrum obtained are identical with those shown in Figures 8-12.

#### 4.2.12 1,1-Bis(4-hydroxyphenyl)-1-phenyl-2,2,2-trifluoroethane (No Solvent)

To a three-necked round bottomed flask equipped with a stirrer, an addition funnel, and a condenser fitted with a gas inlet tube and a thermometer, a mixture of 94 g of phenol (1.0 mol) and 40 g (0.23 mol) of trifluoroacetophenone was added under an atmosphere of dry nitrogen. The contents were heated to 50°C to liquefy the mixture. A charge of 20 g (0.133 mol) of trifluoromethanesulfonic acid was added dropwise with stirring such that the mixture did not exceed 55°C. Over a period of one hour, 10.7 g (0.06 mol) of trifluoromethanesulfonic acid was added until the reaction mixture could no longer be stirred. The reaction mixture was allowed to cool to room temperature and 200 mL of water was added with stirring. The slurry was filtered through a coarse glass frit and the solid substance was washed repeatedly with three 500 mL portions of boiling water to remove the acid and phenol. The product was air dried and then triturated three times with 800 mL portions of methylene chloride. Filtration gave a white solid which was dried in air for 6 hours. Further drying under vacuum (60°C/5 torr) for 24 hours gave 60.0 g (75%) of a white solid, mp 230°C (mp 225-226°C (148); 226-227°C (149)).

The proton, carbon, and 2D NMR spectra, the mass spectrum, and infrared spectrum are shown in Figures 13-17.

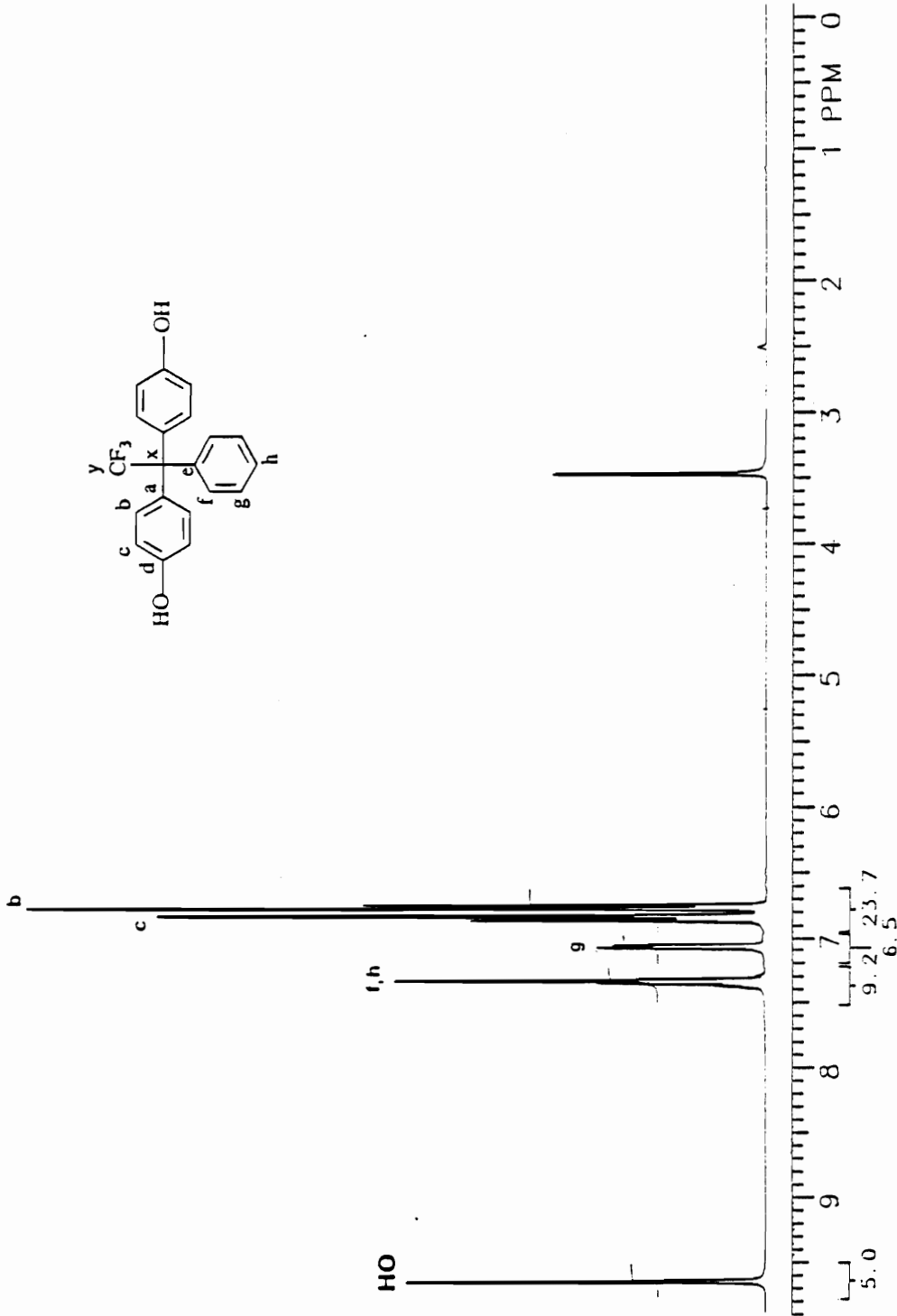


Figure 13. <sup>1</sup>H NMR spectrum of 1,1-bis(4-hydroxyphenyl)-1-phenyl-2,2,2-trifluoroethane.

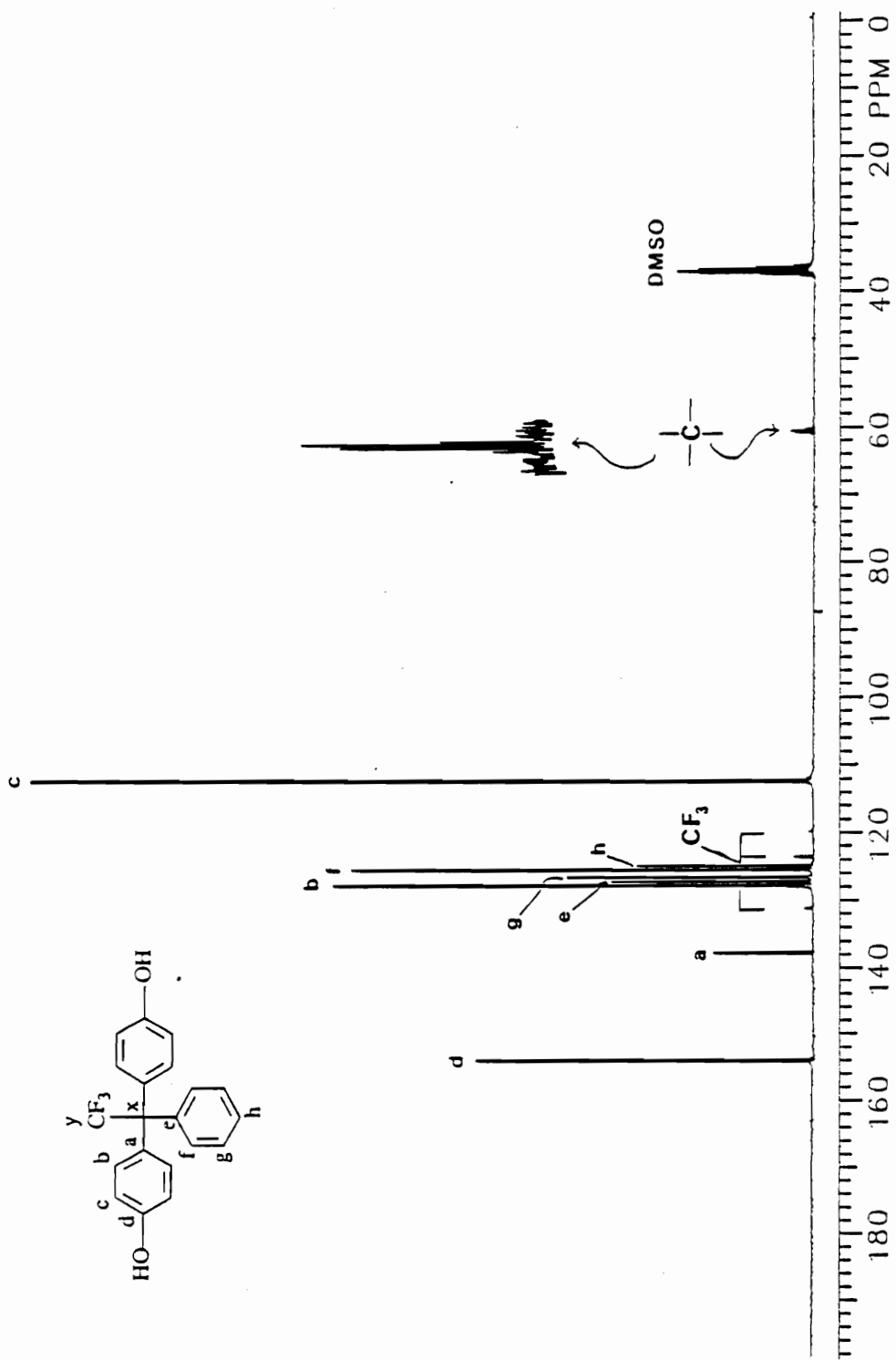


Figure 14.  $^{13}\text{C}$  NMR spectrum of 1,1-bis(4-hydroxyphenyl)-1-phenyl-2,2,2-trifluoroethane.



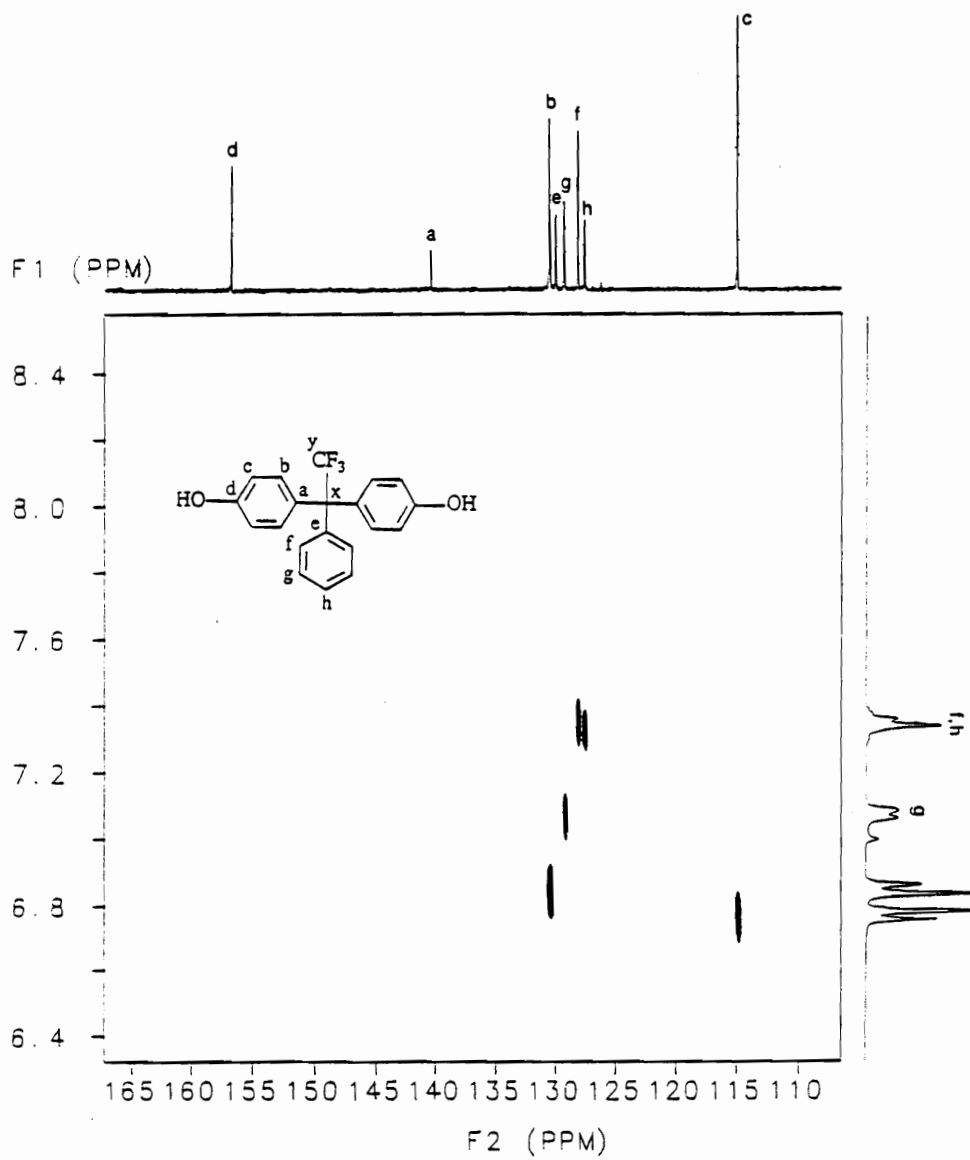


Figure 15. 2D HETCOR NMR spectrum of 1,1-bis(4-hydroxyphenyl)-1-phenyl-2,2,2-trifluoroethane.

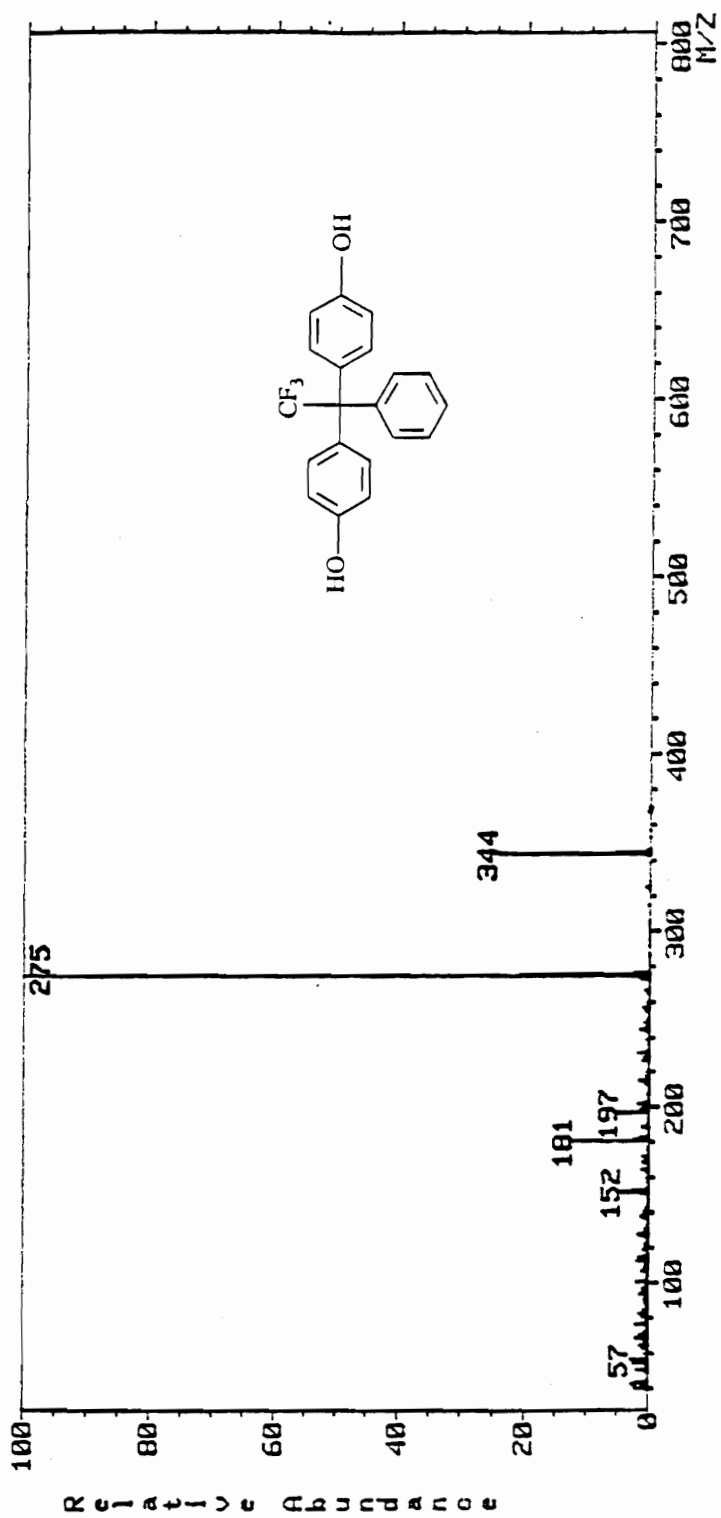


Figure 16. Mass spectrum of 1,1-bis(4-hydroxyphenyl)-1-phenyl-2,2,2-trifluoroethane.

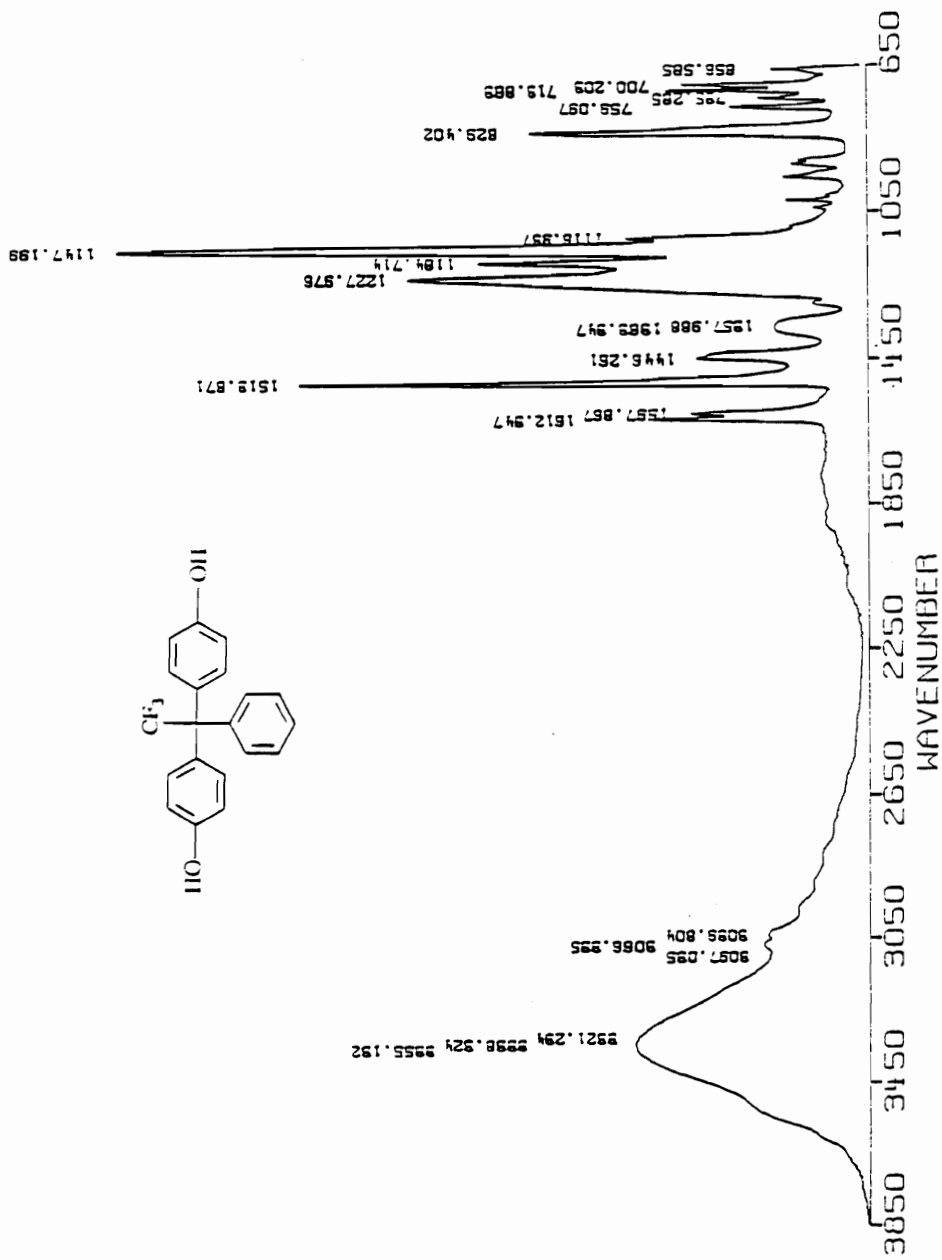


Figure 17. IR spectrum of 1,1-bis(4-hydroxyphenyl)-1-phenyl-2,2,2-trifluoroethane.

#### 4.2.13 1,1-Bis(4-hydroxyphenyl)-1-phenyl-2,2,2-trifluoroethane (Tetrachloroethylene Solvent)

To a 5-L three-necked flask equipped with stirrer, an addition funnel, a thermometer and a condenser fitted with a gas inlet tube, a mixture of 300 g (1.7 mol) of trifluoroacetophenone with 950 g (10.2 mol) of phenol in 2 liters of tetrachloroethylene was added under an atmosphere of dry nitrogen. With no heating or cooling, 150 g (1.0 mol) of trifluoromethanesulfonic acid was added over a period of eight hours such that the temperature of this reaction mixture did not exceed 35°C. After completion of addition, the reaction was stirred an additional twelve hours. One liter of water was then added with stirring and the mixture was filtered through a coarse glass frit. Seventy-five gram portions of the product were washed with three 600 mL portions of boiling water to remove phenol and trifluoromethanesulfonic acid. The crude product was then triturated with three 750 mL portions of methylene chloride, filtered, and allowed to air dry for five hours. Subsequent vacuum drying for 24 hours at 5 torr gave 514 g (84%) of white solid, mp 230-231°C (mp 225-226°C (148); 226-227°C (149)).

The proton, carbon and 2D NMR spectra, the mass spectrum and infrared spectrum obtained are identical with Figures 13-17.

#### 4.2.14 1,1-Bis(4-hydroxyphenyl)-1-phenyl-2,2,2-trifluoromethane (Methylene Chloride Solvent)

To a 5-L three-necked flask equipped with a stirrer, an addition funnel, and a condenser fitted with a gas inlet tube and thermometer, a mixture of 300 g (1.7 mol) of trifluoroacetophenone and 960 g (10.2 mol) of phenol in 2 liters of methylene chloride was added under dry nitrogen. With no provision for heating or cooling, the trifluoromethanesulfonic acid was added over a period of four hours. The rate of addition was such that solvent reflux was minimal. The reaction mixture was stirred for an

additional twenty hours and quenched with one liter of water. The mixture was filtered with a coarse glass frit and subsequently washed with four two liter portions of boiling water. The product was filtered, air dried for six hours and dried under vacuum 60°C for 18 hours. This gave 538 g (88%) of finely divided white product, mp 231°C (lit. mp 225-226°C (148); 226-227°C (149)).

The proton and carbon NMR spectra, the mass spectrum and infrared spectrum obtained are identical with Figures 13-17.

#### 4.2.15 1,1-Bis(4-methylphenyl)-1-phenyl-2,2,2-trifluoromethane

A mixture of 2800 mL (26.4 mol) of toluene and 200 g (1.5 mol) of trifluoroacetophenone was added to a five liter four-necked flask equipped with stirrer, an addition funnel, and a condenser fitted with a gas inlet tube and a thermometer. Trifluoromethanesulfonic acid (200 g, 1.33 mol) was added dropwise over a period of six hours such that the maximum temperature observed was 28°C. Upon completion of addition, the reaction was allowed to stir at room temperature for 48 hours. The toluene solution obtained was extracted with two liters of water, two liters of aqueous saturated sodium bicarbonate, and a final two liters of water. After drying over anhydrous magnesium sulfate and filtering, removal of solvent under reduced pressure gave a waxy solid. The solid product was triturated with three 500 mL portions of benzene-heptane solution (90/10 vol/vol) to yield a fine white powder. The product was dried at 100°C for 24 hours at 5 torr to yield 351 g (90%) of a fine white powder, mp 171-172°C (lit. mp 168-169°C (122)).

The proton, carbon, and 2D NMR spectra, the mass spectrum and infrared spectrum are shown in Figures 18-22.

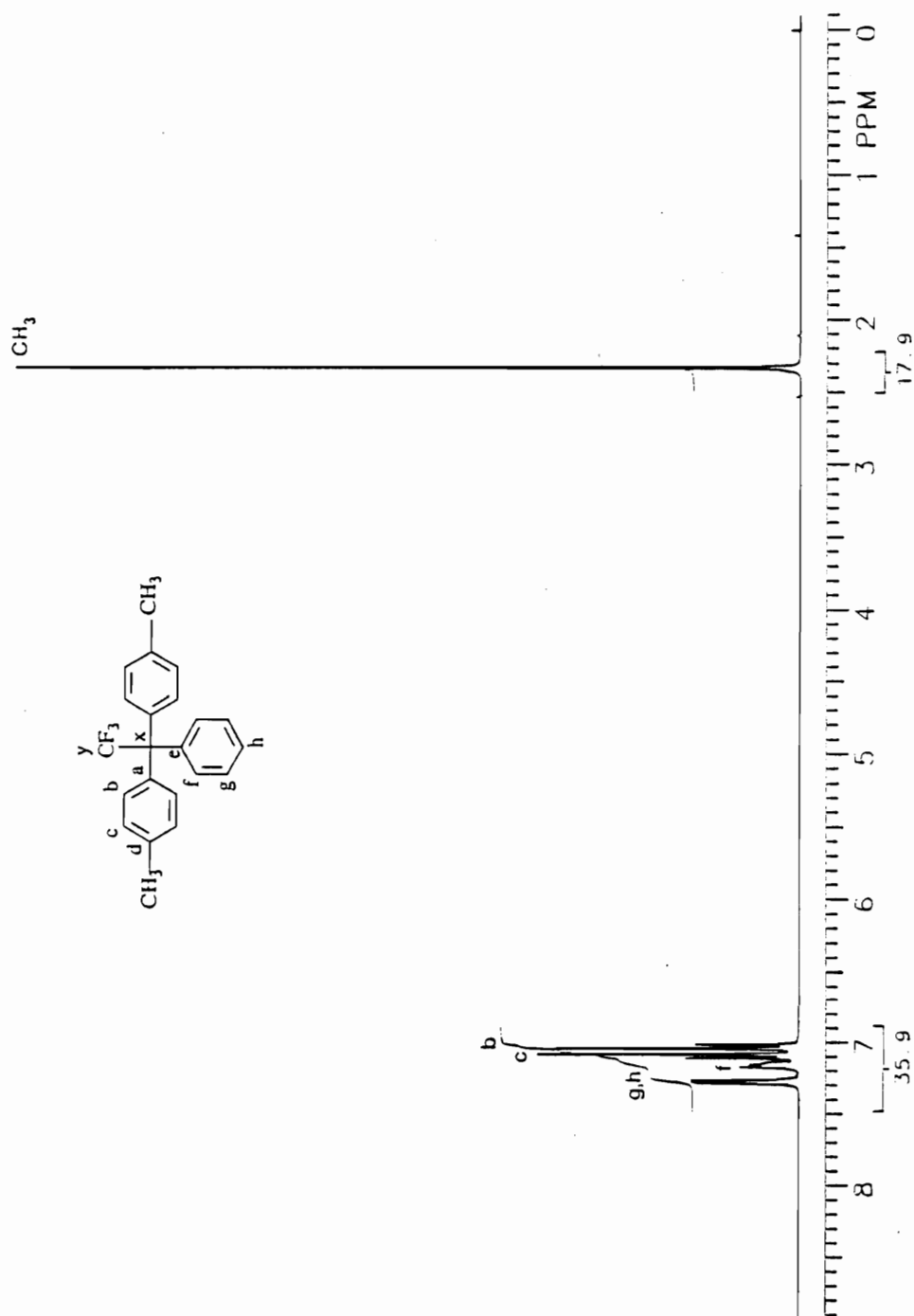


Figure 18.  $^1\text{H}$  NMR spectrum of 1,1-bis(4-methylphenyl)-1-phenyl-2,2,2-trifluoroethane.

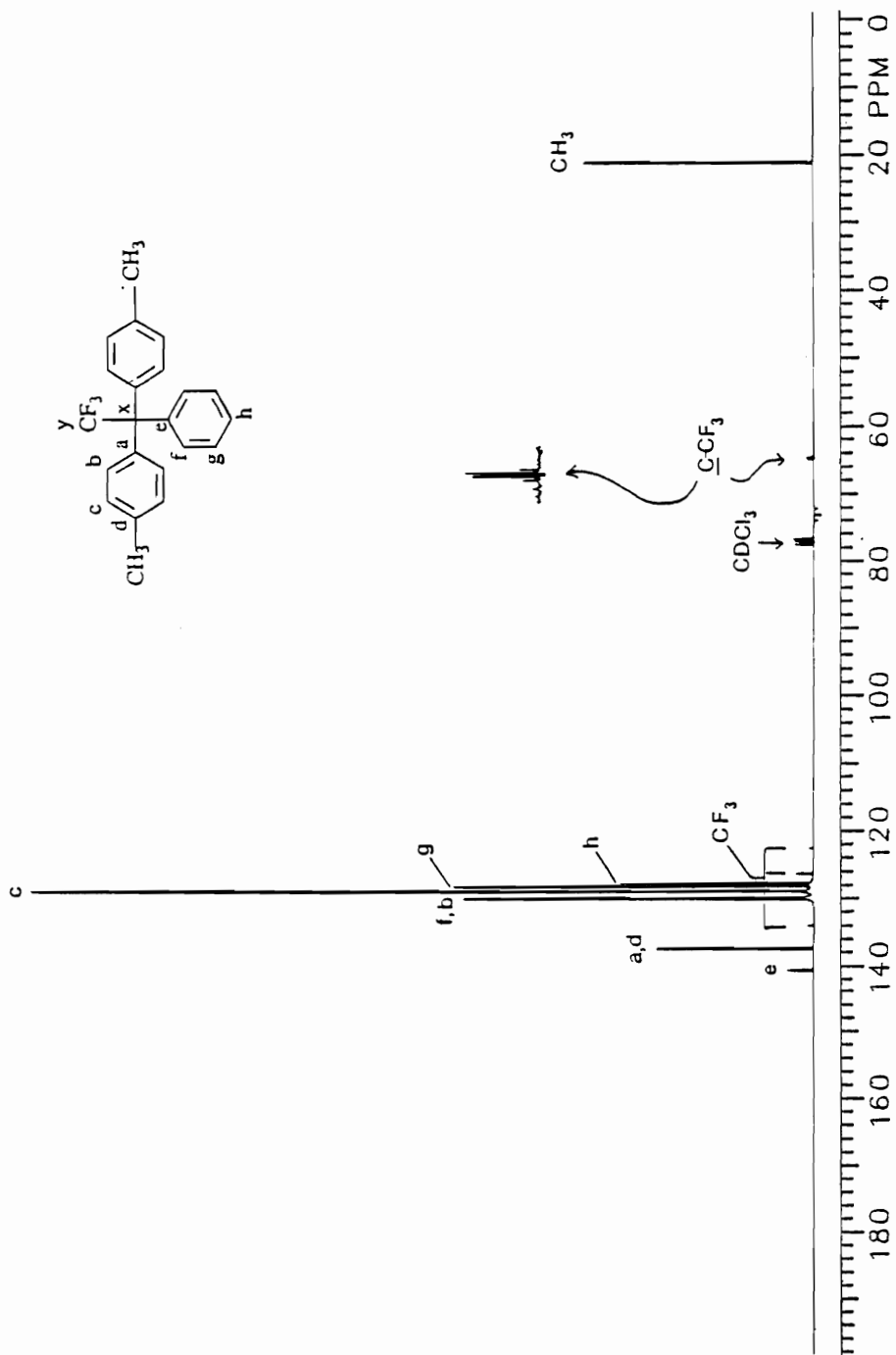


Figure 19.  $^{13}\text{C}$  NMR spectrum of 1,1-bis(4-methylphenyl)-1-phenyl-2,2,2-trifluoroethane.

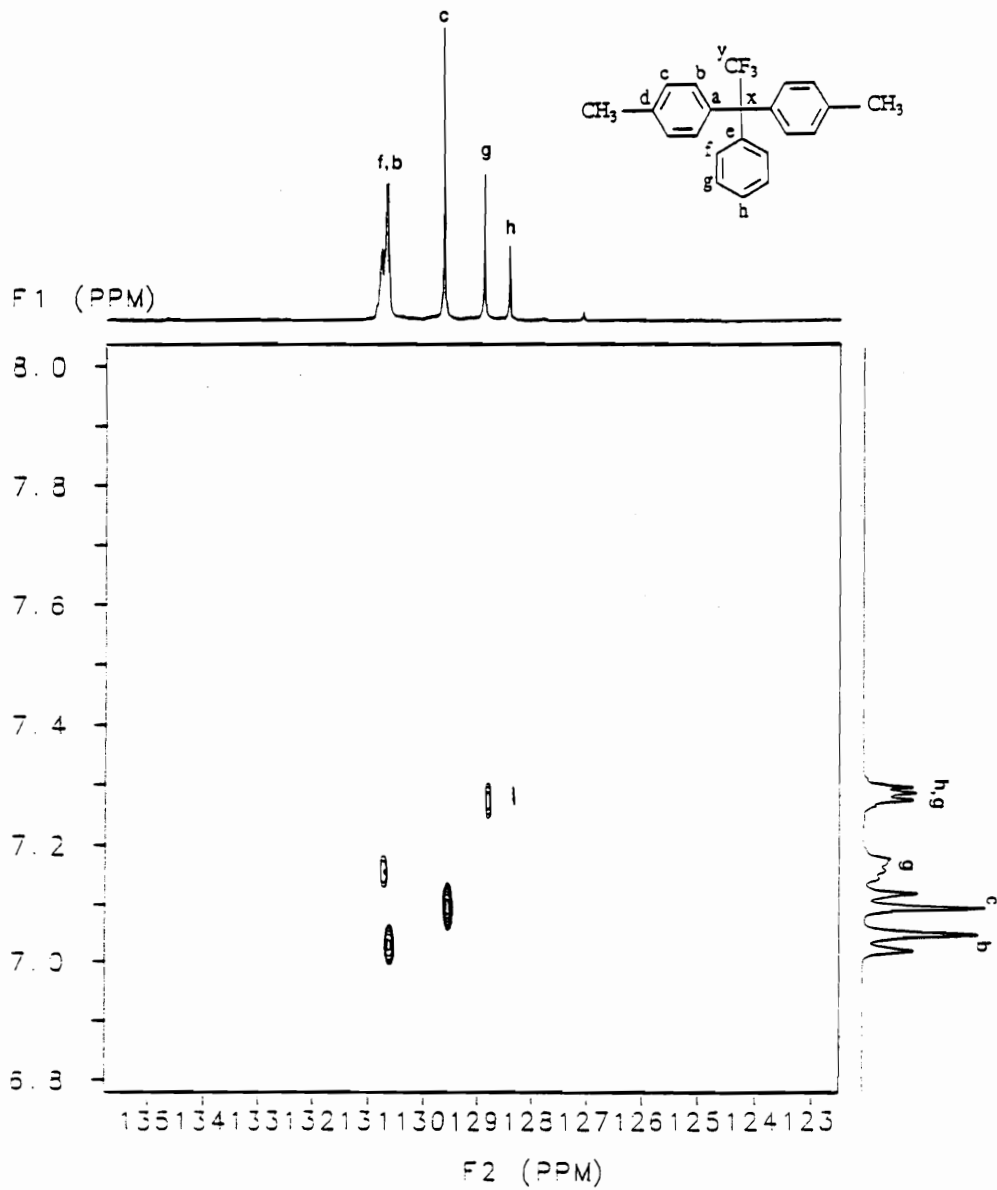


Figure 20. 2D HETCOR NMR spectrum of 1,1-bis(4-methylphenyl)-1-phenyl-2,2,2-trifluoroethane.



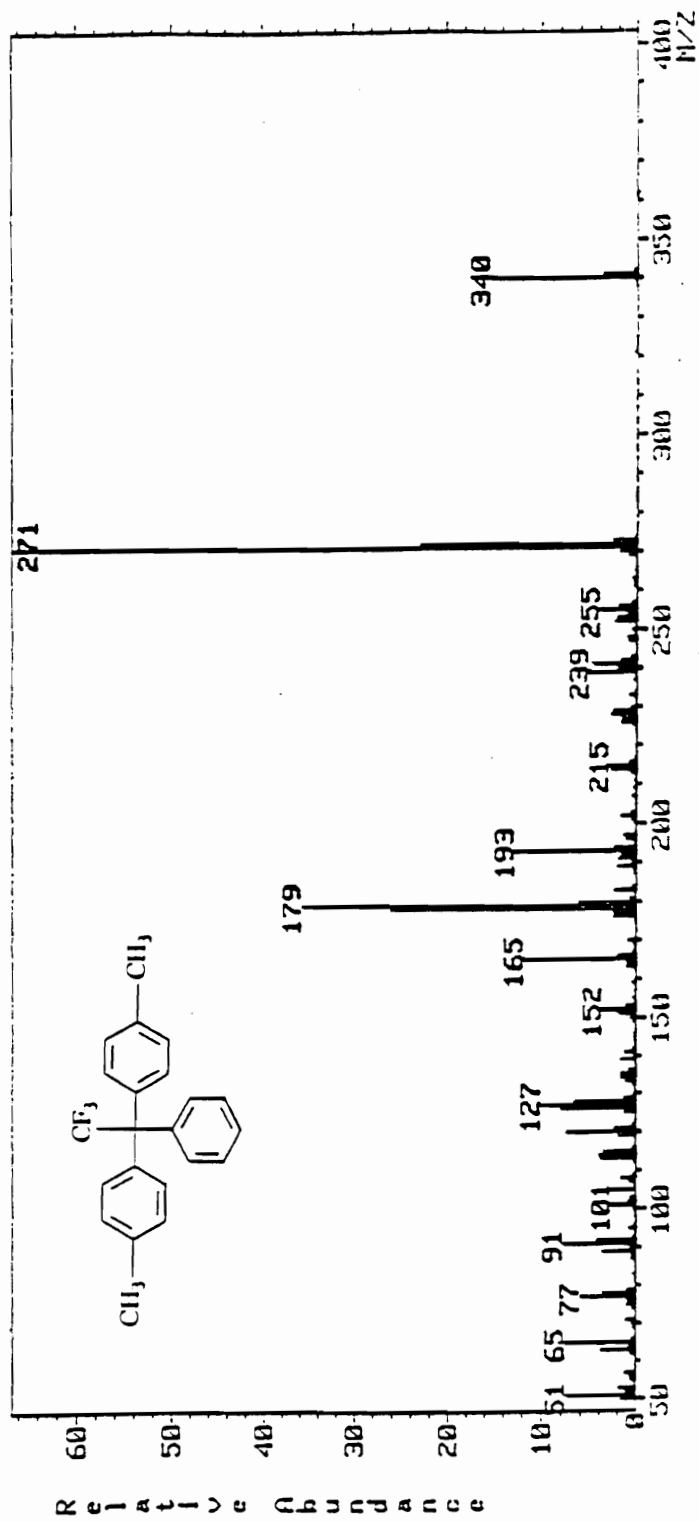


Figure 21. Mass spectrum (EI) of 1,1-bis(4-methylphenyl)-1-phenyl-2,2,2-trifluoroethane.

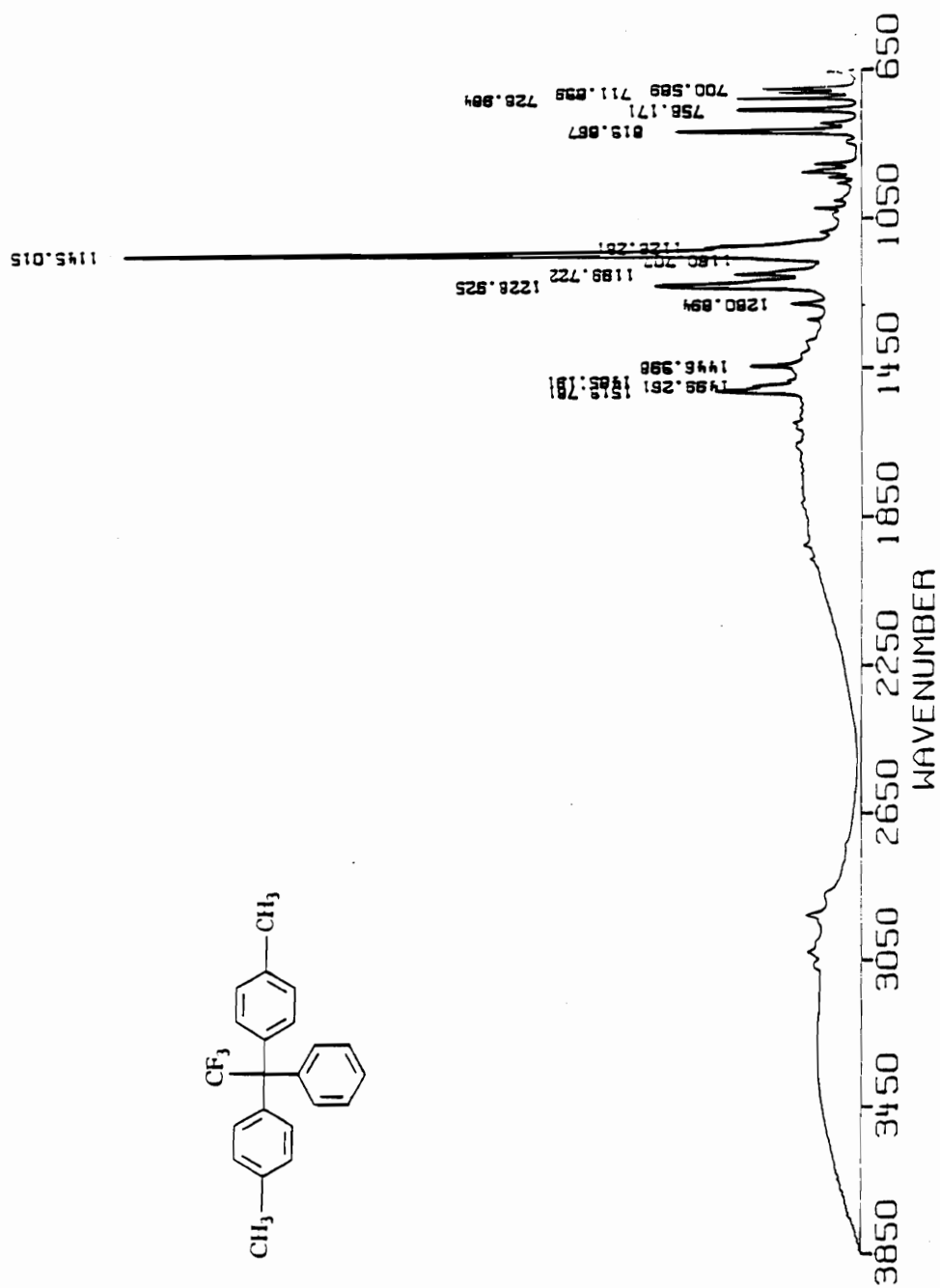


Figure 22. IR spectrum of 1,1-bis(4-methylphenyl)-1-phenyl-2,2,2-trifluoroethane.

#### 4.2.16 1,1-Bis(4-ethylphenyl)-1-phenyl-2,2,2-trifluoroethane

To a 1-L three-necked flask equipped with stirrer, an addition funnel, a thermometer and a condenser fitted with a gas inlet tube, a mixture of 300 g (2.85 mol) of ethylbenzene and 50 g (0.285 mol) of trifluoroacetophenone was added under an atmosphere of dry nitrogen. Fifty grams (0.33 mol) of trifluoromethanesulfonic acid was added dropwise over a period of two hours. After addition, the reaction was stirred at room temperature for an additional 48 hours. Removal of volatiles by distillation (to 160 °C/20 torr) gave an oily residue which was crystallized by trituration with two 250 mL portions of benzene-heptane solution (90/10). Drying (50°/5 torr) of the crystalline solid for 18 hours gave 1.0 g (10%) of product, sharp mp 137°C (lit. mp 135-136°C) (148)).

The proton and carbon NMR spectra, the mass spectrum and infrared spectrum are shown in Figures 23-26.

#### 4.2.17 1,1-Bis(4-fluorophenyl)-1-phenyl-2,2,2-trifluoroethane

To a 1-L three-necked flask equipped with a stirrer, an addition funnel, a thermometer and a condenser fitted with a gas inlet tube, a mixture of 50 g (0.285 mol) of trifluoroacetophenone and 500 g (5.2 mol) of fluorobenzene was added under an atmosphere of dry nitrogen. Over a period of one hour, 50 g (0.33 mol) of trifluoromethanesulfonic acid was added such that the reaction temperature did not exceed 28°C. After addition, the reaction mixture was allowed to stir for an additional 48 hours. The reaction mixture was washed with three 200 mL portions of water, three 200 mL portions of saturated aqueous sodium bicarbonate, and a 200 mL portions of water. The organic phase was dried over anhydrous magnesium sulfate, filtered, and excess fluorobenzene was removed at 100 torr at room temperature. The waxy solid obtained was recrystal

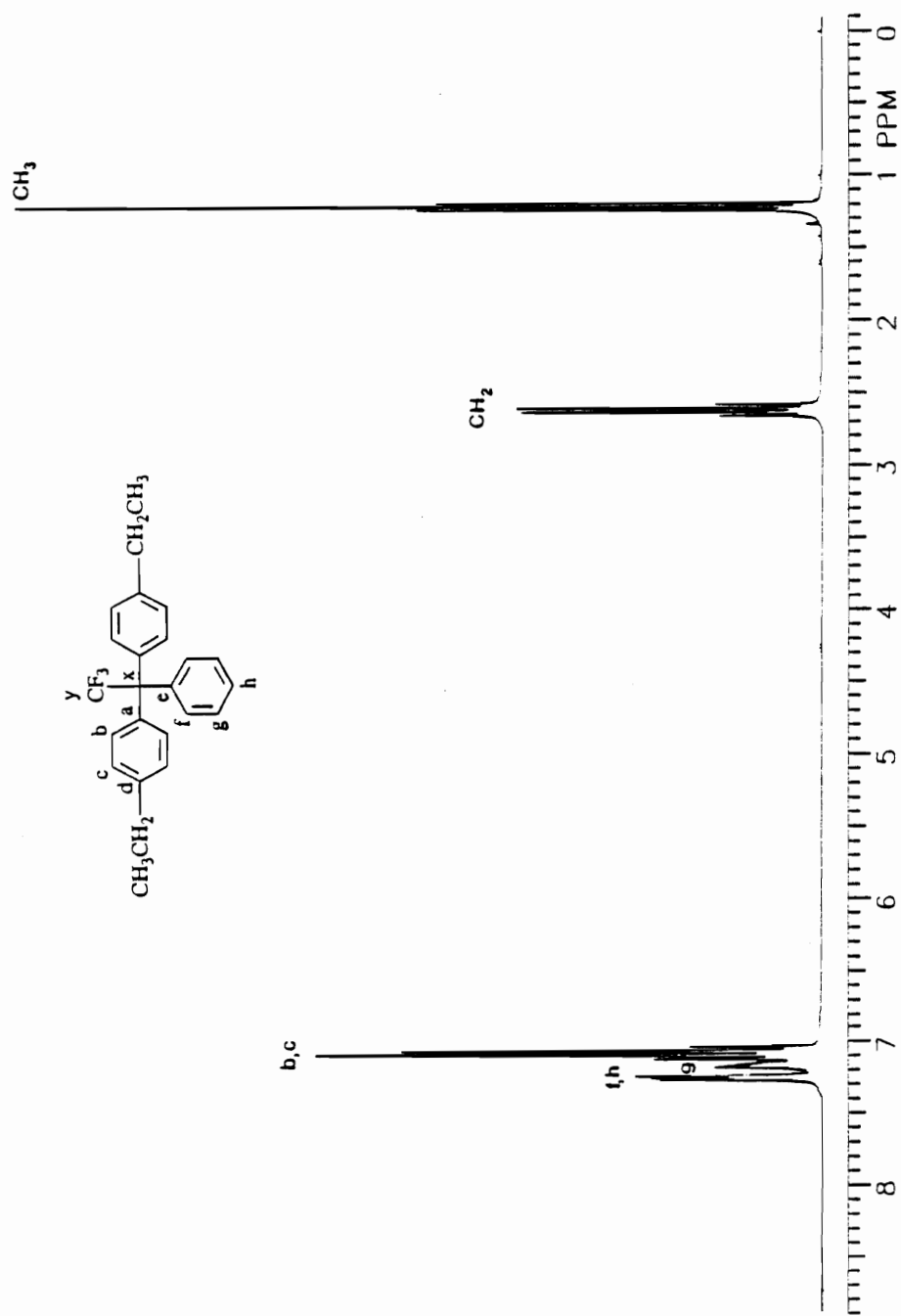


Figure 23.  $^1\text{H}$  NMR spectrum of 1,1-bis(4-ethylphenyl)-1-phenyl-2,2,2-trifluoroethane.

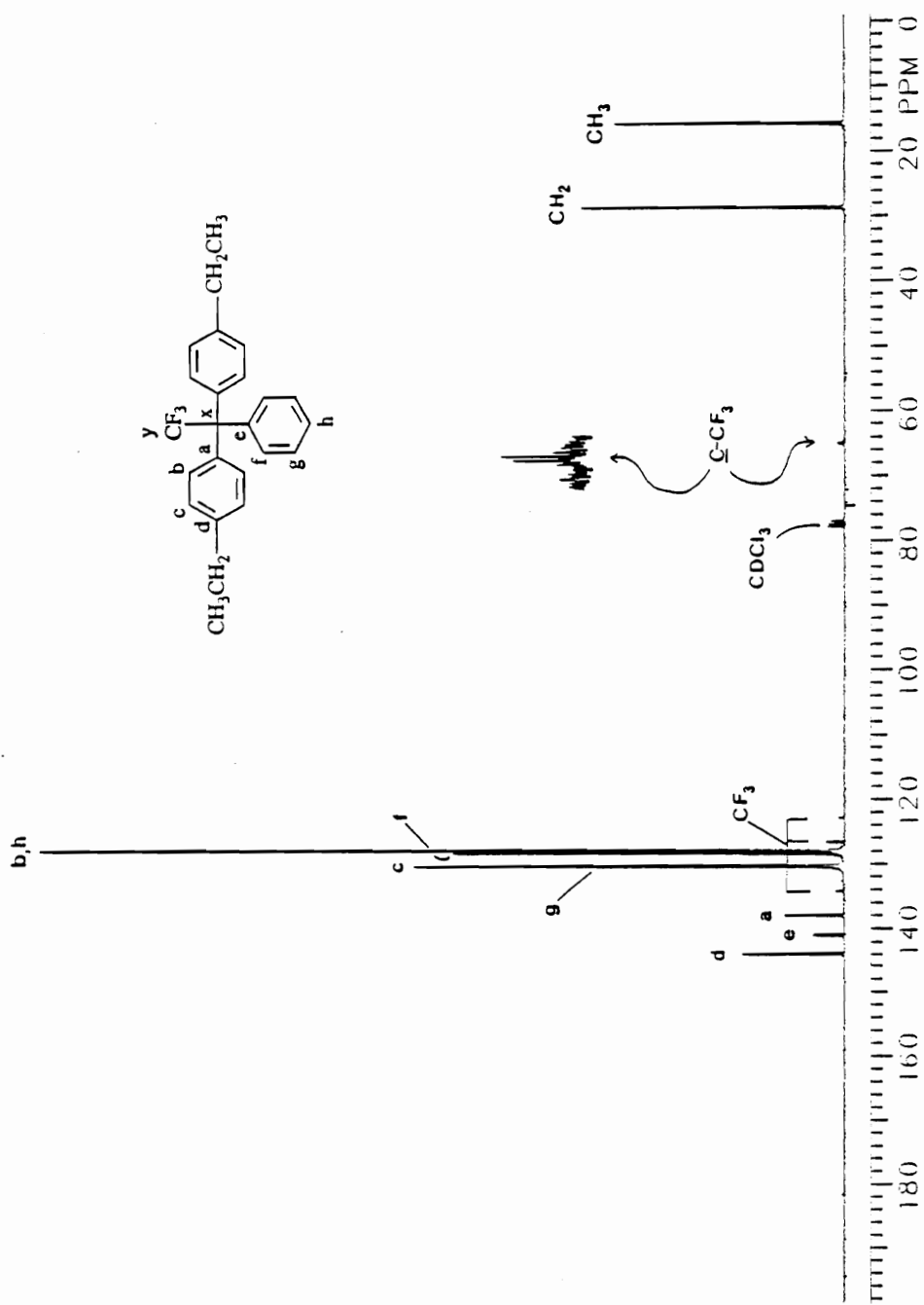


Figure 24.  $^{13}\text{C}$  NMR spectrum of 1,1-bis(4-ethylphenyl)-1-phenyl-2,2,2-trifluoroethane.

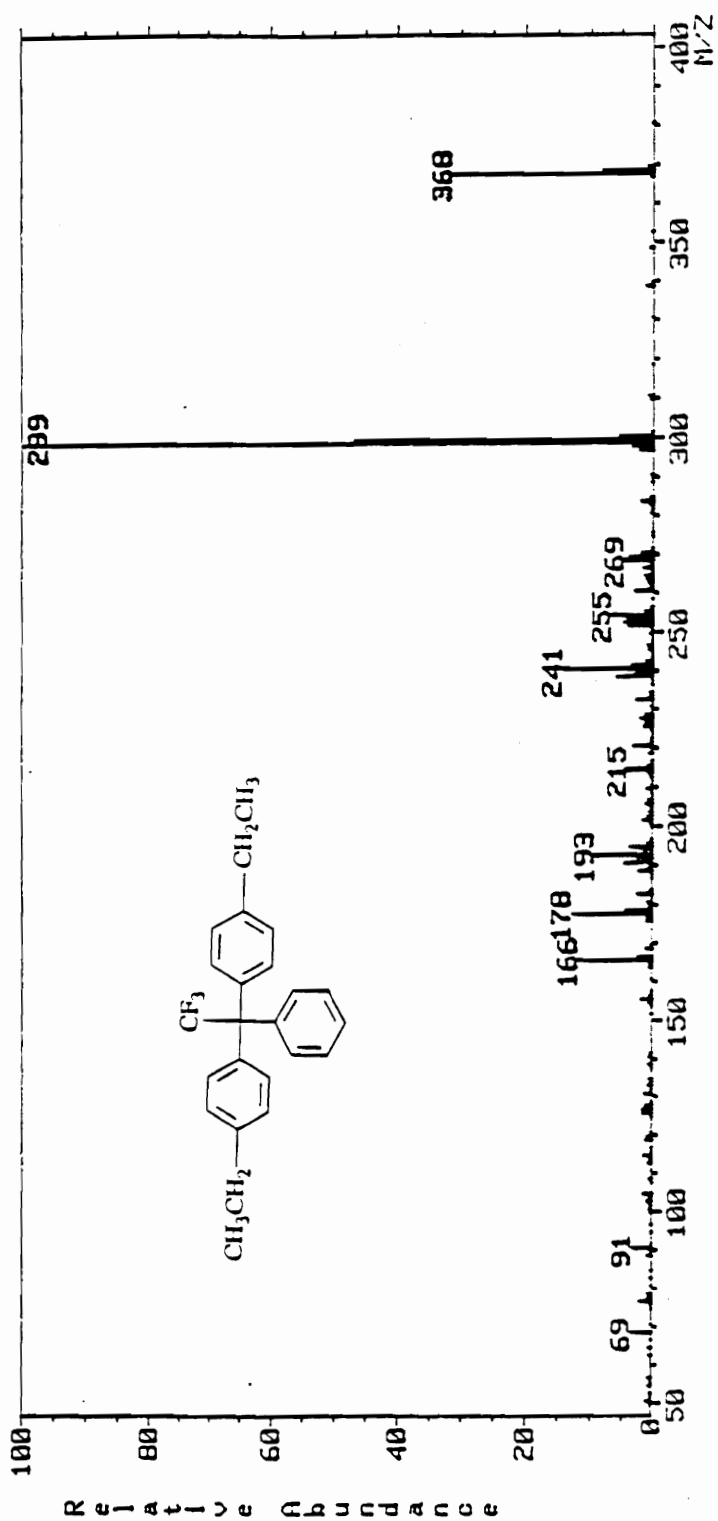


Figure 25. Mass spectrum (EI) of 1,1-bis(4-ethylphenyl)-1-phenyl-2,2,2-trifluoroethane.

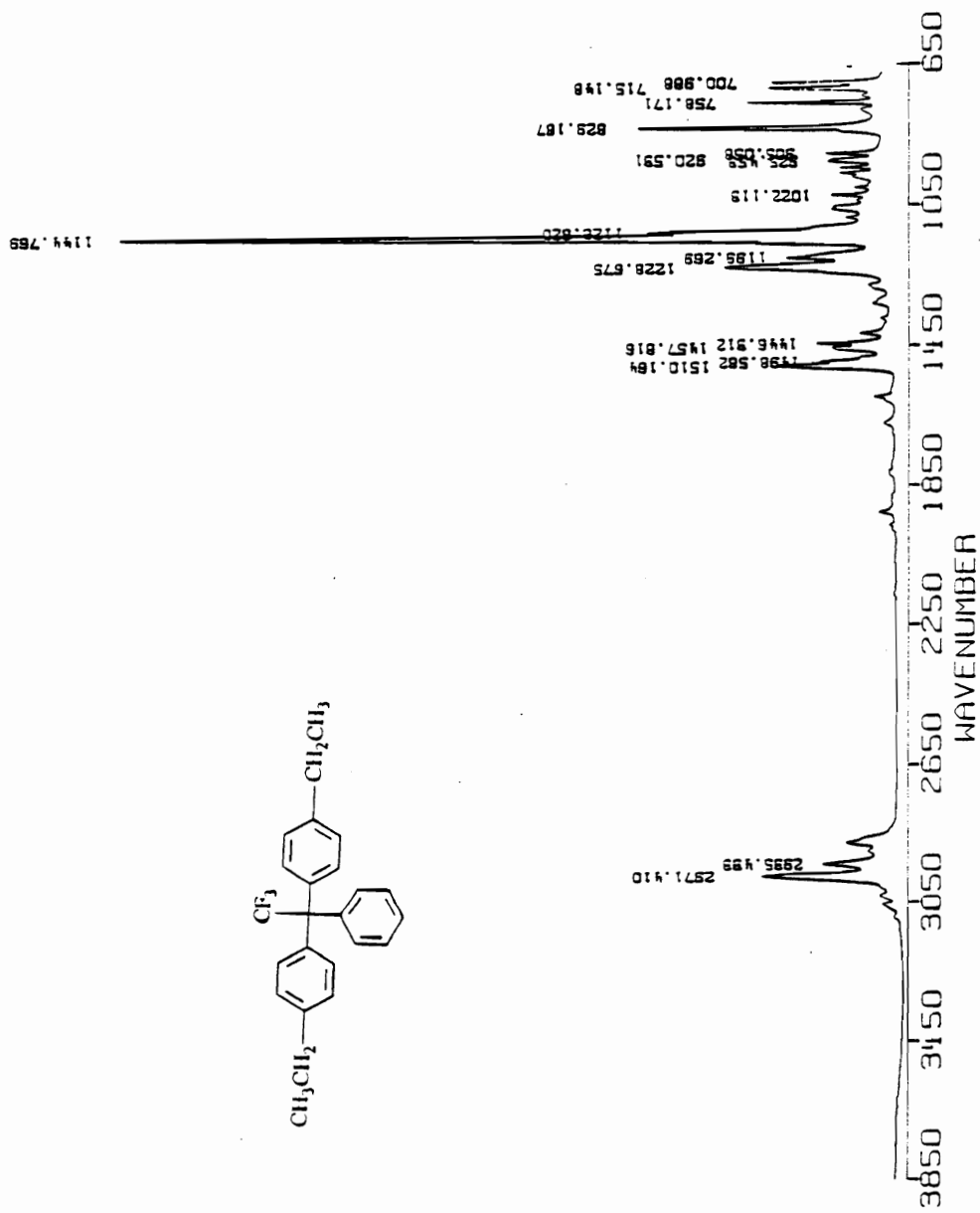


Figure 26. IR spectrum of 1,1-bis(4-ethylphenyl)-1-phenyl-2,2,2-trifluoroethane.

lized from 500 mL of methanol-water solution (90/10), and filtered. Drying (50°C/5 torr) for 18 hours gave 48 g (48%) of white solid mp 97°C (lit. 92-93°C) (148)).

The proton and carbon NMR spectra, the mass spectrum and infrared spectrum are shown in Figures 27-30.

#### 4.2.18 1,1-Bis(4-bromo-4-phenoxyphenyl)-1-phenyl-2,2,2-trifluoroethane

To a 1-L three-necked flask equipped with an addition funnel, thermometer, stirrer, and a condenser fitted with a gas inlet tube, a mixture of 200 g (0.8 mol) of 4-bromodiphenyl ether and 27.8 g (0.16 mol) of trifluoroacetophenone was added under an atmosphere of dry nitrogen. Over a period of one hour, 24.0 g (0.16 mol) of trifluoromethanesulfonic acid was added such that the temperature did not rise above 45°C. After stirring for 2.5 hours following addition, the reaction became a solid cake which could not be stirred. The reaction cake was broken up and stirred with 150 mL of water. The water was poured off and the residue was added to 3-L of methanol with stirring to produce a white granular product. The granules were filtered through a coarse glass frit. Drying (60°/5 torr) gave 98.0 g (93%) of white solid, mp 149-149.5°C.

The proton and carbon NMR spectra, the mass spectrum and infrared spectrum are shown in Figures 31-34.

#### 4.2.19 1,1-Bis(4-phenoxyphenyl)-1-phenyl-2,2,2-trifluoroethane

To a 2-L three-necked flask equipped with a stirrer, an addition funnel, thermometer, and a condenser fitted with a gas inlet tube, a mixture of 60 g (0.344 mol) of trifluoroacetophenone and 300 g (1.17 mol) of diphenyl ether was added under an atmosphere of dry nitrogen. Over a period of two hours, 50 g (0.33 mol) of trifluoromethanesulfonic acid was added at a rate that did not allow the reaction mixture to exceed 40°C.



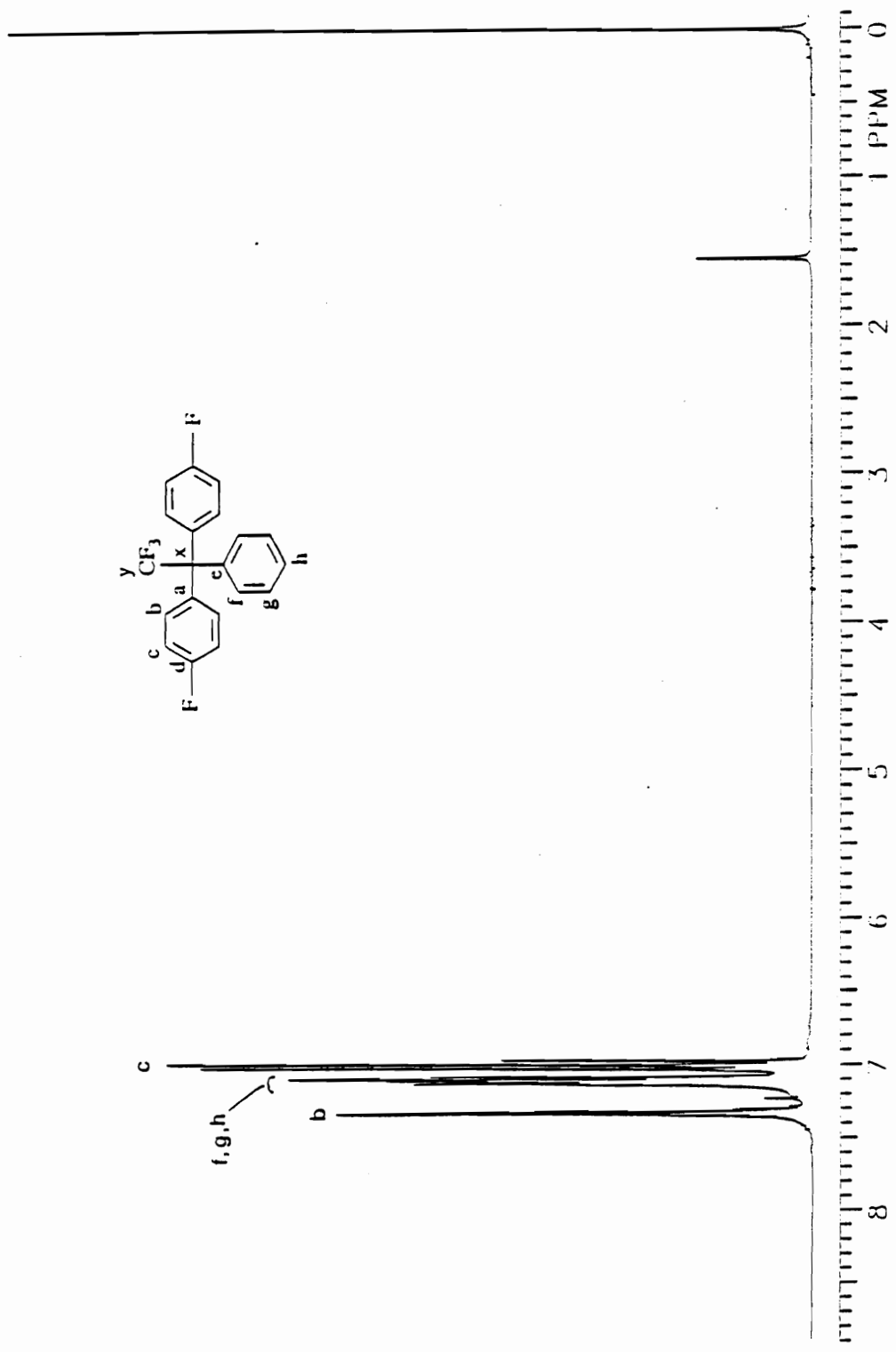


Figure 27. <sup>1</sup>H NMR spectrum of 1,1-bis(4-fluorophenyl)-2,2,2-trifluoroethane.

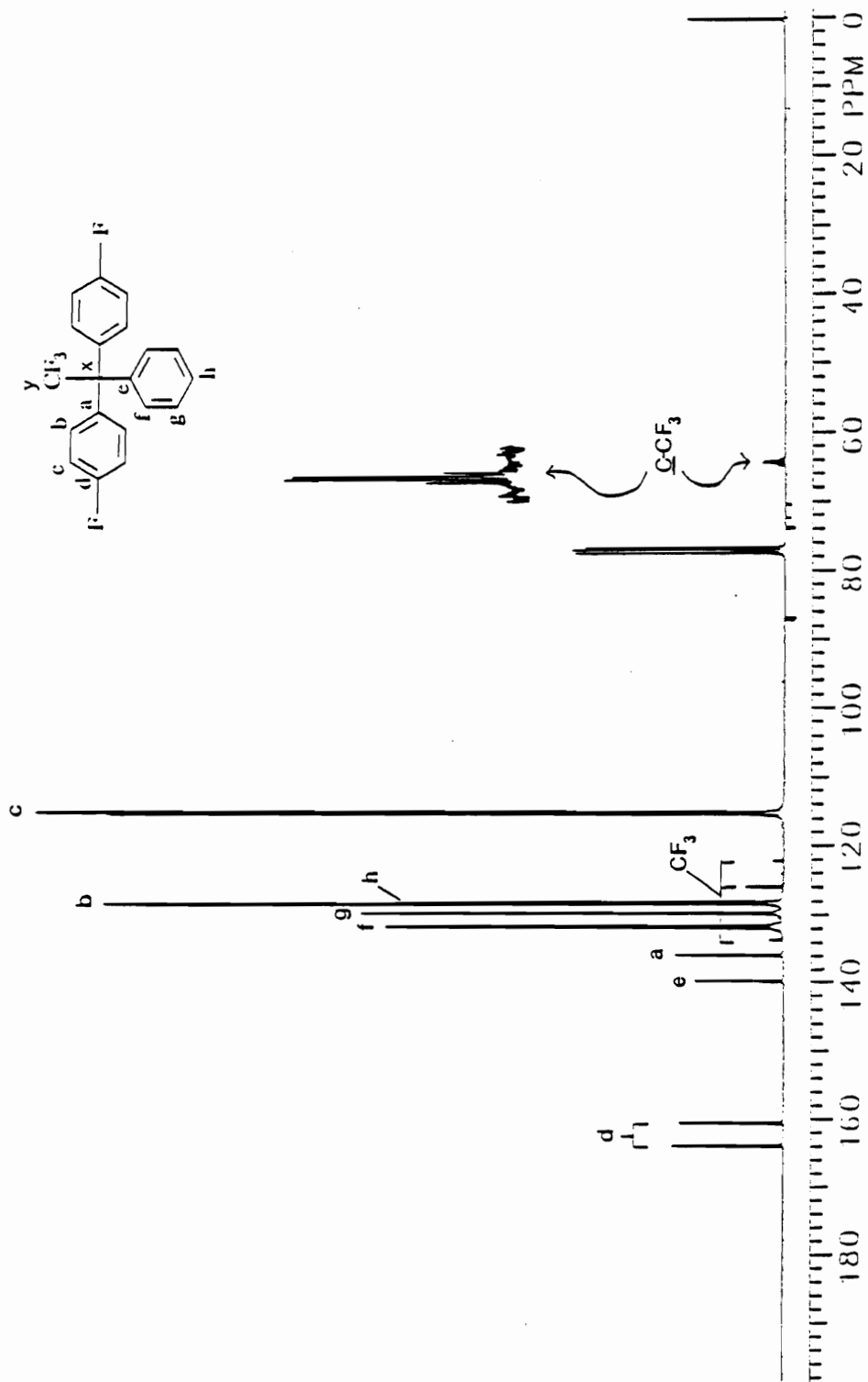


Figure 28.  $^{13}\text{C}$  NMR spectrum of 1,1-bis(4-fluorophenyl)-1-phenyl-2,2,2-trifluoroethane.

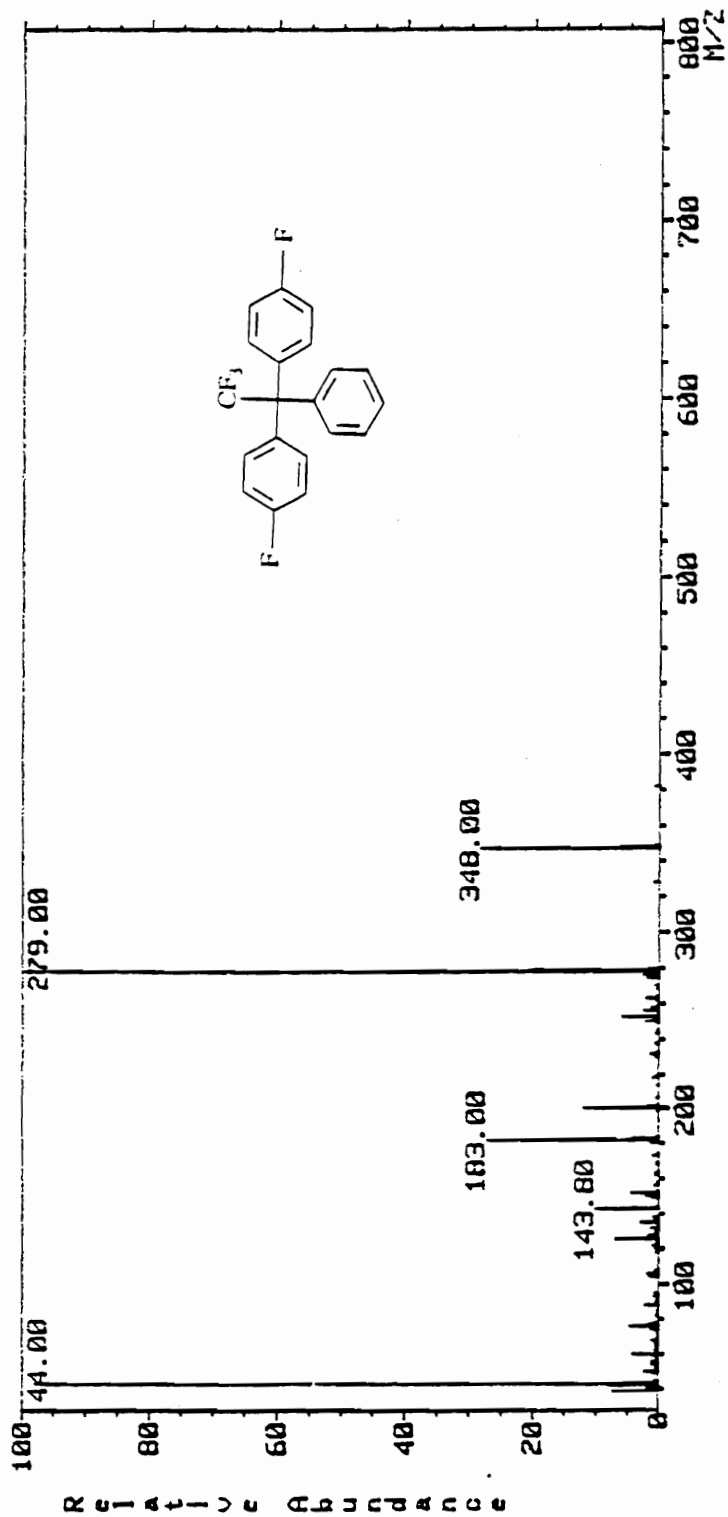


Figure 29. Mass spectrum (EI) of 1,1-bis(4-fluorophenyl)-1-phenyl-2,2,2-trifluoroethane.

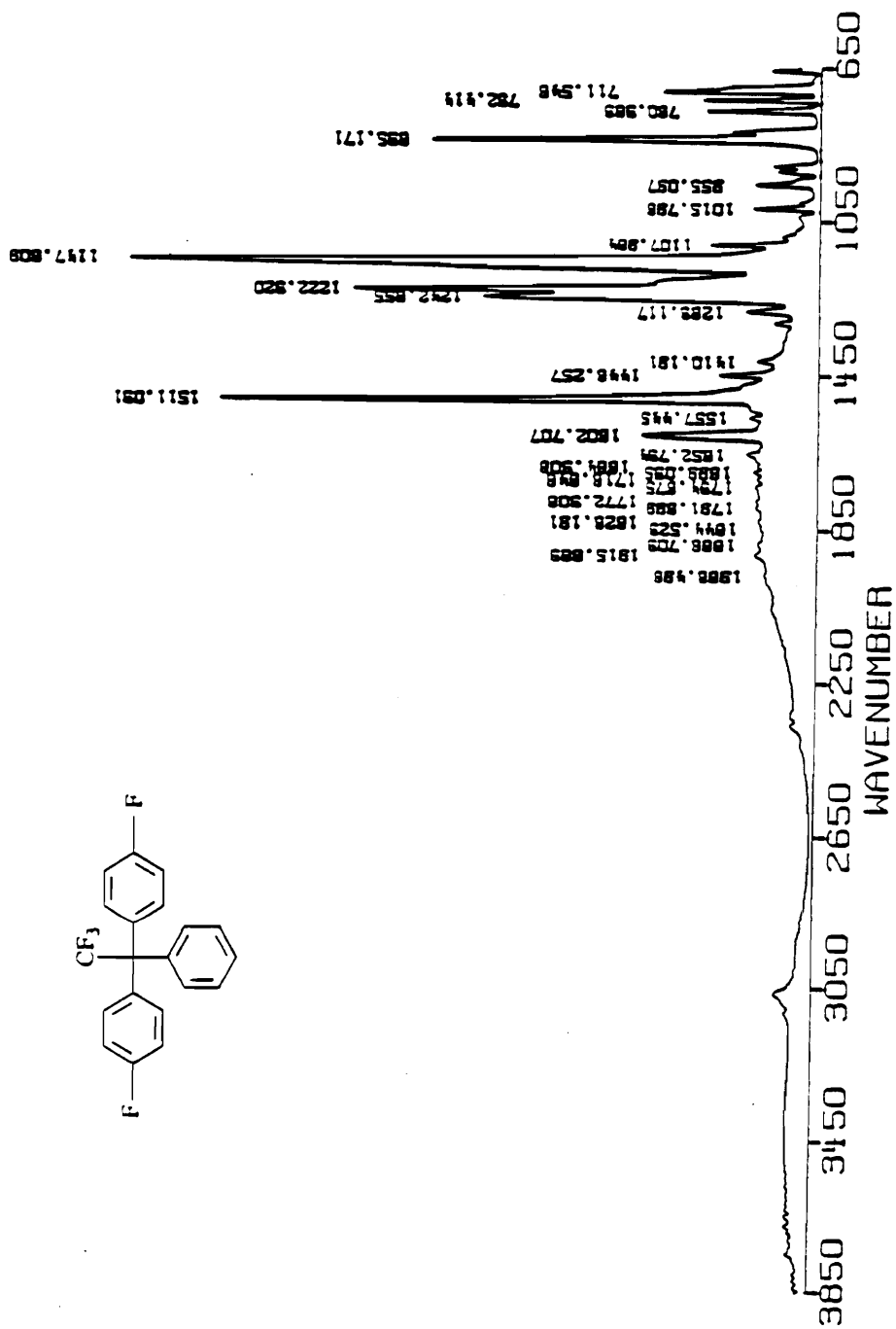


Figure 30. IR spectrum of 1,1-bis(4-fluorophenyl)-1-phenyl-2,2,2-trifluoroethane.

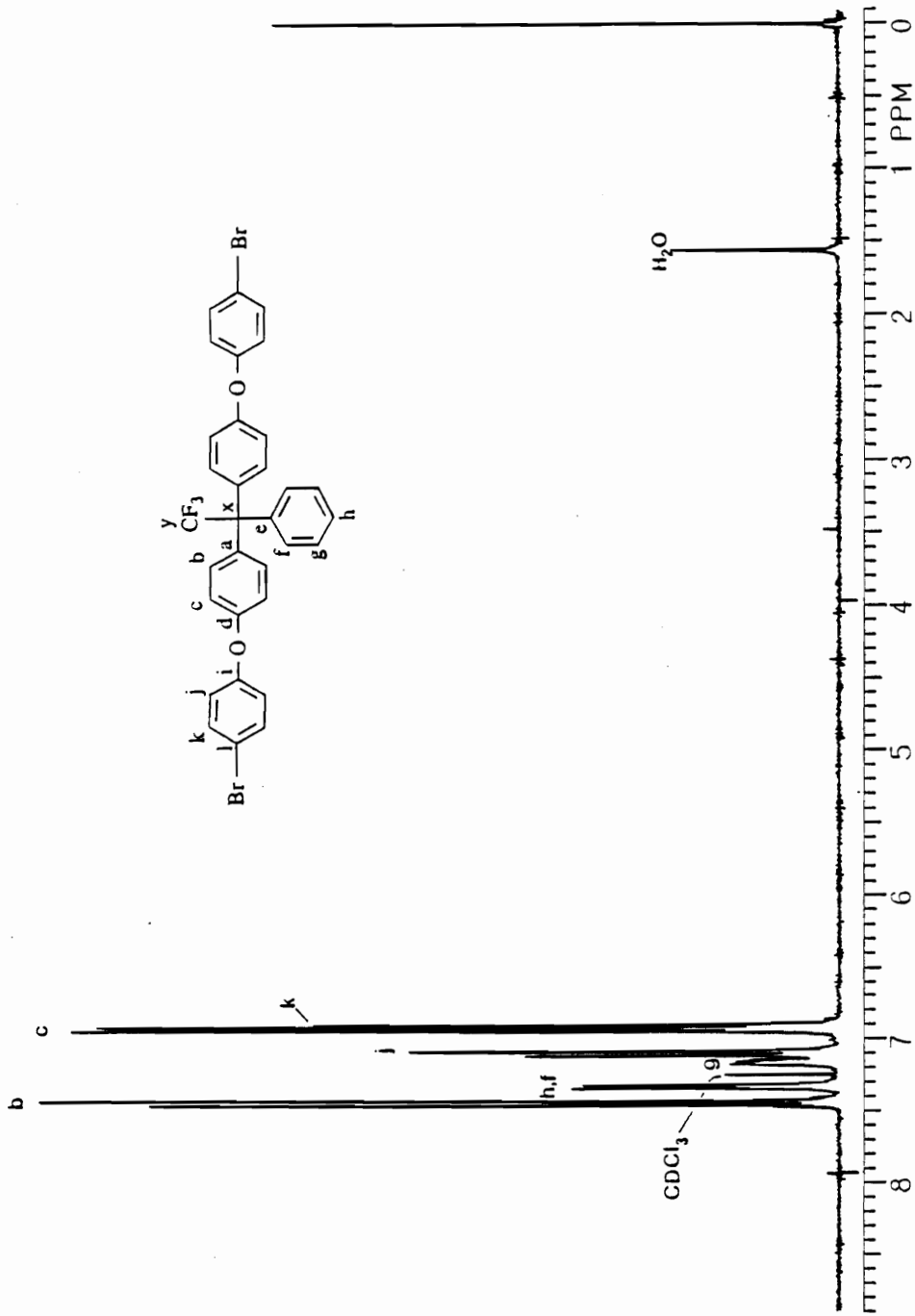


Figure 31. <sup>1</sup>H NMR spectrum of 1,1-bis[4-(4-bromophenoxy)phenyl]-1-phenyl-2,2,2-trifluoroethane.

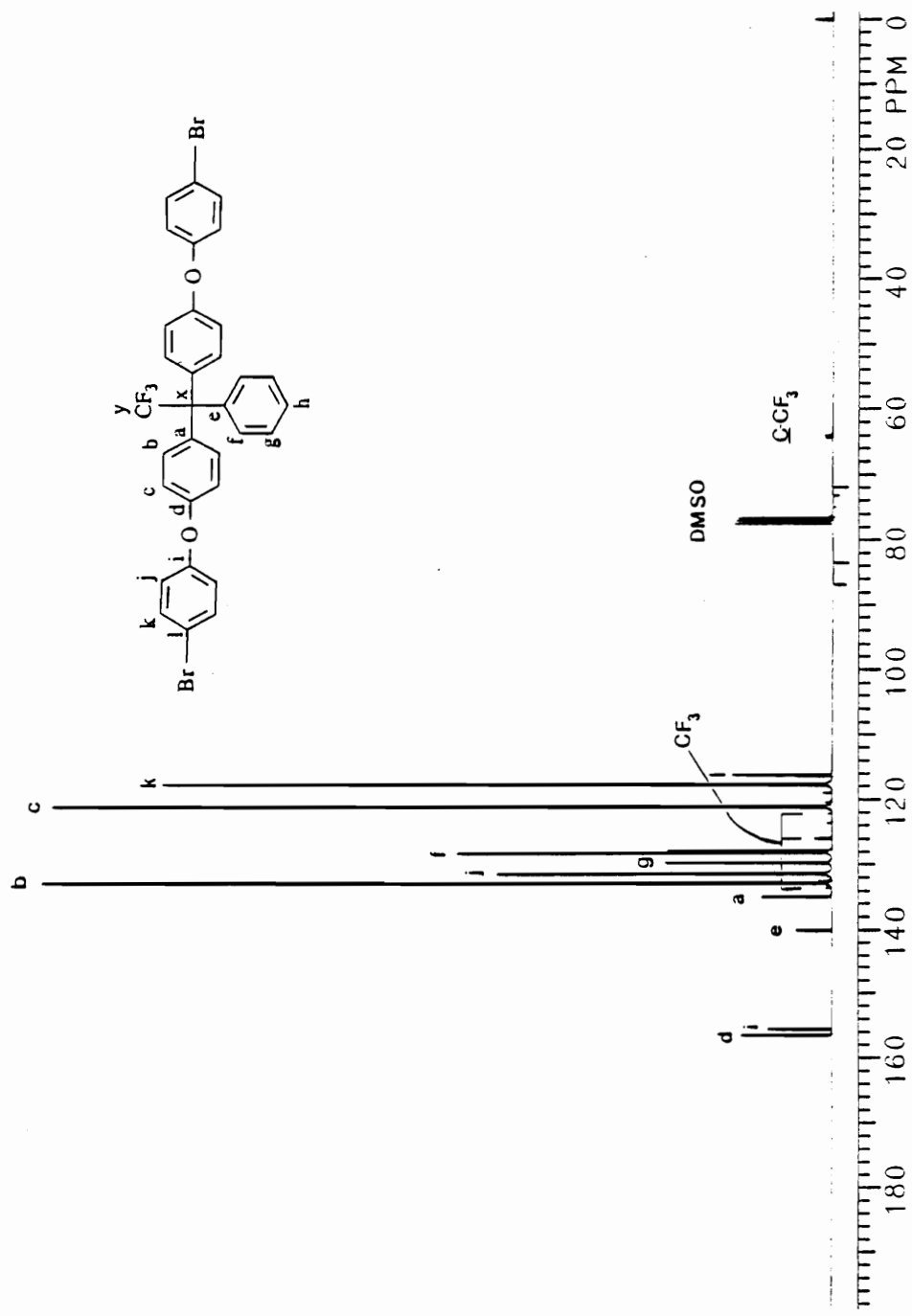


Figure 32. <sup>13</sup>C NMR spectrum of 1,1-bis[4-(4-bromophenoxy)phenyl]-1-phenyl-2,2,2-trifluoroethane.

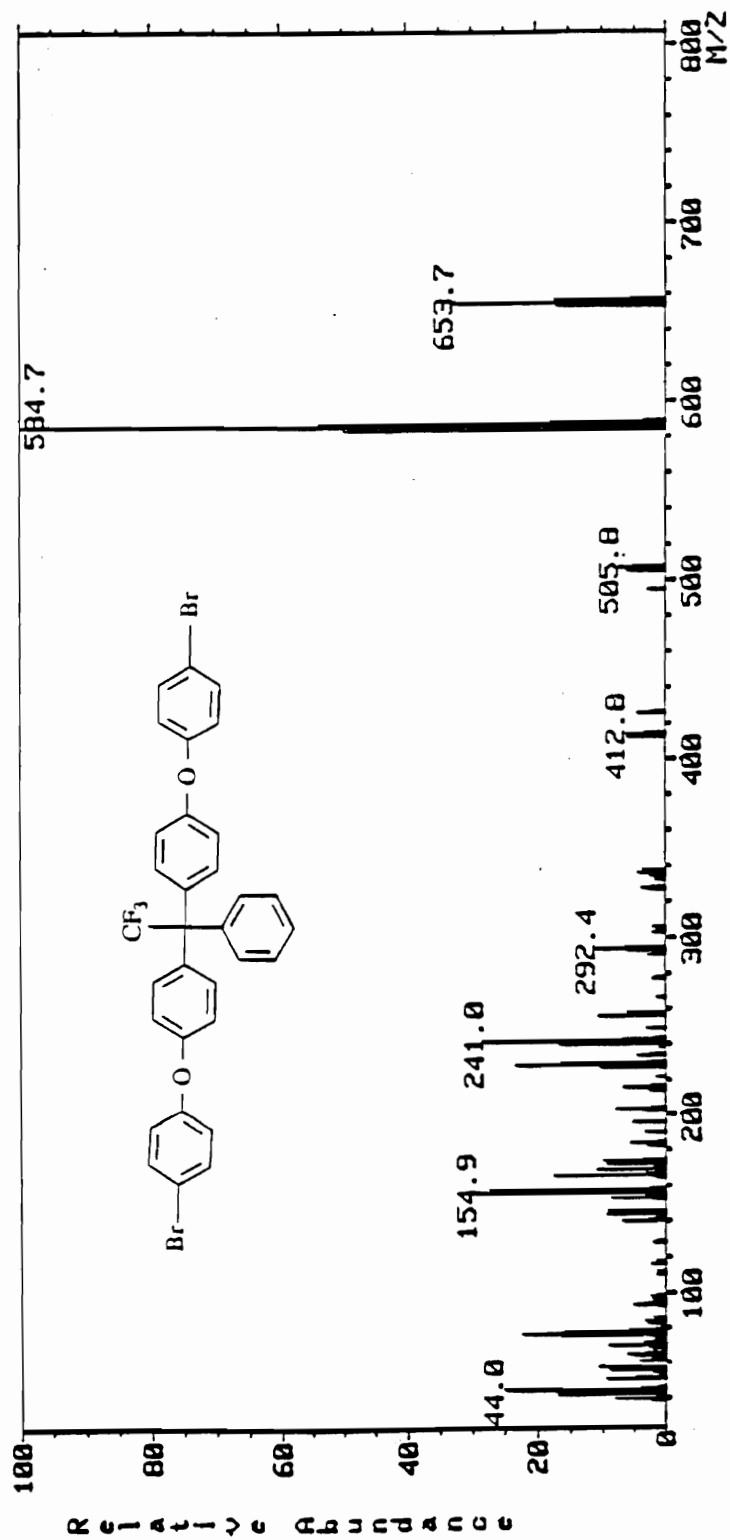


Figure 33. Mass spectrum (EI) of 1,1-bis[4-(4-bromophenoxy)phenyl]-1-phenyl-2,2,2-trifluoroethane.

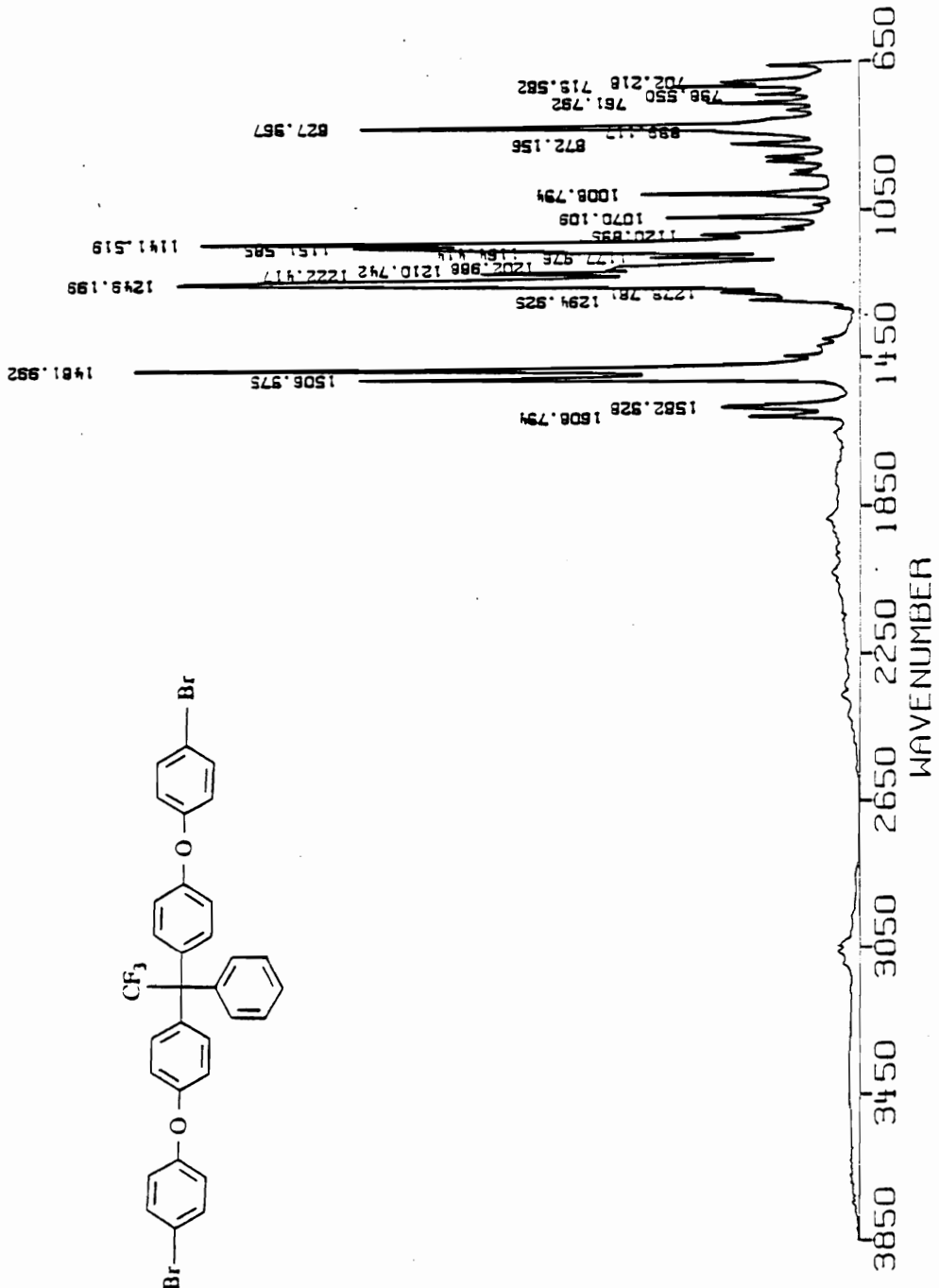


Figure 34. IR spectrum of 1,1-bis[4-(4-bromophenoxy)phenyl]-1-phenyl-2,2,2-trifluoroethane.



After addition, the mixture was allowed to stir at room temperature for seven hours. The mixture was transferred to a separatory funnel and extracted with three 300 mL portions of water, three 150 mL portions of aqueous saturated sodium bicarbonate, and a final three 150 mL portions of water. The organic phase was separated, dried over anhydrous magnesium sulfate and filtered. The volatile components were removed at 60°C and 100 torr to yield a waxy solid. The solid was dispersed with rapid stirring into four liters of 95% ethanol and the particles were allowed to settle for eighteen hours. The white solid was filtered. Drying (50°C/5 torr) for 24 hours gave 124.2 g (72%) of white solid, mp 111-111.5° (lit. mp 109-110°C) (148).

The proton and carbon NMR spectra, the mass spectrum and the infrared spectrum are shown in Figures 35-38.

#### 4.2.20 Perfluoroacetophenone

A 500 mL four-necked jacketed Grignard flask was equipped with a mechanical stirrer, reflux condenser, pressure equalized addition funnel, and nitrogen inlet adapter and coupled to a 1-L four-necked flask equipped with a magnetic stirrer, a nitrogen inlet, and a low temperature thermometer. This system was oven dried at 110°C for 24 hours and assembled under a flow of dry nitrogen. Magnesium turnings (3.06g, 0.126 mol) were placed in the upper flask and the system was further dried with an electrical heat gun under a flow of dry nitrogen. Ether (25 mL) was added and bromopentafluorobenzene (25.2.4g, 0.102 mol) was placed in the addition funnel with sufficient ether to obtain a total volume of 60 mL. The condenser was cooled with water from a refrigerated circulating bath held at 10°C. A single crystal of iodine was added to the upper flask and bromopentafluorobenzene solution was added slowly with stirring. The iodine color disappeared immediately. Addition was carried out at a rate sufficient to maintain

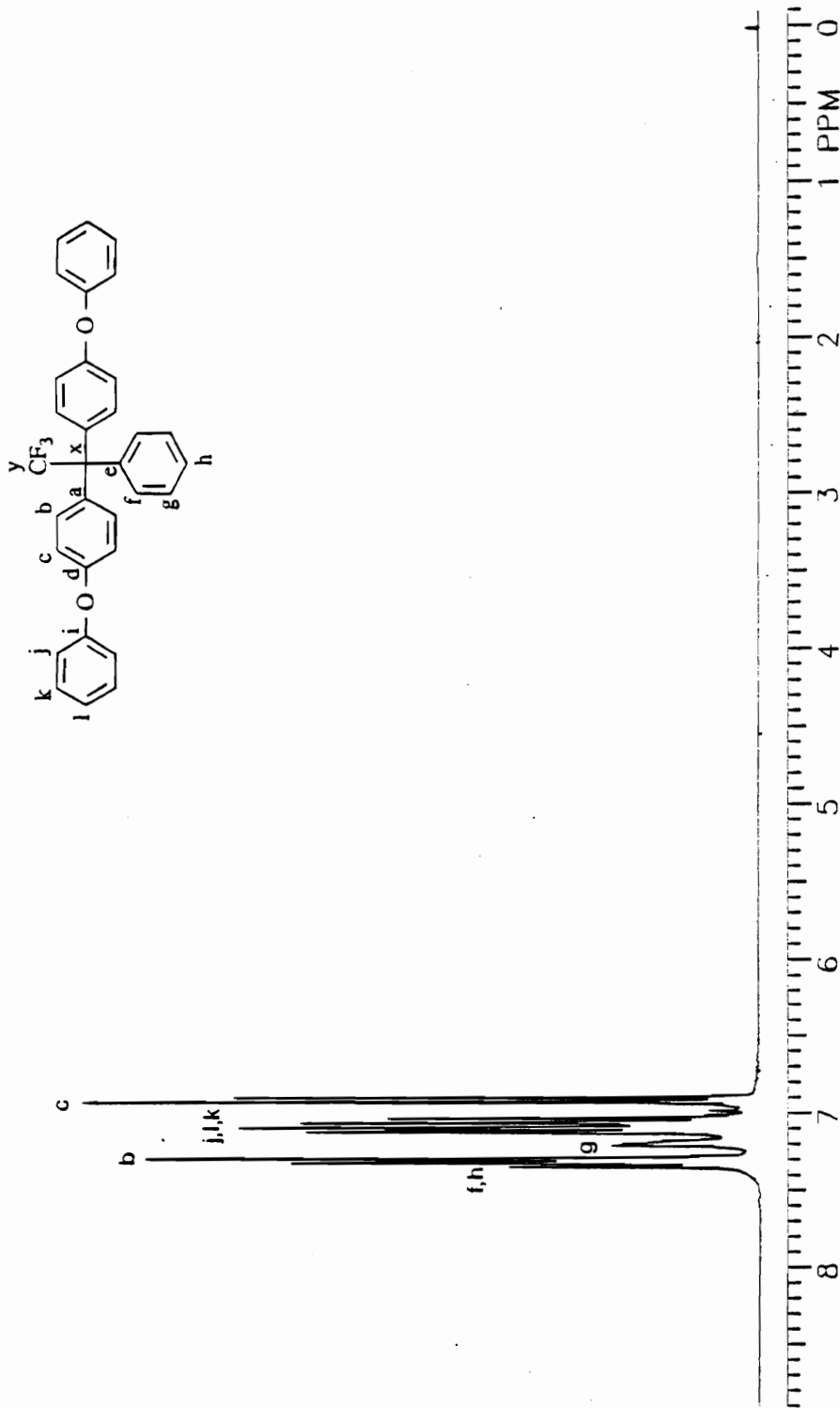


Figure 35. <sup>1</sup>H NMR spectrum of 1,1-bis(4-phenoxyphenyl)-1-phenyl-2,2,2-trifluoroethane.

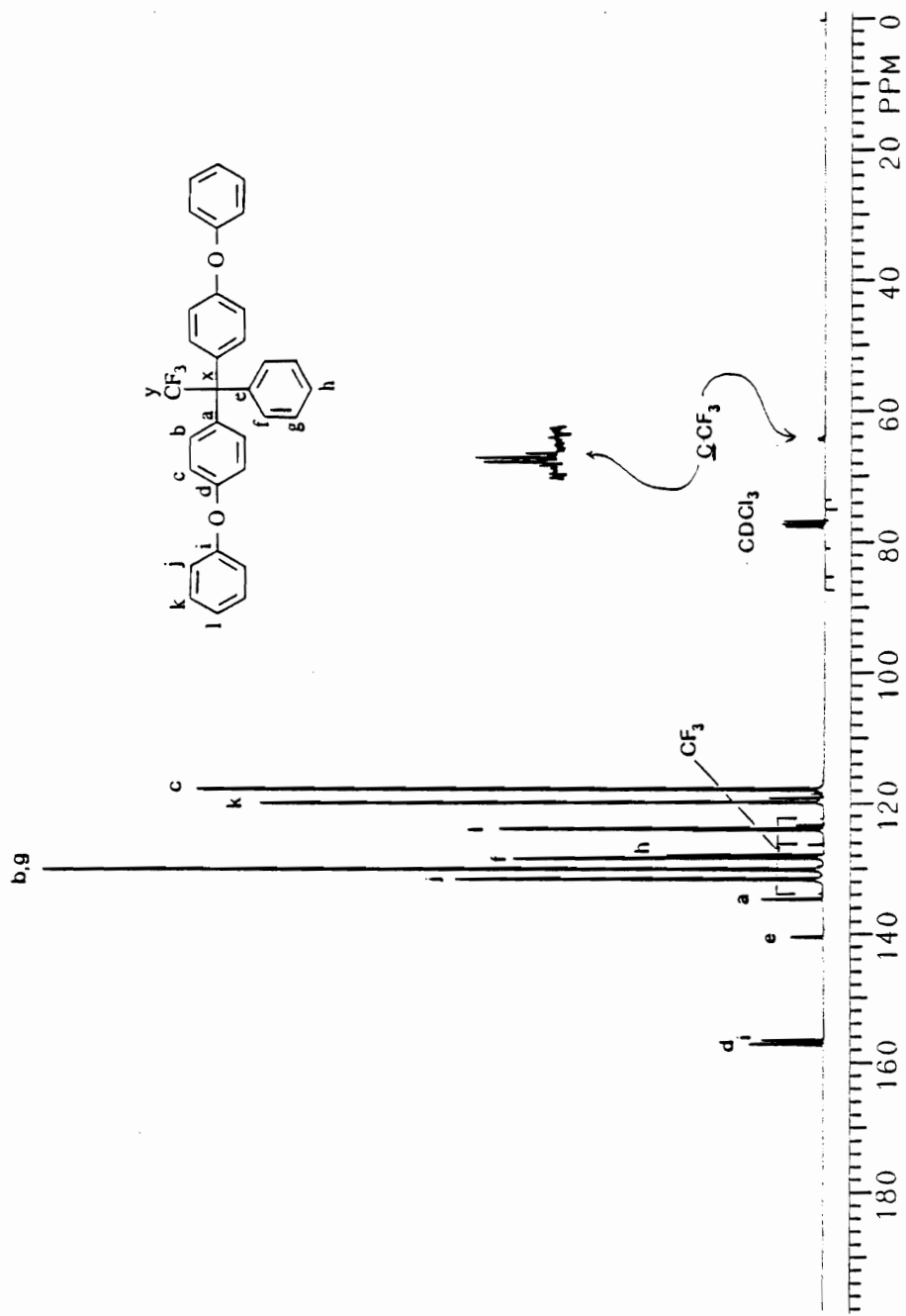


Figure 36.  $^{13}\text{C}$  NMR spectrum of 1,1-bis(4-phenoxyphenyl)-1-phenyl-2,2,2-trifluoroethane.

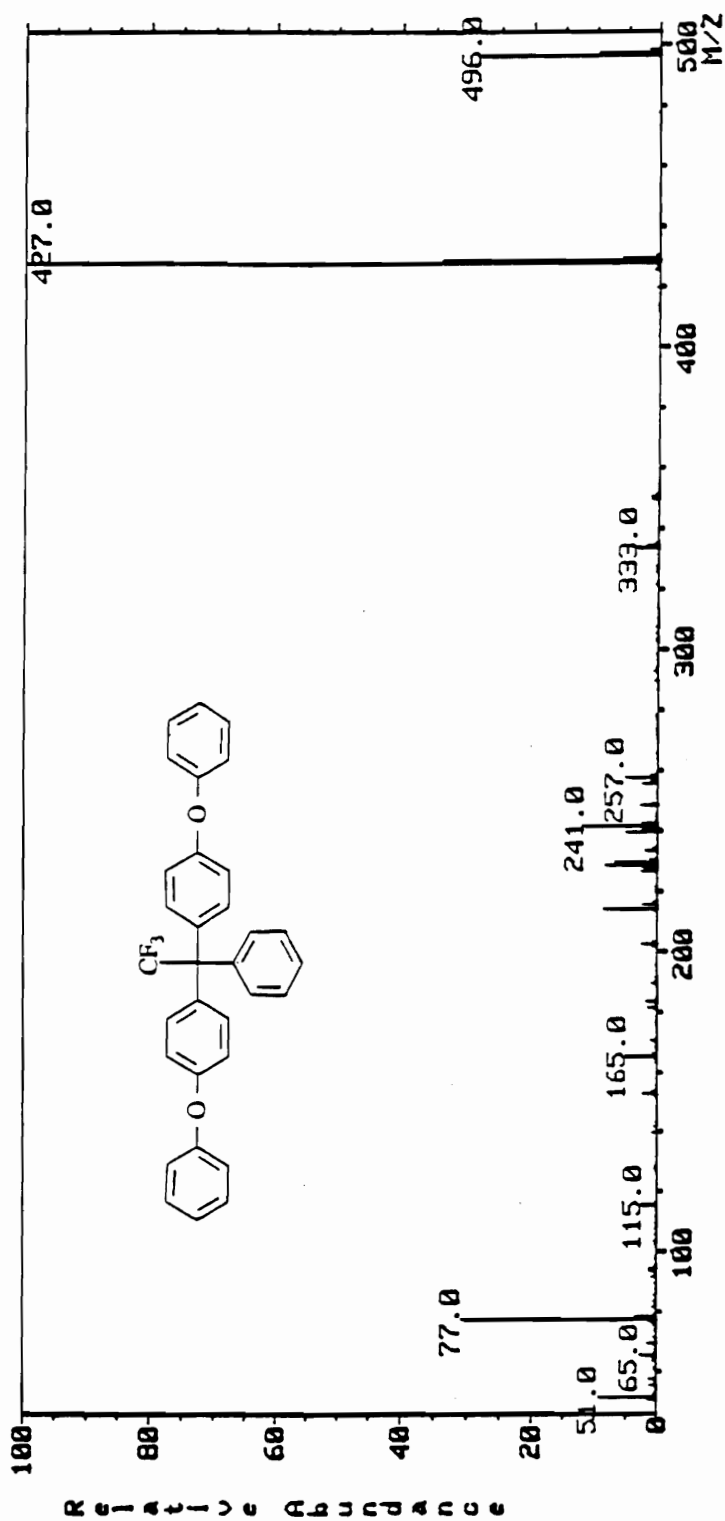


Figure 37. Mass spectrum (EI) of 1,1-bis(4-phenoxyphenyl)-1-phenyl-2,2,2-trifluoroethane.

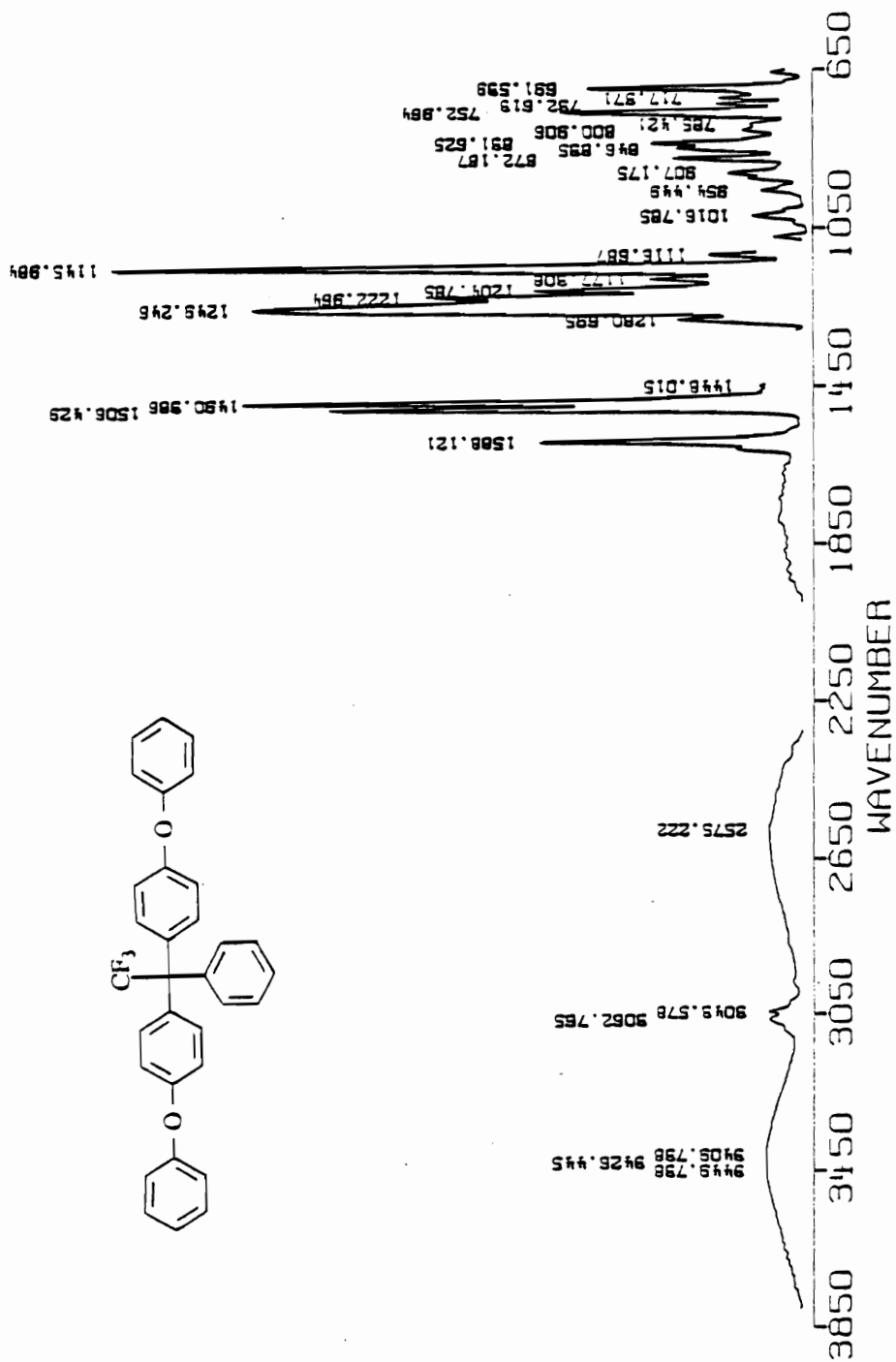


Figure 38. IR spectrum of 1,1-bis(4-phenoxyphenyl)-1-phenyl-2,2,2-trifluoroethane.

a gentle reflux. As the reaction progressed, the mixture became black. After addition, the reaction was stirred for approximately 45 minutes.

Lithium trifluoroacetate (14.24 g, 0.119 mol) was placed in the lower flask along with 250 mL of ether. This mixture was cooled to 0°C under nitrogen with stirring. The solution in the upper flask was then added dropwise to the lower flask. The reaction mixture was stirred for one hour and then allowed to warm to 10°C.

The upper flask was then removed and the lower flask was fitted with a reflux condenser and a pressure equalized addition funnel. Two hundred mL of 10% hydrochloric acid was added via the addition funnel. The mixture was stirred for 30 minutes and then transferred to a separatory funnel. The phases were separated and 250 mL of ether was added to the organic phase. This ethanol solution was then washed successively with two 200 mL portions of water, and two 200 mL portions of half-saturated sodium bicarbonate solution. The ethanol solution was then dried over magnesium sulfate, filtered, and the ether solvent removed by careful distillation through a three inch Vigreux column and a total reflux head. The remaining residual ether was removed by distillation through a 9 inch Vigreux column and a total reflux head. Distillation of the residue (19.74g, 73% crude yield) through a short path still gave 8.04 g of product, bp 79°C to 125°C. Redistillation through a short path still gave 7.28 g (26.9%) of product, b.p. of 127 - 131°C (lit. b.p. 130-131°C) (150)). The carbon NMR is shown in Figure 39.

#### 4.2.21 1,1-Bis(4-hydroxyphenyl)-1-pentafluorophenyl-2,2,2-trifluoroethane

Octafluoroacetophenone (5.61g, 0.02 mol), phenol (7.87g, 0.08 mol), 4 mL of 1,2-dichloroethylene, and 0.1g of anhydrous calcium chloride were stirred in a 100 mL reaction kettle equipped with a thermometer, an addition funnel, and a nitrogen

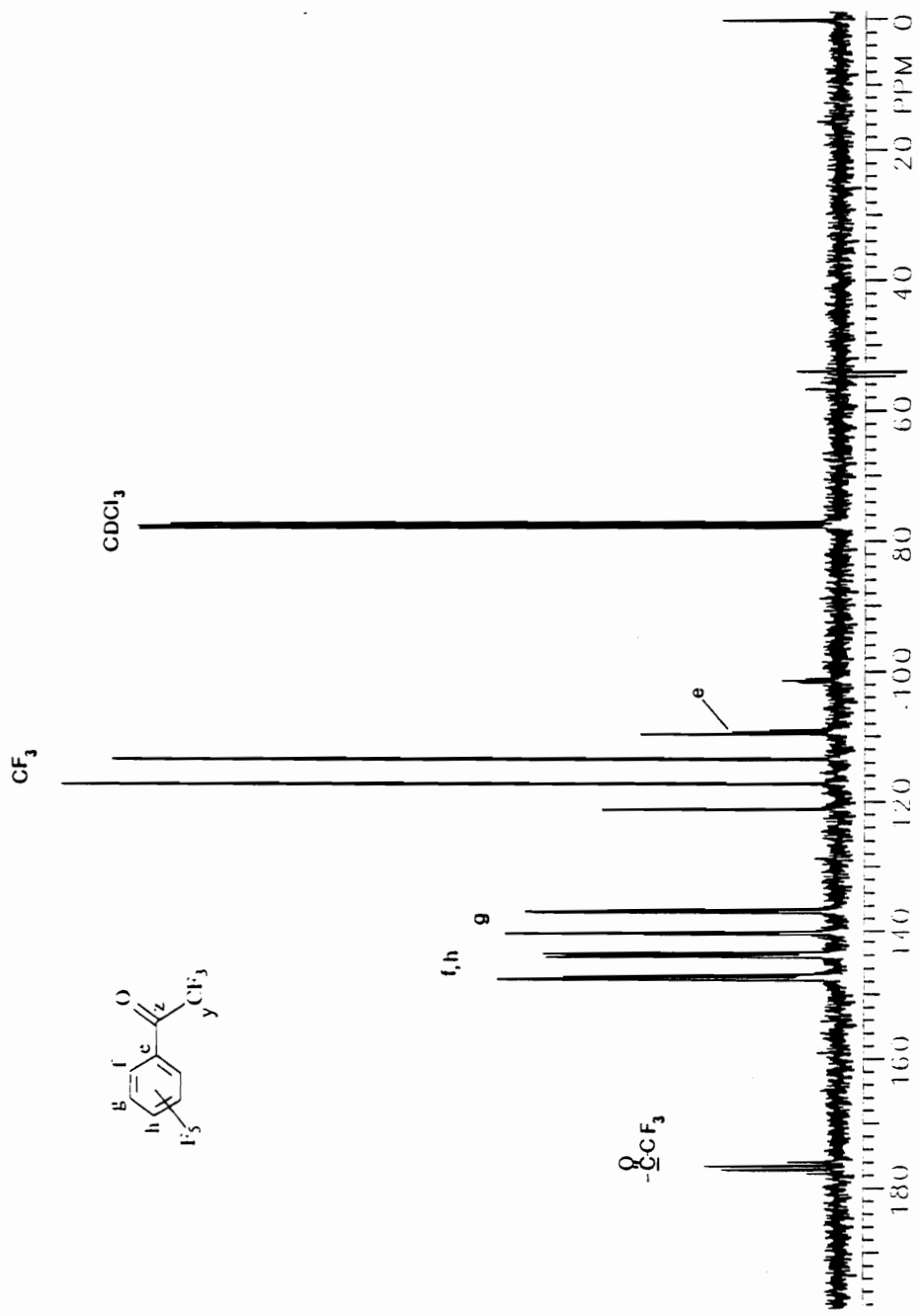


Figure 39.  $^{13}\text{C}$  NMR spectrum of perfluoroacetophenone.

inlet. After flushing with nitrogen for 10 minutes, trifluoromethanesulfonic acid (2.84g, 0.02 mol) was added dropwise over a period of 10 minutes. After addition, the reaction mixture was heated at 45°C for four hours. After cooling to room temperature, the reaction mixture was dispersed with rapid stirring in 600 mL of water. The granular product was filtered, and washed with five 100 mL portions of boiling water. It was then dried at 55°C and 0.1 torr to yield a waxy solid which melted at 175-177°C. Recrystallization from chloroform gave a white crystalline solid (3.60 g, 39.1%) mp 192-193°C. An additional recrystallization did not change the melting point. The proton and carbon NMR spectra, the mass spectrum, and infrared spectrum are shown in Figures 40-43.

#### 4.3 RESULTS AND DISCUSSION

The basic route chosen for the synthesis of monomers of the 1,1,1-triaryl-2,2,2-trifluoroethane type is that just reported by Kray and Rosser (122) in 1977. Various triaryl-2,2,2-trifluoroethanes were reportedly prepared from 2,2,2-trifluoroacetophenone by condensation of aromatic compounds under highly acidic conditions to yield the corresponding 1,1,1-triaryl-2,2,2-trifluoroethanes. Using the procedures as specified by Kray and Rosser (122), 1,1-bis(4-aminophenyl)-1-phenyltrifluoroethane was prepared and subjected to preparation conditions for polyimide formation. Low molecular weight brittle polymer films were obtained and attempts to prepare controlled molecular weight polymer failed. The present study addresses modification of the reaction sequence and purification scheme needed to prepare monomer grade diamine. The present study also focuses on the preparation of monomer grade 1,1-bis(4-hydroxyphenyl)-1-phenyl trifluoroethane.



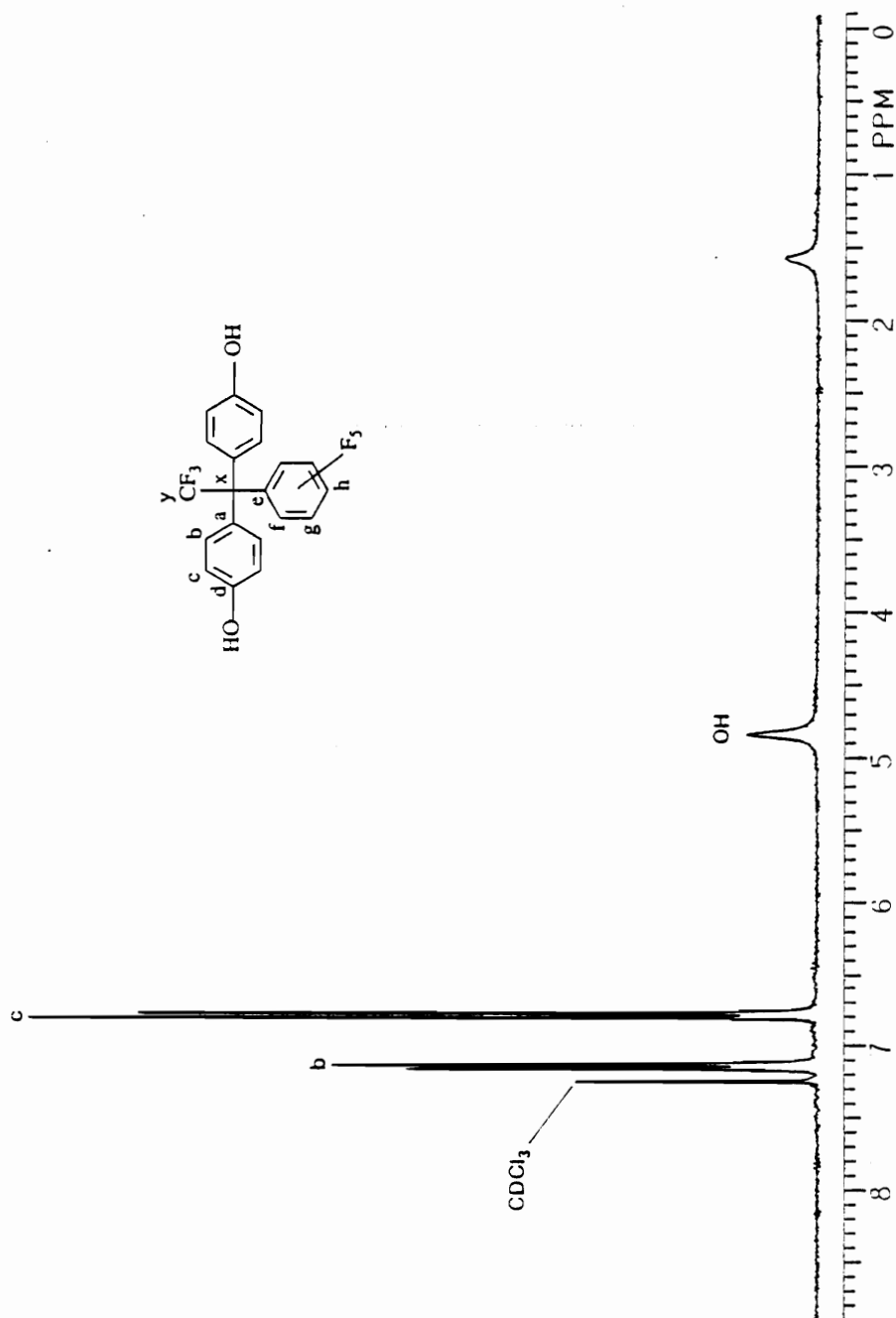


Figure 40.  $^1\text{H}$  NMR spectrum of 1,1-bis(4-hydroxyphenyl)-1-pentafluorophenyl-2,2,2-trifluoroethane.

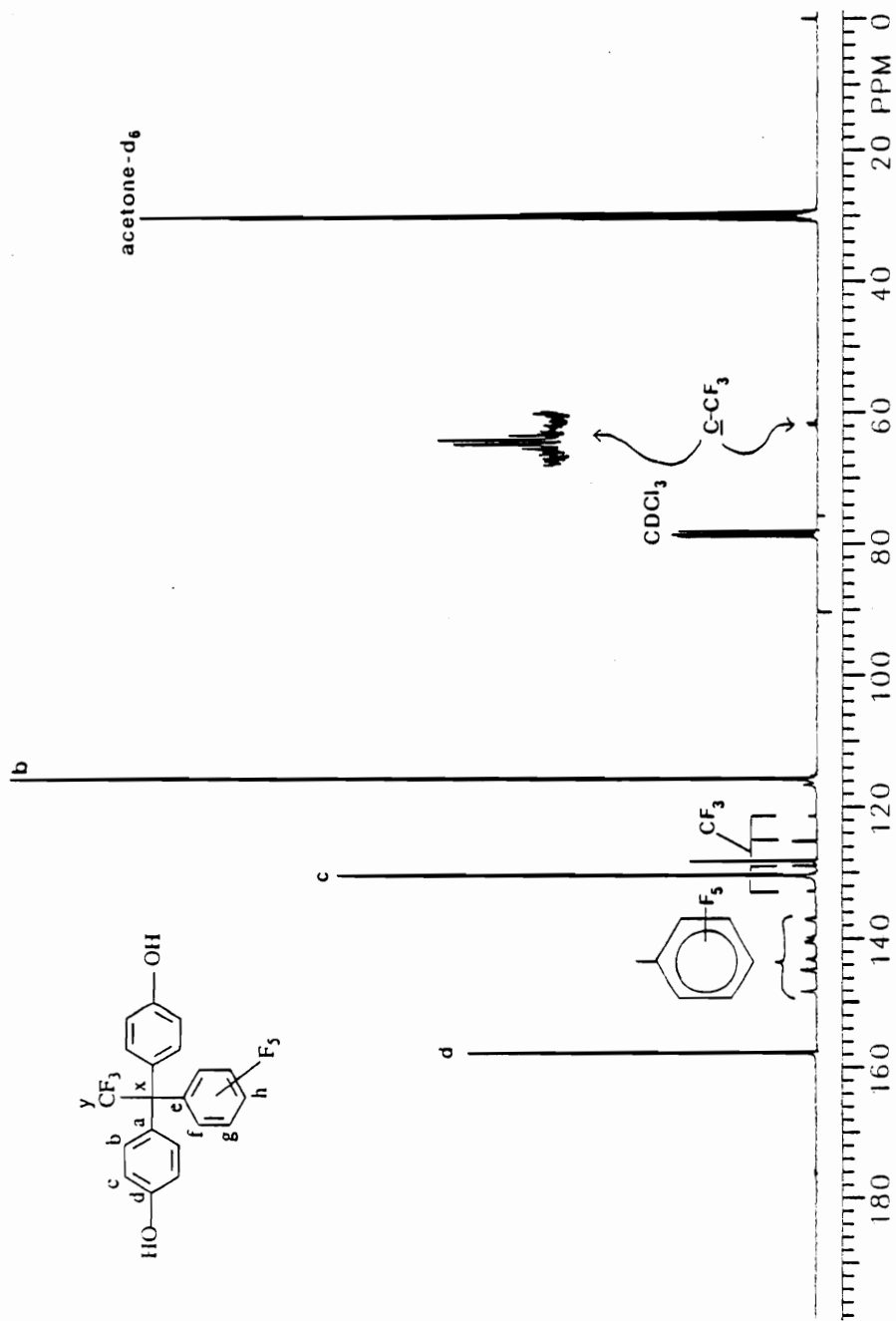


Figure 41.  $^{13}\text{C}$  NMR spectrum of 1,1-bis(4-hydroxyphenyl)-1-pentafluorophenyl-2,2,2-trifluoroethane.

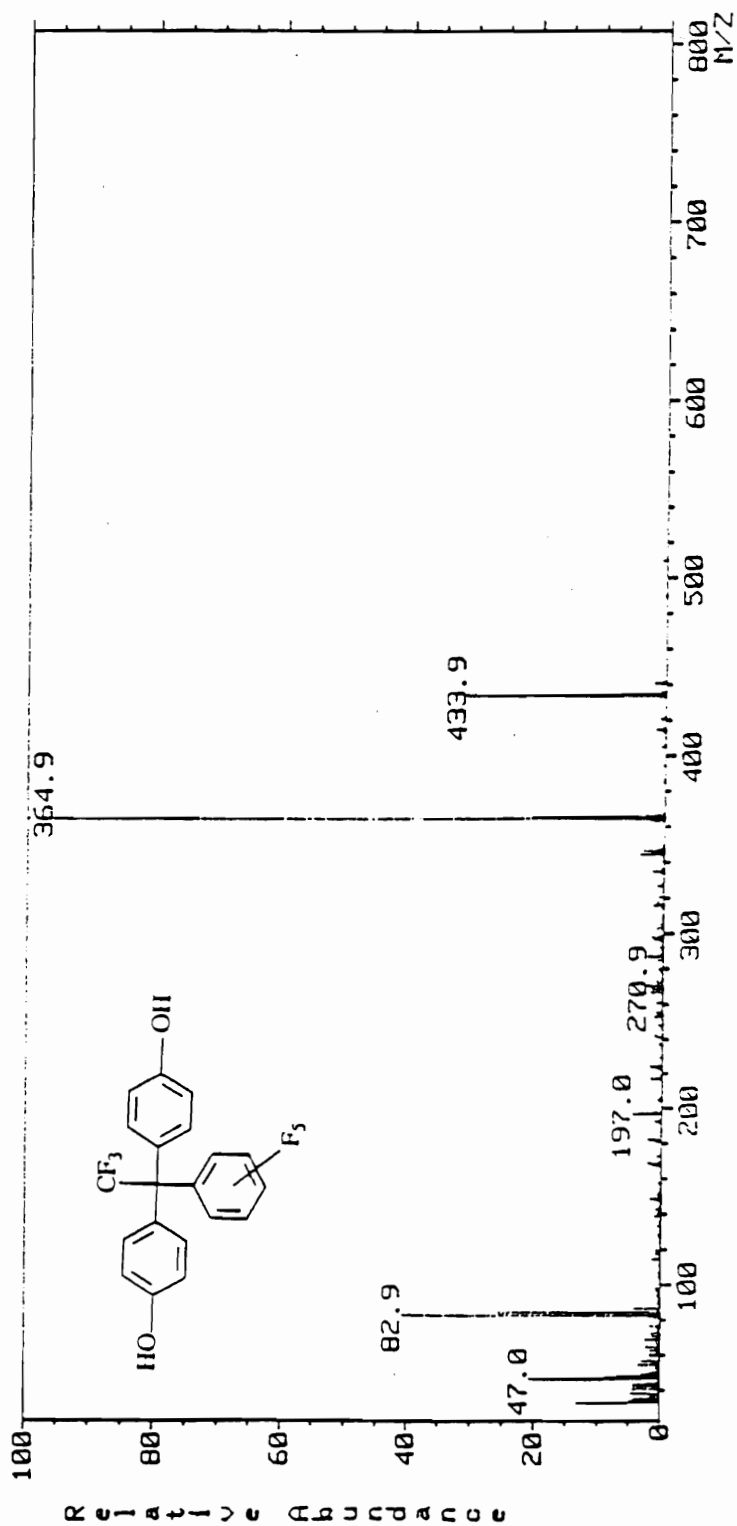


Figure 42. Mass spectrum (EI) of 1,1-bis(4-hydroxyphenyl)-1-pentafluorophenyl-2,2,2-trifluoroethane.

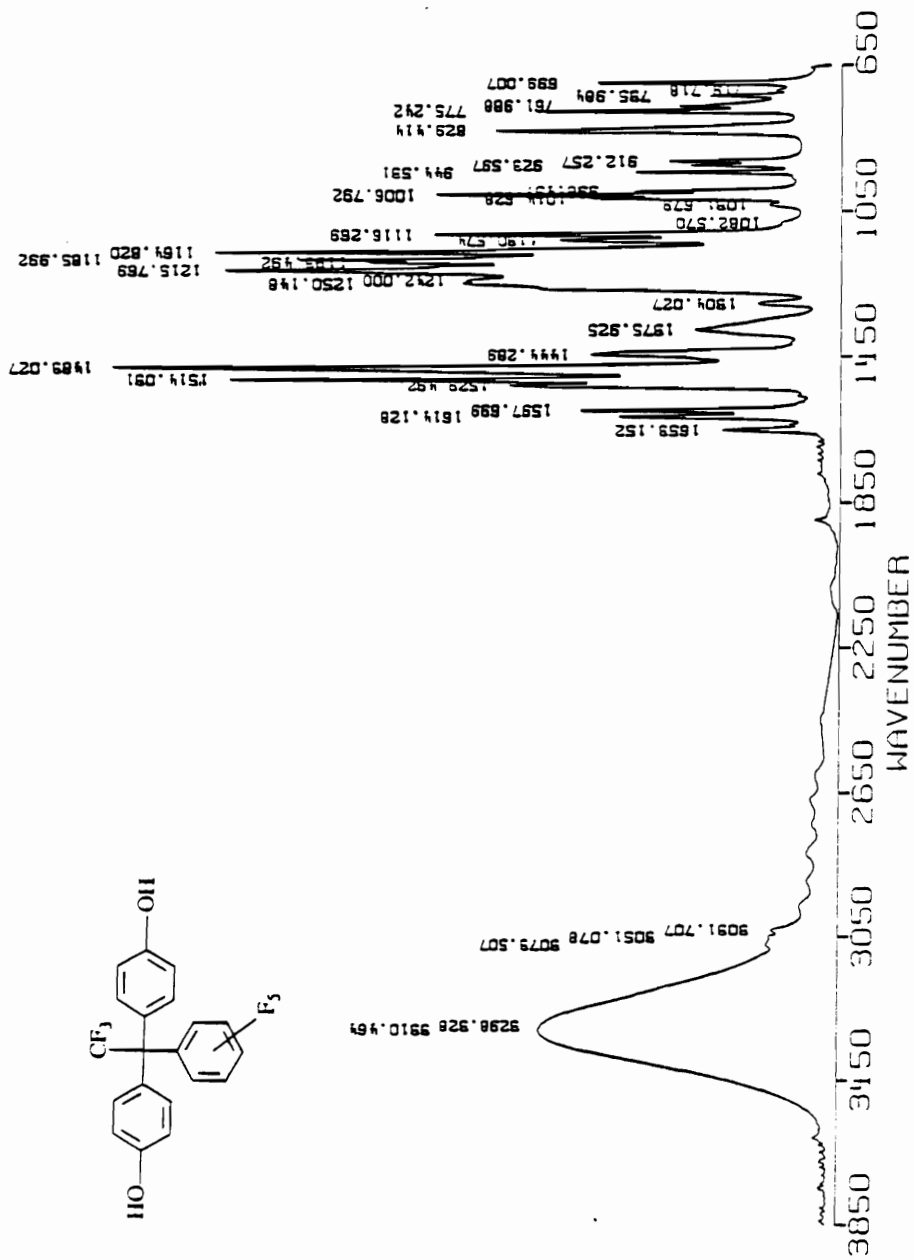


Figure 43. IR spectrum of 1,1-bis(4-hydroxyphenyl)-1-pentafluorophenyl-2,2,2-trifluoroethane.

The basic synthetic methodology is a modified hydroxyalkylation of trifluoroacetophenone. As this ketone is the starting point for all subsequent examples of the targeted 1,1,1-triaryl-2,2,2-trifluoroethanes, a number of synthetic routes for an efficient and economical preparation were explored.

#### 4.3.1 Survey of the Properties and Preparative Techniques of Trifluoromethyl Ketones

In trifluoromethyl ketones, the strong electron-withdrawing nature of the trifluoromethyl group alters the properties of the carbonyl group (147). The trifluoromethyl group also significantly reduces the basicity of the carbonyl group. Trifluoroacetone and acetone differ in proton affinity by 17Kcal/mol (152). This effect reduces protonation or complexation of fluoroketones by soft Lewis acids or metal cations. This also enhances the reactivity of the ketone towards nucleophiles. The ability of fluorinated ketones to form stable hydrates in aqueous media illustrates the enhanced stability of the tetrahedral adduct between a nucleophile and the carbonyl group (153-155). This observation can be explained as a stabilization of the anionic tetrahedral intermediate by the electron-withdrawing trifluoromethyl group which reduces the reversibility of the nucleophilic addition (157,158).

The synthesis of fluoroketones has made extensive use of the reaction between organometallic reagents and trifluoroacetic acid derivatives. The limiting factor in this approach is the availability and cost of the organometallic reagents and the formation of secondary and tertiary alcohols as by-products. Tamborski *et al.* (159) has shown that the subsequent formation of product and by-products is governed by the stability of the initial tetrahedral adduct of the organometallic reagent as shown in Figure 44. In some cases, the stability of this intermediate is dependent on the nature of the substituents and the reaction conditions. These observations explain the many

low yields and the large distribution of reaction products reported. The intermediate is sufficiently stable to be isolated or trapped as shown in Figure 45. The products which have been frequently reported since the first pioneering work in the 1950's are shown in Figure 45 (160-166).

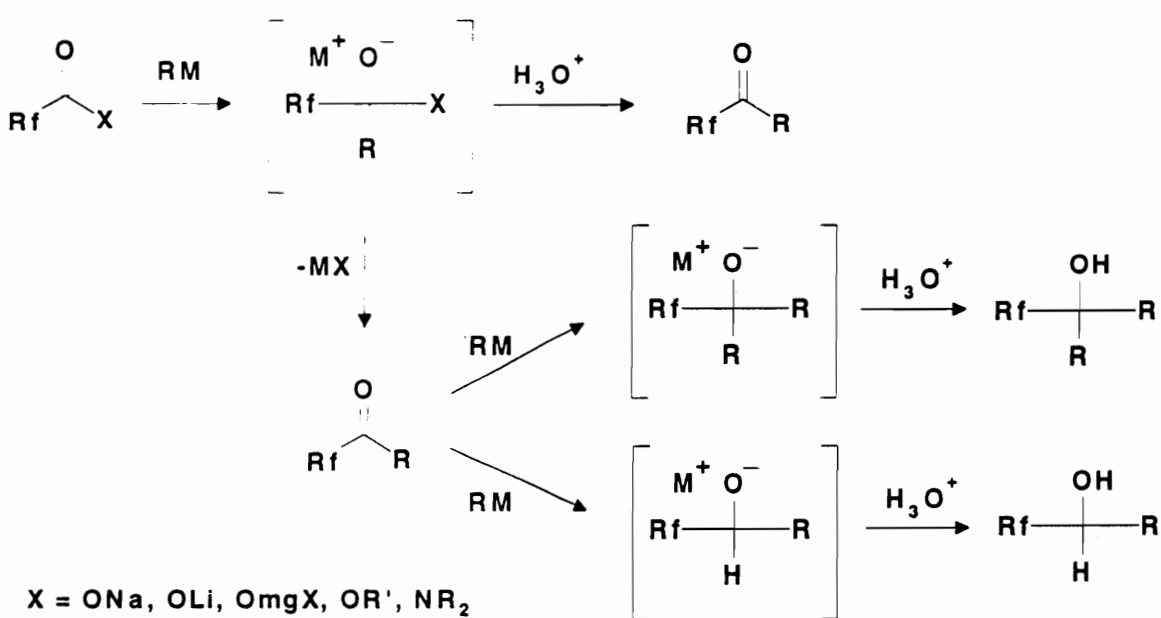


Figure 44. Stable tetrahedral intermediate.

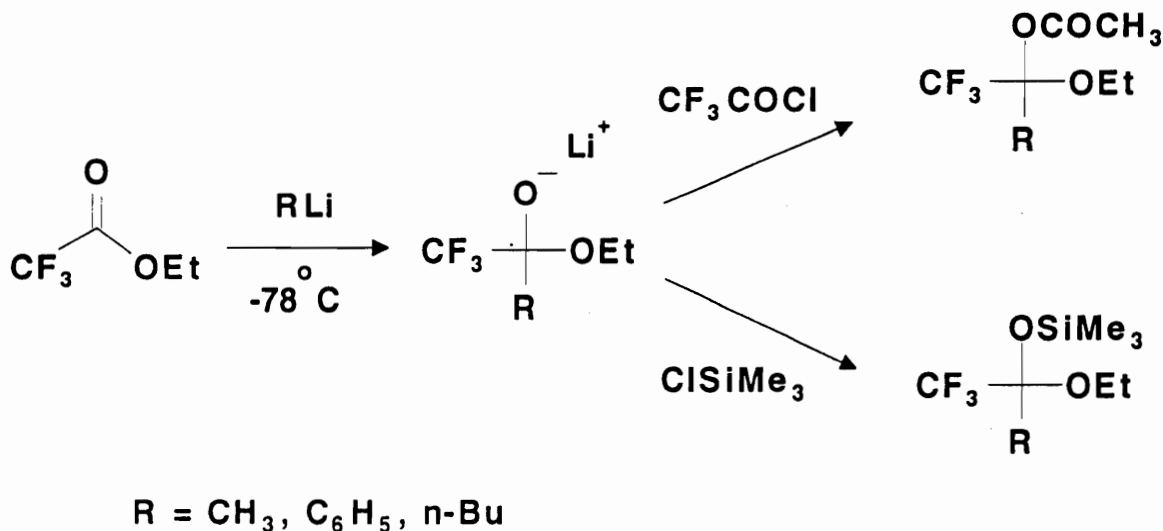
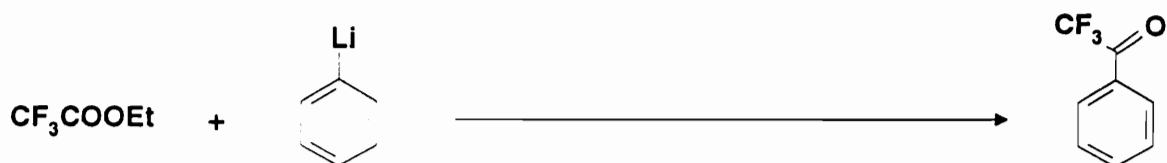


Figure 45. Trapping of stable intermediate.

The reaction temperature and the mode of addition are important factors in determining the stability of the tetrahedral intermediates. Low temperature stabilizes the intermediate and reverse addition favors the formation of alcohol by-products (159). The isolated preparative yields are shown in Table 6. The first three results are from addition of phenyllithium to ethyl trifluoroacetate. The second set of three results is from an inverse addition. Here, the ethyl trifluoroacetate is slowly added to the required amount of phenyllithium, effectively holding phenyllithium in large excess until the addition is nearly complete. It is readily seen that low temperature favors the formation of the stable tetrahedral intermediate. While phenyllithium costs are moderately high, a very useful laboratory scale preparation in quite high yields is obtained. The best yield of trifluoroacetophenone is based on the conclusions of Tamborski (159) and is further exemplified by Creary's procedure (167) for the addition at low temperature of Grignard or organolithium reagents to ethyl trifluoroacetate.



Temperature °C (Time)	Yield
-78° (10 minutes)	92%
+20° (10 minutes)	68%
+20° (10 min → 48 hours)	58%
-40° (10 minutes)	92%
-40° (10 min → +20° (48 hours))	90%
+20° (10 minutes)	0%

(INVERSE ADDITION)

Table 6. Exploration of Phenyllithium Route to Trifluoroacetophenone



One of the earliest routes to trifluoromethyl ketones was the acylation of aromatic compounds with electrophilic trifluoroacetylating reagents. Simons, in 1943, prepared trifluoroacetophenone by the reaction of trifluoroacetyl chloride with benzene in the presence of aluminum chloride (146). As shown in the examples, this procedure works quite well and produces quite acceptable yields. Several replicate synthetic reactions up to a scale of 3 mol gave consistent yields. Due to the difficulty of handling trifluoroacetyl chloride, most references to classical Friedel-Crafts reaction conditions use trifluoroacetic anhydride (168-172). Yields are often quite low using this procedure because arylated by-products, which arise from further reaction of the product trifluoromethyl ketone with the aromatic substrate used, frequently form (173-174). The very high electrophilicity of trifluoroacetic anhydride allows an uncatalyzed reaction to occur with nucleophilic aromatic compounds. Trifluoroacetic anhydride is the basis for a very good preparative procedure with activated aromatic and activated heterocyclic aromatic systems for the preparation of trifluoromethyl ketones (175-182). Recently (1990) Keumi *et al.* (183) reported the use of 2-(trifluoroacetoxy)pyridine for trifluoroacylation of aromatic compounds under Friedel-Crafts conditions. Benzene, alkylbenzenes and naphthalene have been treated with this reagent in the presence of aluminum chloride in dichloromethane to produce the corresponding trifluoromethyl aryl ketones in yields of 60 to 90%.

Perhaps the most economical and practical laboratory procedure is that based on a modification of the procedure reported by Hull *et al.* (184). In this procedure, phosphorous pentachloride is used to prepare trifluoroacetyl chloride directly from trifluoroacetic acid. The trifluoroacetyl chloride produced is distilled into a reactor containing benzene, carbon disulfide, and aluminum chloride. As shown in the example section, this procedure was scaled up to three moles with no change in the

yield of trifluoroacetophenone. A summary of the synthetic routes explored is shown in Figure 46.

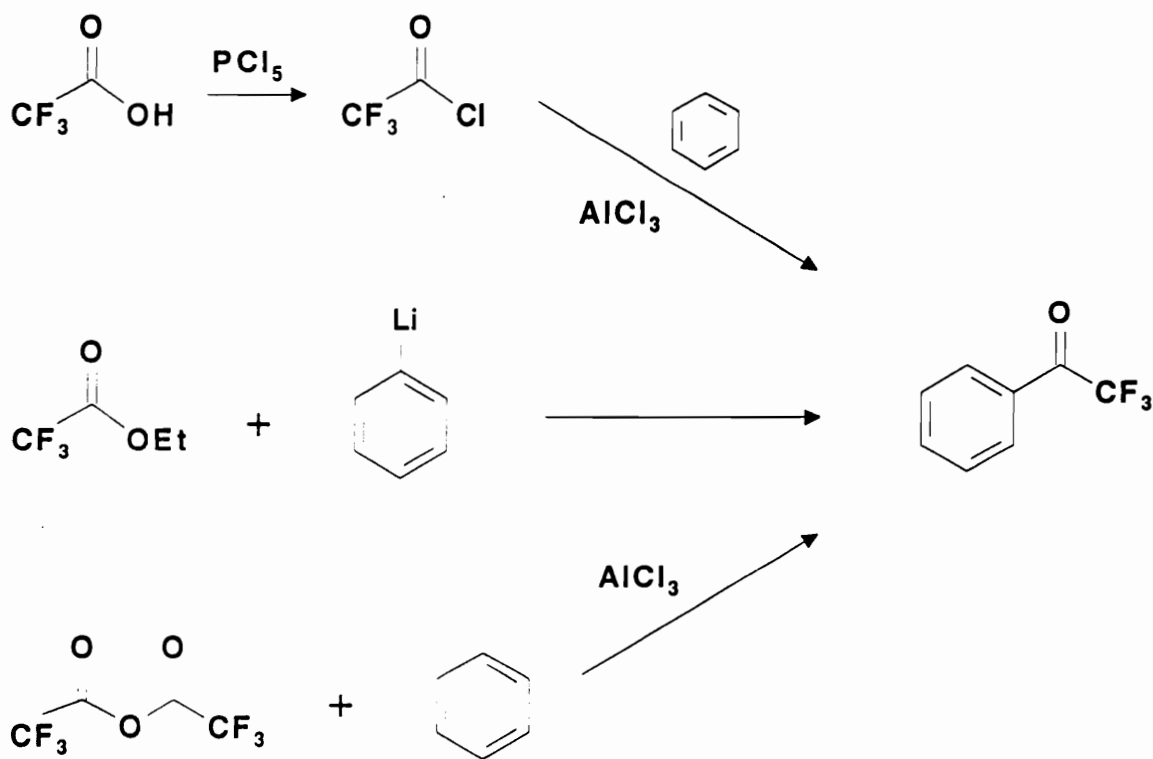
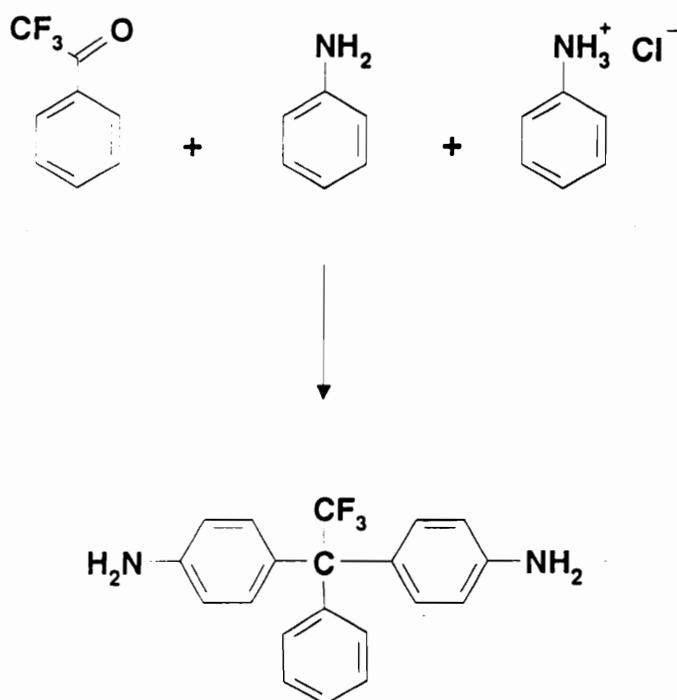


Figure 46. Routes explored to trifluoroacetophenone.

#### 4.3.2 Preparation and Characterization of 1,1-Bis(4-aminophenyl)-1-phenyl-2,2,2-trifluoroethane

The first reported preparation of 1,1-bis(4-aminophenyl)-1-phenyl-2,2,2-trifluoroethane was that of Kray and Rosser (122) in 1977. As shown in Scheme 2, 2,2,2-trifluoroacetophenone was condensed with aniline using an acid catalyst (aniline hydrochloride) to produce the corresponding diamine. A yield of 86% of rose-colored crystals with a melting point of 201-204°C was reported. Treatment of this material



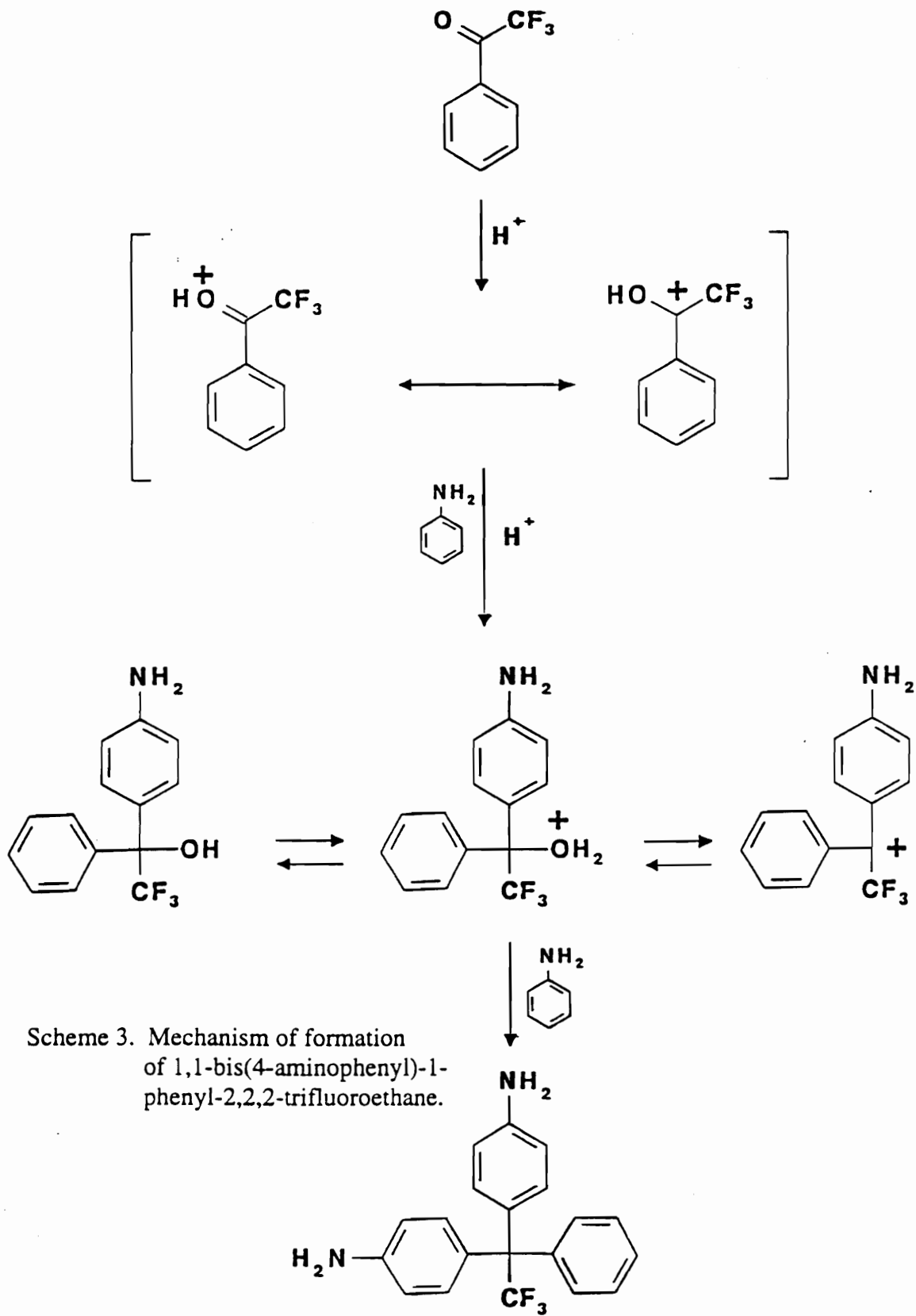
Kray and Rosser reported the preparation of the above compound and described the isolation of an 88% yield of rose colored crystals which melted at 201-204°C.

Ref: William D. Kray and Robert W. Rosser, *J. Org. Chem.*, 42(7), 1186-89 (1977).  
 William B. Alston and Roy F. Gratz, U.S. Patent 4,758,380, July 19, 1988.

Scheme 2. Preparation of 1,1-bis(4-aminophenyl)-1-phenyl-2,2,2-trifluoroethane.

with pyromellitic dianhydride failed to produce polyimide polymers with useful properties. Very dark, brittle films were obtained. Controlled molecular weight polymerizations were also unsuccessful. As a consequence of these results, a detailed study was carried out to investigate the preparation and purification of 1,1-bis(4-aminophenyl)-1-phenyl-2,2,2-trifluoroethane (3F-diamine) for the successful preparation of monomer quality 3F-diamine.

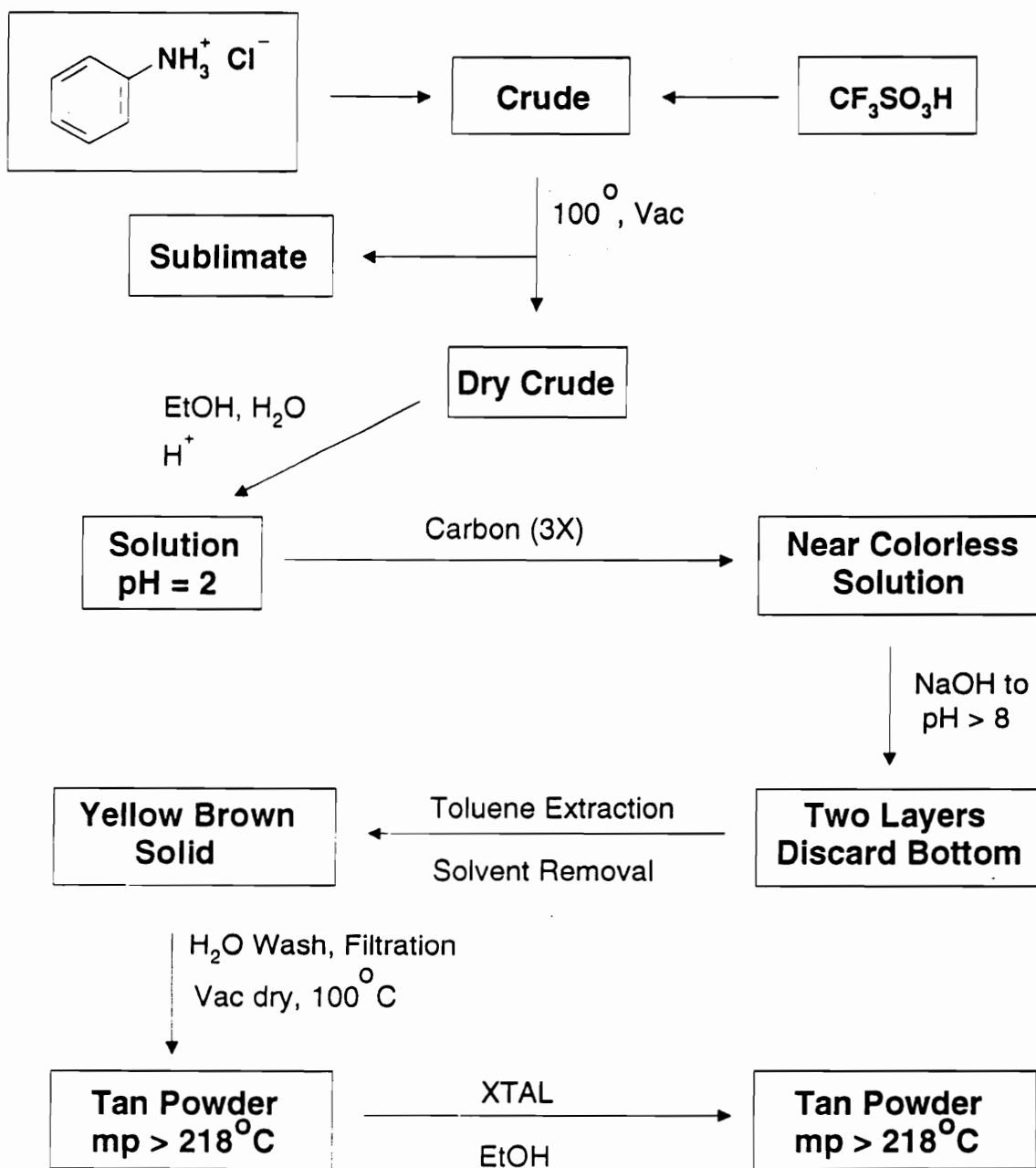
As reported by Kray and Rosser (122) the basic reaction mechanism is a modified hydroxyalkylation of trifluoroacetophenone (Scheme 3). While there are numerous examples of hydroxyalkylation in the literature (138-140), most cases reported involve a ketone or an aldehyde which can be readily protonated by an acid catalyst to produce a reactive ionic species. The cation produced acts as an electrophile in the subsequent reaction with an aromatic system as shown in Scheme 1. A variety of aromatic substrates have been treated with fluoro ketones (141-143). The usual reaction pathway stopped at the carbinal stage or reacted further only if a perfluoroalkyl ketone or an aldehyde were used as the carbonyl component. Kray and Rosser reported the first known example of an acid-catalyzed condensation of trifluoroacetophenone with aromatic substrates to yield 1,1,1-triaryl-2,2,2-trifluoroethanes. The synthetic technique developed by Kray and Rosser (122) is a modification of the procedures developed by Baeyer and Villiger (145) and by Patai and Dayagi (144) for the preparation of 1,1,1-tris(4-aminophenyl)methane derivatives from substituted aldehydes.



As shown in Scheme 3, the Kray and Rosser (122) procedure involves heating a mixture of aniline, aniline hydrochloride (acid source) and trifluoroacetophenone at reflux for 24 hours. Neutralization with sodium bicarbonate and steam distillation removed excess aniline and produced a deep blue solid crude product. The crude product was dissolved in benzene and chromatographed on a silica gel column. This product was recrystallized from benzene/petroleum ether to give rose-colored crystals which melted at 201-204°C. Attempts to prepare polyimides using pyromellitic dianhydride (PMDA) using solution techniques with N-methylpyrrolidone (NMP) (136) failed. Evidence of the presence of poly(amic acid) was seen; subsequent ring closure attempts failed to produce polyimides other than brittle low melting solids. The crude product obtained by the Kray and Rosser procedure could be recrystallized from ethanol to yield monomer grade CF<sub>3</sub> diamine. Generally, six to eight recrystallizations were needed to produce material that was suitably pure for controlled molecular weight polyimide preparation (136). An alternative preparative procedure was subsequently developed.

Scheme 3 shows the acid catalyzed process proceeding by an hydroxyalkylation pathway. In the experimental section, use of both the aniline hydrochloride and the trifluoromethane sulfonic acid methods is presented. Both systems produce a crude yield of 3F-diamine in excess of 90%.

An alternative isolation scheme was developed based on the aqueous solubility of the crude 3F-diamine dihydrochloride salt. The isolation purification procedure is summarized in Scheme 4. Crude 3F-diamine, prepared from the aniline hydrochloride and the trifluoromethanesulfonic acid methods, was vacuum dried. In each case, sublimate was obtained having a weight approximately 5% that of the starting crude. The dry crude product was dissolved in ethanol (95%) and acidified with hydrochloric



Scheme 4. Purification of 1,1-bis(4-aminophenyl)-1-phenyl-2,2,2-trifluoroethane.

acid to pH 2. The ethanol solution was treated with active carbon treated three times to yield a nearly colorless solution. This solution was treated with aqueous sodium hydroxide to raise the pH above eight and was subsequently extracted with toluene to remove the free base. The crude free base was isolated by removal of toluene under reduced pressure and the yellow/brown solid was washed with water to neutrality. Drying under vacuum gave a tan powder with a melting point above 218°C. A single recrystallization from ethanol produced a less colored solid product with a melting point above 218°C.

#### 4.3.3 Mass Spectrometric Investigations

To help identify the origin and understand the nature of the impurities formed in the preparation of 3F-diamine, an in-depth mass spectral investigation was conducted. The mass spectral investigations included both electron impact (EI) and fast atom bombardment (FAB) analyses as well as tandem experiments MS/MS and MS/MS/MS (MS<sup>3</sup>).

All experiments were performed using a JEOL SX 102/SX 102 tandem mass spectrometer. This instrument is a high performance reverse geometry instrument of the configuration magnet-ESA-magnet-ESA(BEBE). Plate lensing is minimized by the use of quadrupole lenses, a feature which facilitates sensitivity. The instrument is typically operated at a resolving power of 1000. The MS-I section of the instrument was operated in the positive ion electron impact (EI) mode with a source temperature of 200°C, 70 eV electron impact excitation, 300  $\mu$ A emission and 10 KeV acceleration. MS-I was also operated in the positive ion fast atom bombardment (FAB) mode with xenon as the FAB gas, ambient source temperature, FAB emission of 10  $\mu$ A, and 10 KeV acceleration. All FAB samples were dissolved in either a nitrobenzyl alcohol



(NBA) or glycerol matrix. All samples were admitted via the direct inlet probe and the probe was heated as needed.

The MS/MS experiment utilizes all four sectors of the instrument. EI or FAB analysis as described above was used to generate ions in MS-I. A given ion (the parent ion) generated in MS-I was selected and passed to the interface between MS-I and MS-II by setting the magnet and ESA to a fixed position. Helium gas sufficient to generate an approximately 60-70% beam reduction was admitted to the collision cell in the interface and the ions were collisionally activated by helium. The product (daughter) ions were then analyzed using a B/E linked scan on MS-II with detection after the ESA of MS-II.

The general purpose of the MS/MS/MS ( $MS^3$ ) experiments was to link a precursor ion to a given first generation product ion and determine the subsequent product ions of the first generation product ion (*i.e.*, second generation product ions). To accomplish this, ions were generated in the ion source (an EI analysis) and activated in the collision cell in the first field-free region (immediately after the source). The magnet and ESA of MS-I were then set to a fixed position to pass an ion of only the mass and energy of the first generation product ion of interest. Although source generated ions of the same mass are formed, only ions of the energy of the product ion are passed through MS-I. The energy imparted to an ion upon fragmentation is proportional to the mass of the fragment compared to the mass of the entire ion. This first generation product ion is passed to the interface between MS-I and MS-II, collisionally activated with helium gas at 60-70% beam reduction, and analyzed with a B/E linked scan on MS-II.

The objective of this study was to establish spectral evidence for the compound of interest and to identify impurities. Both EI and FAB analyses were

used. The interpretation of the EI data is simpler as there are no matrix ions or sample matrix adduct ions. Figures 47-49 show the EI spectra of three samples ranging from crude material, sublimate, and pure tan powder (not recrystallized) described in Scheme 4. The spectrum of the pure tan powder (Figure 49) shows the  $M^+$  ion of 342 and an abundant ion of  $m/z$  of 273 which corresponds to the loss of  $CF_3$  from the molecular ion. Few other ions are observed in this sample. Notable differences between the spectrum of the pure tan powder and the spectrum of the crude mixture are the ions of  $m/z$  of 423, 354, 267, and 247. The appearance of these ions as major components of the sublimate obtained during purification provides further evidence that these species are related to reaction by-products.

The FAB spectra of the same materials are shown in Figures 50-51. In addition to glycerol matrix ions, the prominent series of ions differing by 92 amu, the crude mixture has the  $(M+H)^+$  ion of  $m/z$  of 343 of the 3F-diamine and an ion of  $m/z$  of 354 which is the same mass as an ion seen in the EI spectrum. The FAB spectrum of the pure sample is unusual in that no  $(M+H)^+$  of  $m/z$  of 343 or  $M^+$  ion of 342 is observed. Instead, a prominent ion of  $m/z$  of 340 is observed. Since this EI spectrum of this sample is quite simple and shows the expected ion, it appears that the pure diamine is reacting with the glycerol matrix.

Since results from FAB analysis of the pure sample show unusual matrix effects, MS/MS analysis of the apparent  $(M+H)^+$  as well as by-product ions were carried out from crude samples. The FAB MS/MS spectra of the higher mass ion of  $m/z$  of 354 and the apparent molecular ion are shown in Figures 52 and 53. Principal ions of the MS/MS spectrum of the impurity of  $m/z$  of 354 (Figure 52) are the ions of  $m/z$  of 336 which is most likely formed by the loss of water and the ion of  $m/z$  of 250 which is observed in both the MS/MS spectrum of the apparent  $(M+H)^+$  and in full

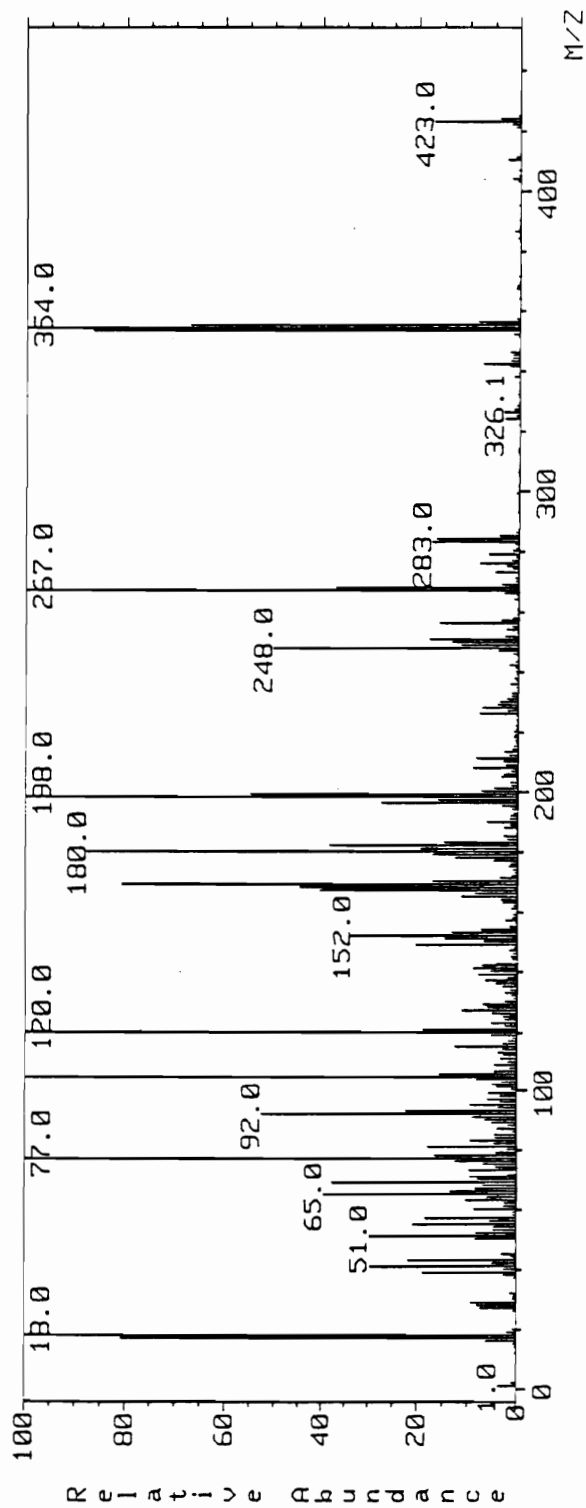


Figure 47. Mass spectrum (EI) of crude 1,1-bis(4-aminophenyl)-1-phenyl-2,2,2-trifluoroethane.

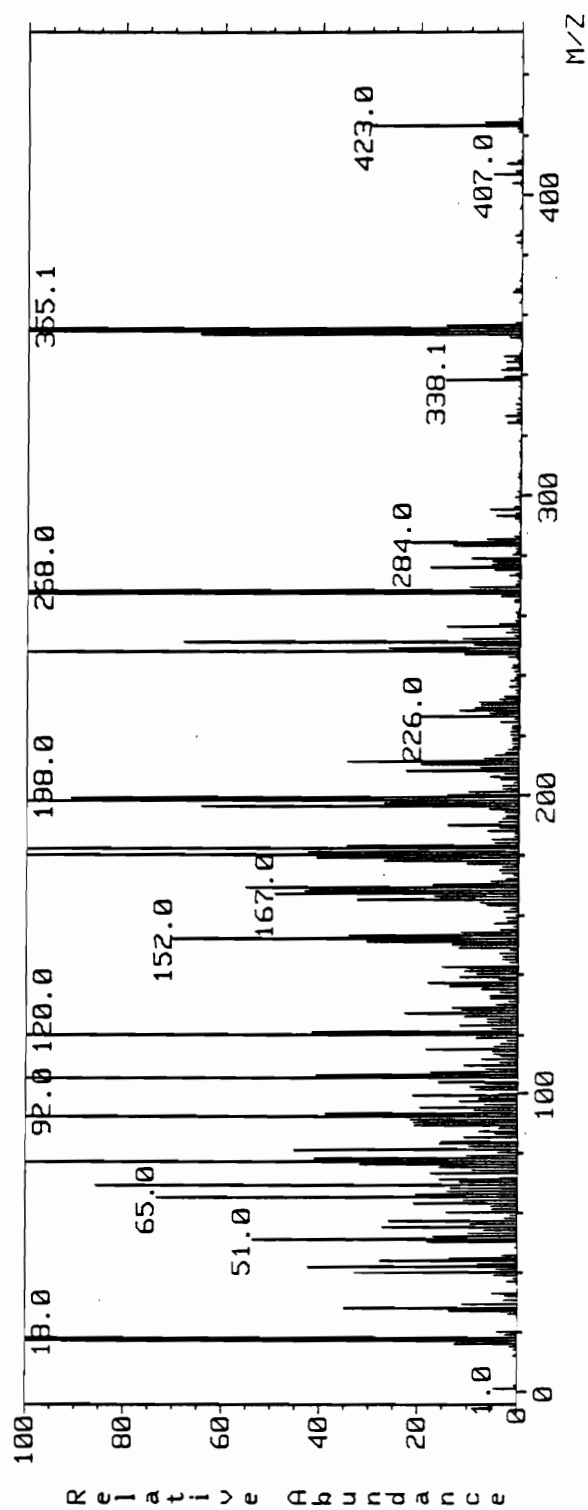


Figure 48. Mass spectrum (EI) of sublimate from crude 1,1-bis(4-aminophenyl)-1-phenyl-2,2,2-trifluoroethane.

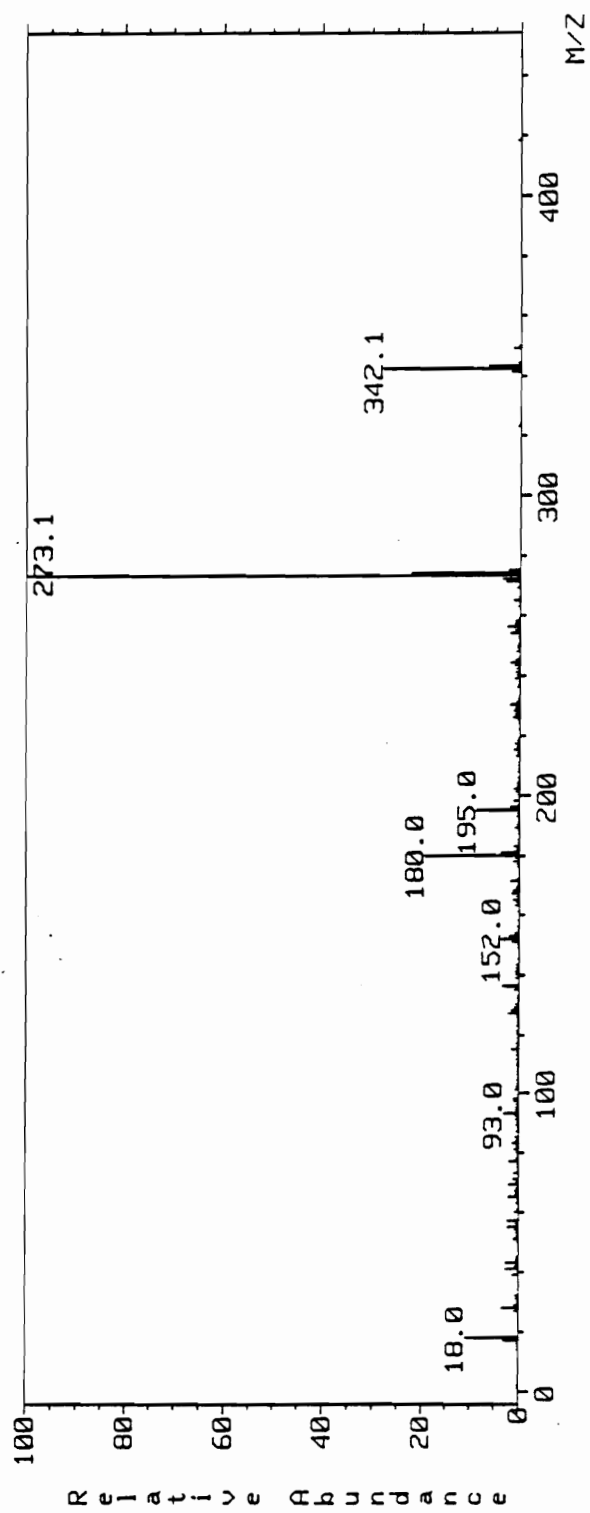


Figure 49. Mass spectrum (EI) of purified 1,1-bis(4-aminophenyl)-1-phenyl-2,2,2-trifluoroethane.

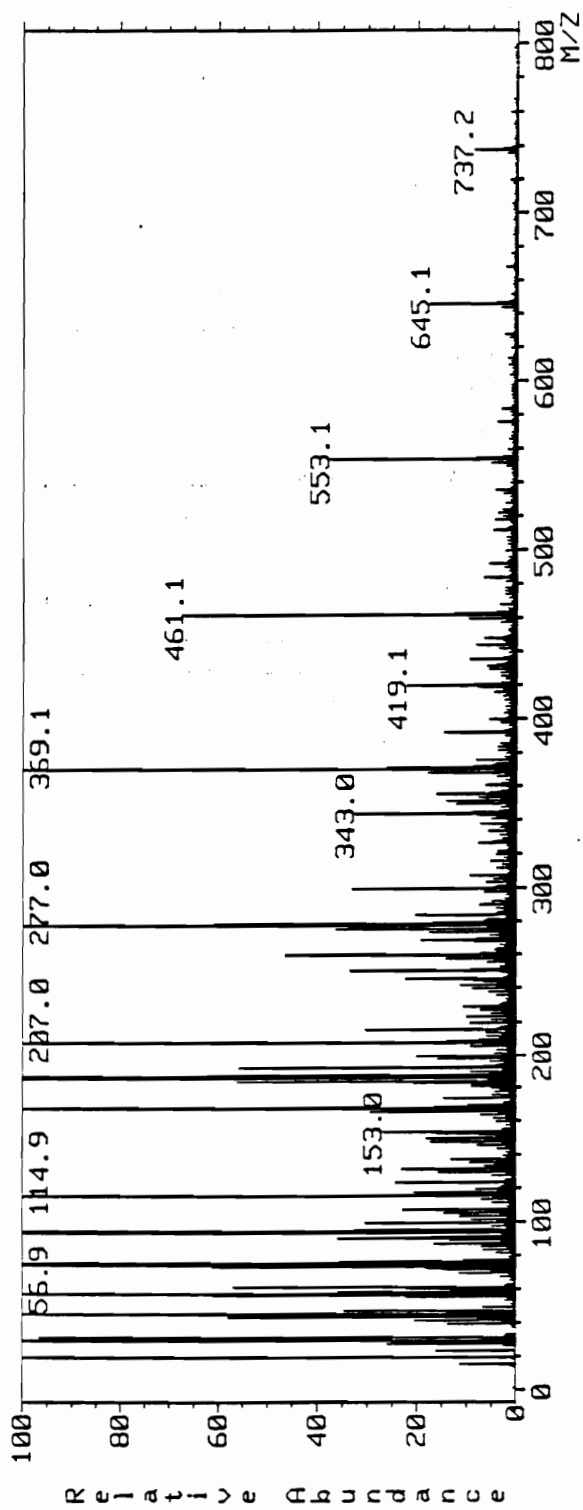


Figure 50. Mass spectrum (FAB, glycerol matrix) of crude 1,1-bis(4-aminophenyl)-1-phenyl-2,2,2-trifluoroethane.

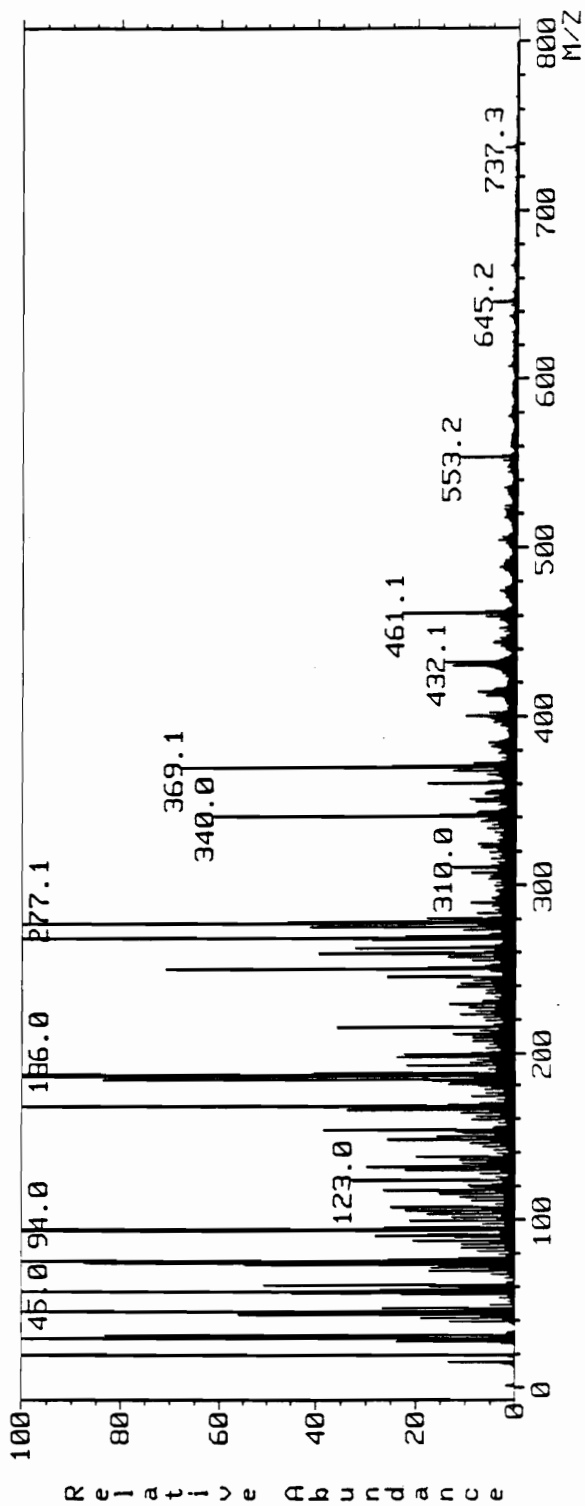


Figure 51. Mass spectrum (FAB, glycerol matrix) of purified 1,1-bis(4-aminophenyl)-1-phenyl-2,2,2-trifluoroethane.

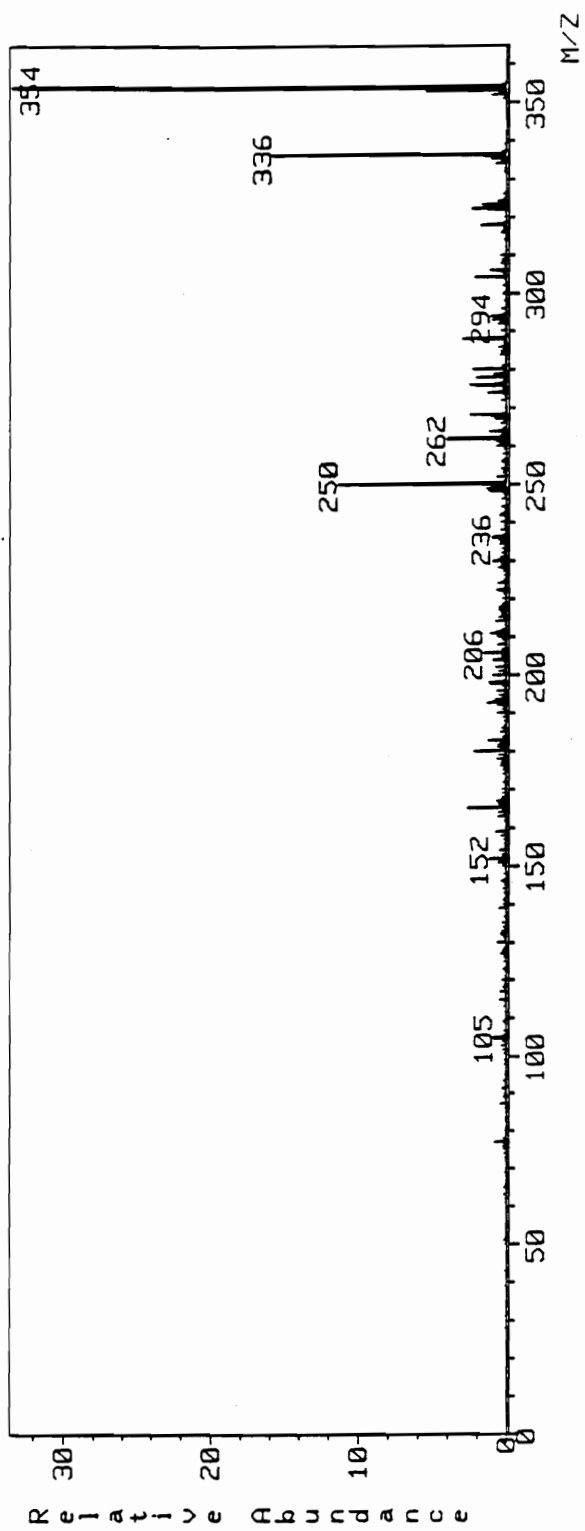


Figure 52. MS/MS of m/z 354 from the FAB mass spectrum (glycerol matrix) of crude 1,1-bis(4-aminophenyl)-1-phenyl-2,2,2-trifluoroethane.



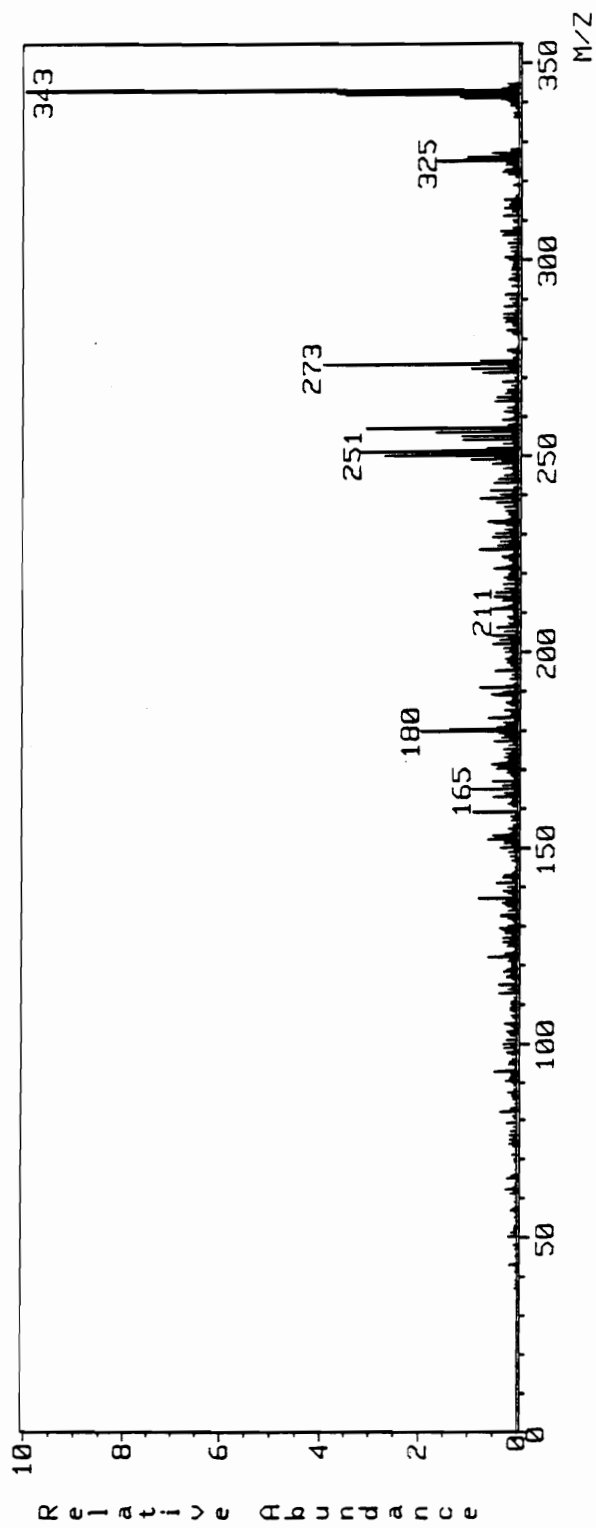


Figure 53. MS/MS of m/z 343 from the FAB mass spectrum (glycerol matrix) of crude 1,1-bis(4-aminophenyl)-1-phenyl-2,2,2-trifluoroethane.

scan FAB spectra. The spectrum for the apparent  $(M+H)^+$  ion (Figure 53) contains ions corresponding to the loss of water ( $m/z$  of 325) and  $HCF_3$  is commonly the major decomposition ion formed from the triphenyl  $CF_3$  series of compounds. However, the loss of water and the ion of  $m/z$  of 257 do not have precedence in the decompositions of other triphenyl- $CF_3$  compounds. This suggests that the impurity is likely a compound having the same mass and similar structure as the target molecule but is probably not identical.

The FAB MS/MS of the ions of 268 and 250 are shown in Figures 54 and 55. For the ion of  $m/z$  of 268 (Figure 54), the loss of water to form the ion of  $m/z$  of 250 is the principal fragmentation. The fragment of  $m/z$  of 180 is also observed as well as low abundance ions of  $m/z$  of 77, 94, 105 and 120. It is noteworthy that these low abundance fragments are not observed in the MS/MS spectrum of the ion of  $m/z$  of 250 and their absence is indicative of substantial structural modification of the ion of  $m/z$  of 268 as it decomposes to the ion of  $m/z$  of 250. The MS/MS spectrum of  $m/z$  of 250 has the principal ions of  $m/z$  of 152, 180, and 230.

The EI MS/MS spectra of significant ions noted in the full scan EI spectra are shown in Figures 56 through 61. The EI MS/MS spectra of the  $M^+$  ion of  $m/z$  of 342 (Figure 56) from a sample of pure 3F-diamine shows only one significant fragmentation which is the loss of  $CF_3$  to form the ion of  $m/z$  of 273. This is a very significant different MS/MS fragmentation than for the apparent  $(M+H)^+$  ion selected from the FAB spectrum (see Figure 51). This provides evidence that the ion of  $m/z$  of 343 is likely a related species rather than the protonated 3F-diamine molecule.

Other ions selected for EI MS/MS study were ions found in impure samples and were analyzed by MS/MS for the purpose of gaining information regarding by-products. Although these ions were detected in the spectra of a number of samples,

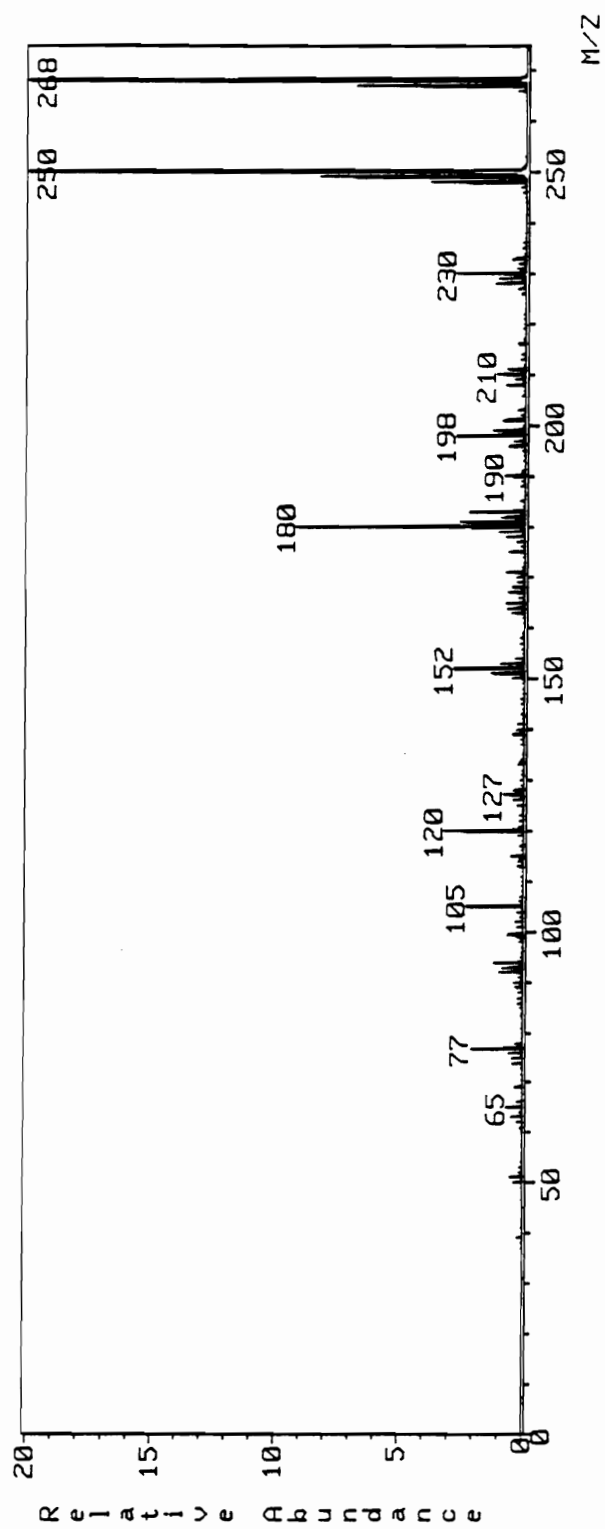


Figure 54. MS/MS of m/z 268 from the FAB mass spectrum of sublimate shown in Figure 48.

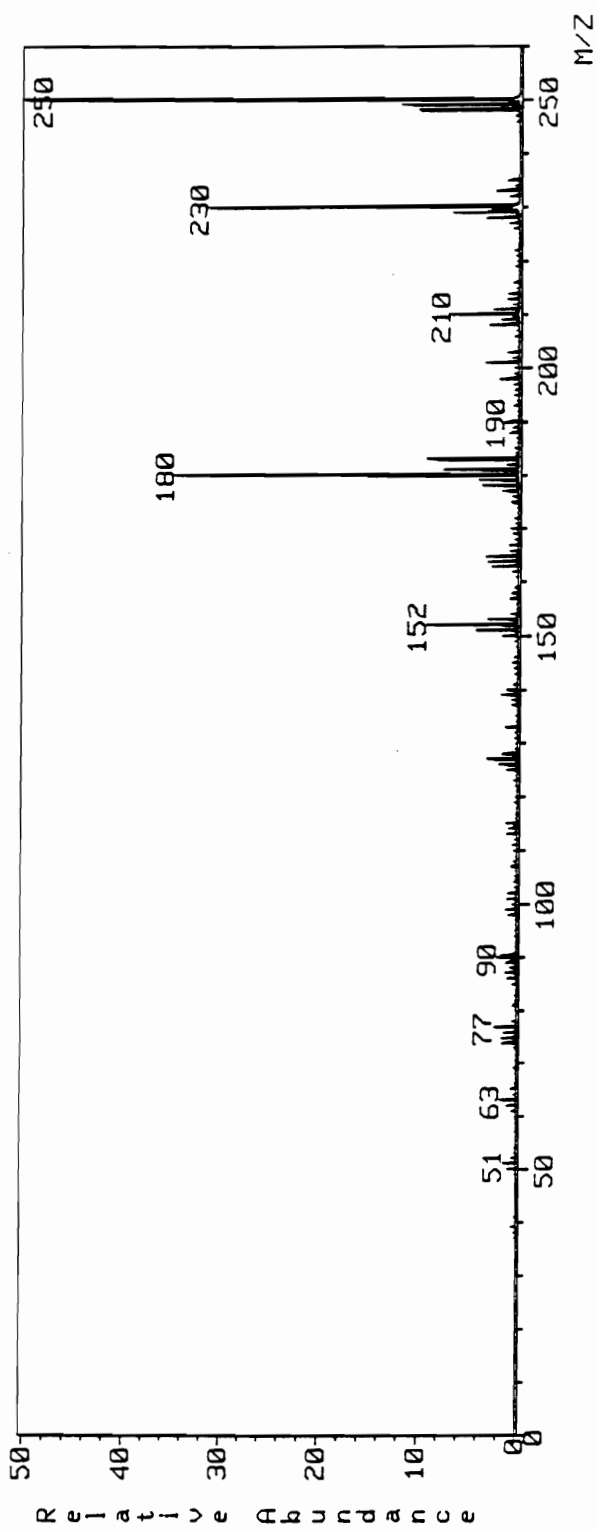


Figure 55. MS/MS of m/z 250 from the FAB mass spectrum of sublimate from crude 1,1-bis(4-aminophenyl)-1-phenyl-2,2,2-trifluoroethane.

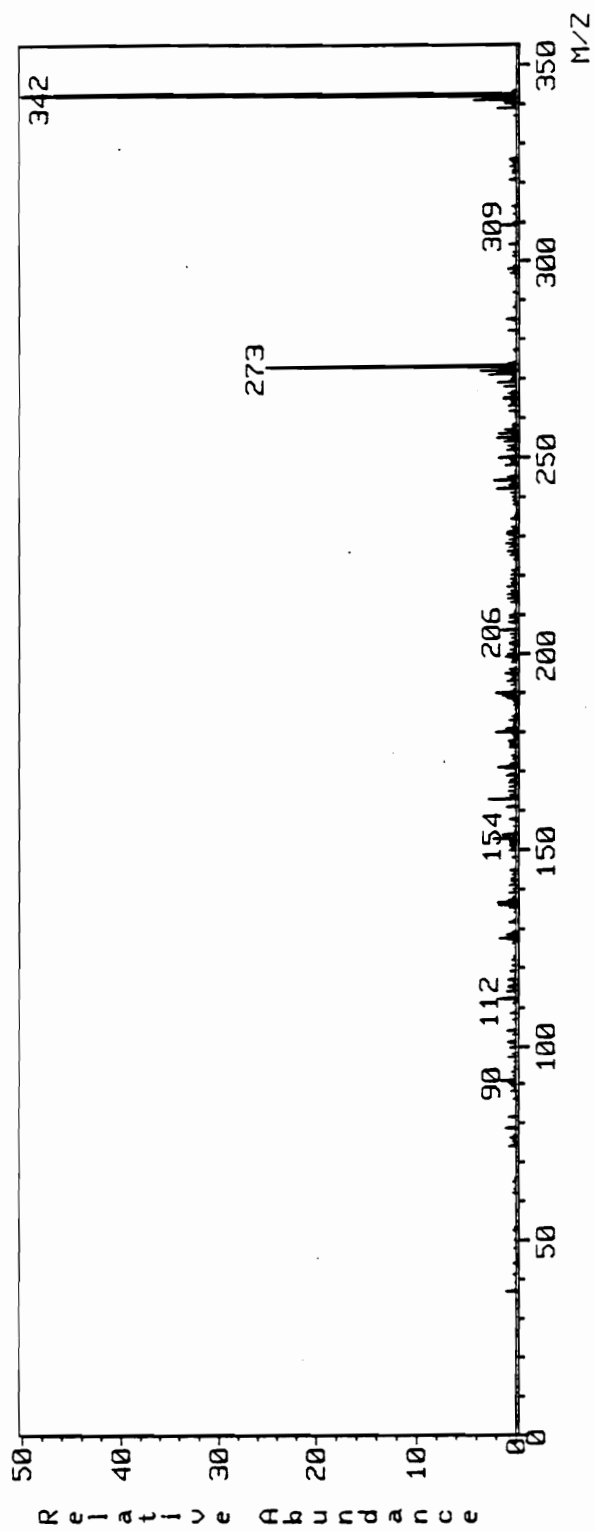


Figure 56. MS/MS of m/z 342 from the mass spectrum of purified 1,1-bis(4-aminophenyl)-1-phenyl-2,2,2-trifluoroethane.

the sublimate sample was selected for analysis due to the high abundance of the ions of interest which simplified the MS/MS analyses.

The EI MS/MS spectrum of the ion of  $m/z$  of 423 (Figure 57) shows that the principal fragmentation is the formation of the ion of  $m/z$  of 354. This difference of 69 amu is characteristic for the loss of  $CF_3$ . The ion of  $m/z$  of 284 may be related to the loss of  $HCF_3$  from the ion of  $m/z$  of 354 providing indication that the ion of  $m/z$  of 423 may be formed from the reaction of a second  $CF_3$  entity with an intermediate product. Ions of  $m/z$  of 77, 104, 248 and 276 are consistent with this explanation.

The EI MS/MS of the ion of  $m/z$  of 354 (Figure 58) is quite similar to the MS/MS spectrum of the ion of  $m/z$  of 423 in the mass range of 0 to 354. This indicates that CAD decompositions of the two ions are quite similar and that most of the ions observed in the MS/MS spectrum of  $m/z$  of 423 are likely the results of a sequential decomposition in which loss of  $CF_3$  is the first step. The dramatic difference between the MS/MS spectrum of the EI generated ion of 354 (Figure 58) and the FAB generated ion (Figure 52) provides strong evidence that these are two distinctly different species of the same nominal mass. Spectra of source-generated ions are likely to differ depending on the mode of ionization, but in the MS/MS experiment a "stable" ion is selected and allowed to collide with a noble gas to generate further fragmentation. The fragmentation process should be independent of the mode of ionization. The different spectra result because the ions are indeed different species. In regards to a reaction mechanism, it is a distinct possibility that two different isomers are formed.

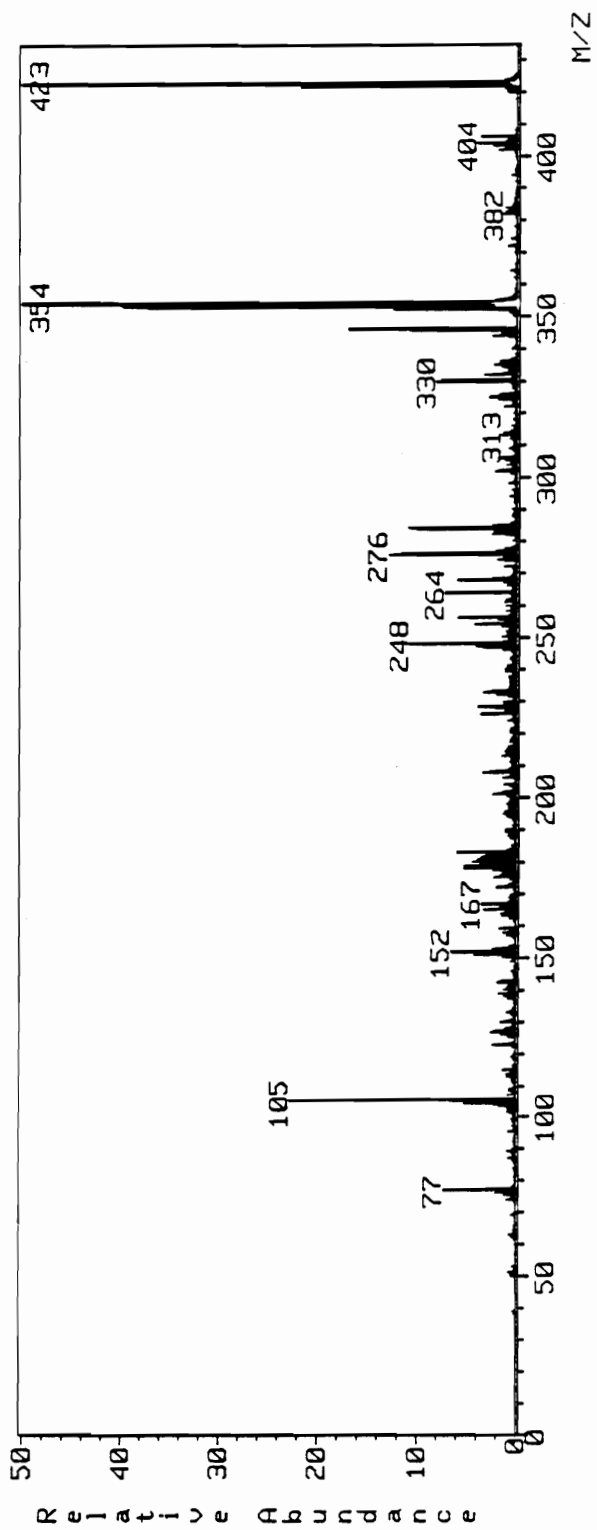


Figure 57. MS/MS of m/z 423 from the mass spectrum of sublimate shown in Figure 48.

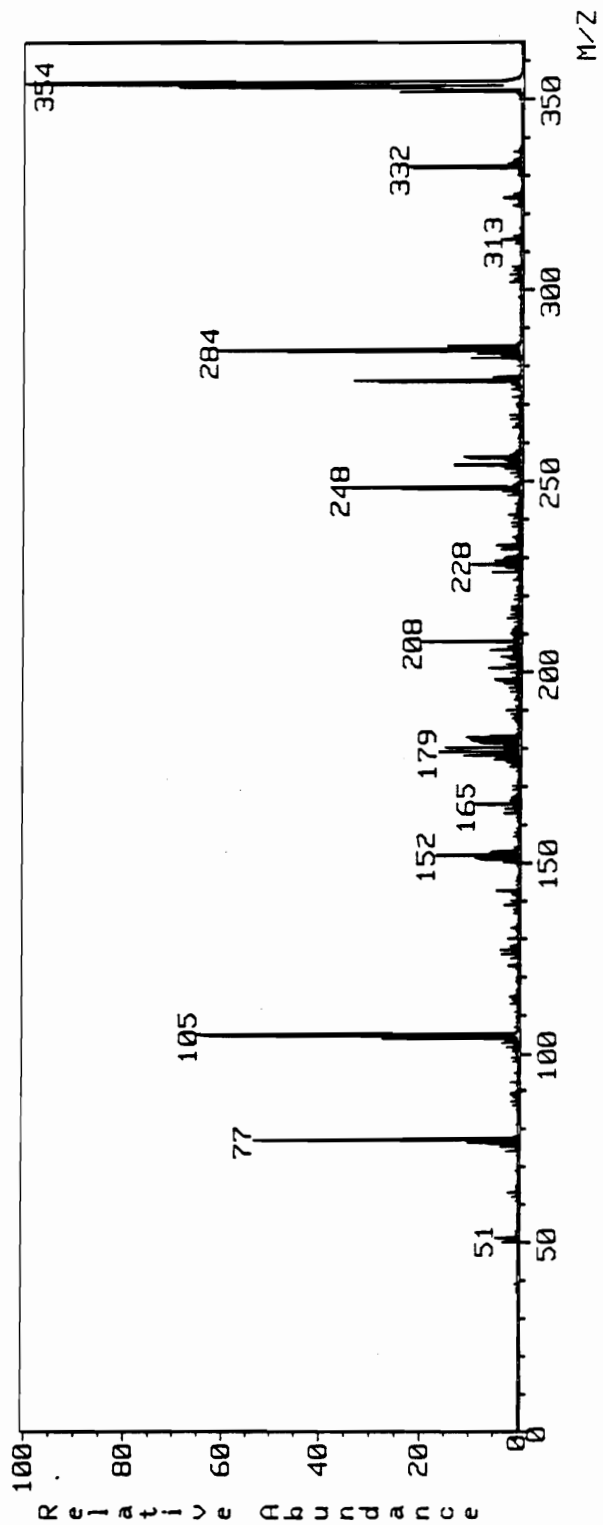
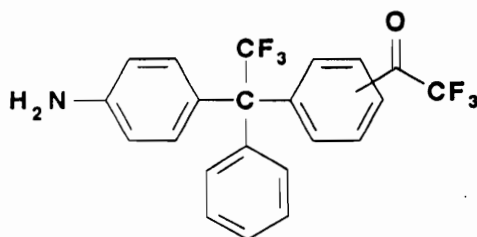


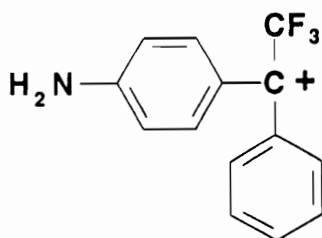
Figure 58. MS/MS of m/z 354 from the mass spectrum of sublimate shown in Figure 48.



The following structure is consistent with these mass spectral interpretations for the compound(s) of  $m/z$  of 423.

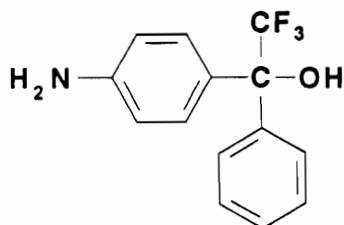


This compound is derived from reaction of the electrophilic species shown below with trifluoroacetophenone.



Multiple isomeric products would be expected with the meta substituted product postulated as the predominant product.

The "independence" of the MS/MS experiment to the mode of formation of the ion is demonstrated by the MS/MS spectra of the ion of  $m/z$  of 267 (Figure 59) and its FAB generated analog, the  $(M+H)^+$  ion of  $m/z$  of 268 (Figure 54). This ion is probably formed from the very undesirable by-product 1-(4-aminophenyl)-1-phenyl-2,2,2-trifluoroethane-1-ol.



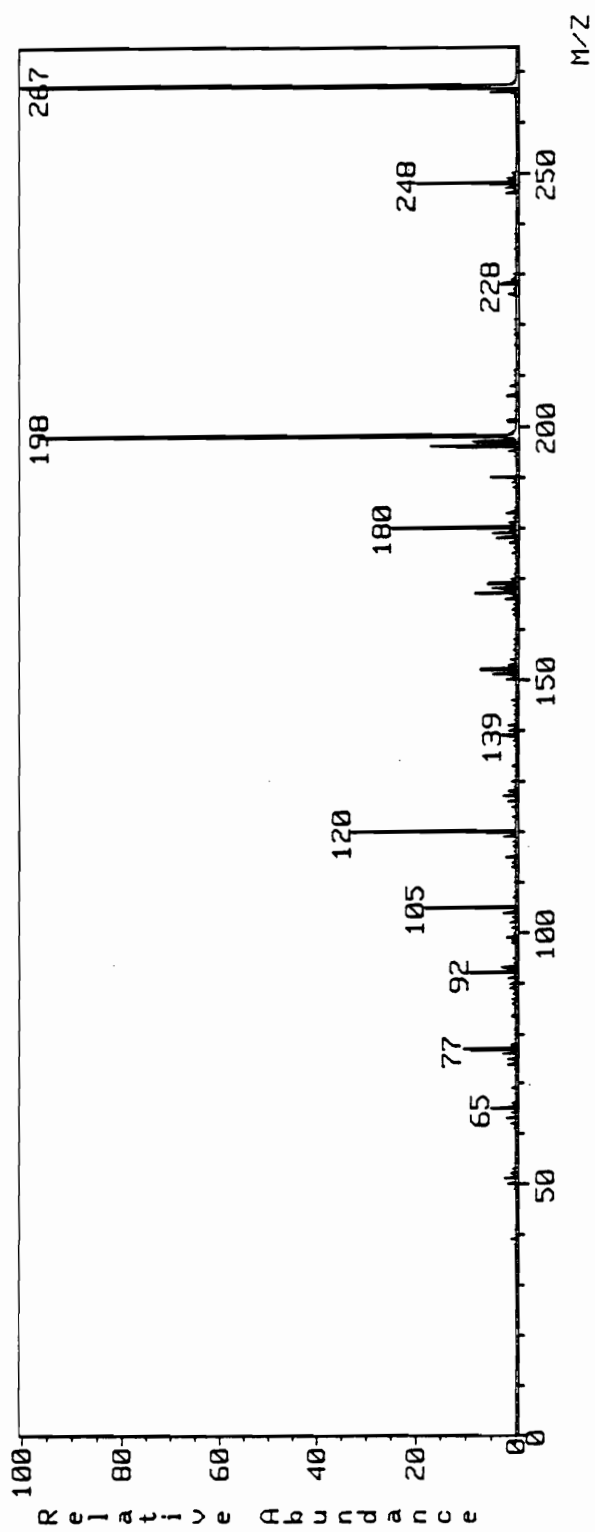


Figure 59. MS/MS of m/z 267 from the mass spectrum of sublimate shown in Figure 48.

With the exception of the loss of water from the protonated species, the spectra are quite comparable in the fragments formed. The fragments are consistent with the proposed structure. The comparison of the EI MS/MS of the ions of  $m/z$  of 251 and 247 is shown in Figures 60 and 61. On first inspection the spectra would be expected to differ by three hydrogens and hence be very similar. There are, however, notable differences. There are no ion clusters observed at  $m/z$  of 197, 99, or 75 for the ion of 251, but these are noteworthy fragments from the ion of  $m/z$  of 248. Also, prominent ion clusters are observed around each major fragment in the MS/MS spectra of  $m/z$  of 248. These differences indicate that these species have substantially different structures.

Comparison of the spectrum of the ion of  $m/z$  of 248 with the MS/MS spectrum of the FAB generated ion of 250 (Figure 55) shows two ions two mass units higher than the corresponding ions for the 248 ion (the ions of  $m/z$  152 and 230) which is consistent with a homologous compound. However the FAB ion of  $m/z$  of 250 (Figure 55) spectrum has no ions corresponding to the ions of  $m/z$  of 75 and 99 which is more like the spectra of the ion of  $m/z$  of 251 (Figure 60). This provides further evidence of chemical distinctiveness of the three species as opposed to simple protonation or deprotonation.

The MS/MS/MS or MS<sup>3</sup> experiment is a relatively new experiment on four sector instruments and has two distinct differences from the multistage experiments performed on ion trap or ICR mass spectrometers. Namely, the collisions are high energy collisions in the sector instrument and the ions are separated in space rather than time. The MS<sup>3</sup> experiments permit the direct experimental correlation of a parent ion not only with a product ion and its decomposition products but also with

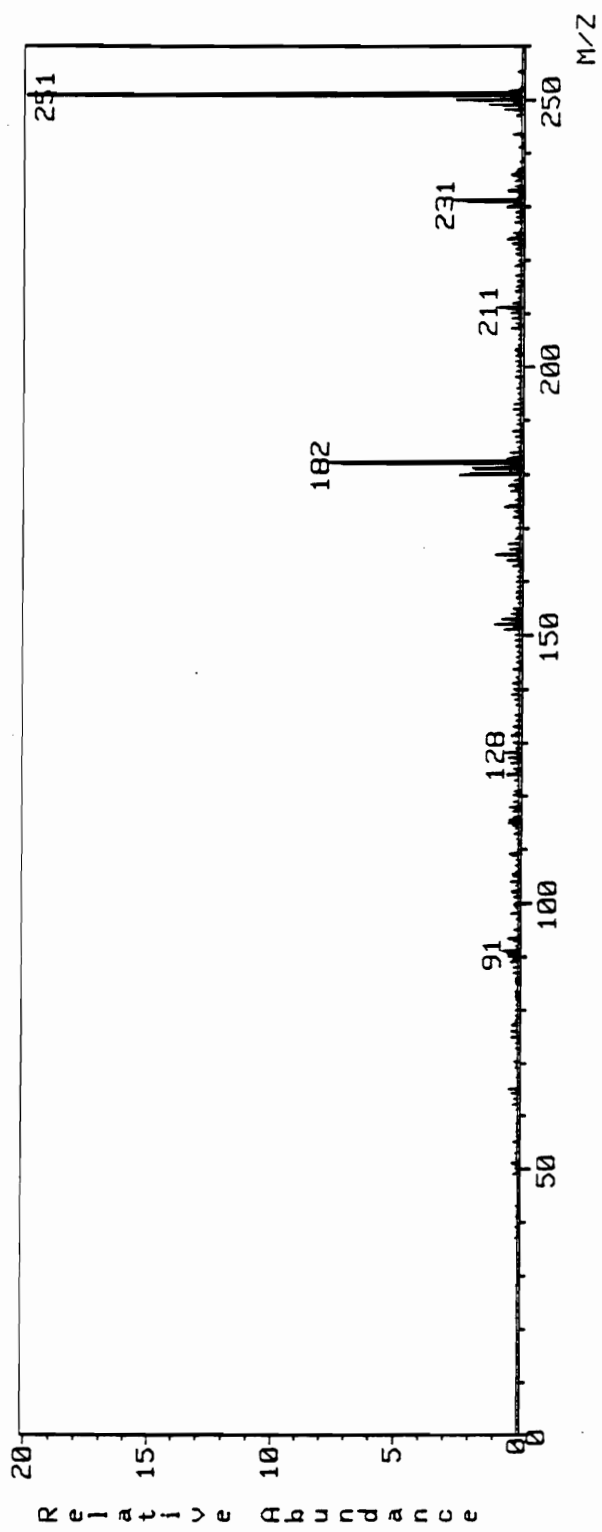


Figure 60. MS/MS of m/z 251 from the mass spectrum of sublimate shown in Figure 48.

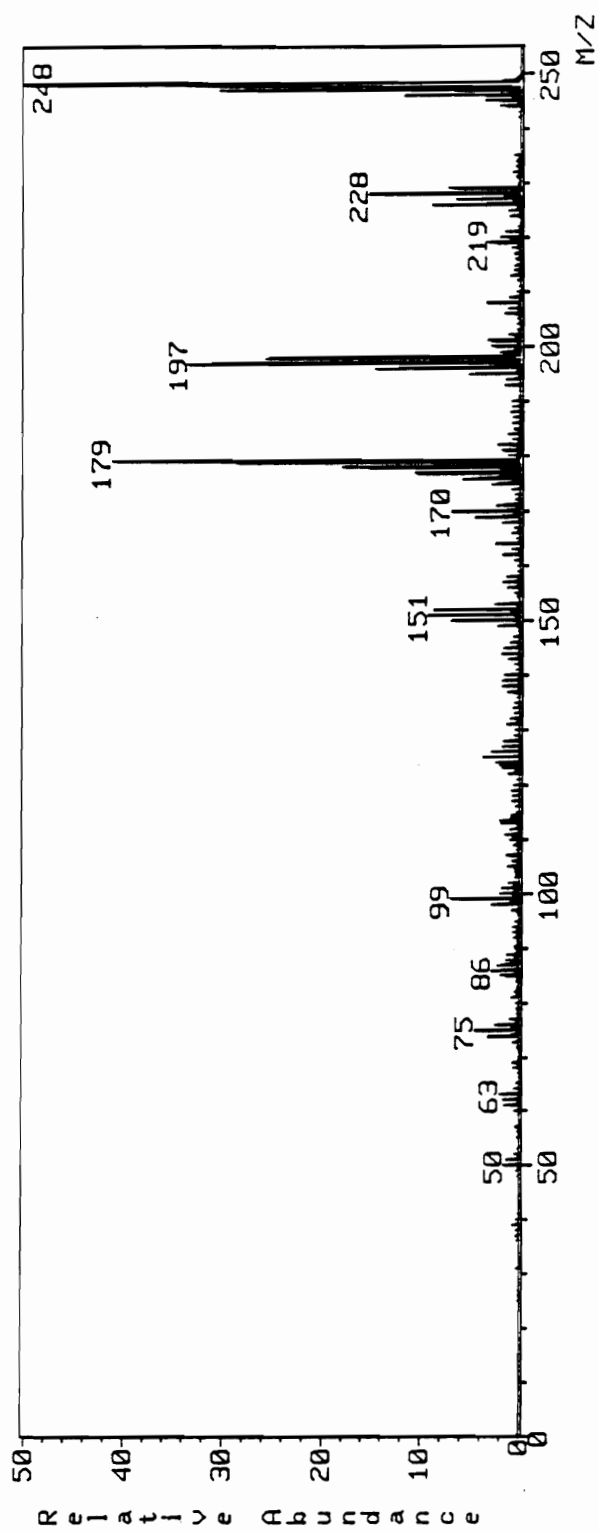


Figure 61. MS/MS of m/z 248 from the mass spectrum of sublimate shown in Figure 48.

the parent ion and the decompositions of the fragments of the first generation product ion. This facilitates establishing relationships of species in a complex mixture and in verification of projected decomposition of ion structures.

Three EI generated ion sequences were selected for the MS<sup>3</sup> experiment. The first was the decomposition of the ion of M/Z of 423 to 354 to second generation product ions (Figure 62). These data, when compared with the MS/MS spectra of the ion of M/Z of 423 (Figure 57) and 354 (Figure 58), definitely establish the link between these ions and the sequential relationship of the decomposition.

The second series of ions selected was that generated by the decomposition of the ion of m/z of 267 to 248 to second generation product ions (Figure 63). This ion series is of particular interest as it is related to an undesirable reaction by-product. The second generation product ions are consistent with the projected structure of the ion of m/z of 267. Comparison of this spectrum with the MS/MS of 248 from the sublimate mixture (Figure 61) provides strong evidence that the EI generated ion of m/z of 248 is a fragment of the by-product 1-(4-aminophenyl)-1-phenyl-2,2,2-trifluoroethan-1-ol. The cluster of ions at each major fragment implies a substantially different character of the bonding of the hydrogen atom. This would be consistent with the hypothesis that "quinoid" structures are formed in these fragmentations.

The last fragmentation series selected for the MS<sup>3</sup> experiment was the series of m/z of 267 to 180 to second generation product ions as shown in Figure 64. Again the parent ion is the by-product 1-(4-aminophenyl)-1-phenyl-2,2,2-trifluoroethan-1-ol and the first generation ion product is in a mass range (178-182) where ions are frequently observed in the study of 3F-diamine. As in the previous example, the spectrum is characterized by clusters of ions. Again, this implies substantial alteration of the bonding of the hydrogen atoms. Further product ion identification is not clear.

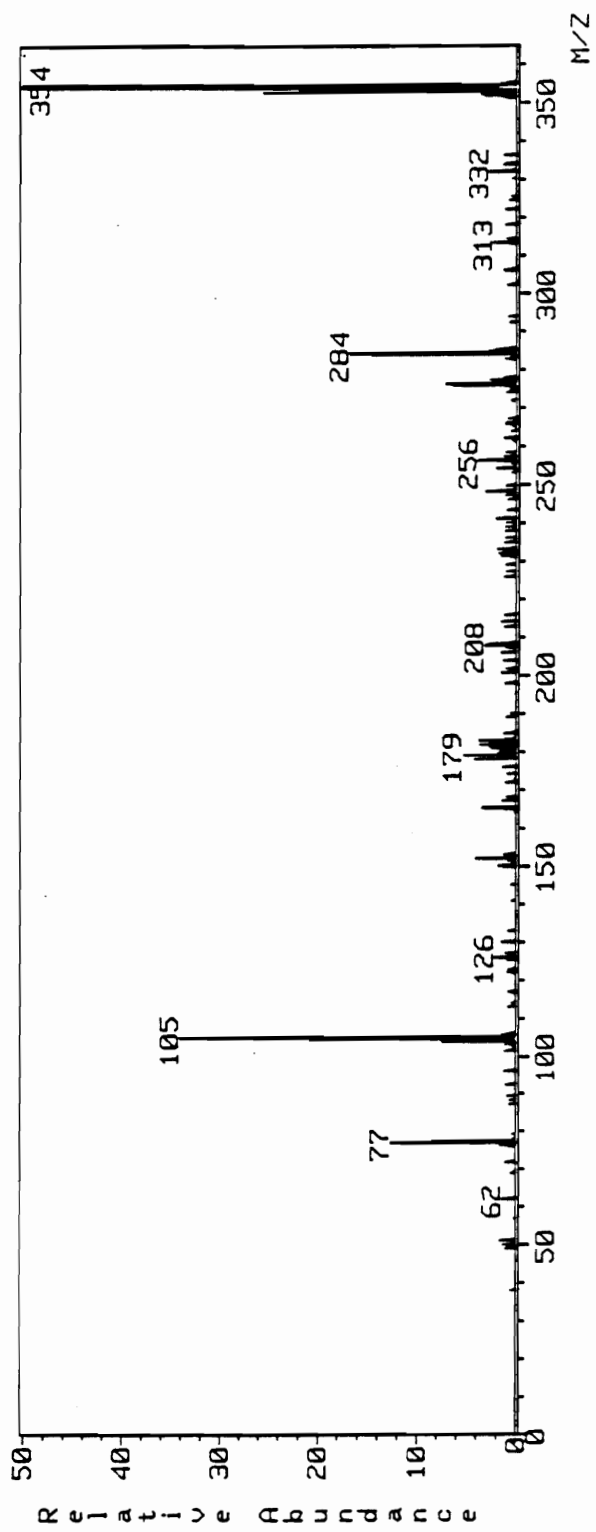


Figure 62. FAB MS' of m/z 423 to 354 to second generation products.

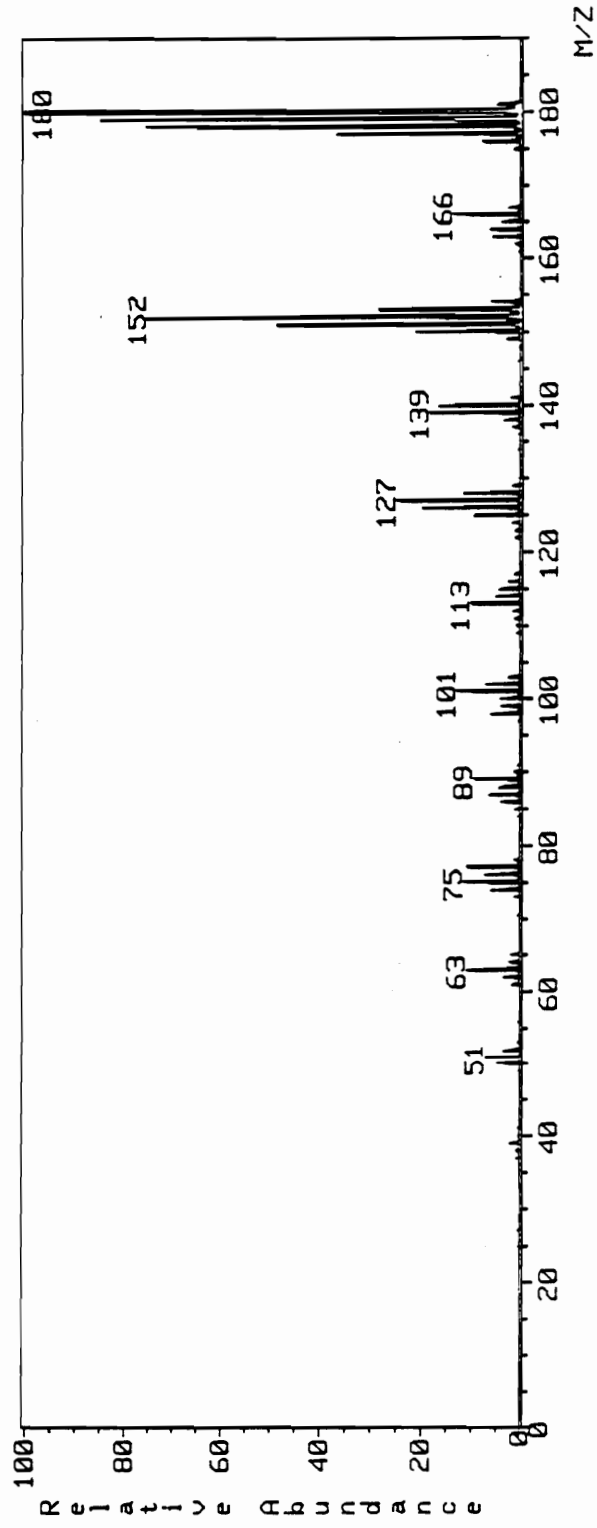


Figure 63. FAB MS<sup>s</sup> of m/z 267 to 248 to second generation products.



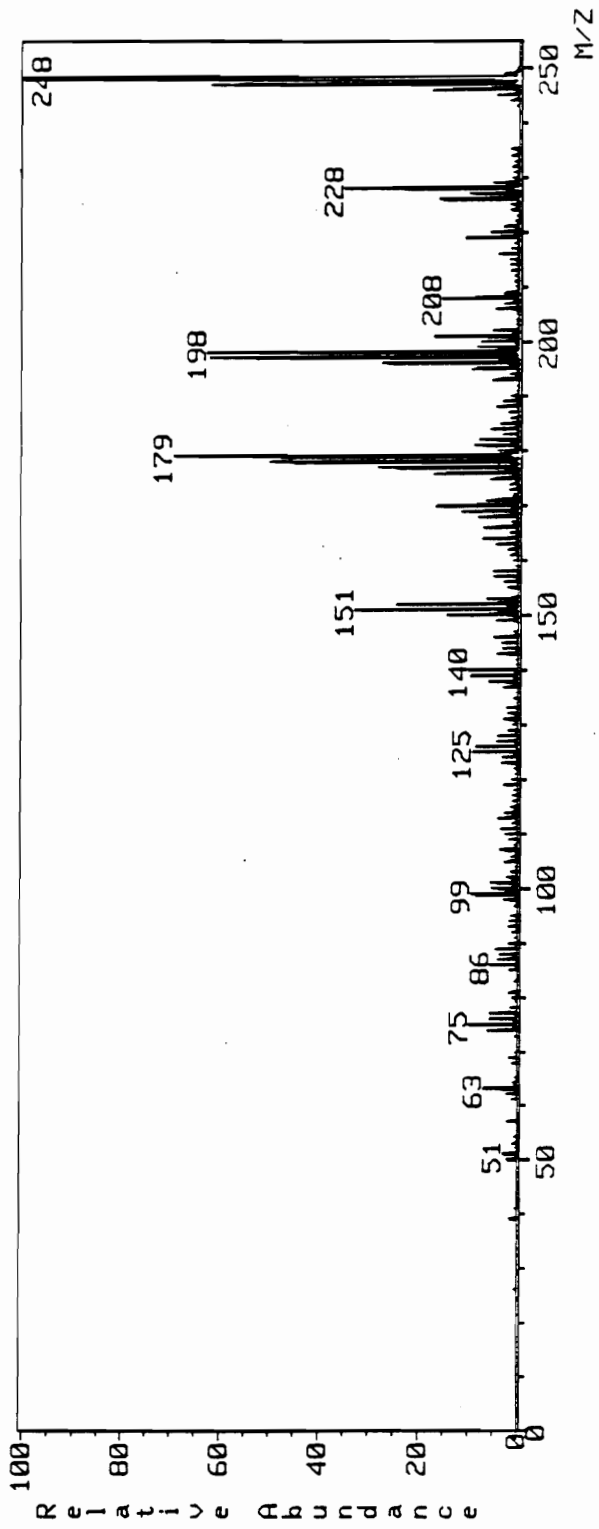


Figure 64. FAB MS' of m/z 267 to 180 to second generation products.

#### 4.3.4 Liquid Chromatographic - Mass Spectrometric Investigations

With the wealth of data obtained by MS/MS and MS<sup>3</sup> experiments with the sublimate fraction, a liquid chromatography-mass spectrometry analysis of the sublimate was carried out. The material was dissolved in methanol and chromatographed using a Waters 600-MS solvent delivery system. A methanol/water gradient was employed. The methanol concentration was increased from 30% at injection to 80% linearly over thirty minutes. The methanol concentration was then raised to 100% and held constant for ten minutes. Glycerol was added to the mobile phase (1.5% by volume) as a FAB matrix. The flow rate was 0.5 mL/min with a Waters Nora-Pak 3.9 x 75 mm phenyl column and a Waters 484 variable wavelength detector set at 260 nm were used.

Analysis by on-line FAB MS was carried out using a JEOL SX 102/SX 102 four sector tandem mass spectrometer. Resolution was 1000, the accelerating potential was 10 KeV, and the range of 0-1000 was scanned in approximately six seconds. For FAB analysis, the primary particles were xenon atoms accelerated through a 6 KeV potential. The LC-MS interface consisted of the "frit-FAB" apparatus, in which the eluent from the LC column is split pneumatically such that approximately 10 mL/min enters the ion source. The volatile components are immediately pumped away, leaving a thin layer of matrix and analyte upon which the xenon beam is directed.

The resulting chromatogram is shown in Figure 65 and the total ion current (TIC) plot is shown in Figure 66. Component one (1) has a retention time of approximately 17 minutes and the corresponding FAB spectra is shown in Figure 67. This compound has a molecular weight of 267 amu. It appears that both the radical cation and the protonated molecular ion are present. The glycerol adduct of the protonated molecular ion is seen at the  $m/z$  of 360. Loss of hydroxyl from  $m/z$  of 267 or water from  $m/z$  of 268 leads to the

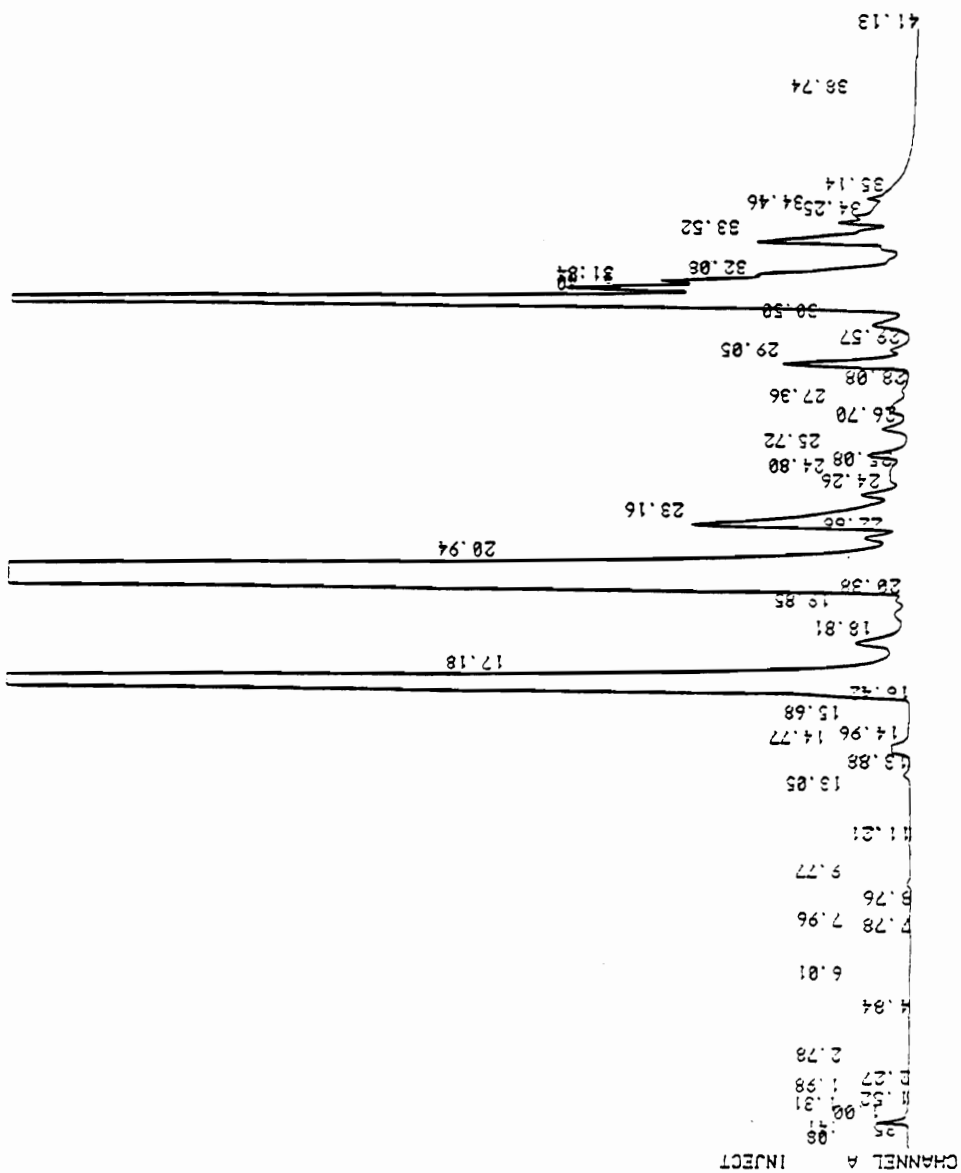


Figure 65. Liquid chromatogram of sublimate.

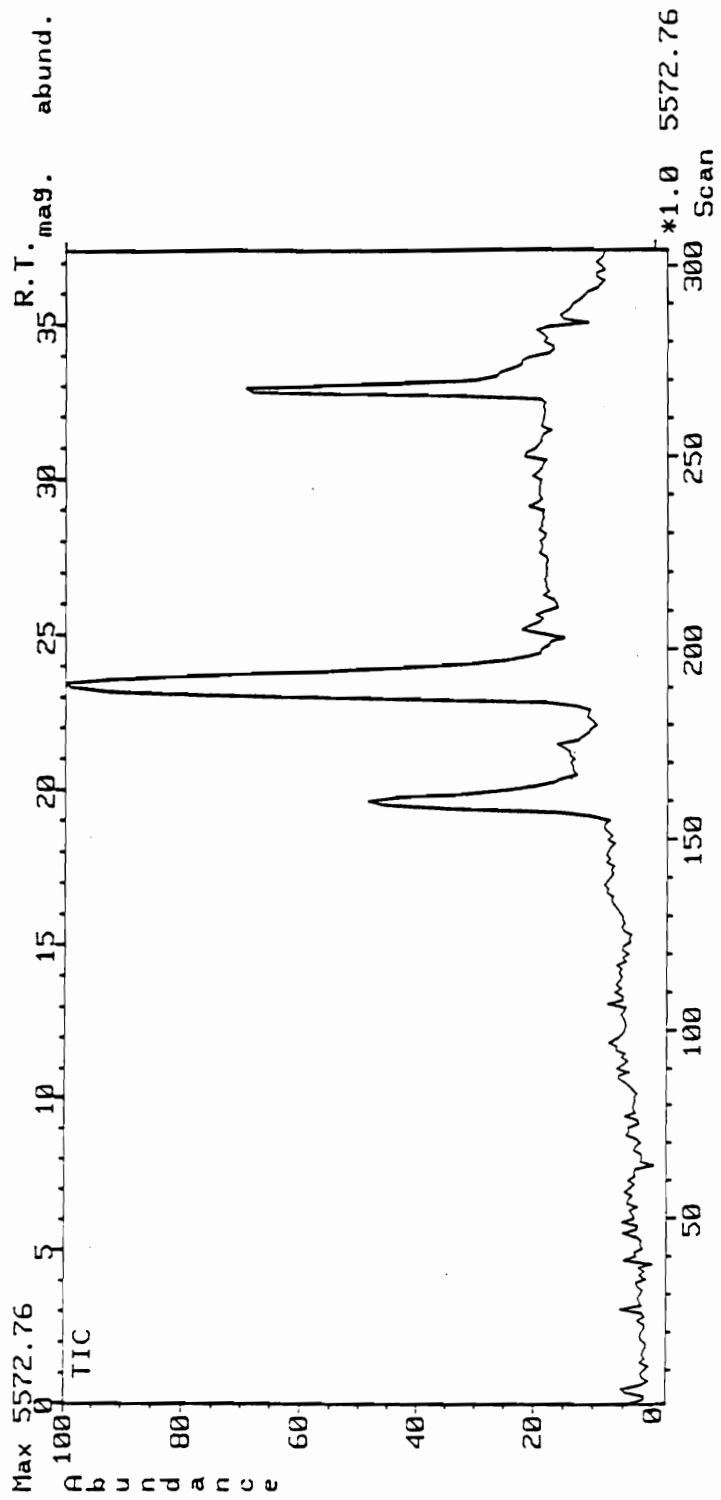


Figure 66. Total ion current plot of the chromatogram shown in Figure 65.

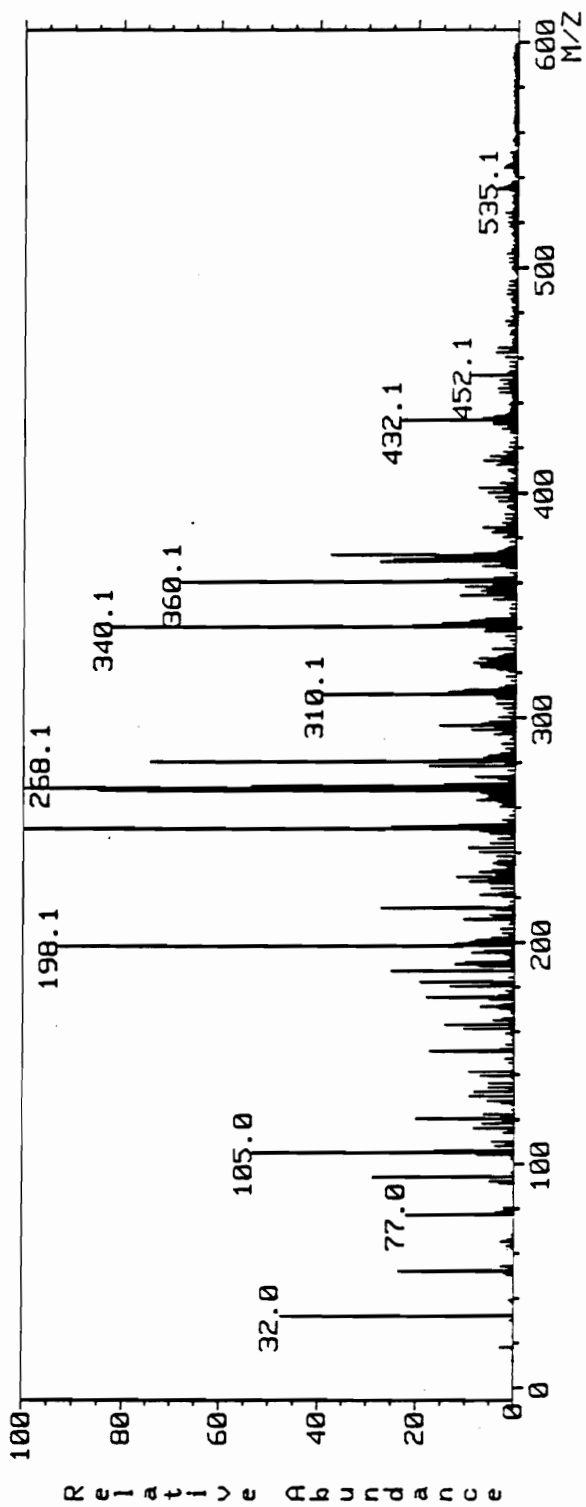


Figure 67. Mass spectrum (FAB) of component 1 of Figure 65.

ion at  $m/z$  of 250. Loss of  $CF_3$  from  $m/z$  of 267 and loss of  $HCF_3$  from  $m/z$  of 268 lead to the ion at 198.

These fragments have been observed previously in the MS/MS spectra of the  $m/z$  of 267 (from EI-generated ions) and 268 (from FAB-generated ions) species. The ion at  $m/z$  of 535 represents the hydrogen-bonded dimer of 1-(4-aminophenyl)-1-phenyl-2,2,2-trifluoroethan-1-ol. The identity of the ions at  $m/z$  of 280, 310, 340 and 372 is uncertain.

Component two (2) has a retention time of approximately 20 minutes and the corresponding FAB spectra is shown in Figure 68. This compound is remarkable in its similarity to component 1. The only obvious difference between the two components is the presence of an ion at  $m/z$  of 262 in the mass spectrum of component 2. Given the baseline separation of the two components it is possible that they represent closely related or perhaps isomeric structures.

Component three (3) has a retention time of approximately 23 minutes and the corresponding FAB spectra is shown in Figure 69. This component appears to be the product 3F-diamine. This is indicated by the protonated molecular ion at the  $m/z$  of 343. This is further supported by the ion at  $m/z$  of 250 which corresponds to the loss of an aniline group.

Component (4) has a retention time of approximately 31 minutes and the corresponding FAB spectra is shown in Figure 70. This component has a molecular weight of 423 amu as shown by the protonated molecular ion at the  $m/z$  of 424. The ion at the  $m/z$  of 354 corresponds to the loss of  $HCF$ . The ion at  $m/z$  250 is most likely the tertiary carbocation postulated previously. The  $m/z$  of 354, 276 and 105 ions present in this spectrum are quite similar to those observed in the MS/MS spectra of 423 (from EI-generated ions). The ion at 250 amu is also found in the MS/MS spectrum of 354 (from

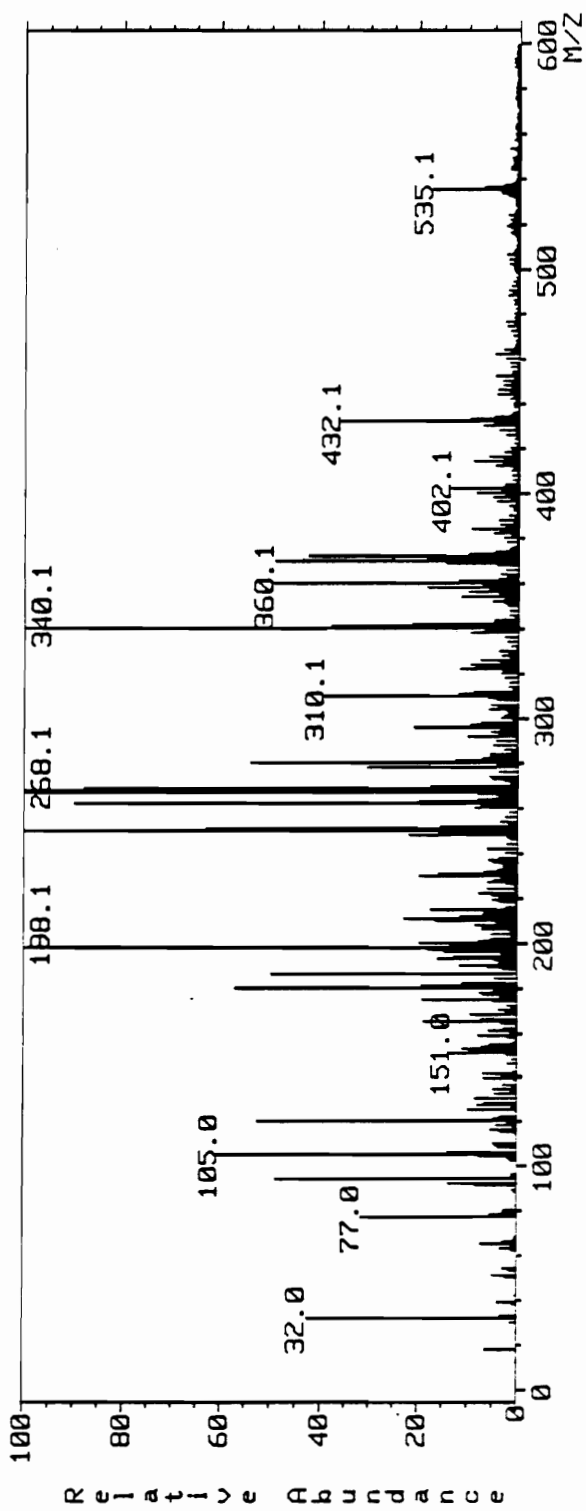


Figure 68. Mass spectrum (FAB) of component 2 of Figure 65.

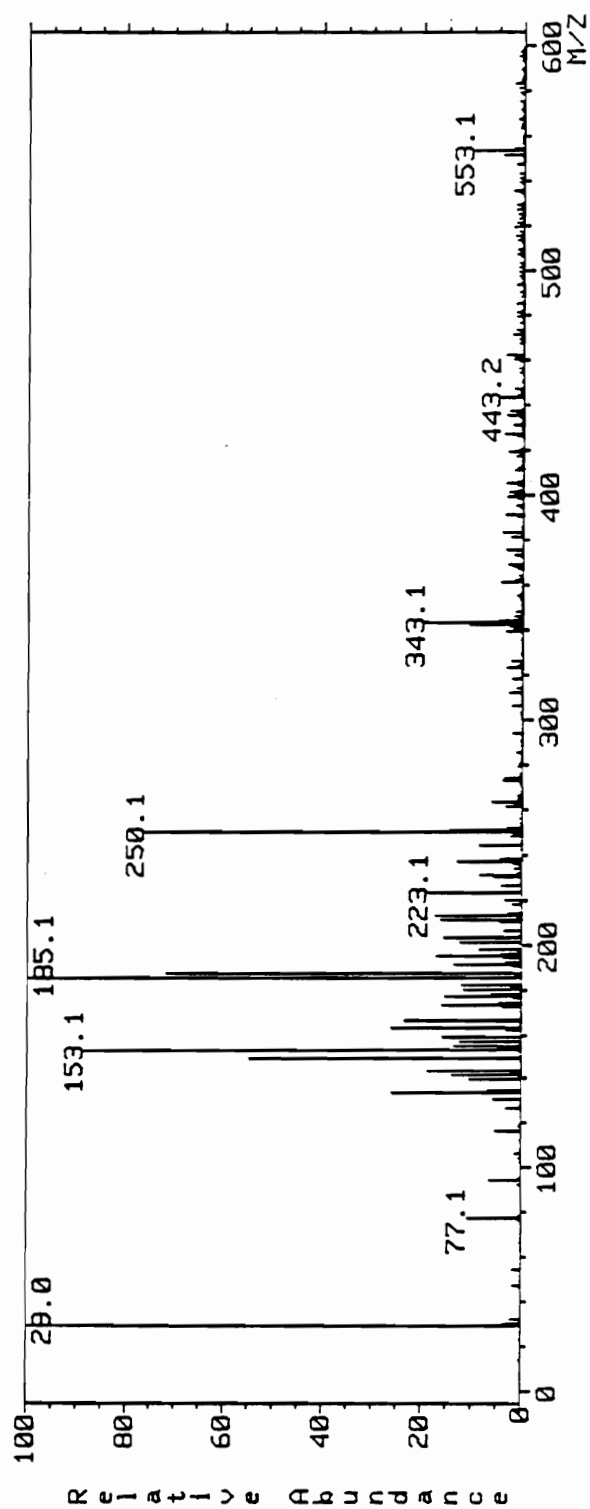


Figure 69. Mass spectrum (FAB) of component 3 of Figure 65.



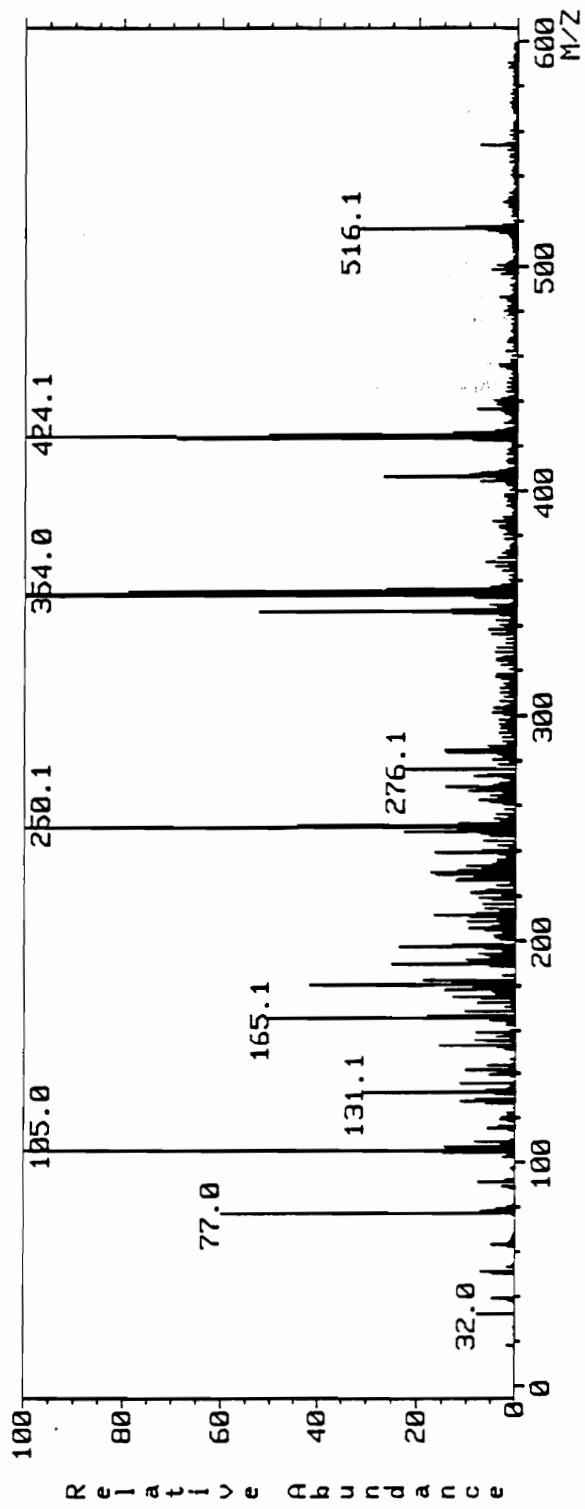


Figure 70. Mass spectrum (FAB) of component 4 of Figure 65.

FAB) but not in the MS/MS spectrum of 423 (even though a 354 ion is generated as a fragment).

#### 4.3.5 Conclusions from the preparation and purification of 1,1-Bis(4-aminophenyl)-1-phenyl-2,2,2-trifluoroethane

A new method for the purification of and a modified preparation route for 1,1-bis(4-aminophenyl)-1-phenyl-2,2,2-trifluoroethane have been developed. By use of mass spectrometry studies, by-products which can prevent polyimide preparation from contaminated  $\text{CF}_3$  diamine have been identified and eliminated by appropriate purification procedures. Figure 71 shows the reaction pathways available to the protonated 1-(4-aminophenyl)-1-phenyl-2,2,2-trifluoroethane-1-ol. Loss of a proton regenerates the alcohol which is monofunctional in the amino substituent. The presence of this compound in crude material and the examined sublimate is clearly shown. Also depicted in Figure 71 is 1-(4-aminophenyl)-1-phenyl-1-(3-trifluoroacetylphenyl)-2,2,2-trifluoroethane. This compound is also clearly shown to be in the crude material and the examined sublimate. As with the alcohol by-product, this material is mono-functional in the amino substituent and would also be a strong chain termination agent in an attempted polyimide preparation. By liquid chromatographic measurement and gravimetric yield based on the sublimate weight, these two compounds represent approximately five to seven percent of the yield of crude 3F-diamine. Other likely by-products are dehydration products of the alcohol. Monomer prepared by this route has been used with success in the preparation of polyimides (136). Controlled molecular weight soluble polyimides have been prepared with pyromellitic dianhydride (PMDA), biphenyl dianhydride (BPDA) and hexafluoroisopropylidene-2,2-bis(phthalic acid anhydride)[6F-DA].

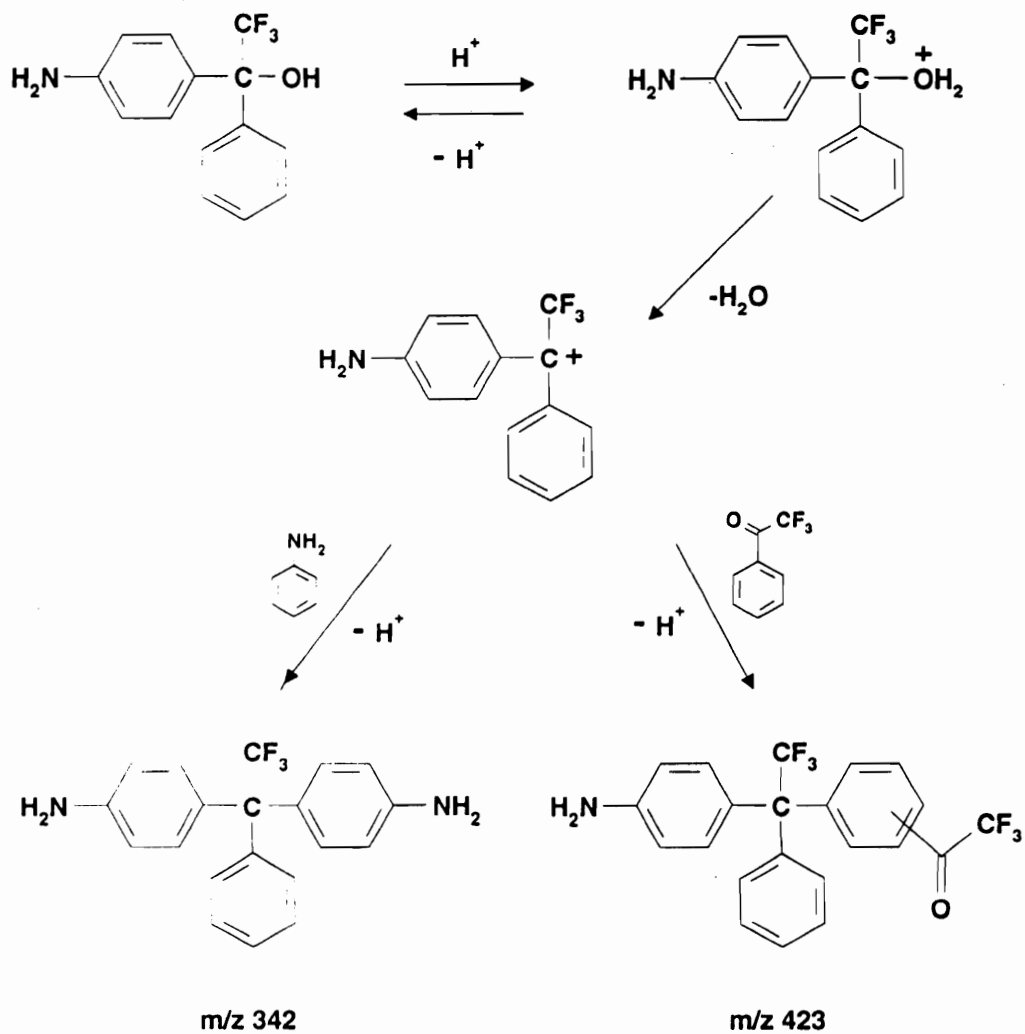
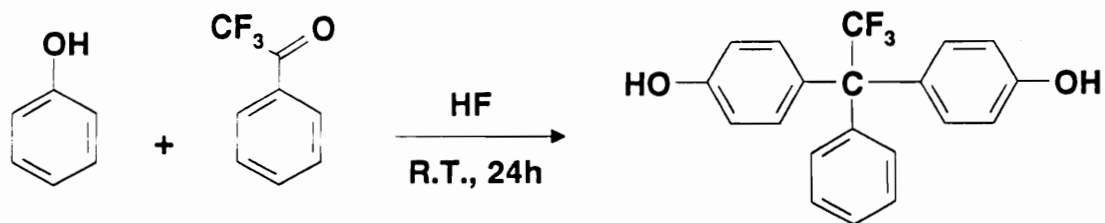


Figure 71. Mechanism for multiple product formation in the synthesis of 1,1-bis(4-aminophenyl)-1-phenyl-2,2,2-trifluoroethane.

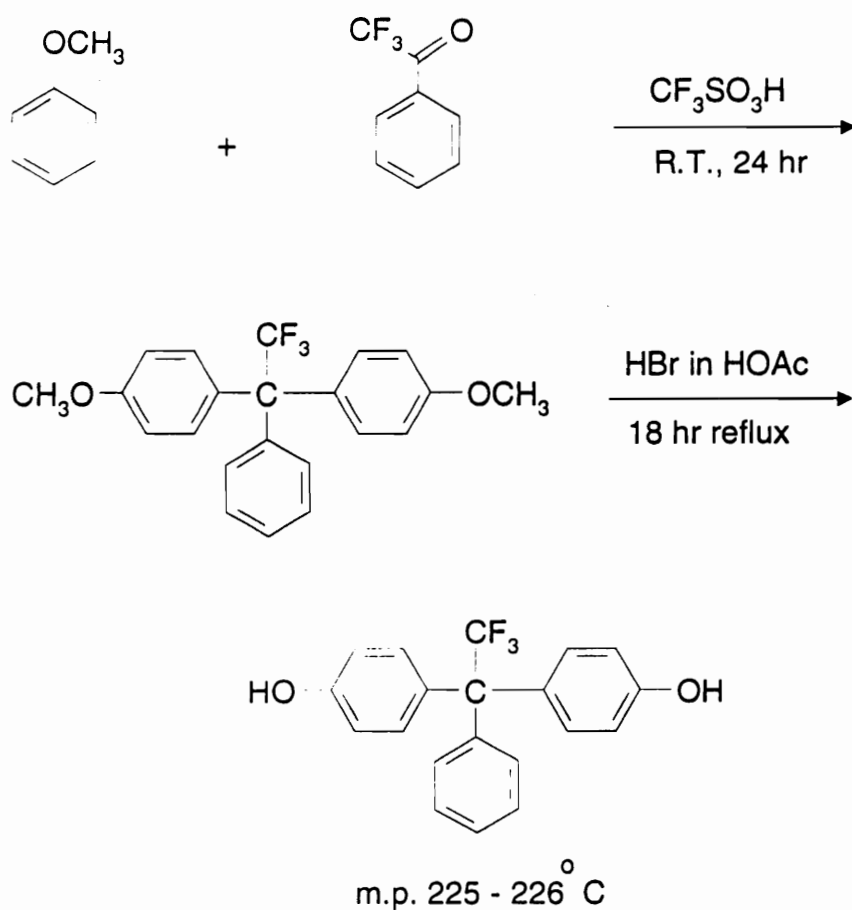
#### 4.3.6 Preparation and characterization of 1,1-Bis(4-hydroxyphenyl)-1-phenyl-2,2,2-trifluoroethane

The first reported preparation of this phenol was that of Vinogradova, *et al.* in 1963 (149). As seen in Scheme 5, trifluoroacetophenone was treated with phenol in anhydrous hydrofluoric acid to yield 1,1-bis(4-hydroxyphenyl)-1-phenyl-2,2,2-trifluoroethane (3F bis-phenol). Korshak, *et al.* first published studies on the preparation of polyarylates formed from the condensation polymerization of 3F bis-phenol with terephthaloyl chloride in 1965 (185). Data were presented to substantiate claims of higher thermal stability and enhanced solubility in organic solvents. No additional synthetic reports were found until 1981 when Frosch, *et al.* patented a procedure (Scheme 6) based on the preparation and subsequent hydrolysis of 1,1-bis-(4-methoxyphenyl)-1-phenyl-2,2,2-trifluoroethane (148). No subsequent synthetic citations could be found.

The synthetic strategy utilized in work presented here was the same as used for the preparation of 3F-diamine from aniline. A modified hydroxalkylation route (122) was chosen as a practical route which would allow large scale preparation under laboratory conditions. As shown in Scheme 7, trifluoroacetophenone is protonated with trifluoromethanesulfonic acid and the electrophilic ion produced reacts with phenol to produce 3F bis-phenol. The reaction could be run in bulk with no added solvent or a solvent could be used to facilitate mixing and transfer. As the protonation step is highly exothermic, preparation in bulk was abandoned. Product was obtained in good yield but was often dark and had a lower melting point. Extensive trituration with methylene chloride or tetrachloroethylene was needed to produce higher purity, high melting 3F bis-phenol by the bulk procedure.

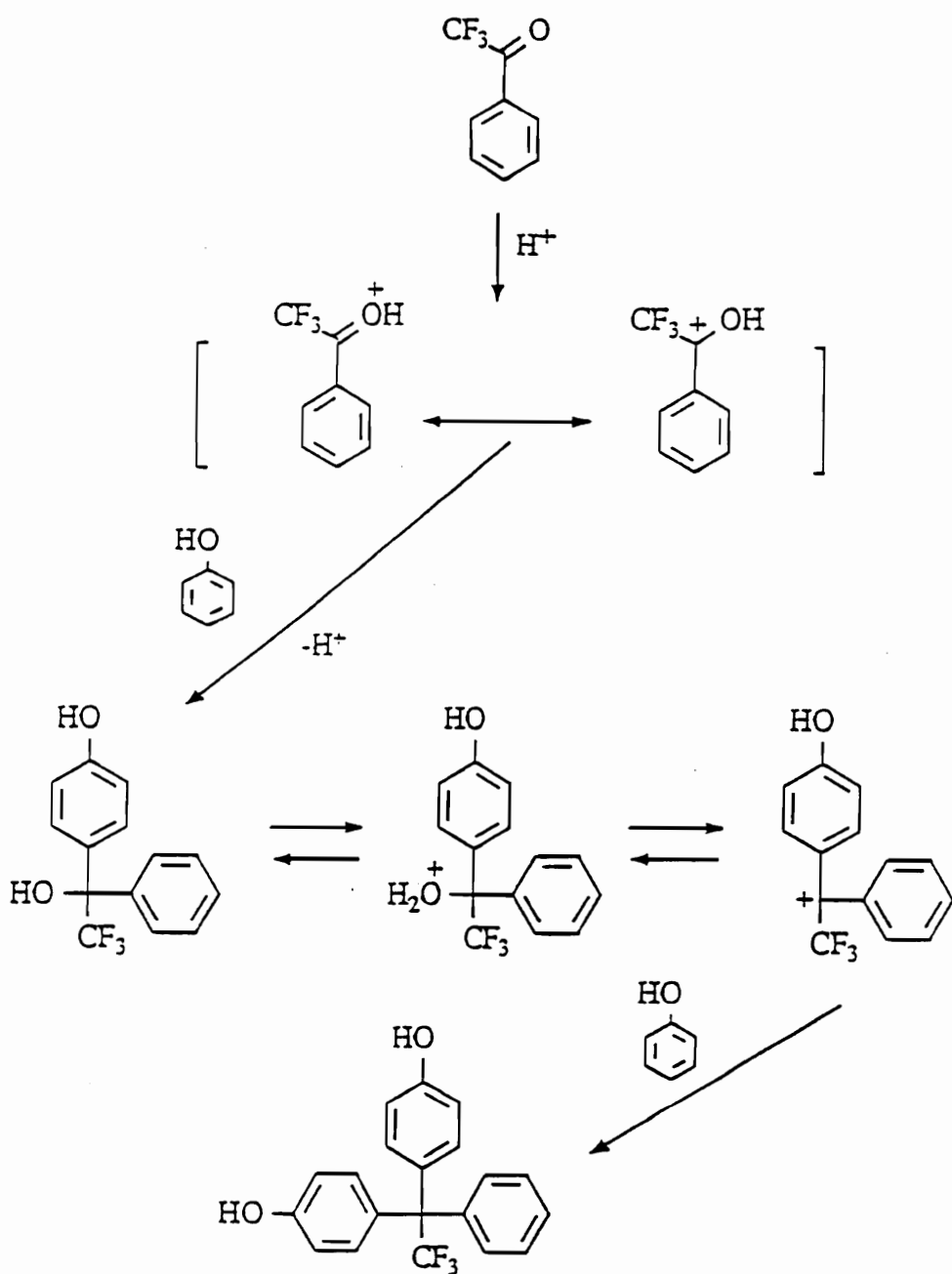


Scheme 5. Hydrogen fluoride mediated preparation of 1,1-bis(4-hydroxyphenyl)-1-phenyl-2,2,2-trifluoroethane.



R. A. Frosh, W. D. Kray, and R. W. Rosser, U.S. Patent 4,307,024, Dec. 22, 1981.

Scheme 6. Preparation of 1,1-bis(4-hydroxyphenyl)-1-phenyl-2,2,2-trifluoroethane by the Frosh method.



Scheme 7. Direct preparation of 1,1-bis(4-hydroxyphenyl)-1-phenyl-2,2,2-trifluoroethane.

Preparation in solution, however, gave better thermal control. The reactants were quite soluble in chlorinated solvents and the product had minimal solubility. As product formed, it rapidly precipitated and was less available for participation in undesirable side reactions. As the exothermic reaction proceeded, solvent reflux temperatures established the upper temperature limit which the reaction system could reach. Methylene chloride was chosen as a particularly good solvent as its low boiling point prevented thermal damage to the purity and the product 3F bis-phenol was very insoluble. Simple filtration of crude product followed by hot water treatment to remove excess phenol and trifluoromethanesulfonic acid residues produced a very pure sample of 3F bis-phenol with a melting point that exceeded literature values substantially.

#### 4.3.7 Mass Spectrometric Investigations

In light of the findings in the characterization of monofunctional contaminants in 3F-diamine, a study was undertaken to explore the possibility of contamination by similar products in the 3F bis-phenol. As traditional spectroscopic techniques such as NMR and IR often fail to identify low level contaminants of similar structure, an in depth mass spectral investigation was carried out.

The instrumentation and the conditions for collection of electron impact and fast atom bombardment analysis data were identical to that described in the 3F-diamine study. The MS/MS experimental conditions were also as previously described. The samples evaluated were those taken from synthetic example number 14. The purified product was used as is and a 25 mL sample of the reaction mixture suspension was taken prior to product isolation and the solvent removed under reduced pressure. The waxy solid obtained was vacuum dried at 0.1 torr and 50°C for 24 hours. An additional 25 mL sample of the reaction mixture suspension was filtered to remove product and solvent

was removed under reduced pressure (0.1 torr) from the clear filtrate. The gum obtained was dried further at 0.1 torr and 50°C for 24 hours. These three samples were examined as pure product, crude product, and methylene chloride residues.

The EI spectrum of pure product is shown in Figure 72. The molecular ion at the  $m/z$  of 344 and the expected loss of  $CF_3$  to give the  $m/z$  of 275 are the predominant ions. It is noteworthy that there are no substantial ions above the  $m/z$  of 344. Figure 73 is the EI spectrum of the crude product. In this spectrum, the molecular ion is protonated  $(M+H)^+$  to produce a  $m/z$  of 345. This spectrum also shows a large number of contaminants at molecular weights above and below the molecular ion.

Figure 74 is the EI spectrum of the methylene chloride residue. It shows that a large number of chemical species are present. The molecular ion appears at the  $m/z$  of 344 and the peak representing the loss of the  $CF_3$  moiety appears at the  $m/z$  of 275. A large number of ions which do not appear in either of the former spectra suggest that an examination of the methylene chloride residue may produce a better understanding of the by-products formed.

A MS/MS study was carried out on selected ions produced in the EI spectrum of the methylene chloride extract. Figure 75 is the MS/MS spectrum of the  $m/z$  of 344. This spectrum clearly shows the molecular ion of  $m/z$  of 344 which corresponds to 3F bis-phenol.

Peaks at  $m/z$  of 275 and 324 represent respectively the loss of  $CF_3$  and the loss of HF. The latter is a low intensity peak. These results support the assigned structure, 1,1-bis(4-hydroxyphenyl)-1-phenyl-2,2,2-trifluoromethane, to the reaction product.



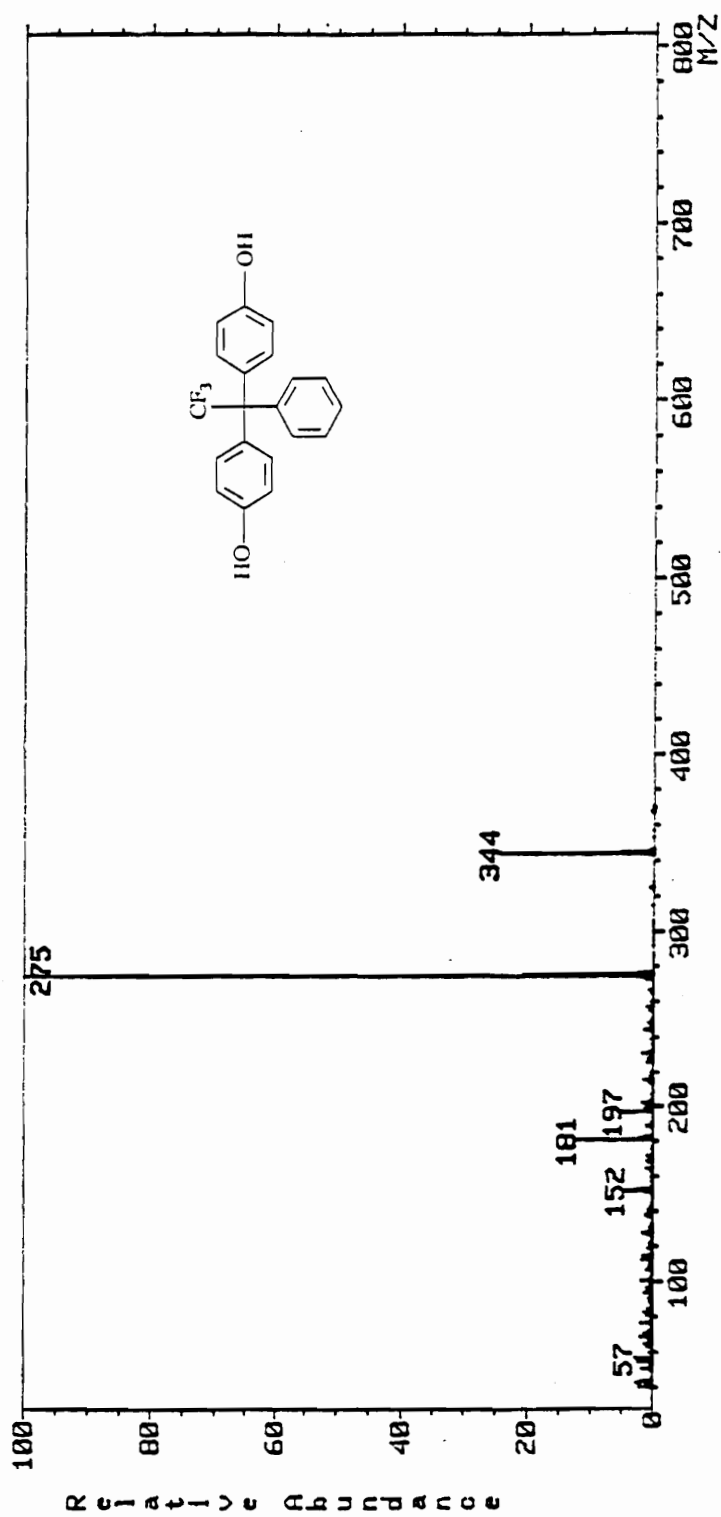


Figure 72. Mass spectrum (EI) of 1,1-bis(4-hydroxyphenyl)-1-phenyl-2,2,2-trifluoroethane.

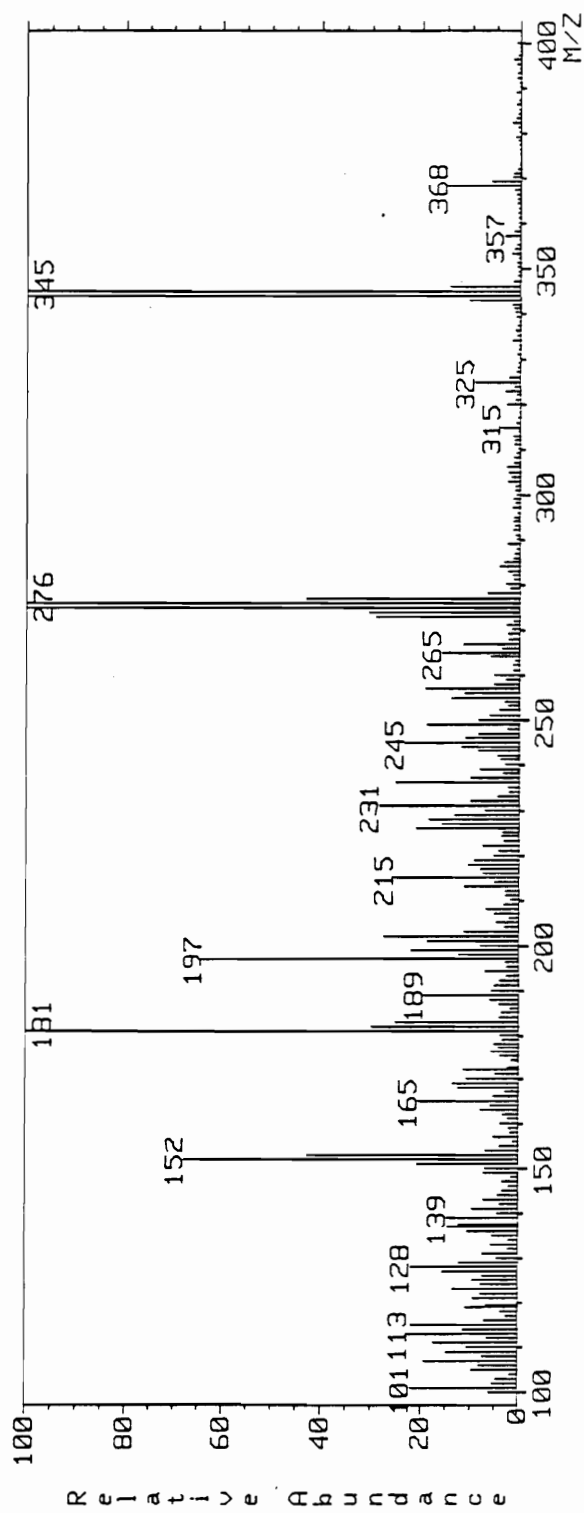


Figure 73. Mass spectrum (EI) of crude 1,1-bis(4-hydroxyphenyl)-1-phenyl-2,2,2-trifluoroethane.

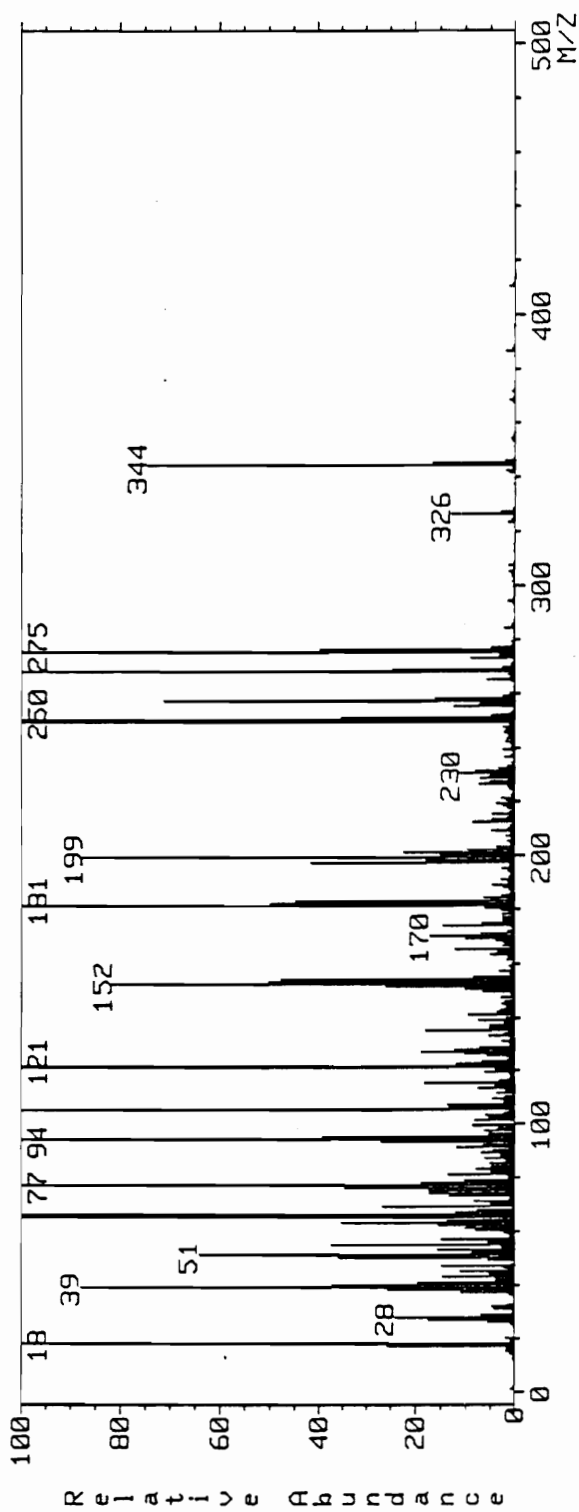


Figure 74. Mass spectrum (EI) of the methylene chloride residue from the isolation of 1,1-bis(4-hydroxyphenyl)-1-phenyl-2,2,2-trifluoroethane.

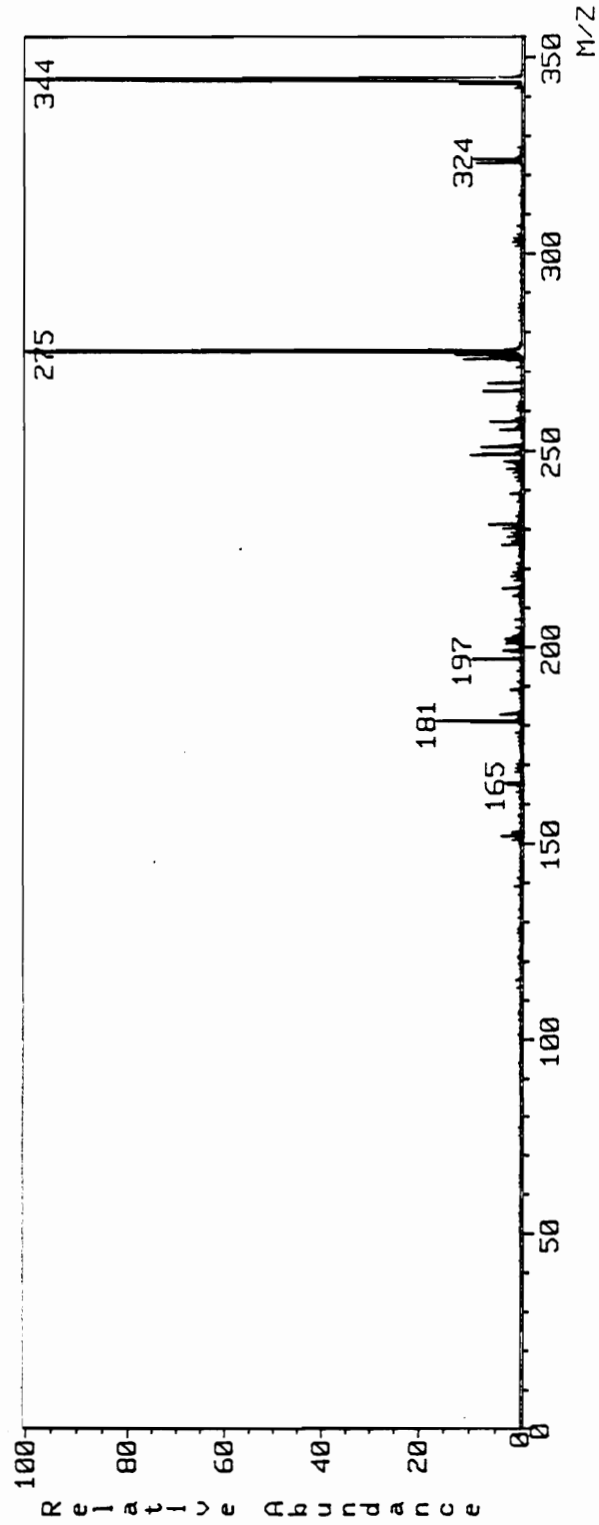


Figure 75. MS/MS of m/z 344 of the spectrum shown in Figure 74.

Figure 76 is the MS/MS of the  $m/z$  268. The most prominent feature of this spectrum is the loss of water, which probably occurs by loss benzylic hydroxyl along with abstraction of a phenolic ring proton. These data would suggest the proposed structure of

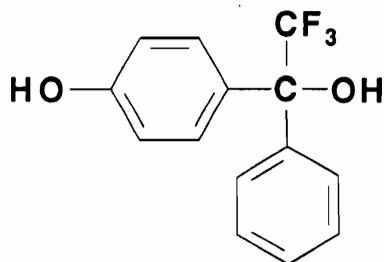
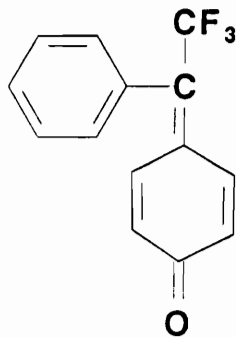


Figure 77 is the EI spectrum of the ion of  $m/z$  of 249. The structure of this ion is uncertain. A loss of 50 amu to yield an ion of  $m/z$  of 199 would mathematically explain the loss of  $CF_2$ . A plausible mechanism for this assignment is not currently available.

Figure 78 is the MS/MS of the ion of  $m/z$  of 250. The major fragment at  $m/z$  181 represents the fragment resulting from the loss of  $CF_3$ . This spectrum is contaminated with the ion and fragments of the  $m/z$  of 249. Attempts to resolve  $m/z$  of 249 and 250 have failed, leading one to suspect that the  $m/z$  of 249 is formed by EI fragmentation of  $m/z$  of 250. A structure proposed for the  $m/z$  of 250 is shown below.



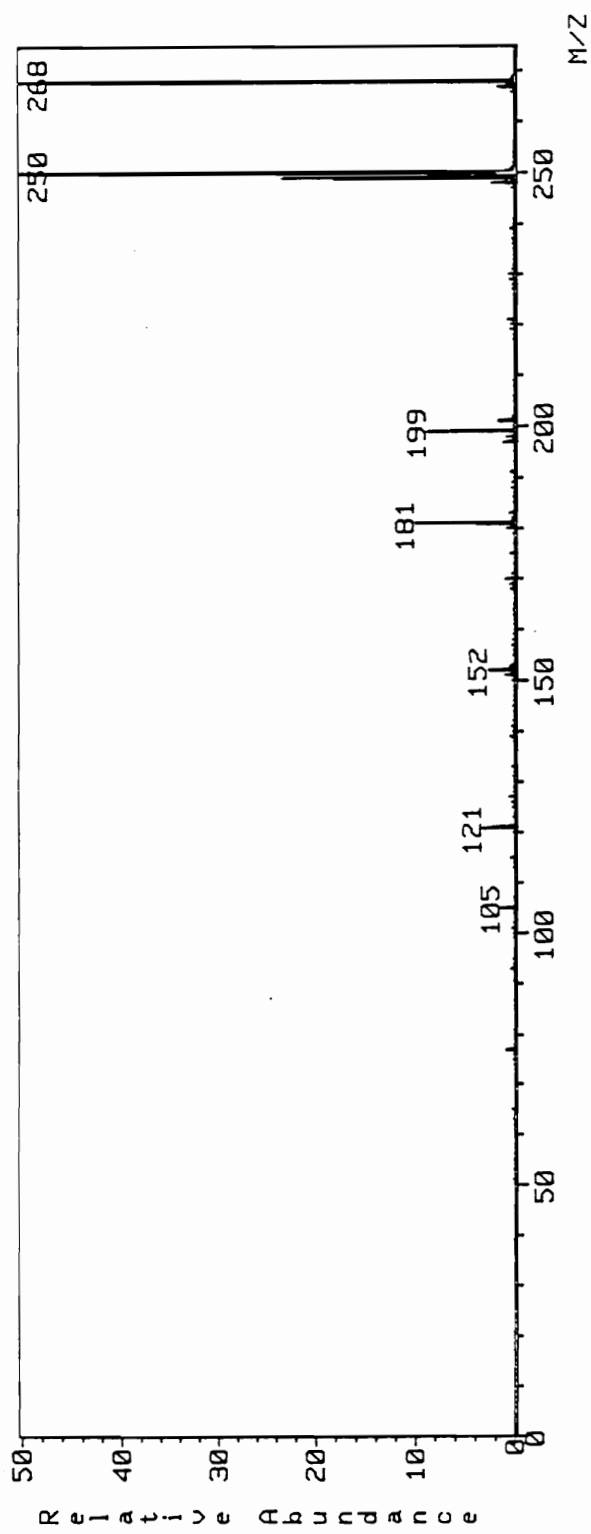


Figure 76. MS/MS of m/z 268 of the spectrum shown in Figure 74.

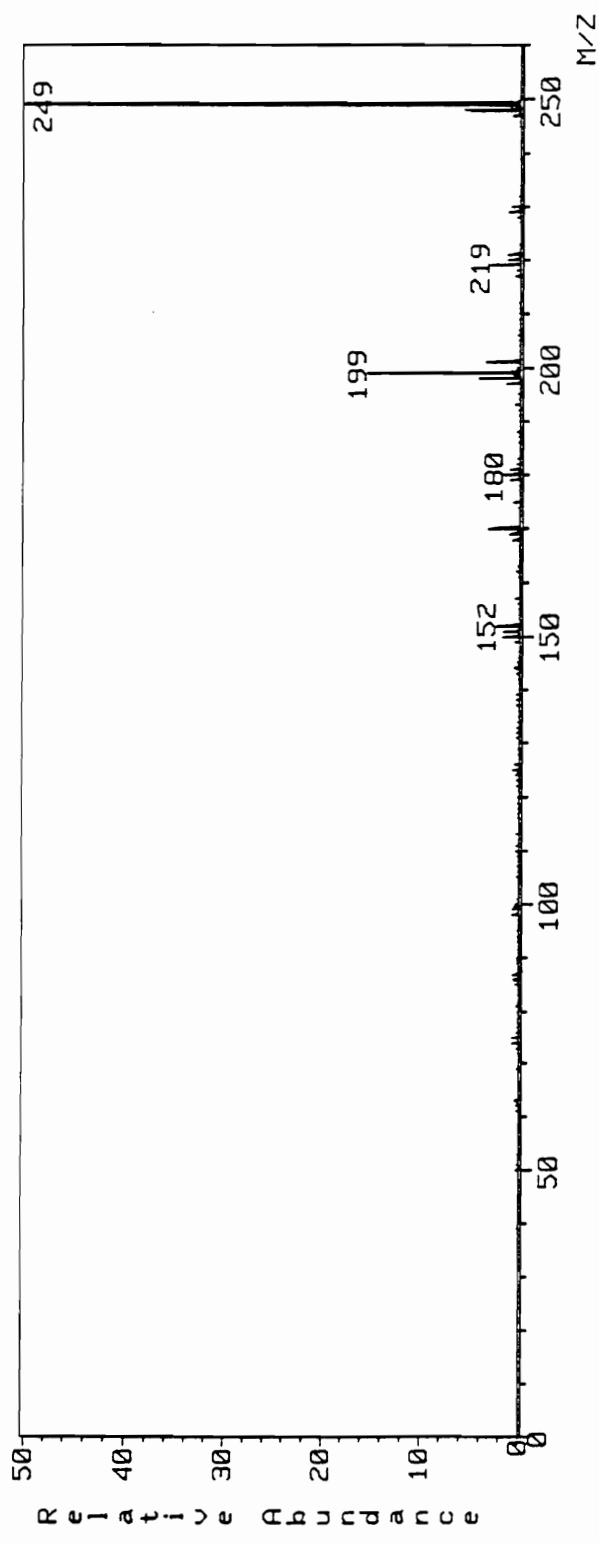


Figure 77. MS/MS of m/z 249 of the spectrum shown in Figure 74.

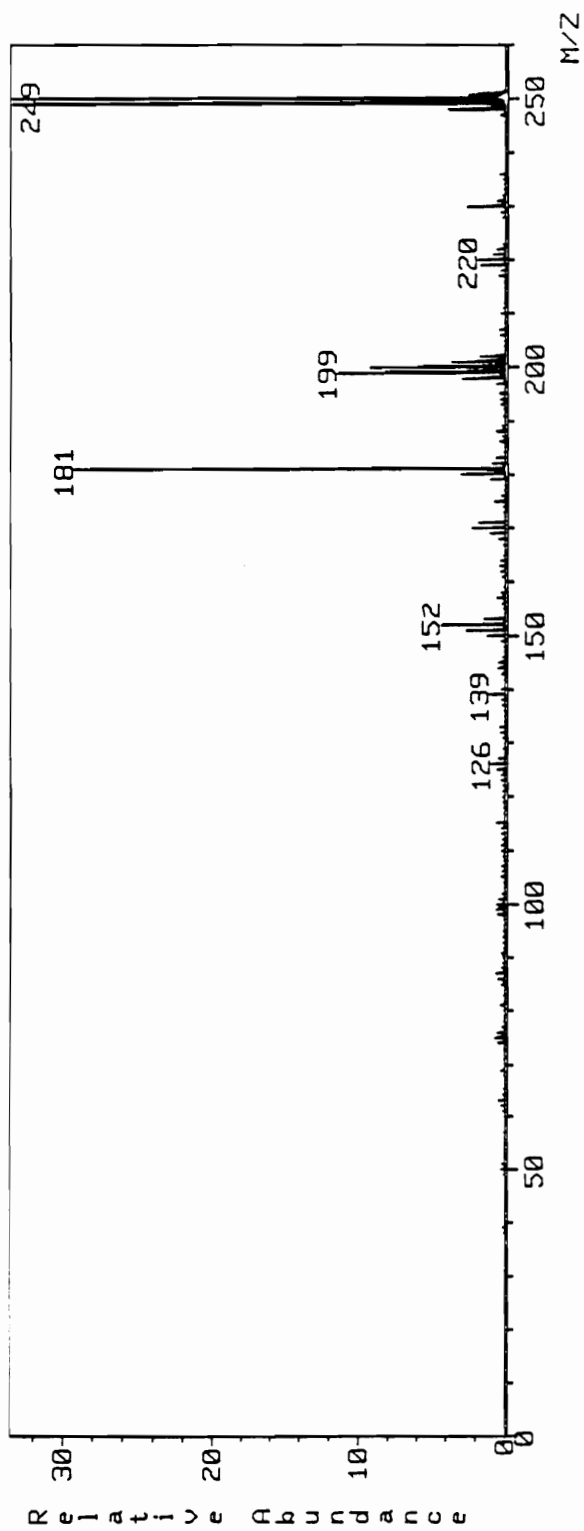
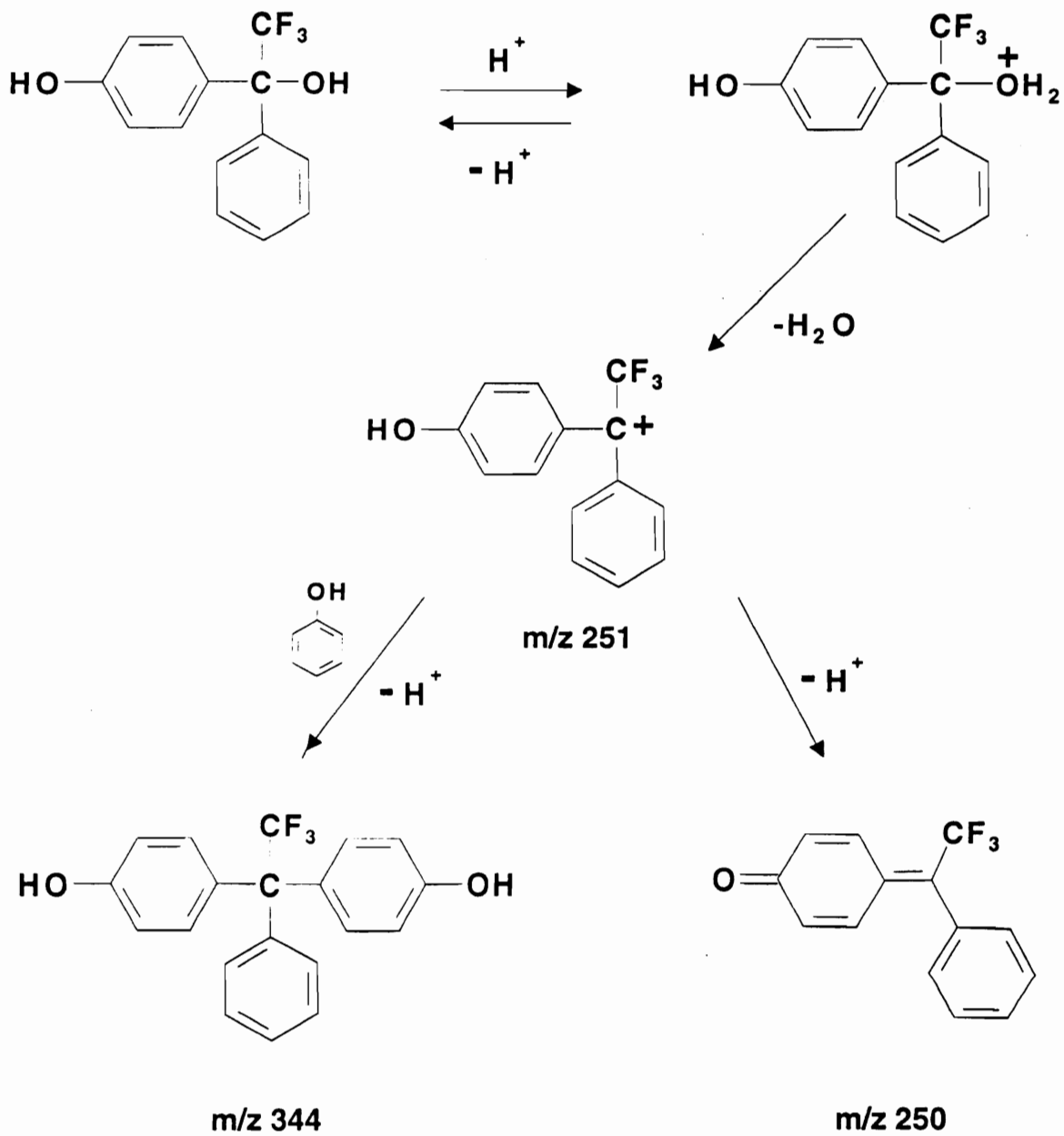


Figure 78. MS/MS of m/z 250 of the spectrum shown in Figure 74.



#### 4.3.8 Conclusions from the Preparation and Purification of 1,1-Bis(4-hydroxyphenyl)-1-phenyl-2,2,2-trifluoroethane

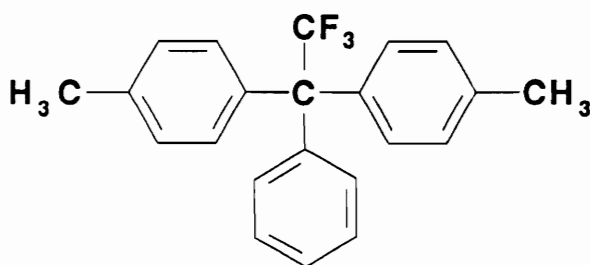
As seen previously in the discussion of 3F-diamine by-product chemistry, 3F bisphenol prepared by the hydroxyalkylation route directly from phenol, is contaminated with by-products. As shown in Scheme 8 the protonated 1-(4-hydroxyphenyl)-1-phenyl-2,2,2-trifluoroethan-1-ol can lead to multiple products. Loss of a proton will yield the substituted ethanol which has only a single phenol moiety. This component would serve as a very effective chain termination agent in polymerizations which require a bifunctional monomer. The protonated species may also dehydrate to yield a carbocation which may rearrange to yield a quinoid product. While this may not interfere with condensation based polymerizations by reaction, it will interfere with correct stoichiometry acting as a diluent.



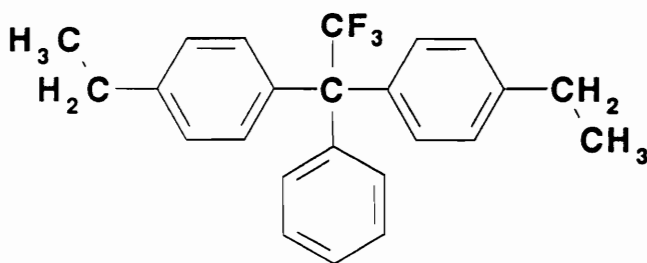
Scheme 8. Alternate product formation from 1-(4-hydroxyphenyl)-1-phenyl-2,2,2-trifluoroethan-1-ol.

#### 4.3.9 Additional Trifluoromethyl Monomers Produced by the Hydroxyalkylation Reaction

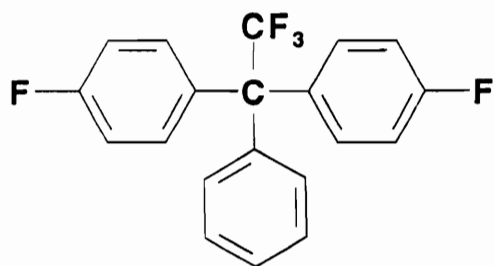
The scope of the hydroxyalkylation reaction of trifluoroacetophenone has been extended by the preparation of additional synthetic examples. 1,1-bis(4-methylphenyl)-1-phenyl-2,2,2-trifluoroethane was readily prepared using toluene as the reactive aromatic substrate.



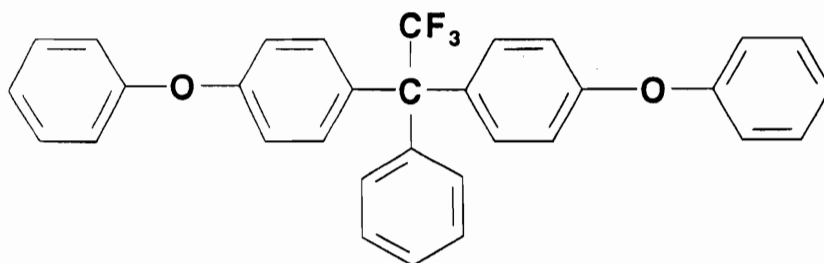
The high yield and purity obtained suggests it could be a useful intermediate to be oxidized to the corresponding dicarboxylic acid and in turn be polymerized to yield novel polyesters and polyamides. The ethyl benzene analogue, 1,1-bis(4-ethylphenyl)-1-phenyl-2,2,2-trifluoroethane was much more difficult to prepare.



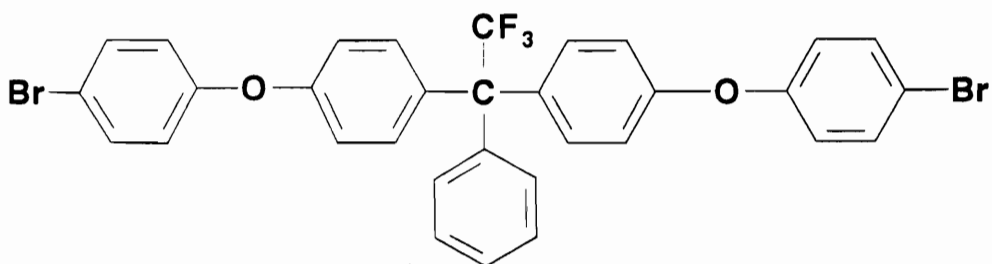
Isolated yields of pure compound were quite low. Reaction of fluorobenzene with trifluoroacetophenone resulted in 1,1-bis(4-fluorophenyl)-1-phenyl-2,2,2-trifluoroethane in high yield and high purity.



This compound may be used to prepare novel poly (arylene ethers) by reaction with suitable bis-phenols. Two compounds were also prepared from diphenyl ether and 4,4'-dibromodiphenyl ether, respectively. 1,1-bis(4-phenoxyphenyl)-1-phenyl-2,2,2-trifluoroethane

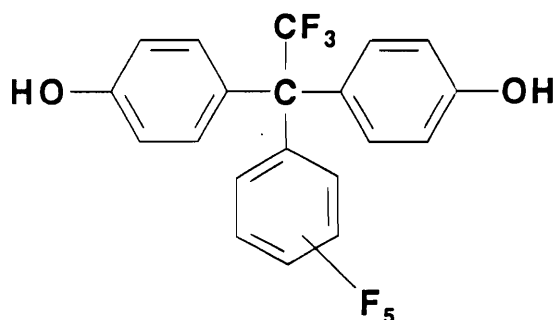


and 1,1-bis(4-bromo-4-phenoxy-phenyl)-1-phenyl-2,2,2-trifluoroethane



were also synthesized in high yield and high purity. These systems are quite interesting and may serve as the starting point for the preparation of novel diamine monomers. 2,2-bis[4-(4-amino-phenoxy)phenyl]hexafluoropropane (4-BDAF) is a commercially available monomer currently utilized to synthesize high performance polyimides. Nitration and reduction of these diphenyl ether adducts may lead to economically attractive novel "3F" analogues of 4-BDAF.

The preparation of 1,1-bis(4-hydroxyphenyl)-1-pentafluorophenyl-2,2,2-trifluoroethane proceeded in moderate yield based on the use of octafluoroacetophenone.



The high fluorine content of this bis-phenol may prove to be of value in the preparation of low dielectric poly (arylene ethers) for optical use.

#### 4.3.10 CONCLUSIONS

A study has been completed on the preparation of 1,1-bis(4-aminophenyl)-1-phenyl-2,2,2-trifluoroethane (3F-diamine) and 1,1-bis(4-hydroxyphenyl)-1-phenyl-2,2,2-trifluoroethane (3F-bis-phenol). The pioneering work of Kray and Rosser (122) utilizing the hydroxyalkylation reaction of 2,2,2-trifluoroacetophenone with active aromatic systems under acid catalysis has been expanded to include the direct preparation of 3F bis-phenol. An extensive mass spectrometric study has been completed for both systems.

This study has assisted in the optimization of purification and isolation of "monomer grade" 3F-diamine and 3F bis-phenol. These practical procedures have been scaled for routine preparation of each of these interesting monomers in our laboratories and further extensive study is underway using these systems for the preparation of high performance thermooxidatively stable thermoplastics. The general utility of this synthetic route has been demonstrated by the preparation of a number of additional examples of 1,1,1-triaryl-2,2,2-trifluoroethanes. Exploration of the chemistry of many of these systems is also under current evaluation.

## 5.0 PHOSPHINE OXIDE MONOMER INVESTIGATIONS

### 5.1 INTRODUCTION AND BACKGROUND

Polymer chemists have for many years been interested in the incorporation of phosphorus into organic polymers. The similarity of carbon and phosphorus in preferred coordination number of four and their similar electronegativity make their interchange in a polymer structure appealing. The most important benefit that phosphorus has offered is the addition of fire-resistance (186). One would not expect drastic change in the general features of macromolecules as a consequence of phosphorus incorporation. There are several organophosphorus chemical systems from which polymer chemists can select. It is somewhat surprising that the history of phosphorus containing macromolecules is quite short and the number of references to phosphorus containing engineering polymers is very limited.

Table 7 depicts the phosphorus systems that have been reported in the polymer literature. This table illustrates phosphorus in all of its common oxidation states from phosphine through phosphates. As one would expect, polymers containing the lower phosphorous oxidation states are quite prone to oxidation. Not included in this table are phosphorous-nitrogen systems. For this work, the focus is on phosphorous carbon bonds located in the polymer backbone. The phosphites and phosphates are included in Table 7 for comparison with polymers which contain phosphorous-carbon bonds in the backbones. While many examples of polymers incorporating the phosphite and phosphate systems are known, as a class, these polymers are very prone to hydrolytic attack. Phosphorous-carbon bond systems are very similar to poly(arylene ether)s in hydrolytic stability whereas phosphorous-oxygen bond systems are similar to polyesters.

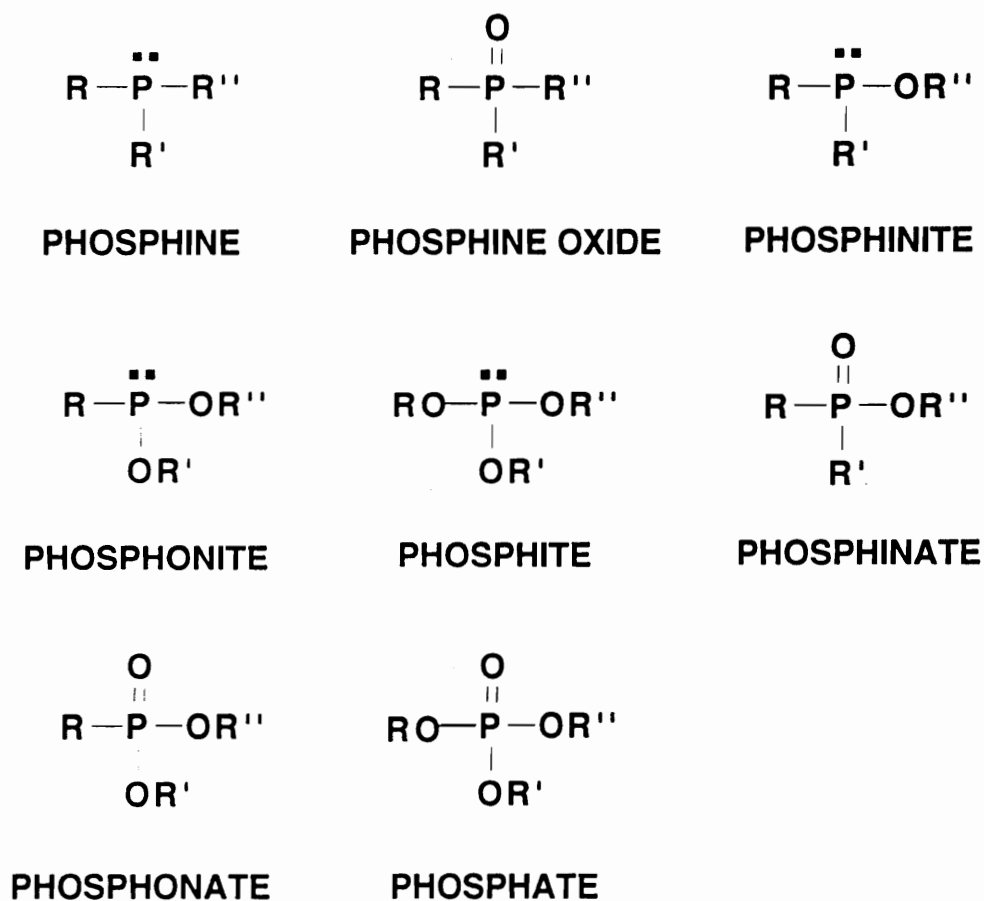
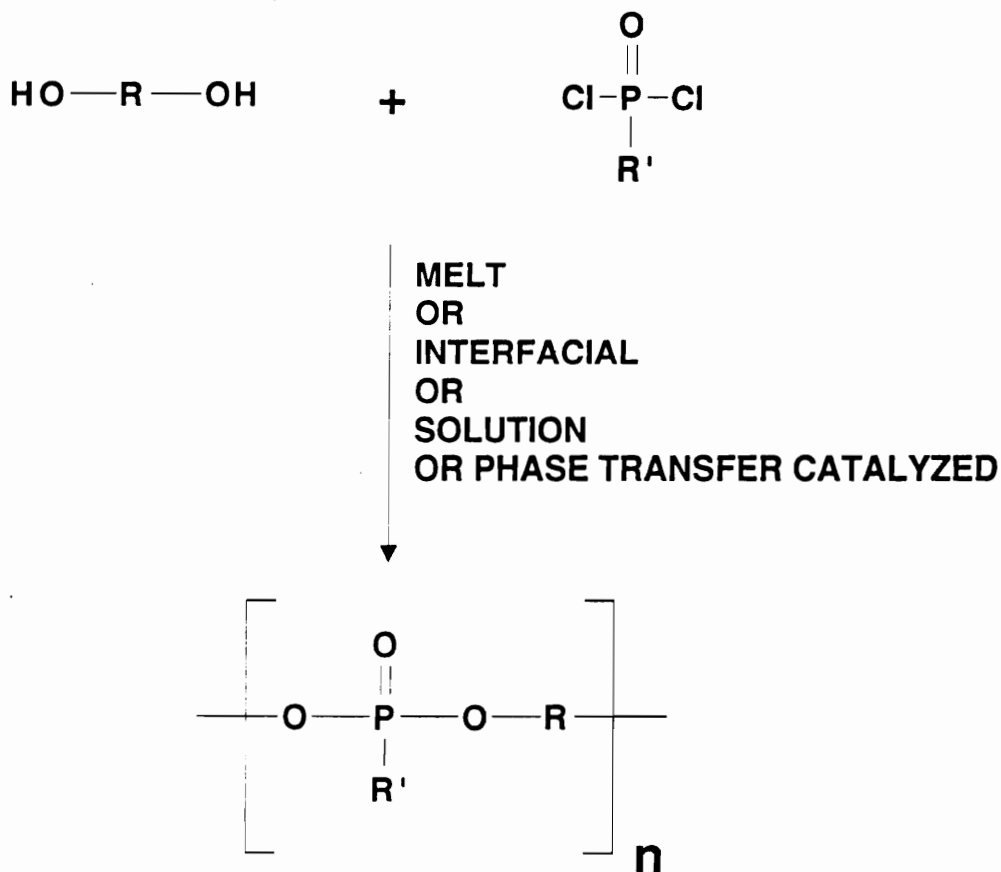


Table 7. Types of Organophosphorus Linkages.

Unsuccessful attempts have been made at chain polymerizations of phosphorous containing unsaturated compounds (187-188) as well as step growth polymerizations (189). These attempts failed due to unacceptable side reactions which present the formation of useful high molecular weight products. Since these reviews in the 1960's, examples of step and chain mechanisms that yield high molecular weight polymers have been elusive. Reported polycondensations which form phosphorous-oxygen bonds have been troubled by hydrolysis problems (190-194). A polyphosphonate synthesis is shown in



Scheme 9. The techniques of melt (195), solution (195,196), interfacial (197) and phase transfer (188, 195, 199) polymerization in each of these cases have failed to give high molecular weight products in acceptable yields. The low molecular weight products obtained have been used primarily as flame retardant additives for



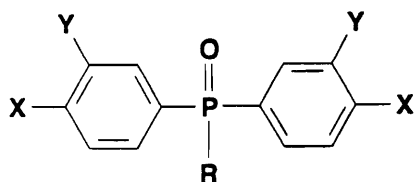
Scheme 9. Polyphosphonate synthesis.

other polymer systems such as polyesters and polyamides. Numerous patents exist in this area, many of them foreign disclosures (195). As previously mentioned, hydrolytic stability is a concern with all of the polymers which contain single bond phosphorous-oxygen linkages (200). The limiting factor for the formation of phosphorous-carbon

linkages has been a lack of appropriate step-growth mechanisms available for polymer formation.

Successful incorporation of phosphorous-carbon linkages in the main chain can occur only through classic step-growth mechanisms. The difficulty in preparing these types of polymers is the lack of suitable monomers. This section will address the successful procedures for monomer synthesis with emphasis on the phosphine oxide system.

A very attractive feature of the phosphine oxide system is the high thermal stability achieved relative to that of traditional organic polymers. It has been well established and long known that triphenyl phosphine oxide is a stable material at 700°C (201). The monomers represented in Figure 79 are very attractive for the preparation of poly(arylene ether)s, polycarbonates, polyamides, polyesters, and polyimides.



**X = F, OH, COOH, NH<sub>2</sub>, COO**

**Y = H, OH, NH<sub>2</sub>, COOH, CO**

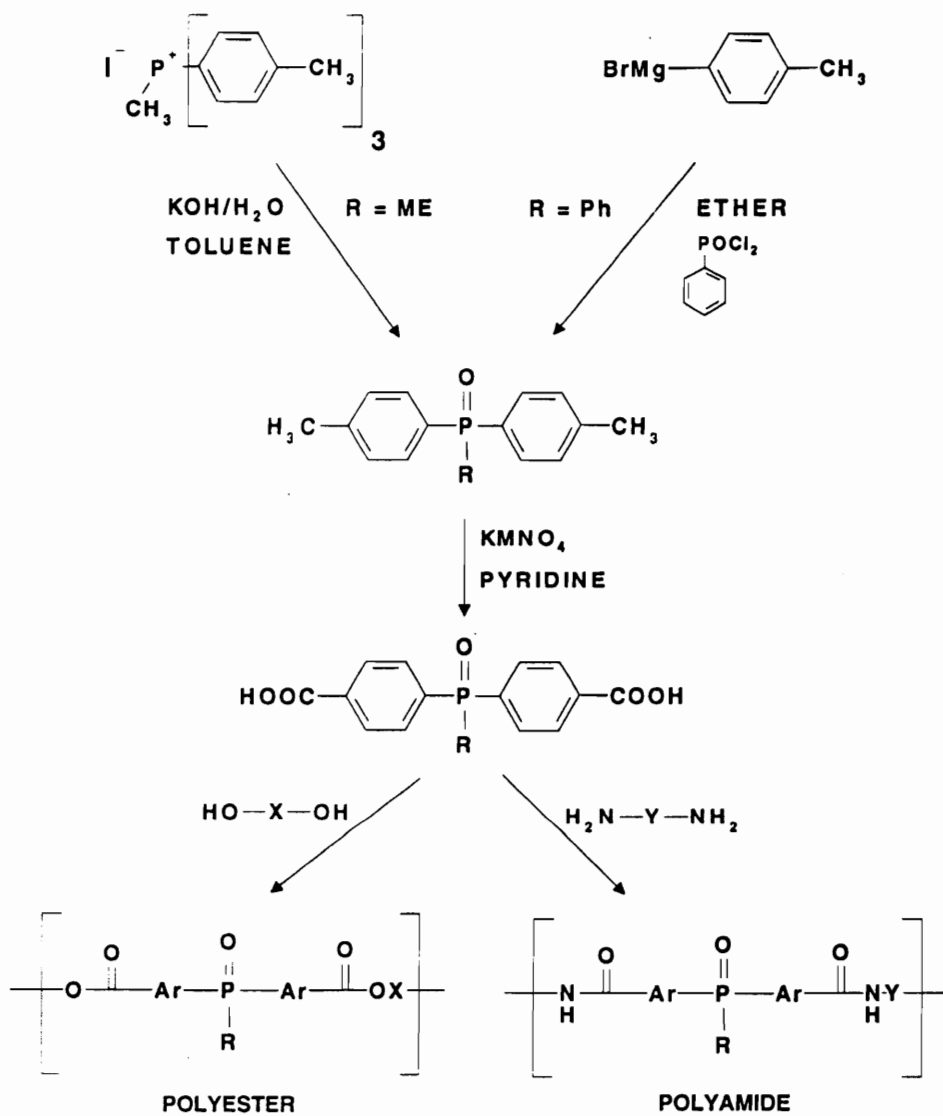
**R = ALIPHATIC, AROMATIC**

**TYPICALLY CH<sub>3</sub> or Ph**

Figure 79. Phosphine oxide monomers.

As early as the 1950's, Morgan and Herr (202,203) examined the potential of polyester fiber production by polymerizing bis(4-carboxyphenyl)phenylphosphine oxide

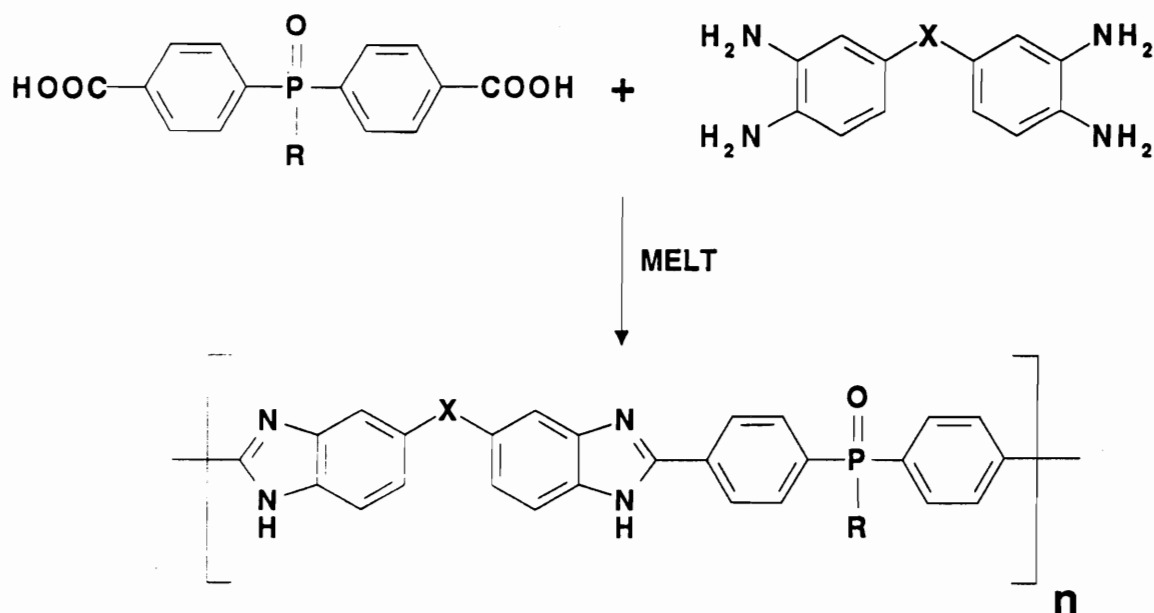
with alcohols to produce polyesters. The process, illustrated in Scheme 10, shows the synthetic strategy used.



Scheme 10. Polyester formation from bis(4-carboxyphenyl)phenylphosphine oxide.

Decomposition of quaternary phosphonium salts or Grignard procedures were used to prepare bis(4-methylphenyl)phenylphosphine oxide. Standard potassium permanganate/pyridine oxidation procedures gave the corresponding bis(4-carboxyphenyl) phenylphosphine oxide in good yield. Using prevailing polymerization techniques (203), polymers were obtained which could be spun into satisfactory fibers. Other workers investigated polyamides (204-207) and polyesters (204,208). There have been no reports of these materials in the open literature since the 1960's.

Additional references to utilization of the phosphine oxide diacids appeared in the mid 1960's. Low molecular weight polybenzimidazoles (PBI's) were prepared from selected aromatic tetramines (209-211) as seen in Scheme 11.



Scheme 11. Preparation of polybenzimidazoles containing phosphine oxide moieties.

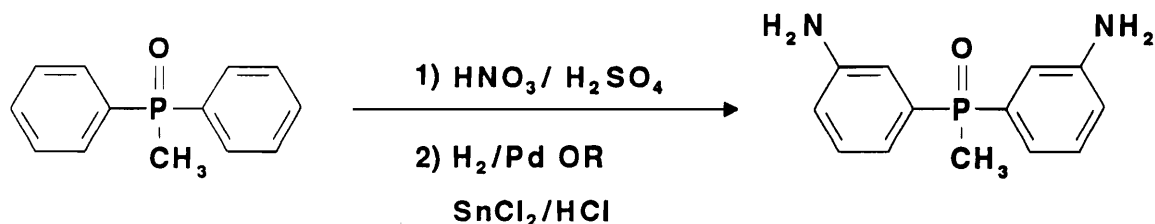
Relative to other available PBI's, these systems had higher thermal stability and solubility due to the presence of the large phenylphosphine oxide unit.

The bisphenol of the phosphine oxide structure shown in Figure 79 was reported in the 1950's (212) and utilized in an epoxy system in the 1960's (213).

This route also used a Grignard procedure for monomer preparation. Bis(4-methoxyphenyl)phenylphosphine oxide was obtained and was subsequently hydrolyzed to give bis(4-hydroxyphenyl)phenylphosphine oxide in acceptable yields. This monomer was used to prepare polyarylates (214) by interfacial and solution techniques. Improved solubility and self-extinguishing behavior as compared to Bis-A polyarylates were noted.

The high bulk which favors solubility, and the high thermal stability imparted by the phenylphosphine oxide group, makes polyimides an attractive area for incorporation of phosphorous-carbon linkages. While possessing superior thermal stability properties, polyimides have earned a reputation of being very difficult to process. The normal preparation of aromatic polyimides has been through a two step process. An aromatic diamine is reacted with an aromatic dianhydride to give a soluble poly(amic acid). This is followed by solution or solid state imide ring formation by thermal or chemical processes. As shown in Figure 2, the dianhydride and diamine functions would be needed for the synthesis of phosphine oxide-based polyimides.

The synthesis of a phosphine oxide diamine was first reported in 1963 (215). Diphenylmethylphosphine oxide was nitrated and then reduced to the diamine. The product, shown in Scheme 12, was obtained in good yield.



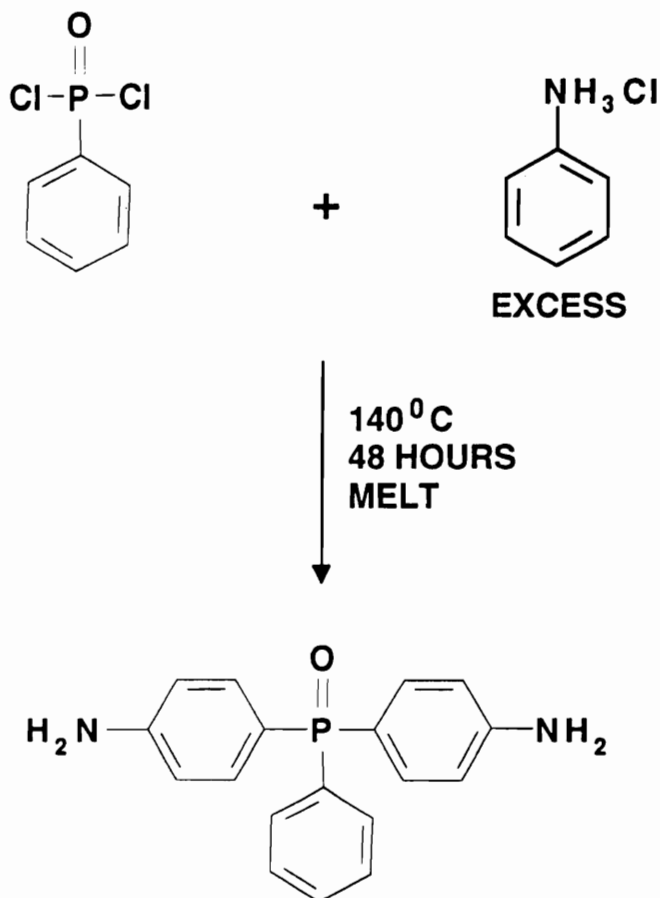
Scheme 12. Preparation of phosphine oxide diamine by nitration and reduction.

The first example of a polyimide from this material was not found until twenty years later (216). Polyamides of high molecular weight were prepared from this monomer (215) and were spun into fibers. Nonflammability and high softening temperatures were claimed.

Phenyl substituted phosphine oxide diamines are cited in the open literature less frequently than any other phosphine oxide monomer systems. The general procedure of triphenyl phosphine oxide preparation by Grignard techniques can not be used with aromatic nitro or amino substitution without the extensive use of protective groups. The use of Friedel-Crafts routes via the phosphine sulfide (217) to produce triphenylphosphine sulfides which may be oxidized to the corresponding oxides will not proceed with nitro-substituted aromatics due to inactivation. The direct nitration of triphenylphosphine oxide and subsequent reduction has been carried out (218, 219). The mixture of isomeric nitro compounds could only be separated by time consuming chromatography techniques.

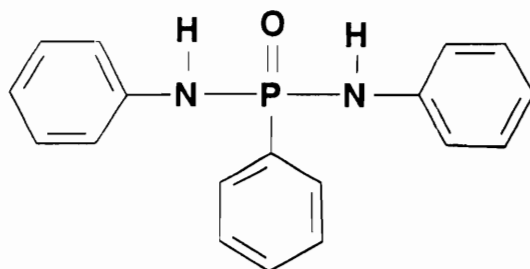
In 1971, Russian workers (220,221) reported a simple one-step procedure to yield bis(4-aminophenyl)phenylphosphine oxide (Scheme 13). Dichlorophenylphosphine was reported to react with aniline hydrochloride at high temperature in a Friedel-Crafts reac-

tion to yield monomer grade diamine after recrystallization from ethanol. Polyimides were reported from diamine prepared by this route (222,223) and in all cases were less stable thermally than conventional polyimides which did not contain phosphorous (224).



Scheme 13. Alleged preparation of bis(4-aminophenyl)phenylphosphine oxide.

A very thorough investigation of this route has identified (225) the compound obtained as the known diamide (226).



In 1985, Schiemenz reported (227) a route to the 4-dinitro compound. This route, reported later in this dissertation, produced a very difficult to separate mixture of isomers. A displacement reaction of bis(4-fluorophenyl)phenylphosphine oxide with lithium nitrite was utilized.

The nitration and reduction of tris(3-nitrophenyl)phosphine oxide to produce the corresponding triamine has been reported (216) as have a number of polyimide-phosphorous-containing resins (228-231). The triamine was reacted with varying ratios of nadic or maleic anhydride and resins produced were investigated for flame retardant properties.

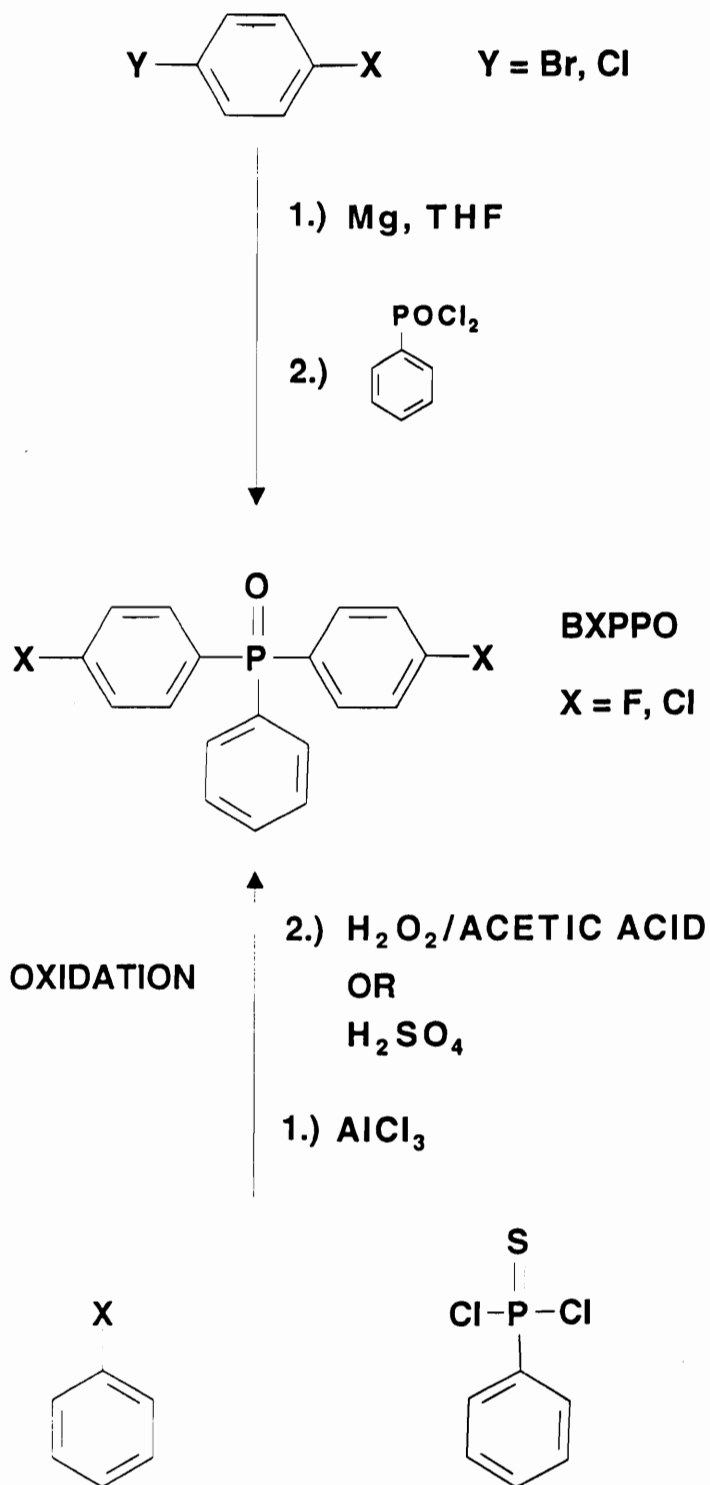
An additional phosphine oxide monomer system was reported in the late 1970's. This system (232) and procedures for preparing poly(arylene ether phosphine oxide) (PEPO) were based on the polycondensation of the sodium salt of bisphenol-A with bis(4-chlorophenyl) phenylphosphine oxide (BCPPO). BCPPO was prepared as outlined in Scheme 14.

The synthesis of bis(4-halophenyl)phenylphosphine oxide by the represented pathways has been investigated by a number of workers (233-239). Both routes to this monomer would appear practical. The Grignard preparation is a single step from the prepared Grignard reagent. Yields are very high and purity is quite good. The Friedel-Crafts route requires two steps as conversion to the phosphine oxide is needed. Use of the oxide or the phosphine systems under identical reaction conditions will not yield the intended



product. Isomeric impurities which form from the reaction of halobenzenes with dichlorophenylphosphine sulfide reduce the yield and purity of monomer obtained by the Friedel-Crafts route.

Nucleophilic displacement polycondensation with aromatic bisphenols and bis(4-halophenyl)phenyl phosphine oxide in dipolar aprotic solvents has been reported (240-244). In all cases, the use of the fluoro-substituted monomer resulted in higher molecular weight polymers due to the higher reactivity in aromatic nucleophilic substitution. Thermally stable, self-extinguishing polymers with Tg's of 150°C to 260°C were reported.



Scheme 14. Preparation of bis(4-halophenyl)phenylphosphine oxides.

## 5.2 SYNTHESIS

### 5.2.1 Bis(4-methylphenyl)phenylphosphine Sulfide

To a 1-L four-necked flask fitted with a stirrer, thermometer, a reflux condenser, and an argon inlet line, 31.65 g (0.15 mol) of phenylthiophosphonic acid dichloride, 106.8 g (0.8 mol) of anhydrous aluminum chloride, and 200 mL of toluene were added. The mixture was heated to reflux with stirring for six hours. After completion of reaction and cooling to room temperature, the mixture was poured into a mixture of 600 mL of 6N hydrochloric acid and 500 g of ice. The phases were separated and the aqueous phase was extracted three times with 200 mL-portions of toluene. The combined organic phases were dried over anhydrous magnesium sulfate, filtered, and the toluene solvent removed under reduced pressure. A glass-like product was obtained which crystallized spontaneously. A yield of 30.1 g (62%) of a tan solid, mp 142.5 - 143.0°C was obtained.

The carbon and proton NMR spectra, the infrared spectrum and mass spectrum are shown in Figures 80-83.

### 5.2.2 Bis(4-carboxyphenyl)phenylphosphine Oxide

To a 1-L three-necked flask, 10.0 g (.030 mol) of bis(4-methylphenyl)phenylphosphine sulfide, 400 mL of water, 4.0 g sodium hydroxide, and 36.0 g (0.24 mol) of potassium permanganate were added and the mixture was refluxed overnight to yield a brown solution. After cooling to room temperature, the solution was filtered through a bed of Celite®. The Celite® filter pad was washed with three 100 mL-portions of hot water and the combined aqueous solutions were acidified with concentrated hydrochloric acid to yield a white solid which on filtering and drying weighed 10.18 g (92%), mp 335.5 - 337.0°C. <sup>13</sup>C and <sup>1</sup>H NMR, infrared, and mass spectra (Figures 84-87) are consistent with the assigned structure.

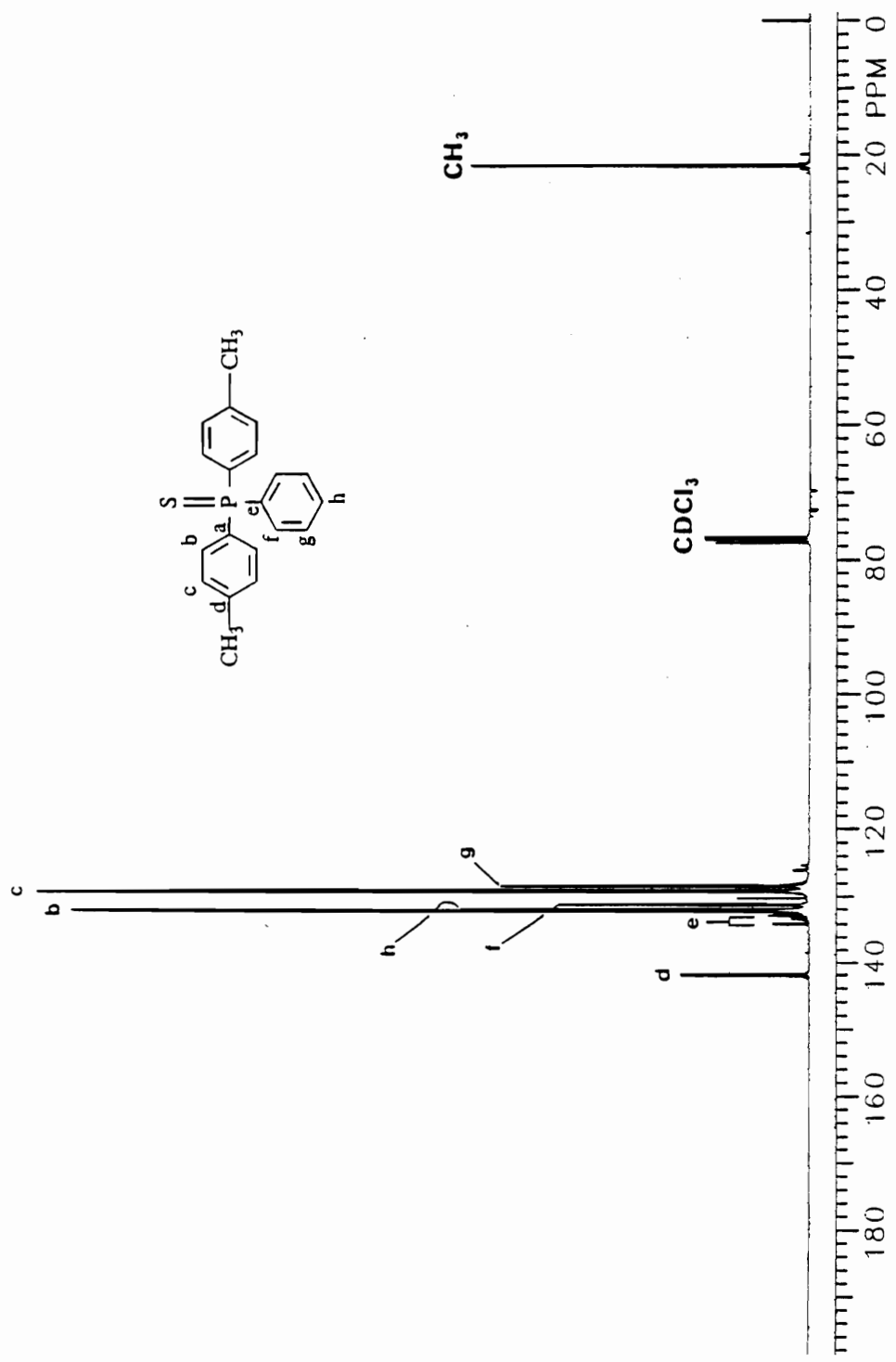


Figure 80.  $^{13}\text{C}$  NMR spectrum of bis(4-methylphenyl)phenylphosphine sulfide.

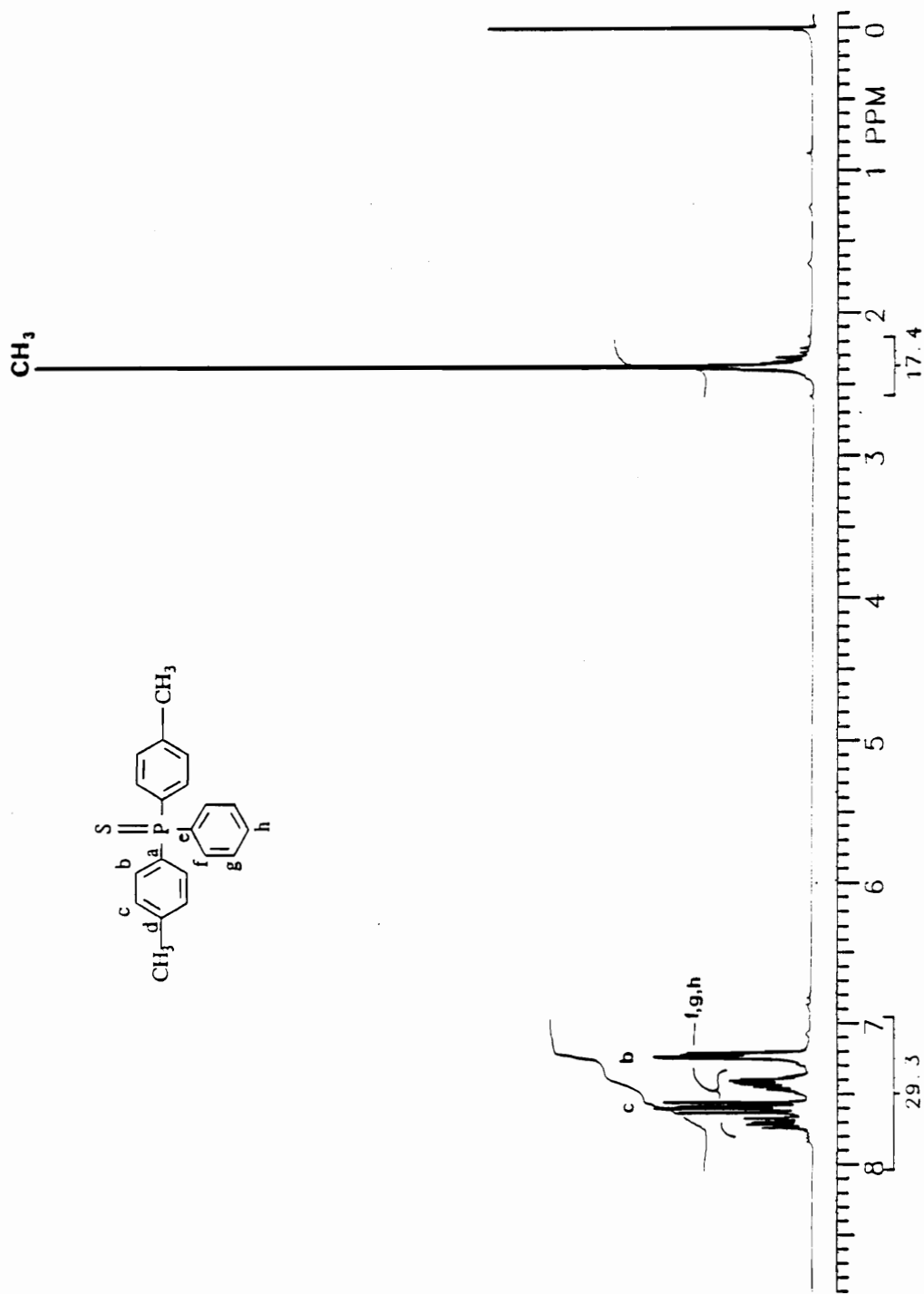


Figure 81.  $^1\text{H}$  NMR spectrum of bis(4-methylphenyl)phenylphosphine sulfide.

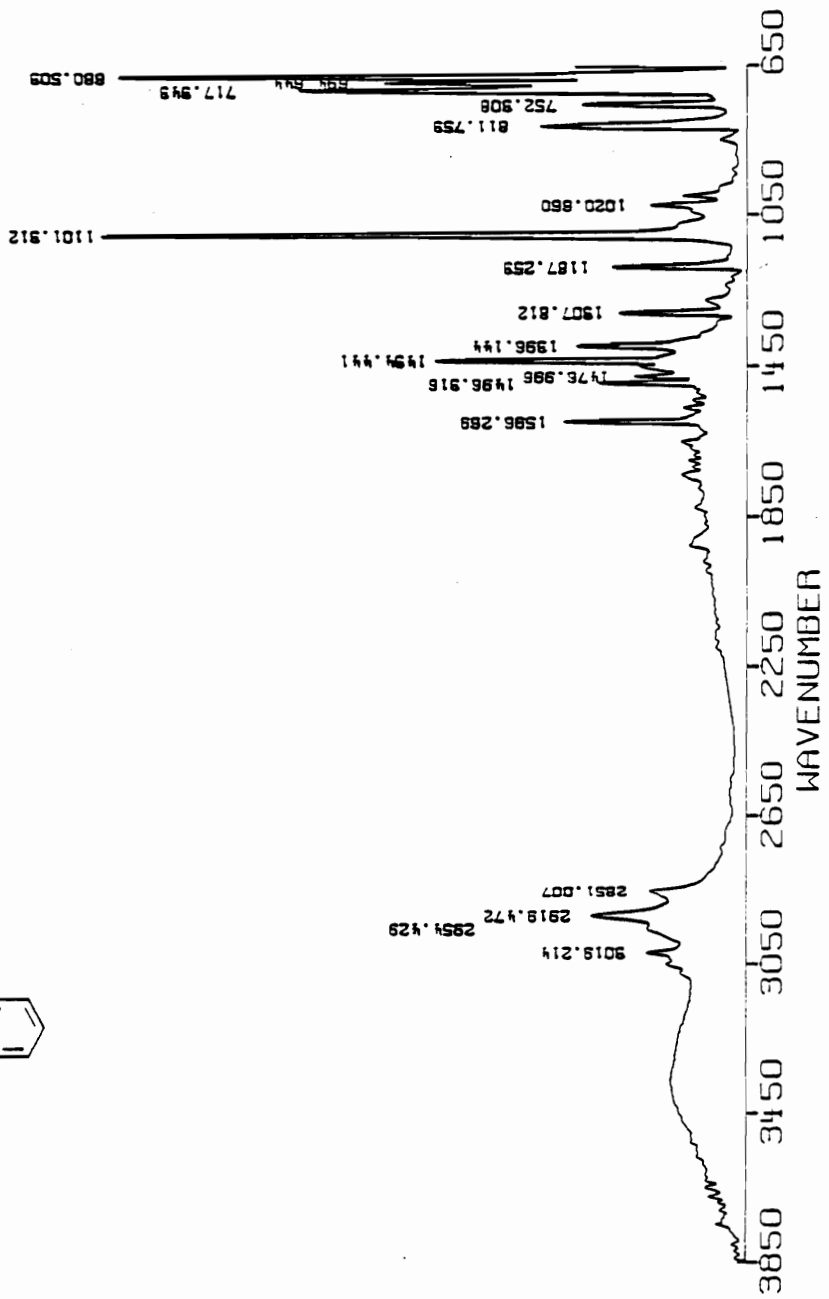
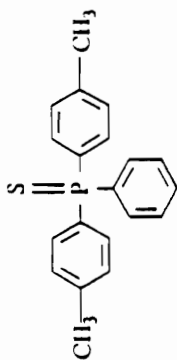


Figure 82. IR spectrum of bis(4-methylphenyl)phenylphosphine sulfide.

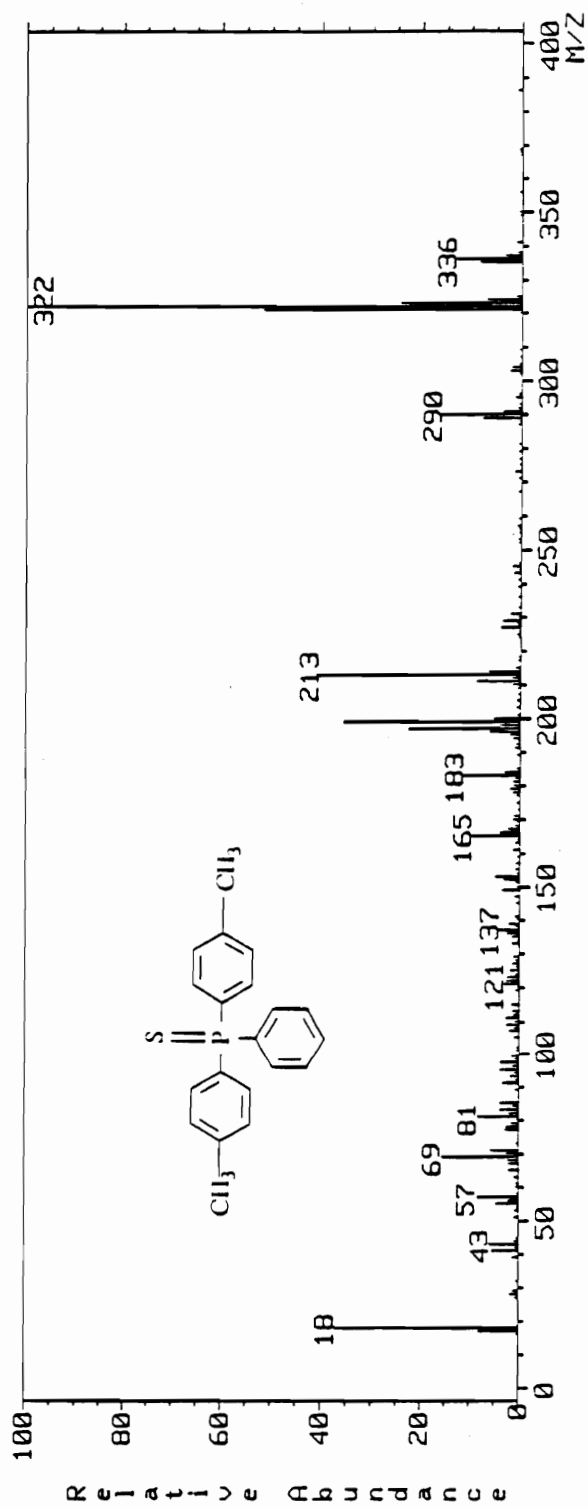


Figure 83. Mass spectrum of bis(4-methylphenyl)phenylphosphine sulfide.

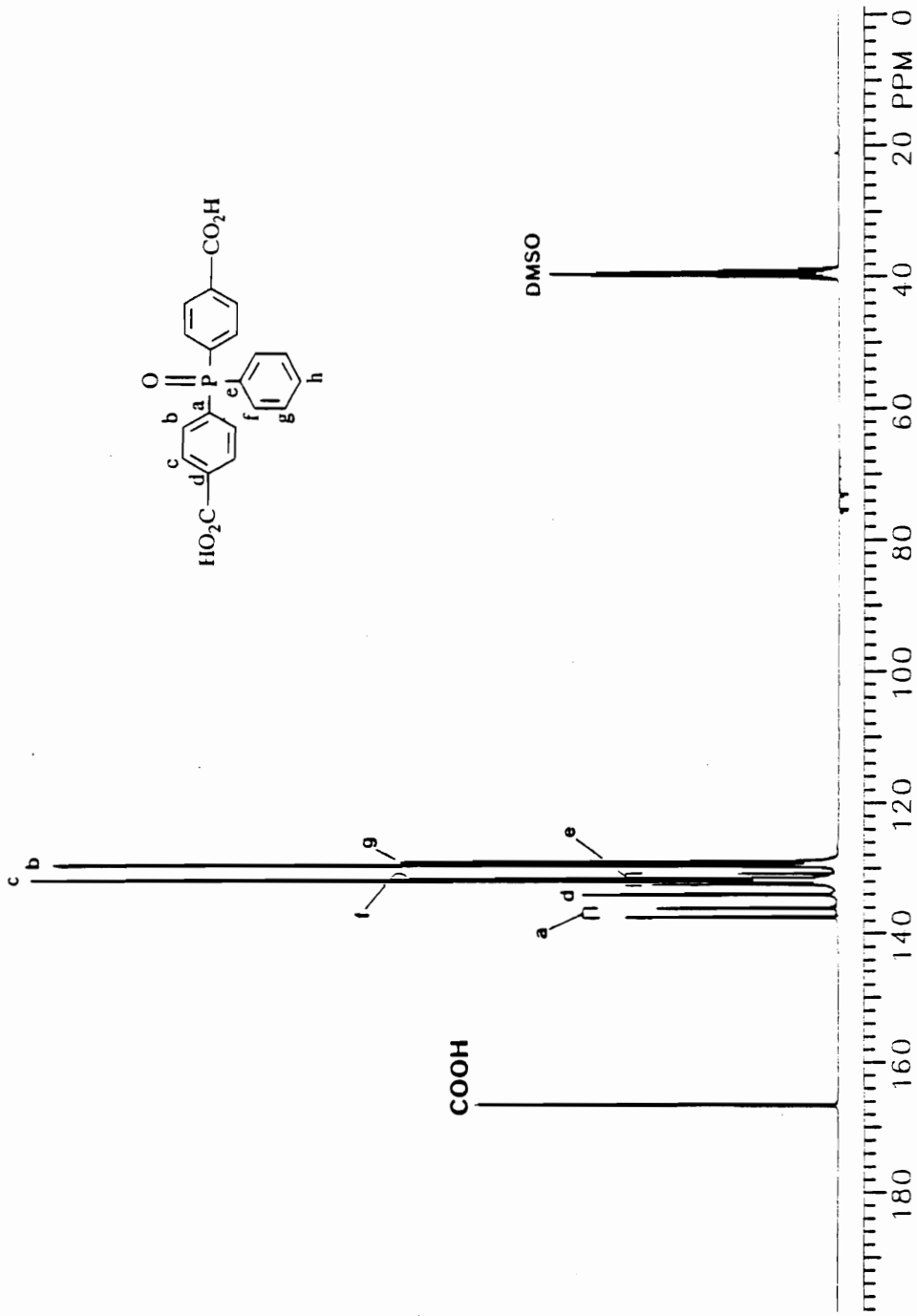


Figure 84.  $^{13}\text{C}$  NMR spectrum of bis(4-carboxyphenyl)phenylphosphine oxide.



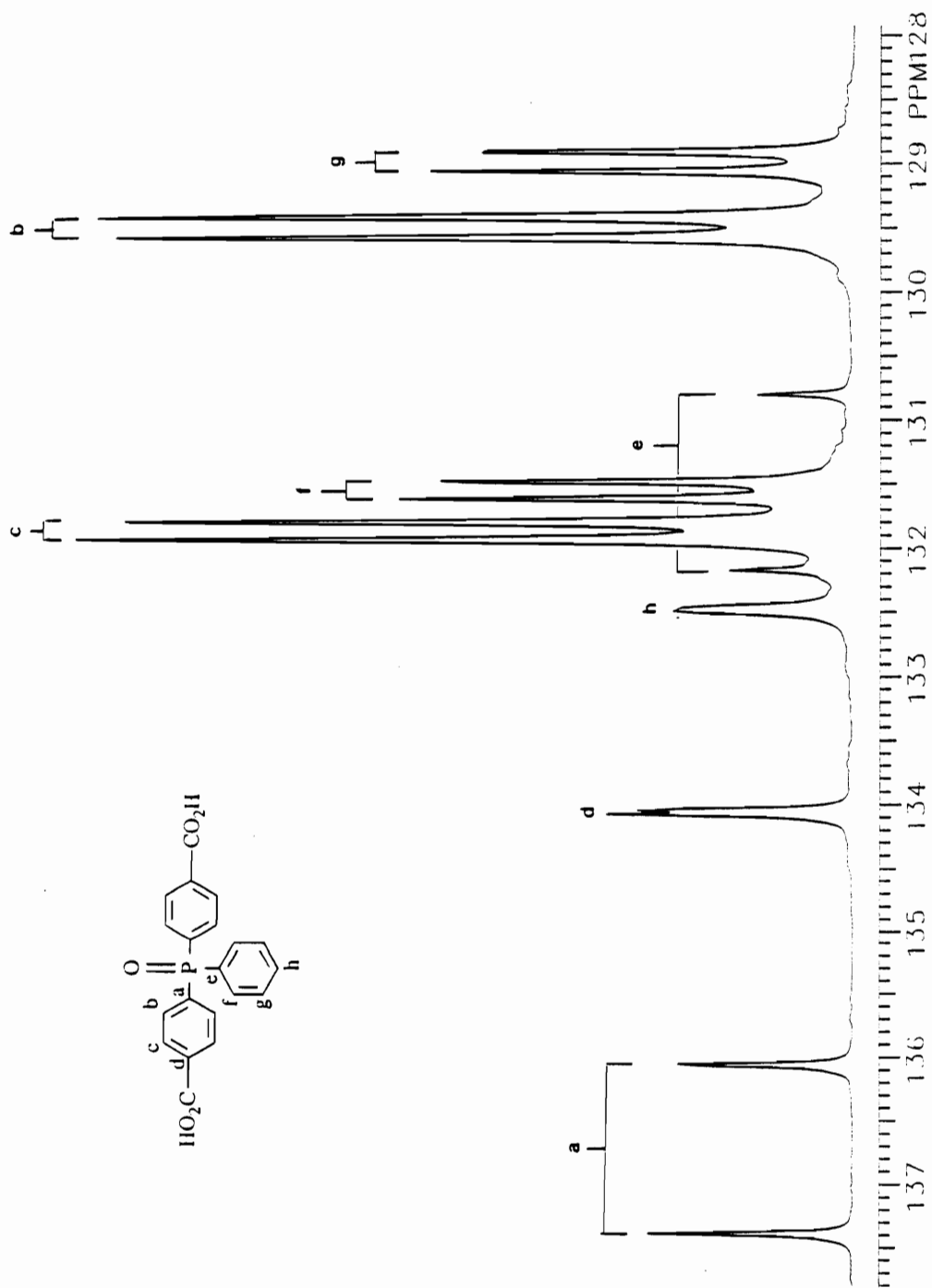


Figure 84a. Expansion of the aromatic region of the  $^{13}\text{C}$  NMR spectrum of bis(4-carboxyphenyl)phenylphosphine oxide.

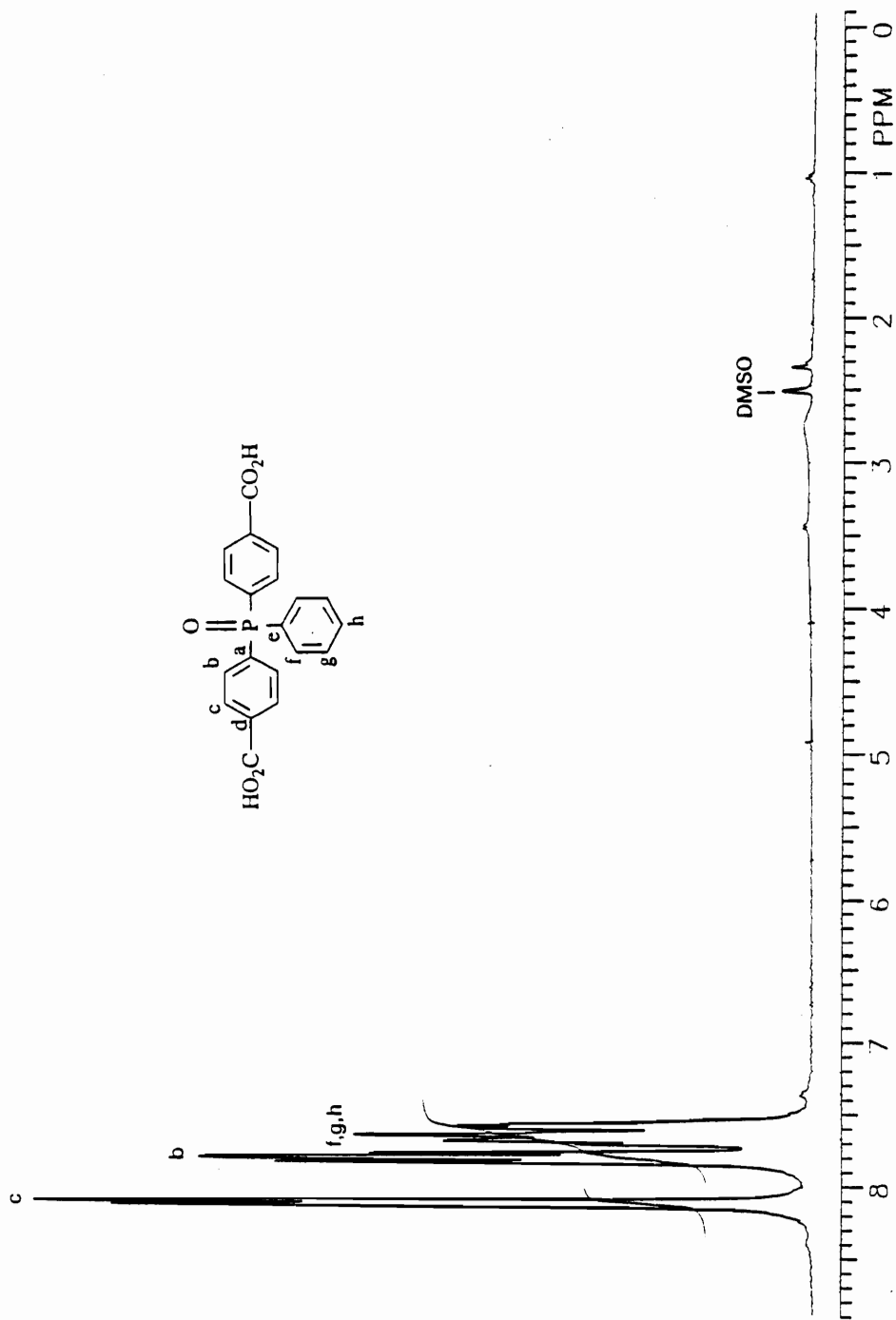


Figure 85.  $^1\text{H}$  NMR spectrum of bis(4-carboxyphenyl)phenylphosphine oxide.

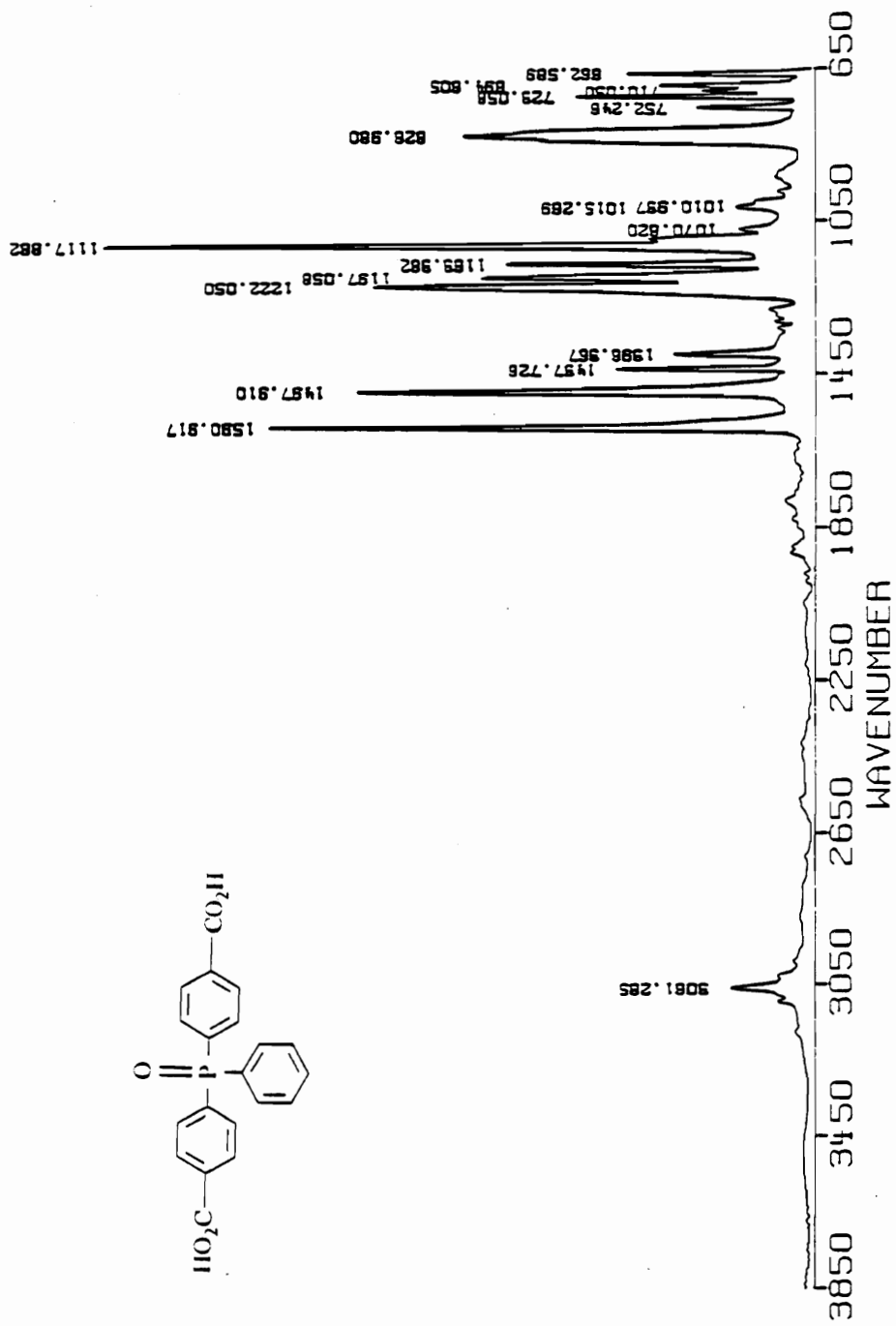


Figure 86. IR spectrum of bis(4-carboxyphenyl)phenylphosphine oxide.

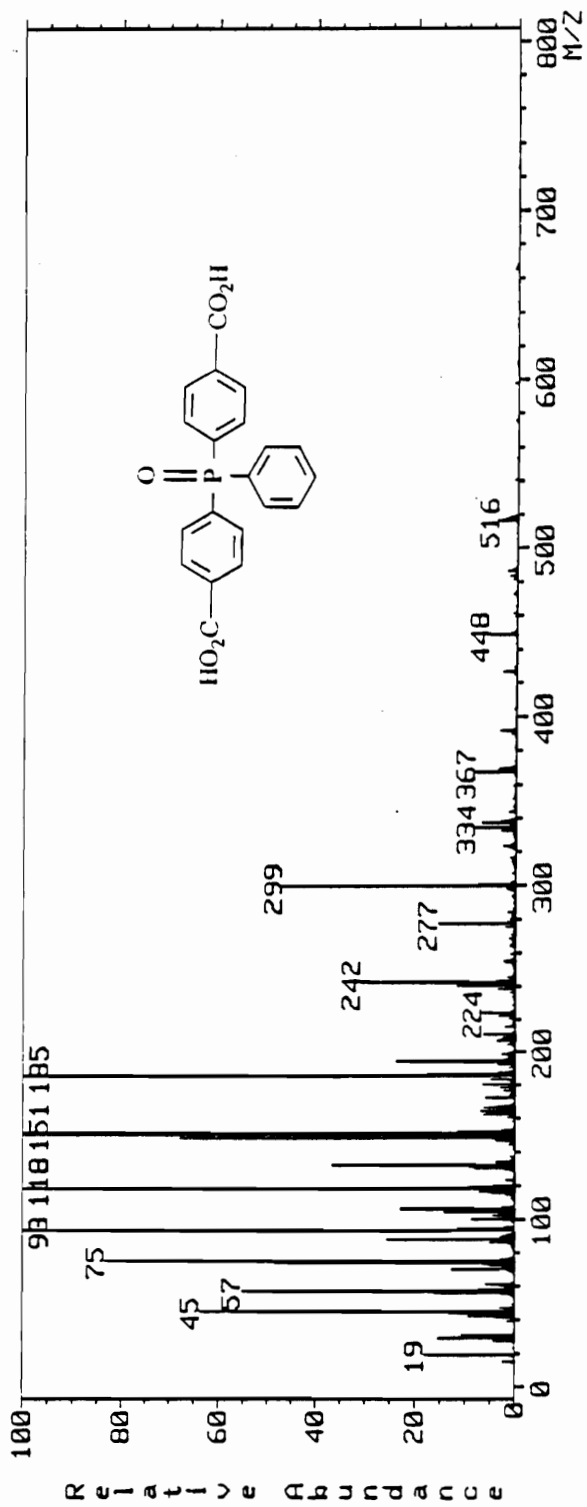


Figure 87. Mass spectrum of bis(4-carboxyphenyl)phenylphosphine oxide.

### 5.2.3 Bis(4-isopropylphenyl)phenylphosphine Sulfide

To a 1-L four-necked flask fitted with a stirrer, thermometer, a reflux condenser and an argon inlet line, 31.7 g (0.15 mol) of phenylthiophosphoric acid dichloride, 106.8 g (0.80 mol) of anhydrous aluminum chloride, and 200 mL of isopropylbenzene were added. The mixture was heated to reflux with stirring for four hours. After cooling to room temperature, the mixture was poured into a mixture of 600 mL of 6N hydrochloric acid and 500 g of ice. The phases were separated and the aqueous phase was extracted three times with 200 mL portions of isopropylbenzene. The combined organic phases were dried over magnesium sulfate, filtered, and the isopropylbenzene solvent removed under reduced pressure. A viscous syrup was obtained which crystallized on standing over a period of 72 hours to give 41.3 g (73%) of a white solid mp 154.5 - 157.0°C.

The carbon and proton NMR spectra, the mass spectrum and infrared spectrum are shown in Figures 88-91.

### 5.2.4 Bis(4-phenoxyphenyl)phenylphosphine Sulfide

To a 1-L four-necked flask equipped with an addition funnel, a reflux condenser, a thermometer, and an overhead stirrer, 85.1 g (0.5 mol) of diphenyl ether and 66.2 g (0.5 mol) of anhydrous aluminum chloride were added under an atmosphere of dry nitrogen. Phenylthiophosphoric acid dichloride (26.4 g, .0125 mol) was added dropwise over a period of 30 minutes. The mixture was heated to 125°C with stirring and allowed to react for 8 hours. After cooling to room temperature, the reaction contents were added to a mixture of 200 mL of 6N hydrochloric acid and 200 g of ice. 200 mL of chloroform was added and the phases separated. The aqueous phase was extracted with two 200 mL portions of chloroform and the organic phases combined. The organic phase was washed with one 100 mL portion of half saturated sodium bicarbonate and two 100 mL portions

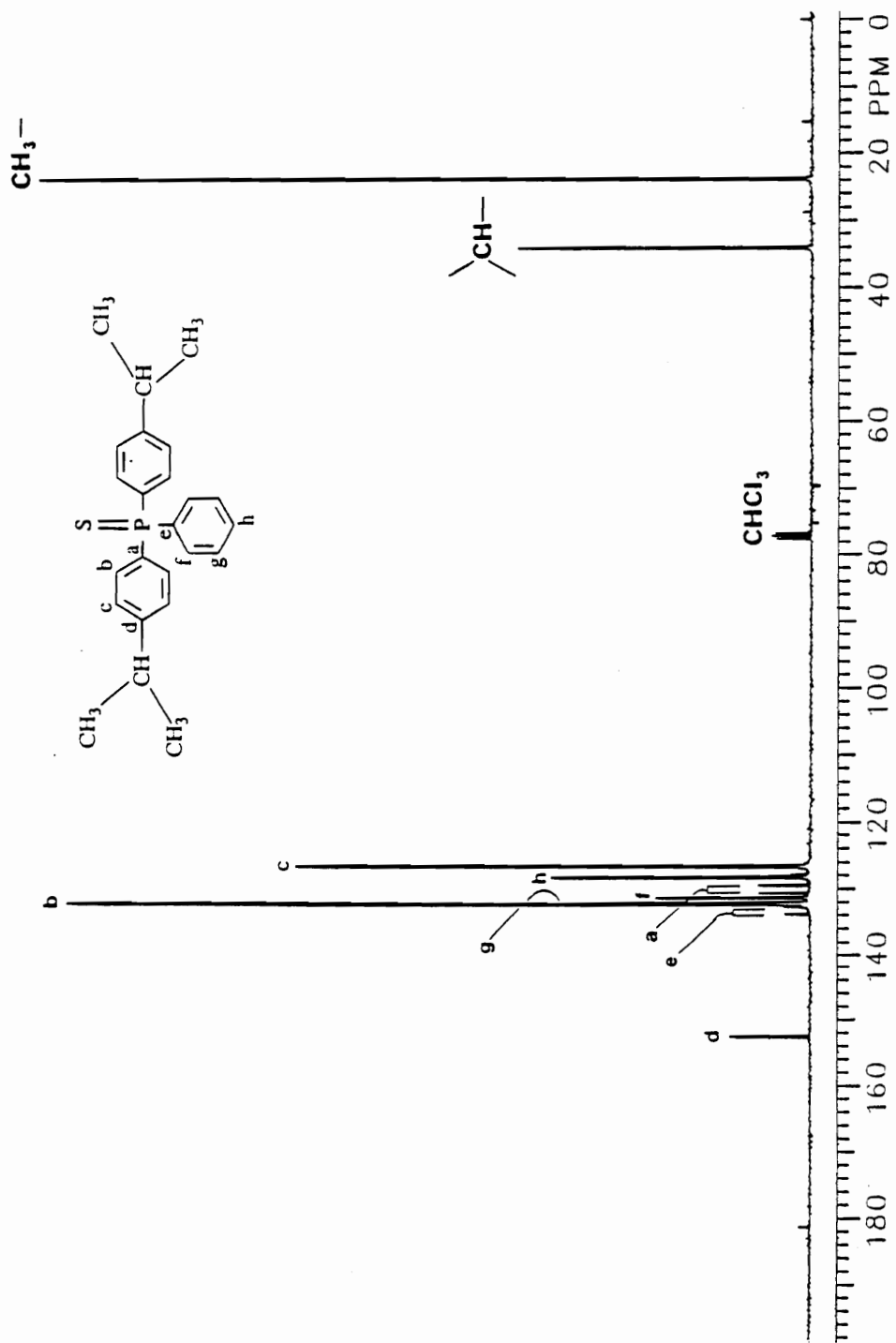


Figure 88.  $^{13}\text{C}$  NMR spectrum of bis(4-isopropylphenyl)phenylphosphine sulfide.

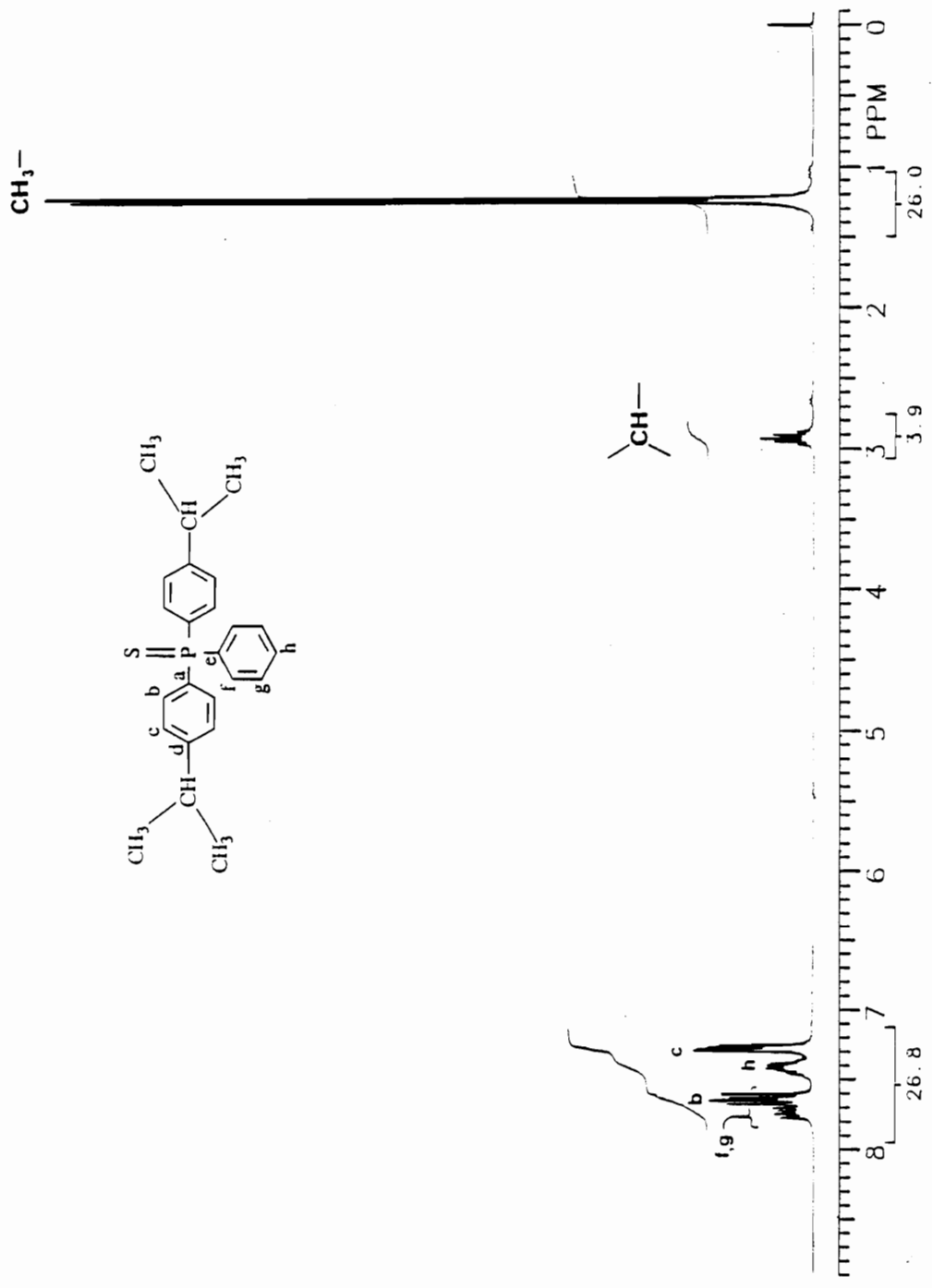


Figure 89. <sup>1</sup>H NMR spectrum of bis(4-isopropylphenyl)phenylphosphine sulfide.

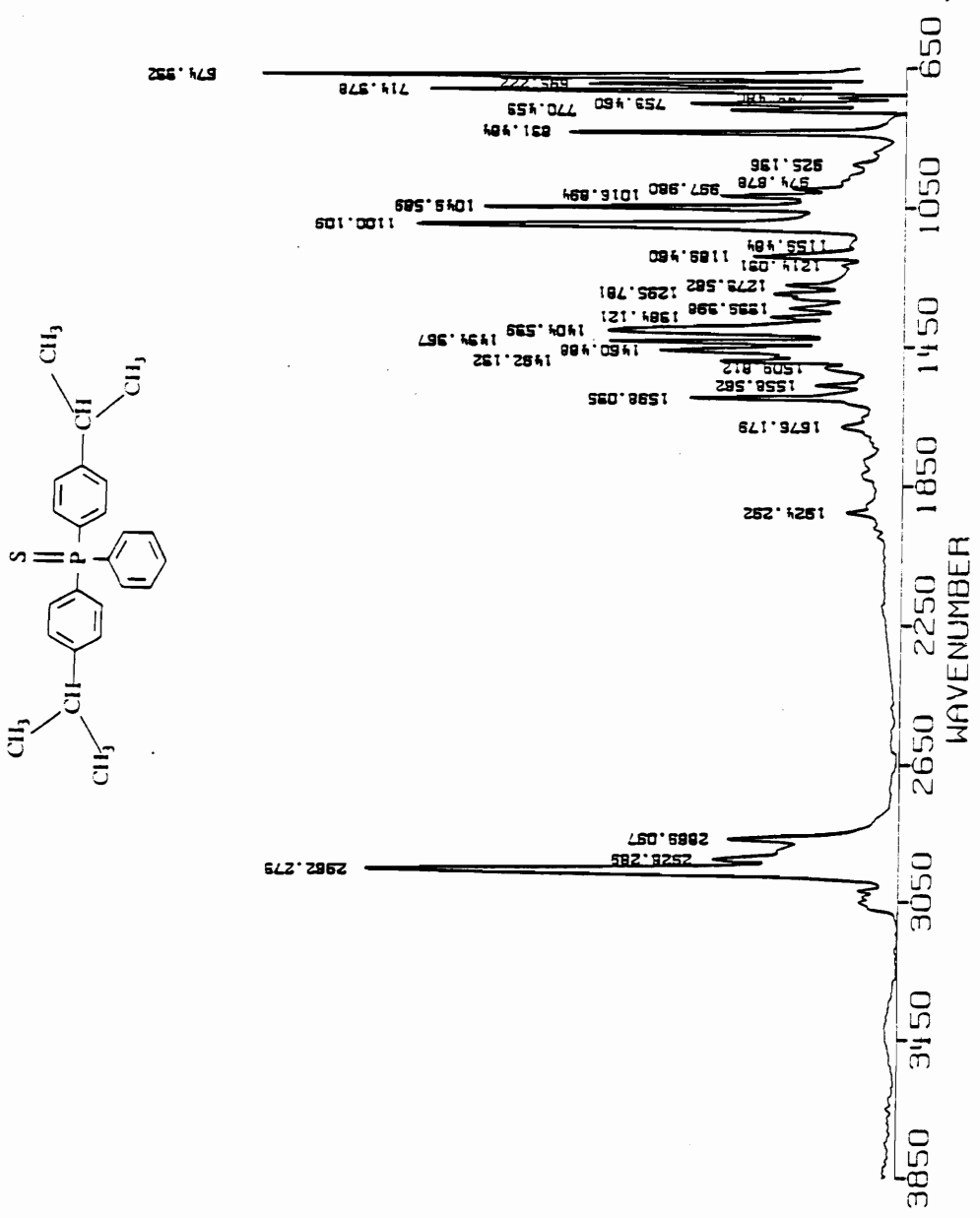


Figure 90. IR spectrum of bis(4-isopropylphenyl)phenylphosphine sulfide.



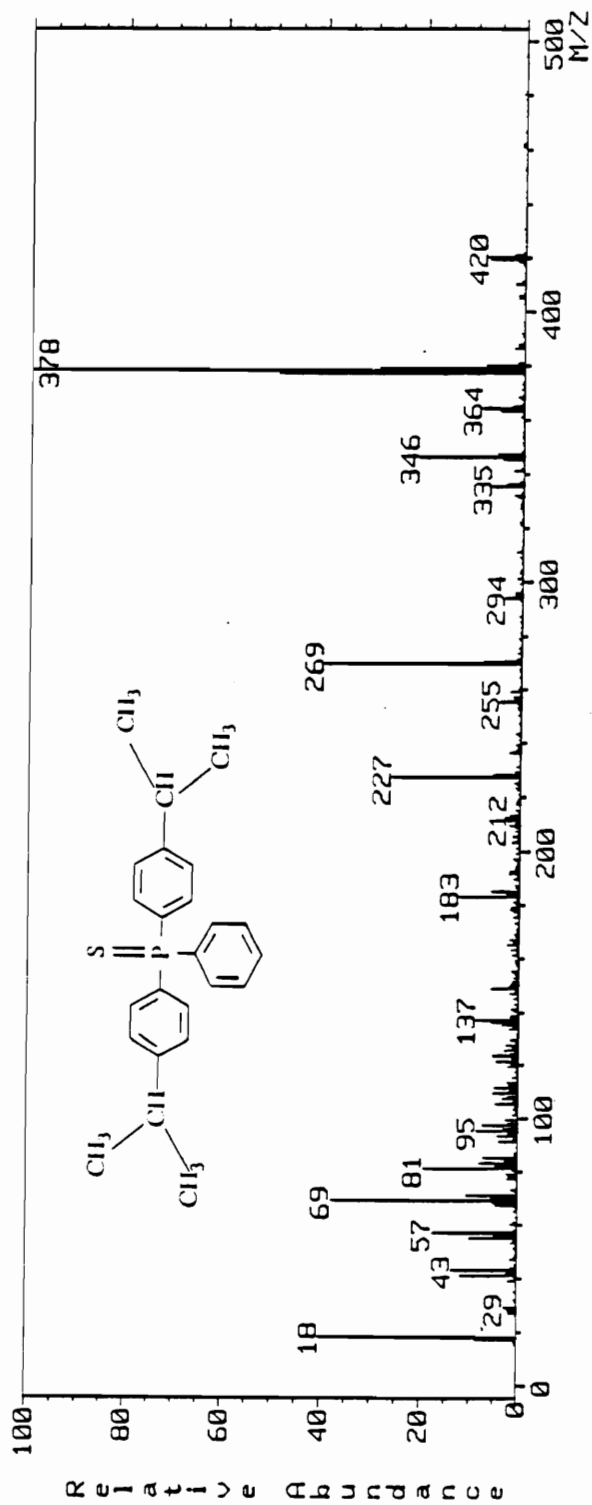


Figure 91. Mass spectrum of bis(4-isopropylphenyl)phenylphosphine sulfide.

of water. The chloroform solution was dried over magnesium sulfate, filtered, and solvent removed under reduced pressure. The viscous liquid obtained was dried at 100°C for 48 hours at 0.5 torr to yield 54.2 g (91%) of tan solid with a softening point of 60°C.

The carbon and proton NMR spectra, the infrared spectrum and the mass spectrum are shown in Figures 92-95.

### 5.2.5 Bis(4-fluorophenyl)phenylphosphine Oxide

To a 1-L four-necked flask fitted with an addition funnel, an argon inlet, an overhead mechanical stirrer and a thermometer, was added 24.3 g (1.0 mol) of magnesium turnings and 400 mL dry tetrahydrofuran. The suspension was cooled in an ice bath and to the stirred suspension was added slowly 176.8 g (1.0 mol) of 4-bromofluorobenzene such that the temperature of the reaction remained at 5°C or lower. After completion of addition, the reaction was allowed to warm to room temperature overnight with stirring. 98.2 g (0.50 mol) of phenylphosphonic dichloride was added dropwise to the cooled (ice bath, 5°C) Grignard solution. After completion of addition, the yellow reaction mixture was allowed to warm to room temperature with stirring overnight. Ten percent sulfuric acid was added to make the solution acidic and the mixture was added to 500 mL of water. 500 mL of ethyl ether was added. The phases were allowed to separate and the organic phase was separated. The aqueous phase was extracted with four 200 mL portions of ethyl ether. The organic phases were combined and were extracted with one 200 mL portion of half saturated aqueous sodium bicarbonate and three 200 mL portions of water. The ether solution was dried over magnesium sulfate, filtered, and organic solvents removed under reduced pressure. The crude product obtained was dissolved in hot toluene (500 mL) and the solution obtained was cooled in an ice bath to yield large white crystals. The crystals were filtered off, dried at 50°C for 24 hours at 0.5 torr and

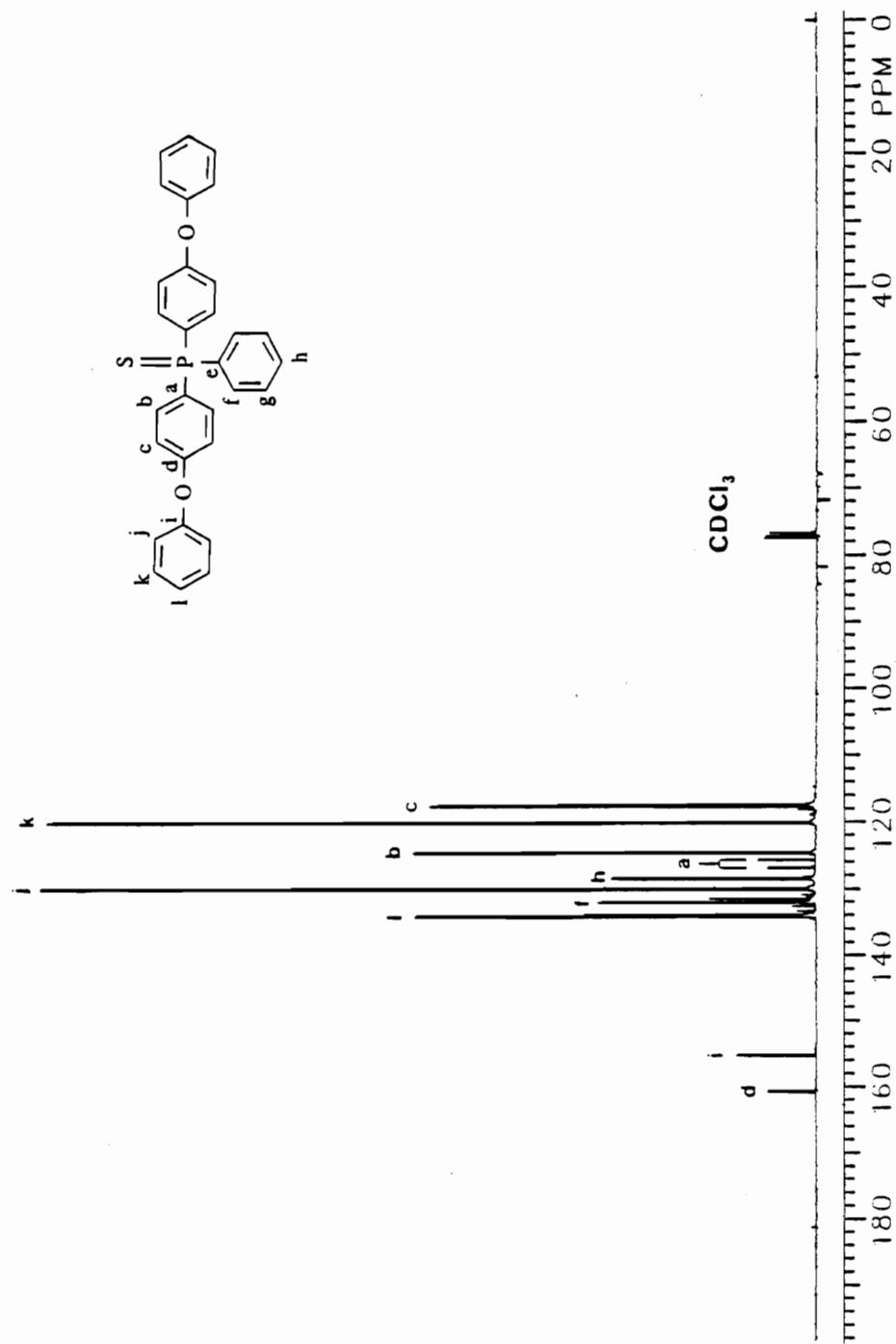


Figure 92.  $^{13}\text{C}$  NMR spectrum of bis(4-phenoxyphenyl)phenylphosphine sulfide.

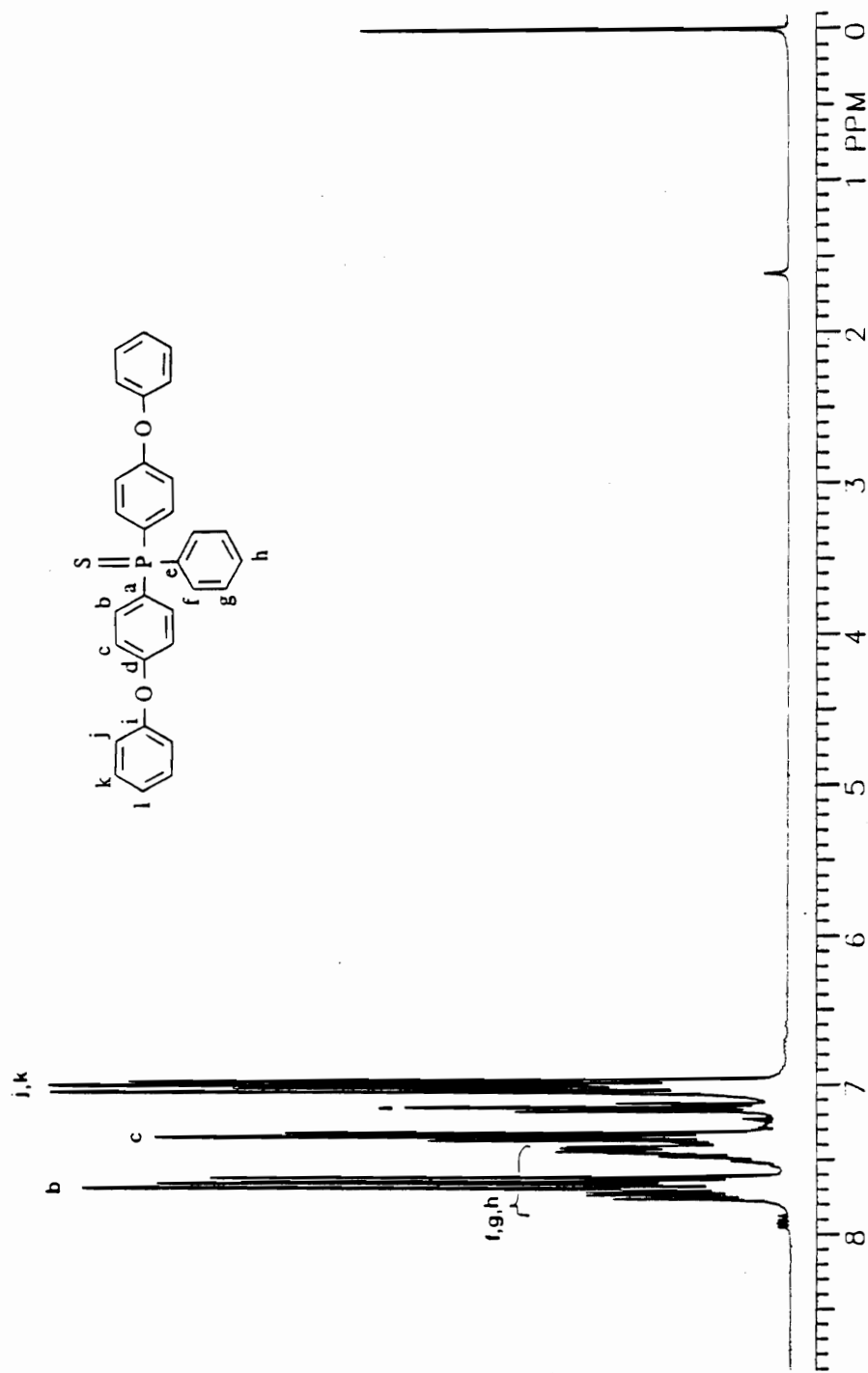


Figure 93.  $^1\text{H}$  NMR spectrum of bis(4-phenoxyphenyl)phenylphosphine sulfide.

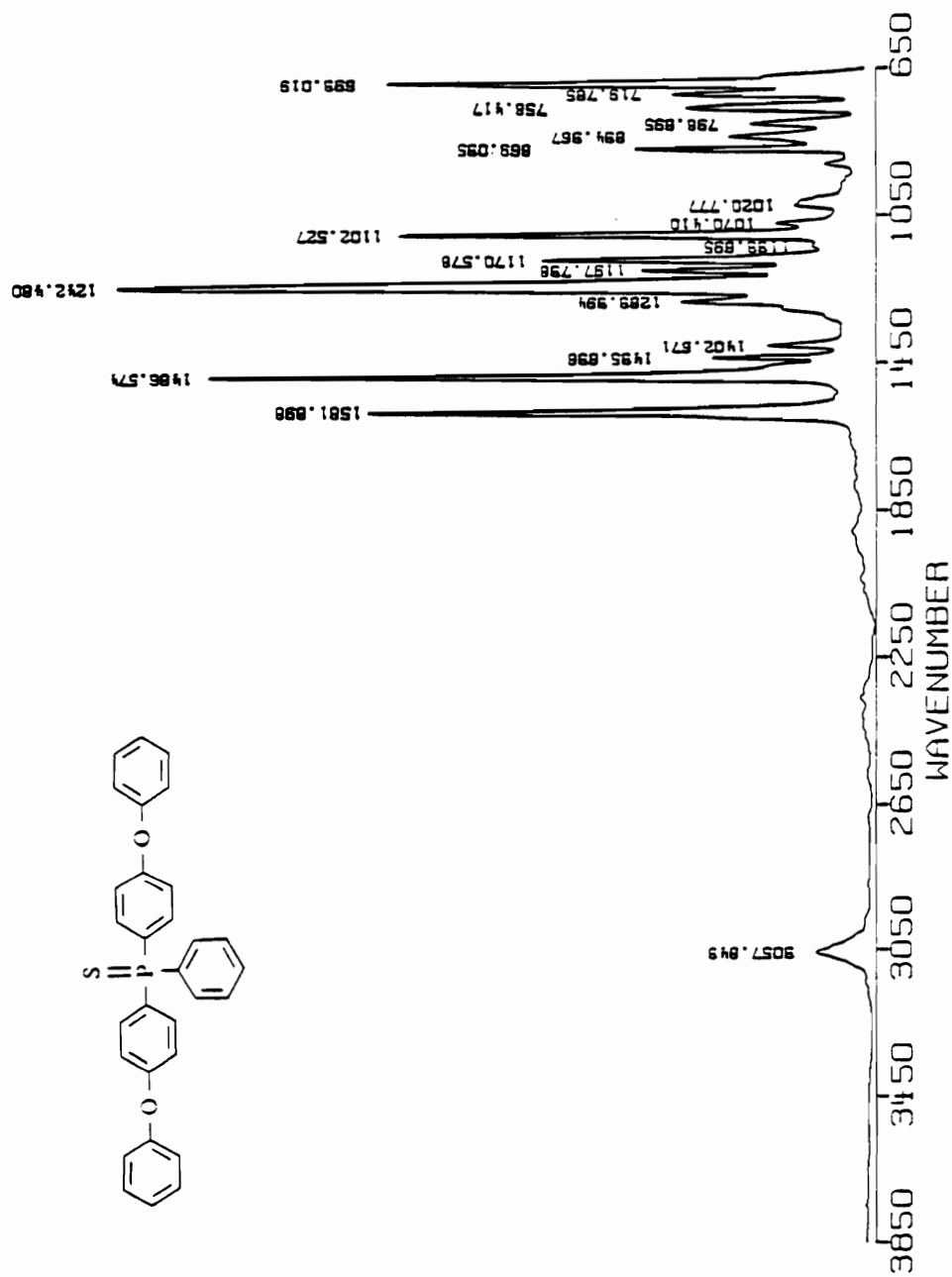


Figure 94. IR spectrum of bis(4-phenoxyphenyl)phenylphosphine sulfide.

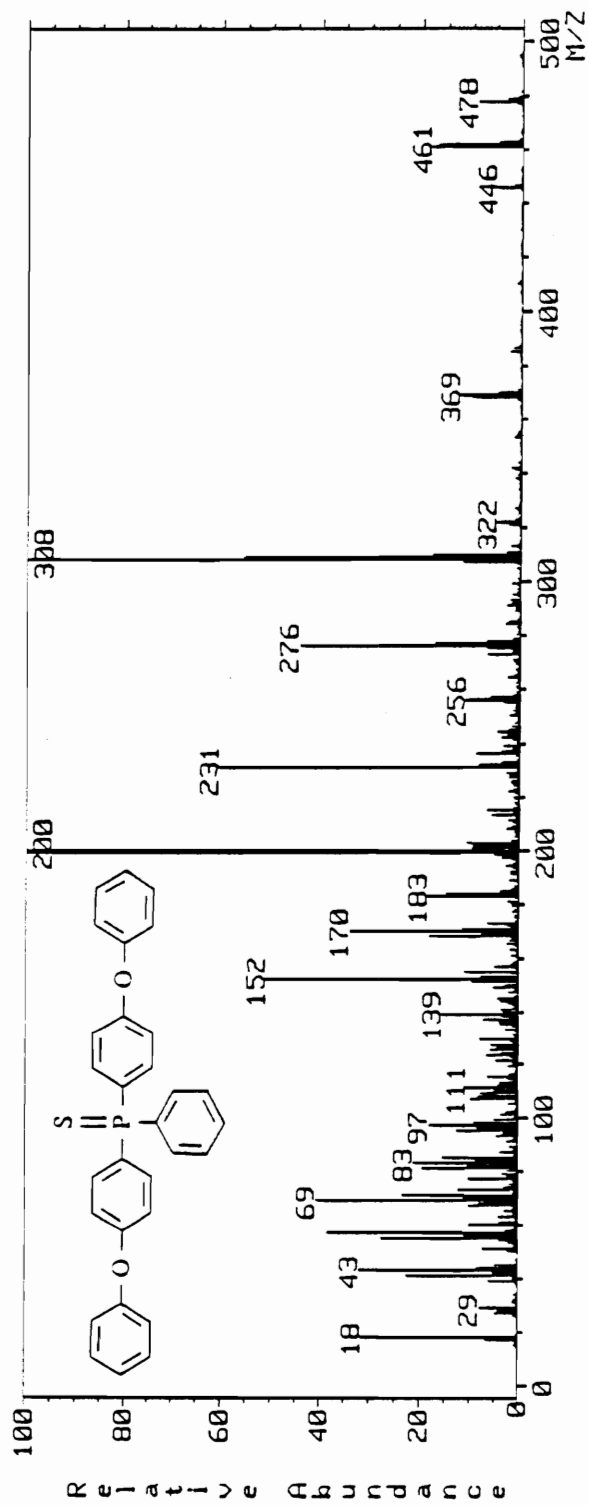


Figure 95. Mass spectrum of bis(4-phenoxyphenyl)phenylphosphine sulfide.

subsequently ground to a fine powder. The powdered material was again dried at 50°C for 24 hours at 0.5 torr to yield 226.1 g (72%) of white product, mp 130.0 - 131.0°C.

The carbon and proton NMR spectra the infrared spectrum and the mass spectrum are shown in Figures 96-99.

#### 5.2.6 Bis(4-hydroxyphenyl)phenylphosphine Oxide

47.8 g (0.1 mol) of bis(4-phenoxyphenyl)phenylphosphine sulfide and 40.0 g (1.0 mol) of sodium hydroxide pellets were placed in a 1-L three-necked flask equipped with a reflux condenser and mechanical stirrer. The mixture is heated to 310°C for eight hours and then allowed to cool to room temperature. 200 mL of water was added and the contents heated to reflux for one hour. After cooling to room temperature, the solution was filtered through a coarse glass frit filter and the aqueous solution was acidified to pH 3 with concentrated hydrochloric acid. A tan solid product was filtered off and washed with three 100 mL portions of boiling water. The product was vacuum dried at 50°C for 24 hours at a pressure of 0.5 torr. The dry product was recrystallized from methanol to yield 26.4 g (81%) of a white crystalline solid, mp 235.0 - 235.5°C.

The carbon, proton and 2D NMR spectra, the infrared spectrum and mass spectrum are shown in Figures 100-104.

#### 5.2.7 N,N-bis(trimethylsilyl)-4-bromoaniline

To a 2-L three necked flask fitted with a stirrer, a short Vigreux column (three inch) with a total reflux distillation head, and an argon inlet, 500 g (3.44 mol) of N,N-diethyl-trimethylsilylamine and 200 g (1.16 mol) of 4-bromoaniline was added. To the stirred solution, 0.5 g of diammonium sulfate was added and the mixture heated to gentle reflux in the head. When the head temperature has dropped to 55°C, the diethylamine

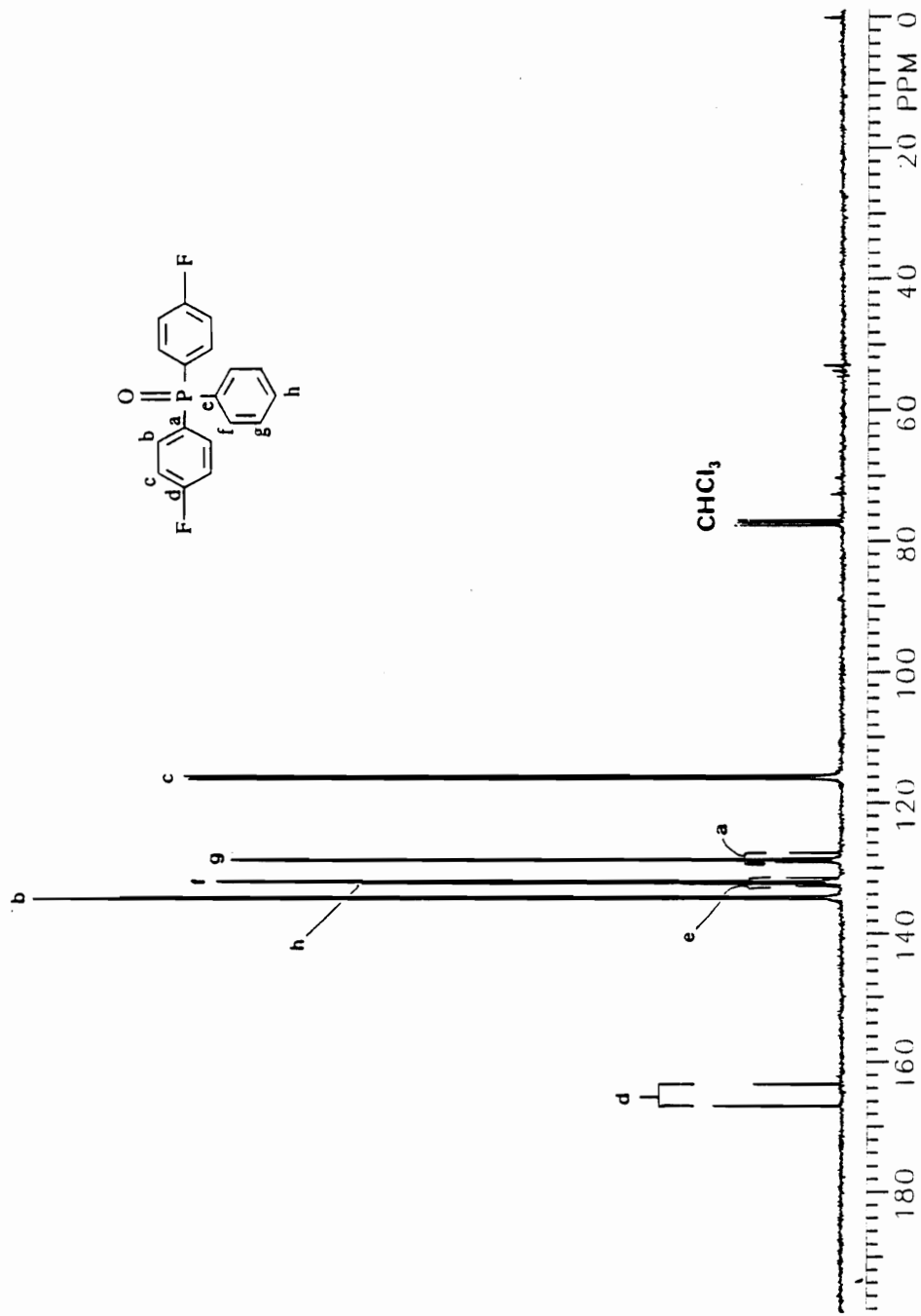


Figure 96.  $^{13}\text{C}$  NMR spectrum of bis(4-fluorophenyl)phenylphosphine oxide.



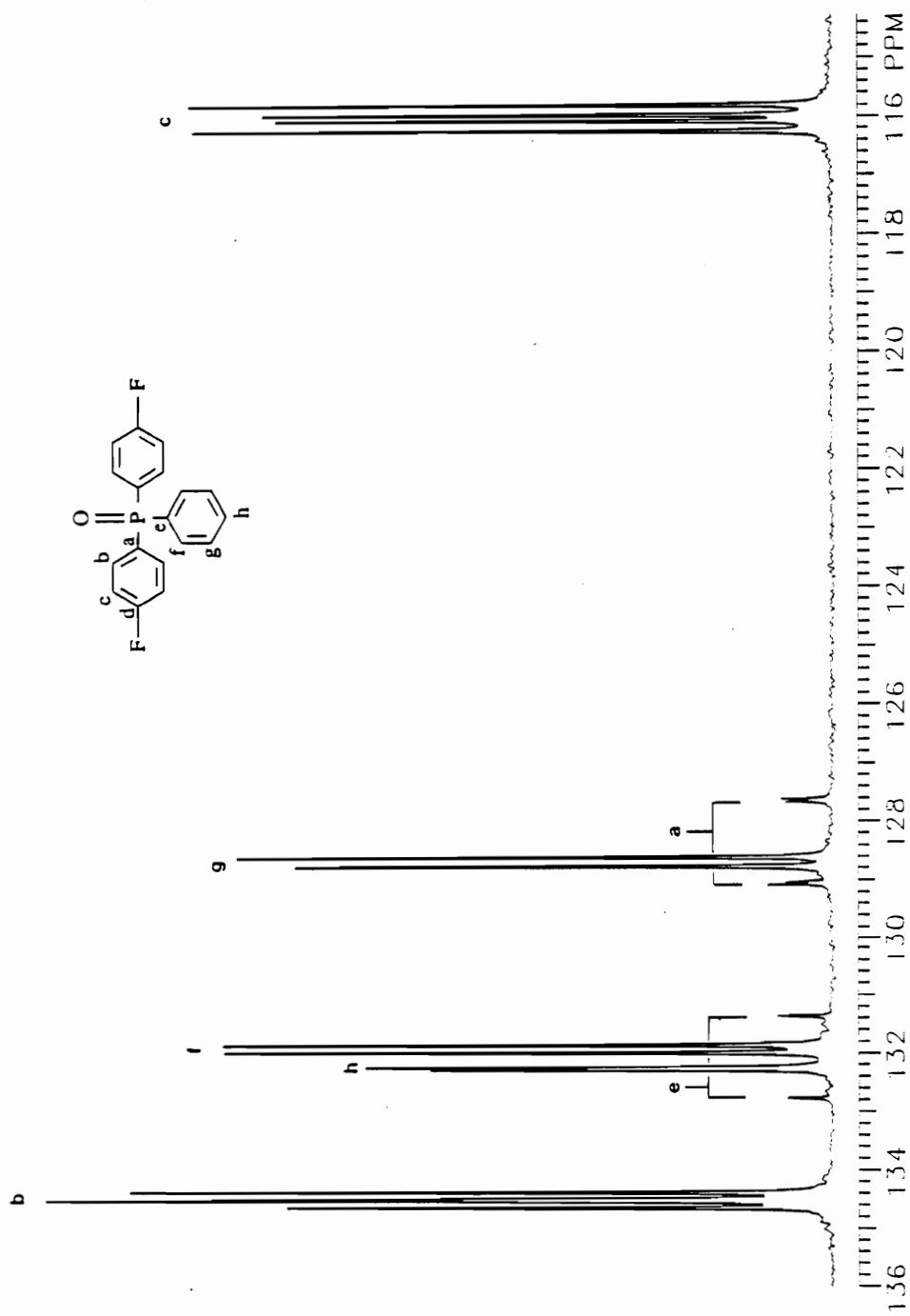


Figure 96a. Expansion of the aromatic region of the  $^{13}\text{C}$  NMR spectrum of bis(4-fluorophenyl)phenylphosphine oxide.

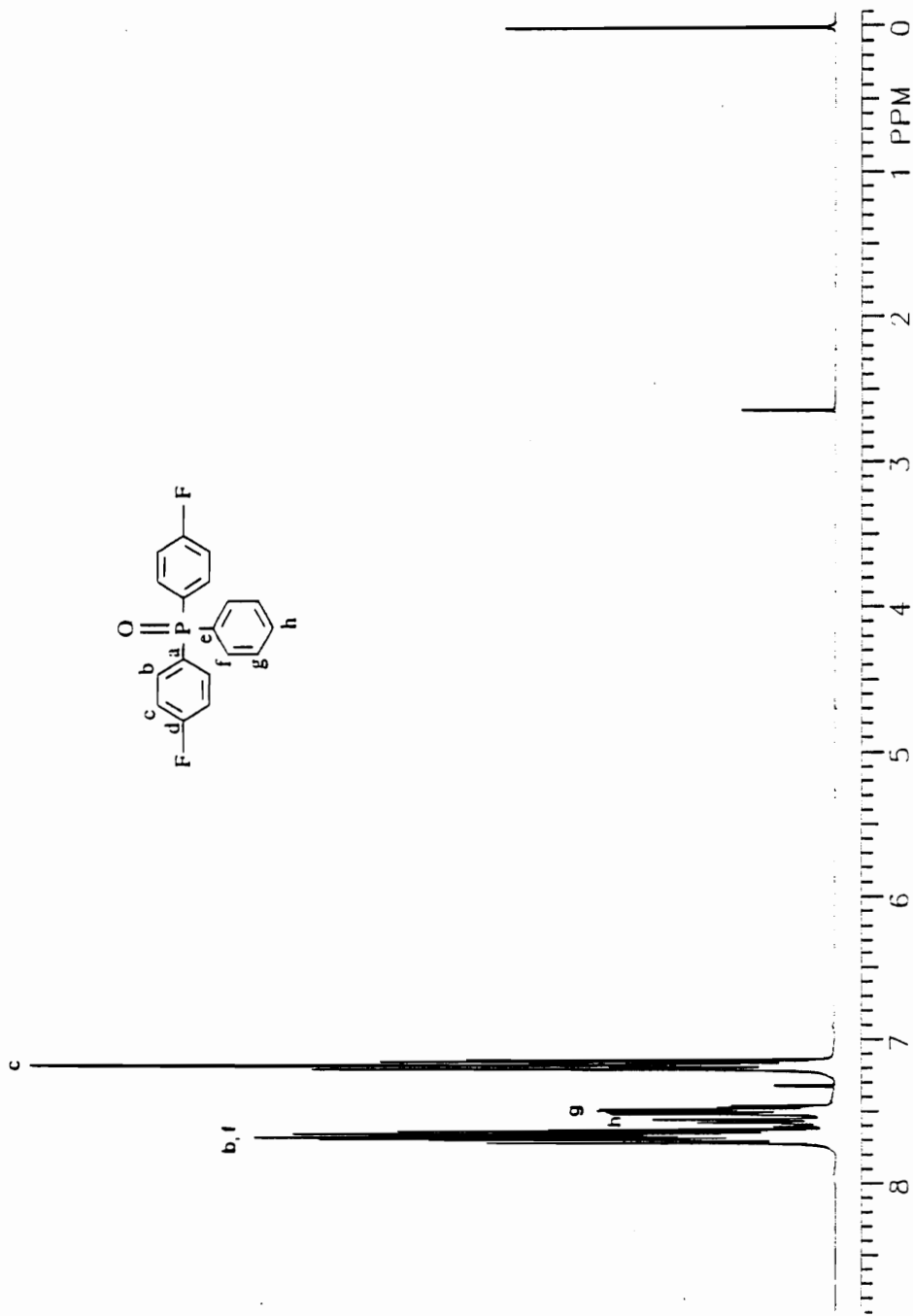


Figure 97.  $^1\text{H}$  NMR spectrum of bis(4-fluorophenyl)phenylphosphine oxide.

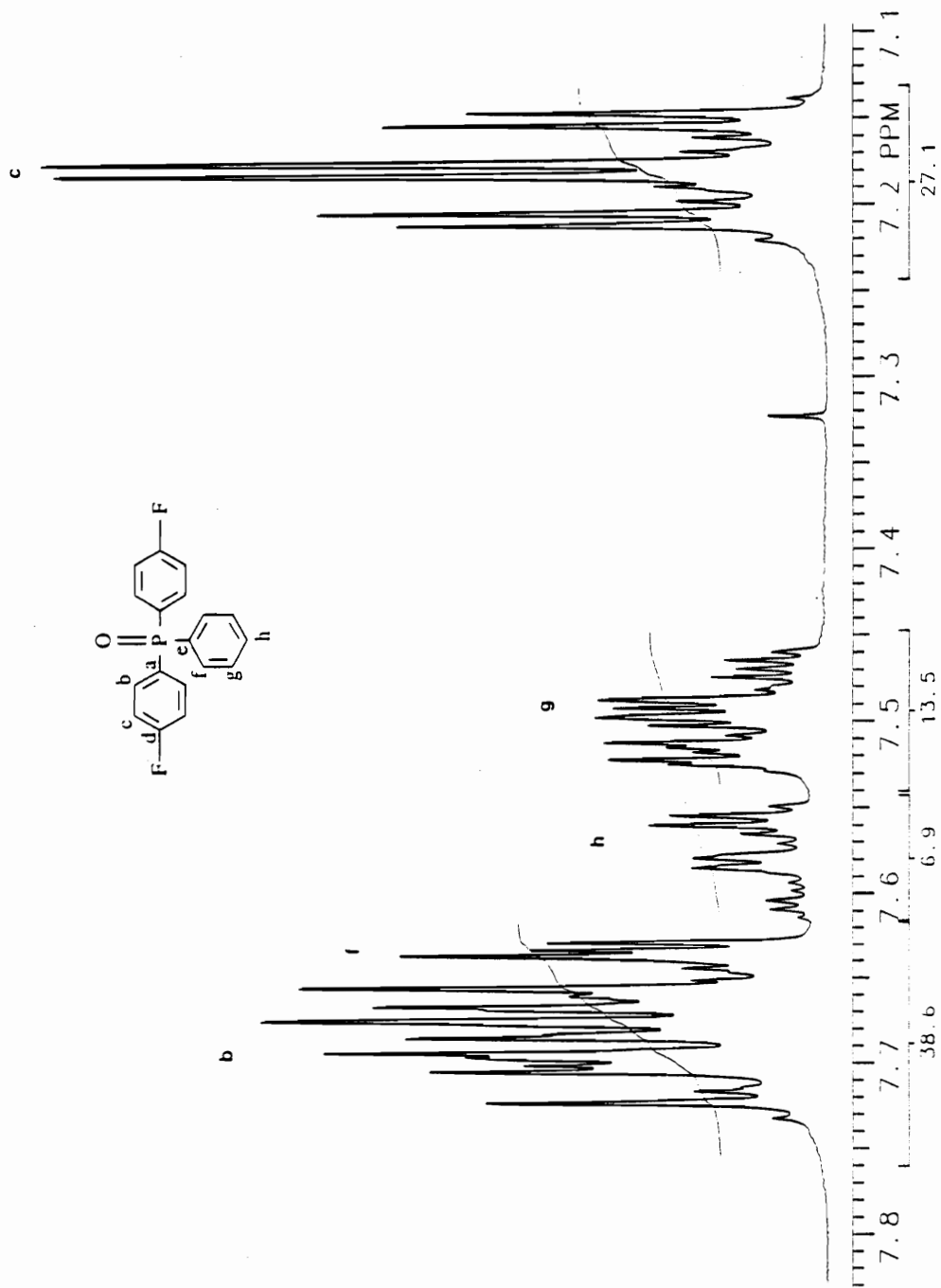


Figure 97a. Expansion of the aromatic region of the  $^1\text{H}$  NMR spectrum of bis(4-fluorophenyl)phenylphosphine oxide.

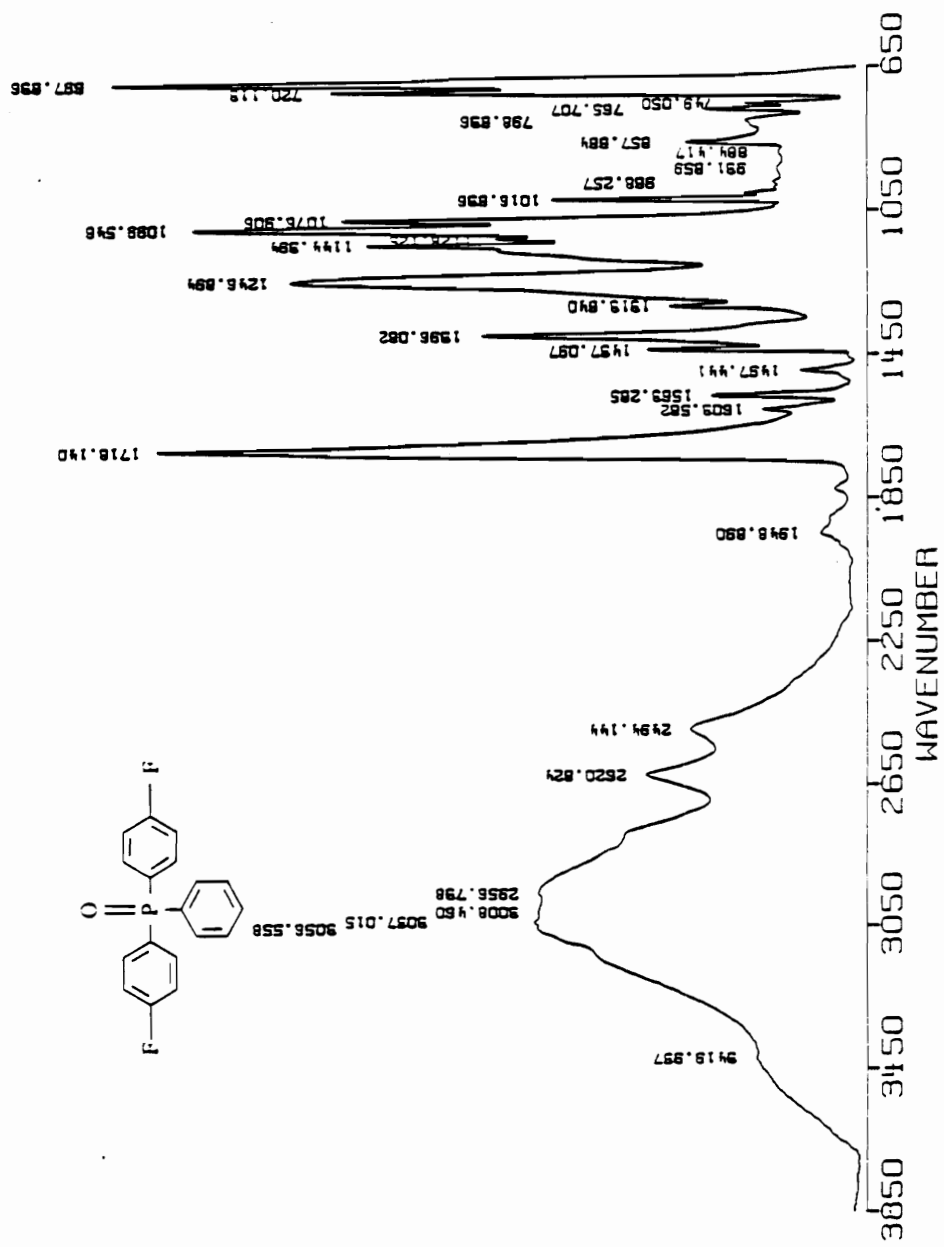


Figure 98. IR spectrum of bis(4-fluorophenyl)phenylphosphine oxide.

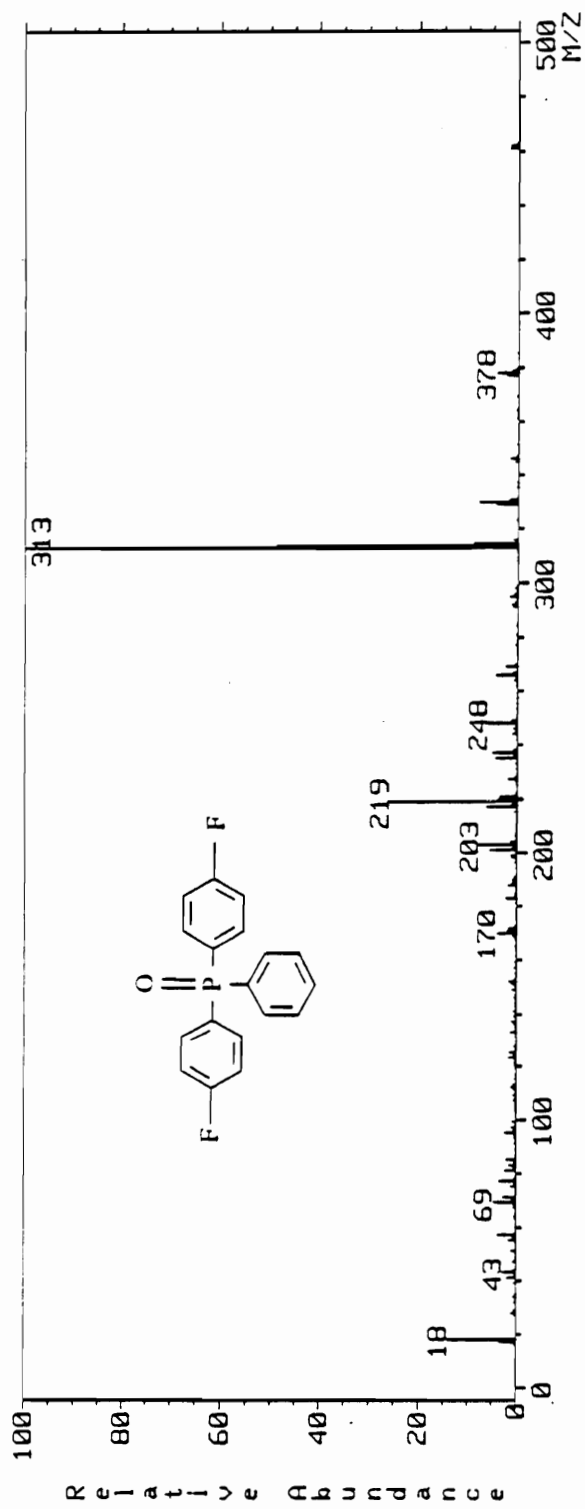


Figure 99. Mass spectrum of bis(4-fluorophenyl)phenylphosphine oxide.

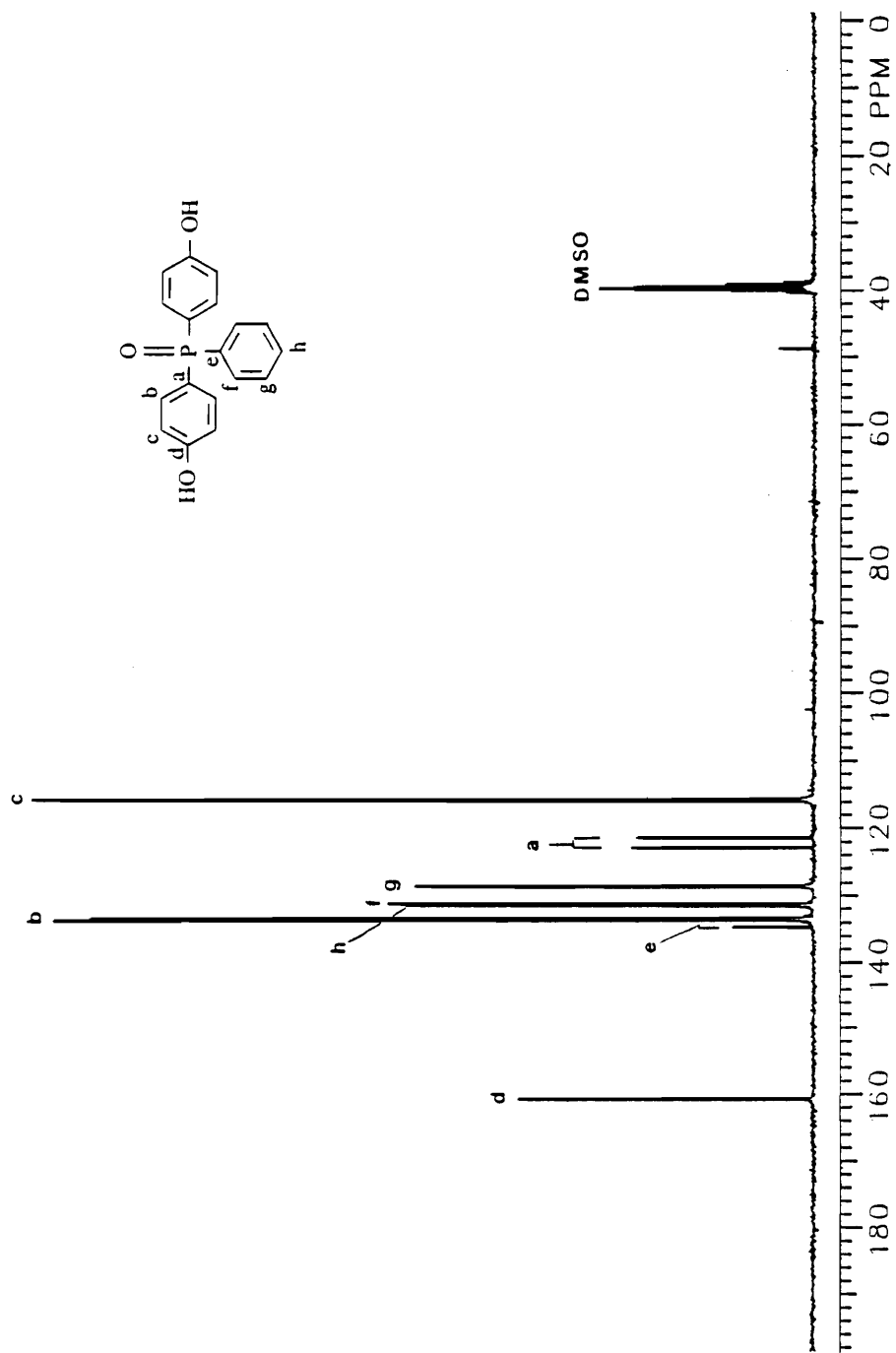


Figure 100.  $^{13}\text{C}$  NMR spectrum of bis(4-hydroxyphenyl)phenylphosphine oxide.

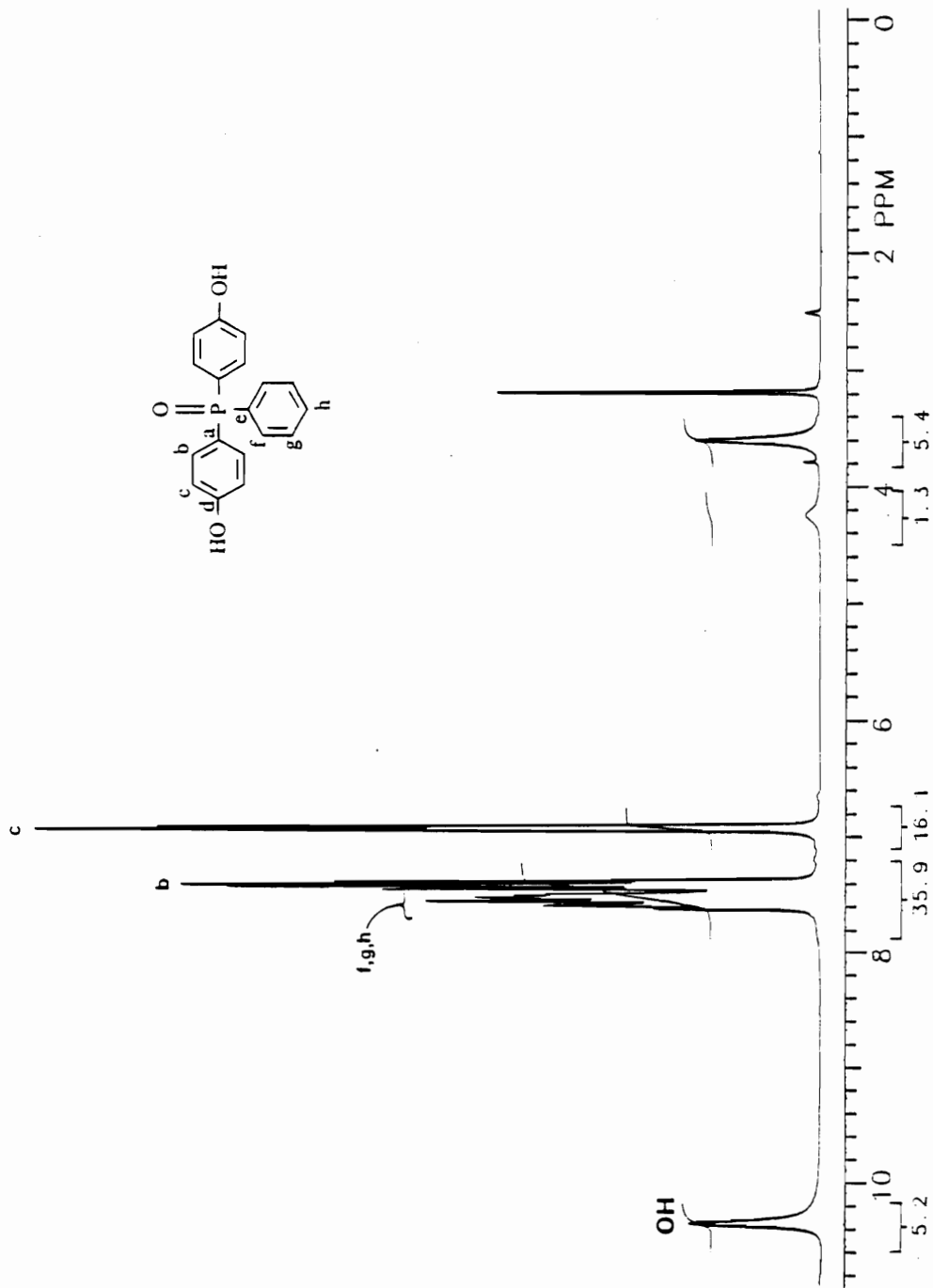


Figure 101.  $^1\text{H}$  NMR spectrum of bis(4-hydroxyphenyl)phenylphosphine oxide.

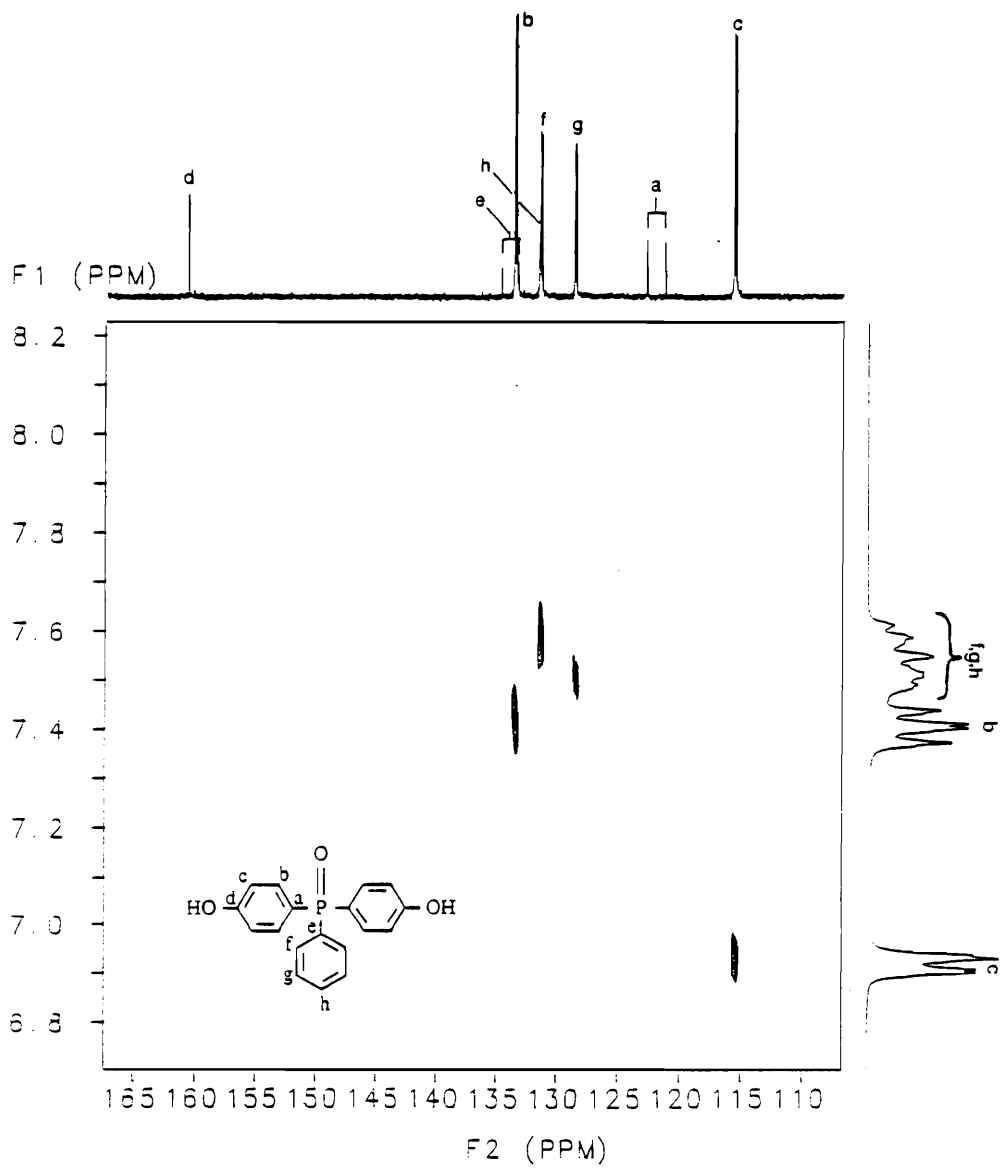


Figure 102. 2D NMR spectrum of bis(4-hydroxyphenyl)phenylphosphine oxide.



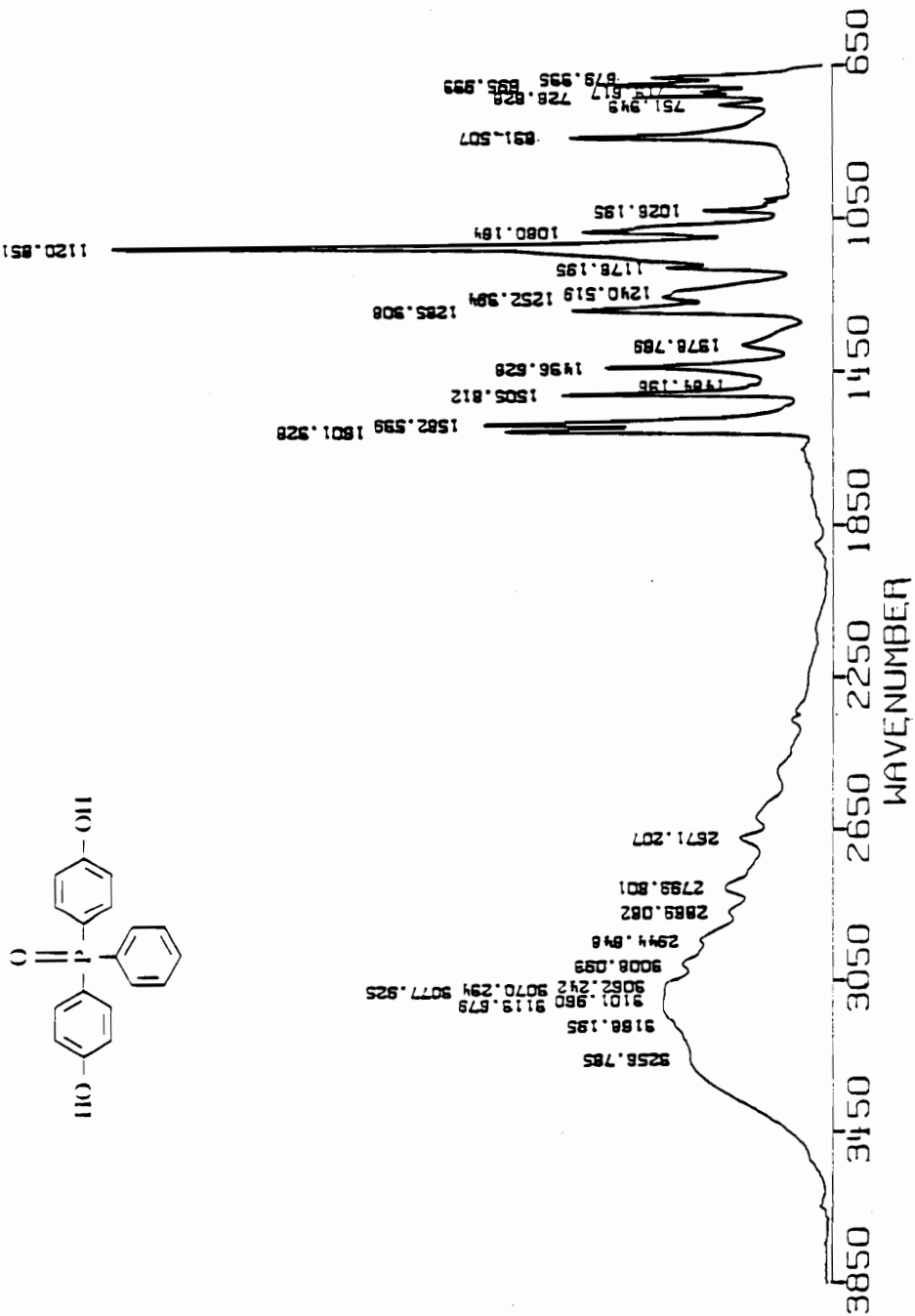


Figure 103. IR spectrum of bis(4-hydroxyphenyl)phenylphosphine oxide.

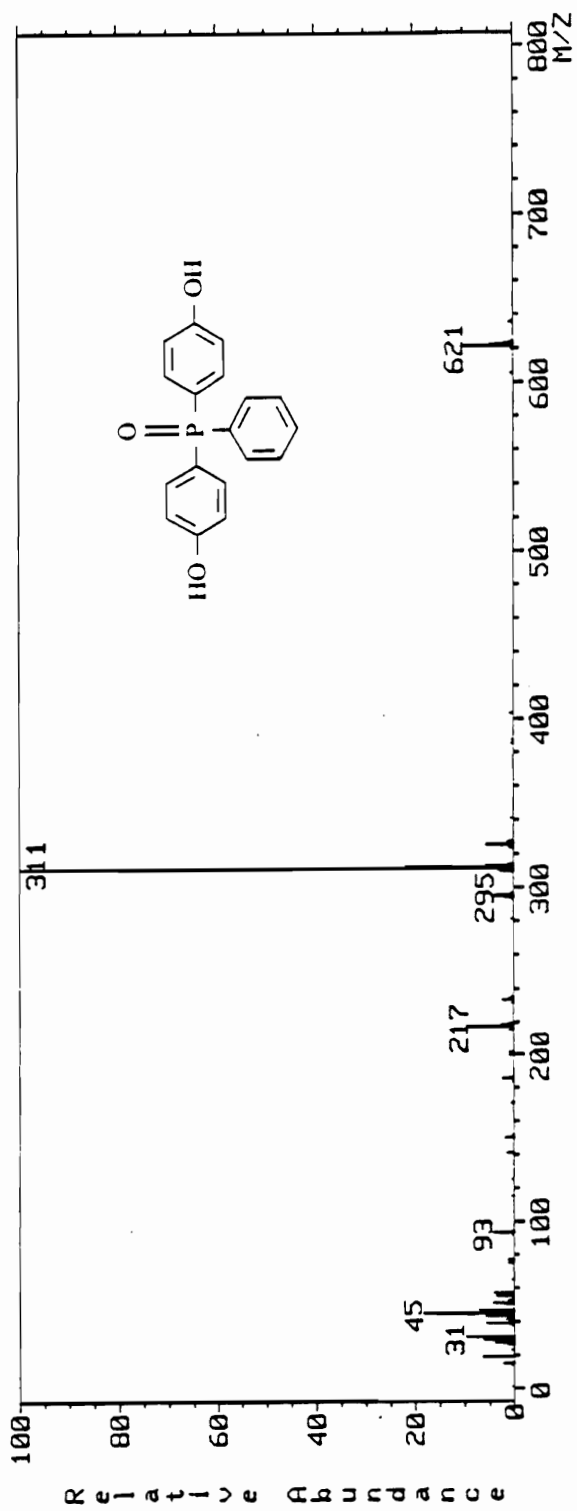


Figure 104. Mass spectrum of bis(4-hydroxyphenyl)phenylphosphine oxide.

formed was taken off by careful distillation. The reaction mixture was periodically sampled and analyzed by gas chromatography on a DB-5 capillary column. Distillation was continued until there was at least 98% conversion to the fully silylated product. At this point the heating bath had reached 195°C. The argon line was replaced with a vacuum line and the product was distilled. 294.2 g (80%) of product distilling at 103-107°C and 0.34 torr was obtained. The product was used without further purification in the subsequent preparation of bis(4-aminophenyl)phenylphosphine oxide.

### 5.2.8 Bis(4-aminophenyl)phenylphosphine Oxide

A 2-L three-necked flask fitted with a mechanical stirrer, a reflux condenser, and a 500 mL pressure equalized dropping funnel was dried overnight in an oven at 110°C. The apparatus was then assembled hot under a flow of dry nitrogen and a low temperature thermometer was added. Magnesium turnings (22.69 g, 0.94 mol) were added with 200 mL of anhydrous ethyl ether and 292.4 g (0.92 mol) of N,N-bis(trimethylsilyl)-4-bromoaniline was added to the addition funnel under dry nitrogen. After addition of approximately 0.1 g of iodine crystals to the ether suspension, dropwise addition of the bromoaniline was started. The iodine color disappeared at once and the magnesium surface became black. Addition of the bromoaniline was completed in two hours with no detected exotherm. The solution obtained was stirred overnight at ambient temperature. Using a glass fritted filter, the solution was filtered under a blanket of nitrogen to remove unreacted magnesium metal. The solution was filtered into a previously dried 3-L three-necked flask equipped with a magnetic stirrer, pressure equalized dropping funnel, and a nitrogen inlet adapter. Dichlorophenylphosphine oxide (90.0 g, 0.462 mol) in 100 mL of ethyl ether was added dropwise via the addition funnel to the Grignard solution. An exotherm was observed and the rate of addition was controlled so that the ethereal solu-

tion was kept at a gentle reflux. Addition was completed in three hours and the reaction mixture was allowed to stir overnight at ambient temperature. A gummy red solid was obtained. The reaction flask was cooled with an ice bath and 400 mL of saturated ethanolic hydrogen chloride was added slowly via the addition funnel. Addition was completed in two hours and the yellow precipitate formed was stirred for an additional two hours. The hygroscopic precipitate was collected and stored over anhydrous calcium chloride for 24 hours. The calcium chloride was replaced by anhydrous sodium hydroxide (to absorb excess hydrogen chloride). A final crude yield of 356 g was obtained.

A 57.1 g sample of the crude material was dissolved in two liters of water containing 40 mL of concentrated hydrochloric acid. This solution was added to a continuous extractor and extracted for 60 hours with ethyl ether. Phases were separated and the aqueous phase was concentrated under reduced pressure. The remainder of the water was removed by lyophilization. The dried residue weighed 47.8 g. Fifteen grams of the lyophilized product was dissolved in a mixture of 520 mL of 95% ethanol, 167 mL of concentrated hydrochloric acid and 167 mL of water. The solution was boiled and treated with 1.0 g of activated carbon for five minutes. The solution was filtered and the filtrate was subjected to the same carbon treatment twice again. The filtrate was added to a mixture of 290 mL of 95% ethanol to which 166 mL of water and 116 mL of 50% (w/w) sodium hydroxide solution has been added. The cloudy suspension obtained was extracted with five portions of 250 mL each of chloroform. The chloroform extracts were combined and the solvent removed under reduced pressure. The solid obtained was washed with three 50 mL portions of hot water and then triturated with two 15 mL portions of chloroform. The slurry was filtered and dried at 50°C for 24 hours at 0.5 torr. A yield of 2.15 g (28.8% based on dichlorophenylphosphine oxide) of white powder with a sharp melting point of 269°C was obtained.

The carbon, proton and 2D NMR spectra, the infrared spectrum and the mass spectrum are shown in Figures 105-109.

### 5.2.9 Bis(4-aminophenyl) phenylphosphine Oxide

In a 450 mL stirred Parr pressure reactor was placed a solution of 0.3139 g (3.182 mol) of bis(4-fluorophenyl)phenylphosphine oxide in 250 mL of DMSO. The reactor was closed, weighed and then cooled in an ice-water bath and ammonia was introduced with stirring. When the addition of ammonia was complete, the reactor was weighed again. A total of 55 g (3.23 mol) of ammonia had been added. The reactor was then heated with stirring from an initial pressure of 40 psi at 19°C. Stirring was continued for three days at 135-136°C and 1360 psi. Heating was then discontinued and the reactor allowed to cool to ambient temperature. A sample was taken and subjected to TLC analysis. TLC (85:14:1 - chloroform:ethanol:ammonium hydroxide) showed no starting material (Rf 0.72), and a spot corresponding to bis(4-aminophenyl)phenylphosphine oxide (Rf 0.23). An unidentified spot of Rf 0.73 was also obtained.

The TLC results were corroborated by HPLC. Samples were analyzed on a Whatman Partsil 5 (5m) 4.6 x 250 mm column using 5:95 methanol:ethyl acetate at a flow of two ml/min and a pressure of 2500 - 3000 psi using a Waters M6000A pump, and an ISCO UA-5 Absorbance Detector. The following results were obtained:

<u>Compound</u>	<u>Retention Times (min.)</u>		
bis(4-fluorophenyl)phenylphosphine oxide			3.0
bis(4-aminophenyl)phenylphosphine oxide			8.5
reaction mixture	4.5	5.0	9.3
	4.3	4.8	8.5

Figure 106

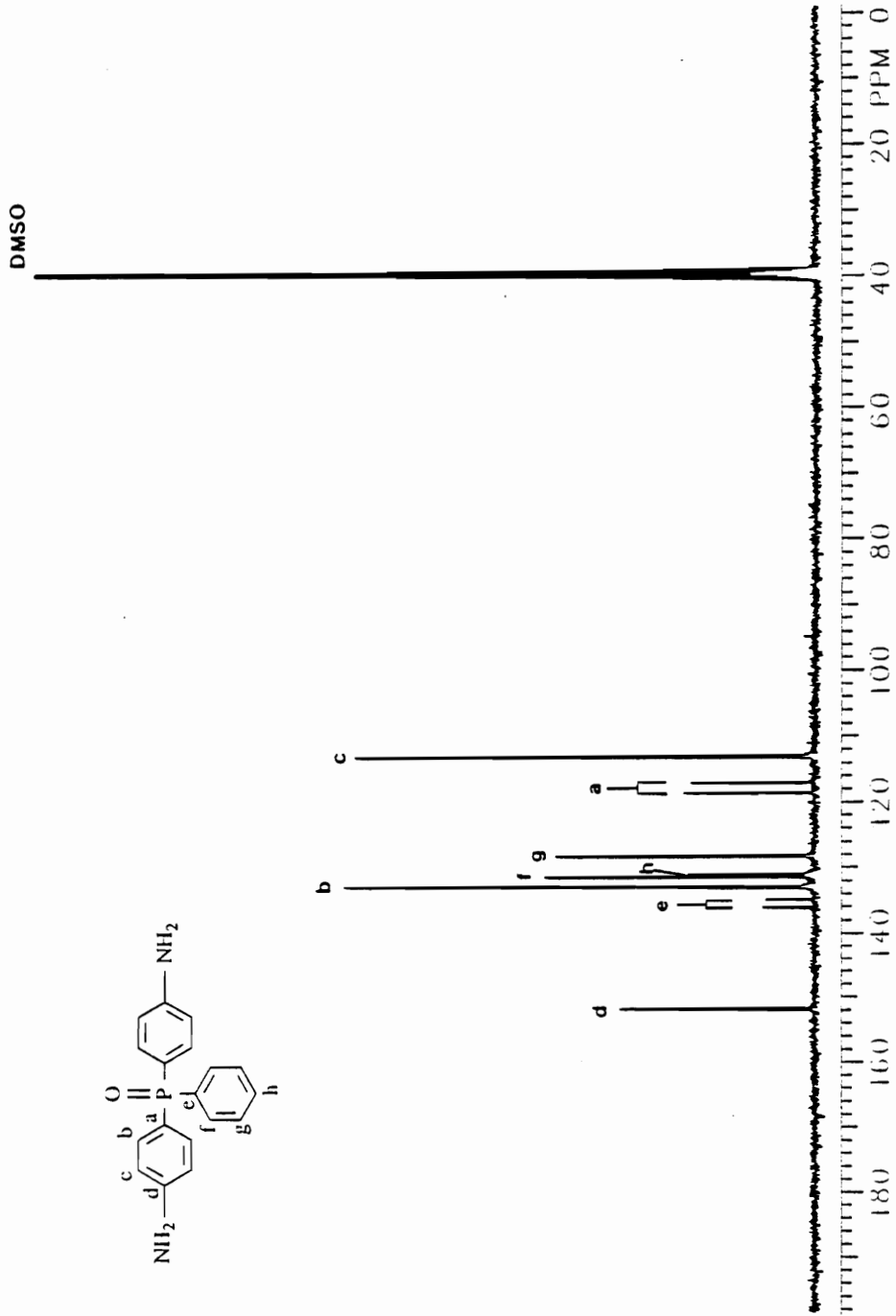


Figure 105.  $^{13}\text{C}$  NMR spectrum of bis(4-aminophenyl)phenylphosphine oxide.

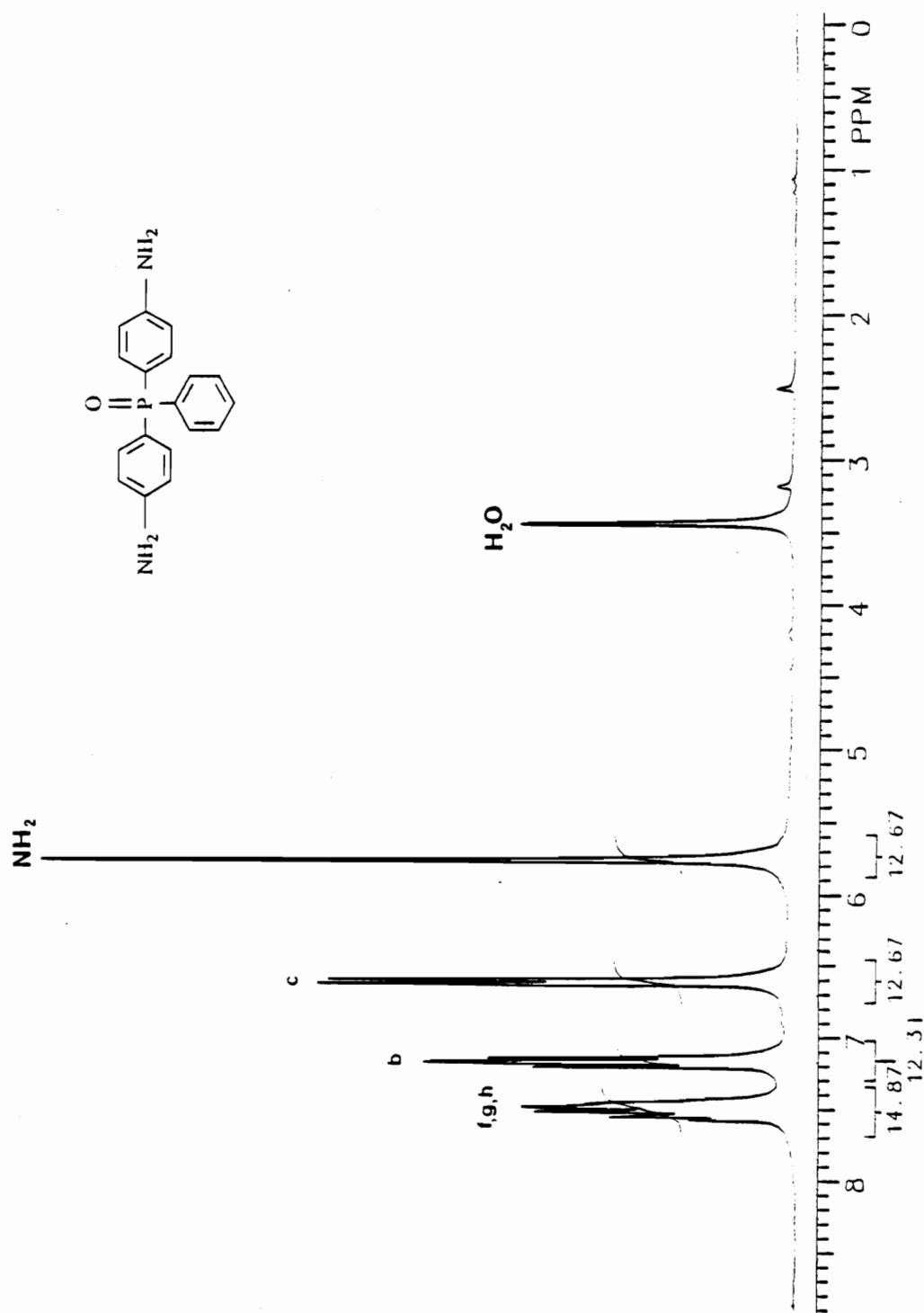


Figure 106.  $^1\text{H}$  NMR spectrum of bis(4-aminophenyl)phenylphosphine oxide.

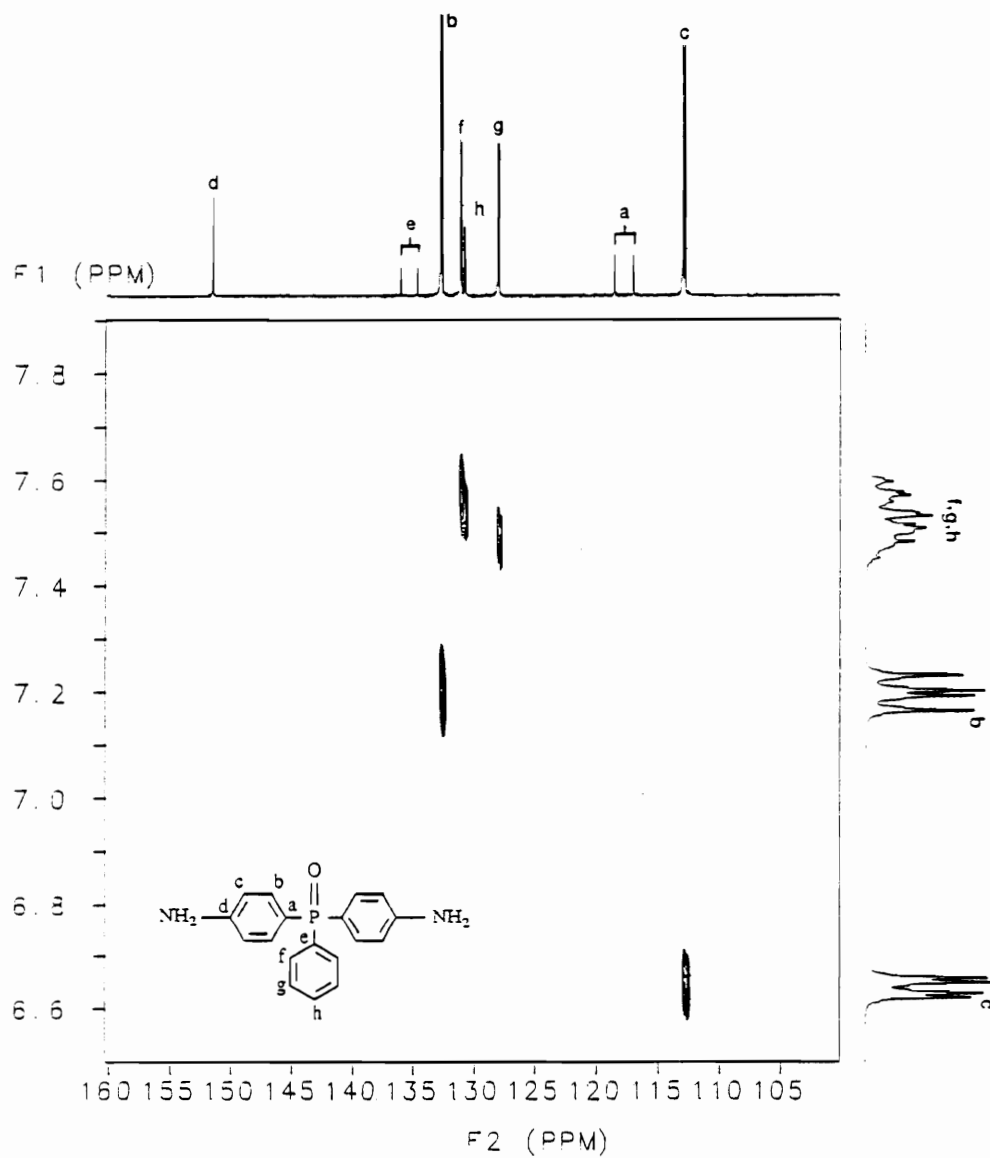


Figure 107. 2D NMR spectrum of bis(4-aminophenyl)phenylphosphine oxide.



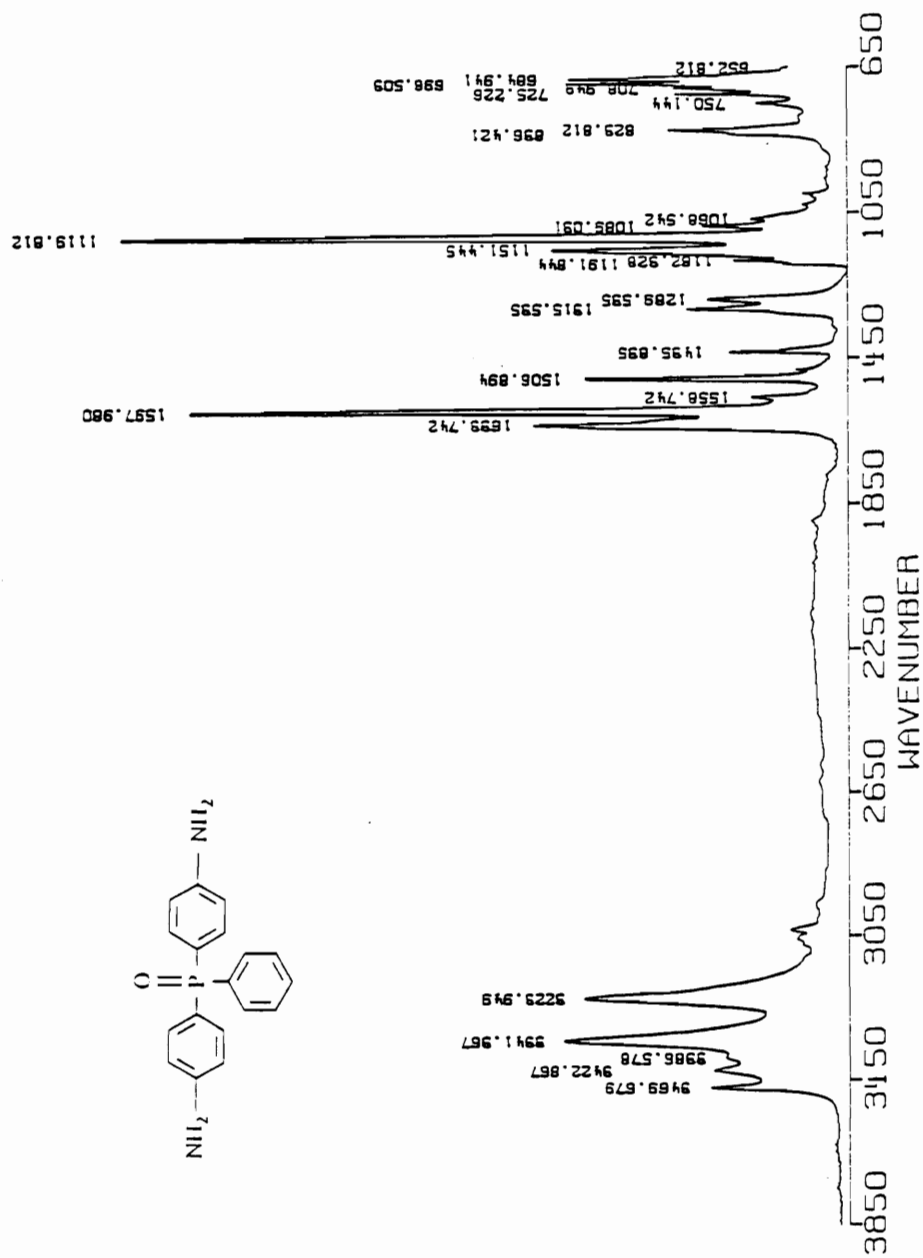


Figure 108. IR spectrum of bis(4-aminophenyl)phenylphosphine oxide.

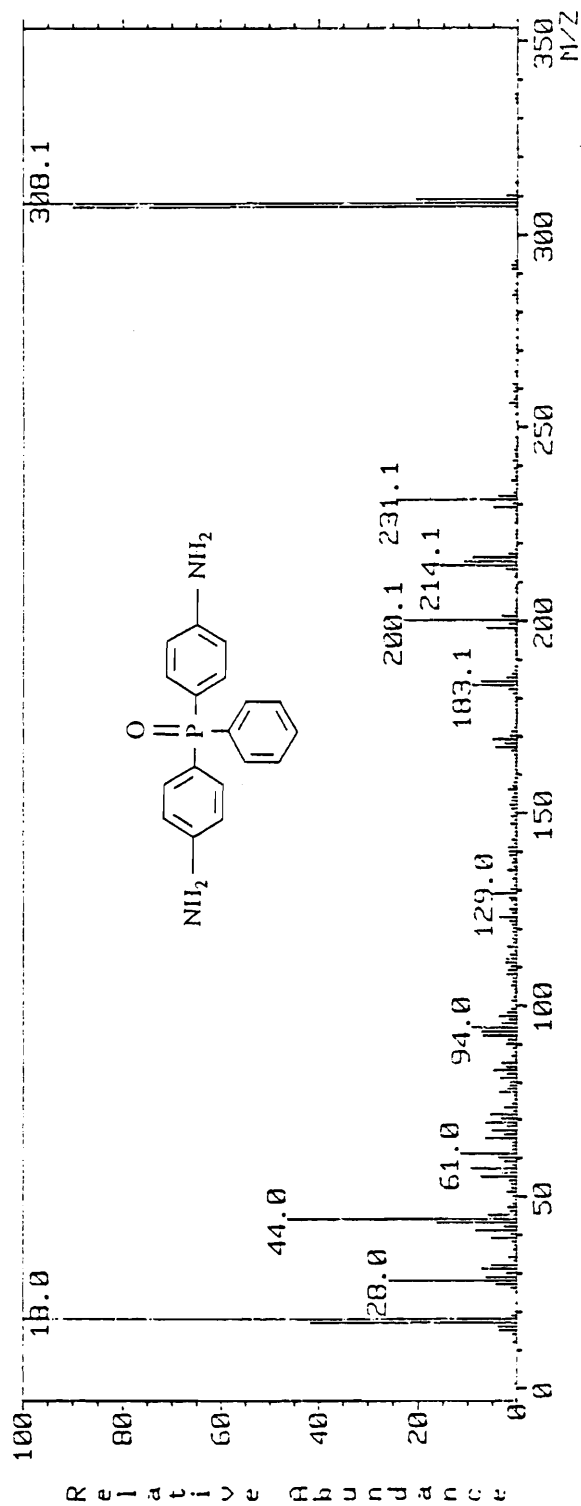


Figure 109. Mass spectrum of bis(4-aminophenyl)phenylphosphine oxide.

Using a calibration response curve obtained from weighed amounts of polymerization grade bis(4-aminophenyl)phenylphosphine oxide, analysis showed the reaction mixture contained  $0.55 \pm .02$  mg/ml of product which corresponds to a reaction yield of 45%.

#### 5.2.10 Attempted preparation of Bis(4-nitrophenyl) phenylphosphine Oxide

Into a 1-L three-necked flask was placed 20 g (0.06 mol) of bis(4-fluorophenyl) phenylphosphine oxide and DMSO. The mixture was heated to 70°C with stirring and 13.5 g (0.26 mol) of lithium nitrite was added in a single portion. The mixture was heated to 150°C for five hours with stirring and then allowed to cool to room temperature. 500 mL of water was added with stirring and the dark red solution was extracted with three 150 mL portions of methylene chloride. The methylene chloride was removed under reduced pressure and the residue obtained was dissolved in 300 mL of benzene and extracted with three 50 mL portions of water. The benzene phase was separated, dried over magnesium sulfate, filtered, and the benzene removed under reduced pressure. A waxy solid was obtained which weighed 5.21 g. Column chromatography on silica gel using ethyl acetate:methylene chloride (10:90) produced a mixture of the desired dinitro compound, and unreacted starting material. TLC and mass spectral analysis confirmed that no effective separation of components was obtained. Under identical reaction conditions and substituting DMF and HMPA for the DMSO solvent, no improvement was noted in the yield or ratio of reaction products. This synthetic approach was abandoned.

#### 5.2.11 Attempted preparation of Bis(2-acetaminophenyl) phenylphosphine

To a 500-mL four-necked round bottom flask equipped with a mechanical stirrer, reflux condenser with a nitrogen inlet adapter, carbon disulfide (150 mL) and acetanilide

(27.0 g, 0.200 mol) was added with stirring. Phenyl dichlorophosphine (18.0 g, 0.100 mol) in 25 mL of carbon disulfide was added rapidly. Aluminum chloride (84.4 g, 0.638 mol) was added in small portions and a slight exotherm from ambient to 40°C was noted. One hour after completion of addition, the reaction mixture was taken to gentle reflux by use of a warm water bath and allowed to stir at reflux for 18 hours. After cooling to room temperature, the liquid phase was decanted and the remaining white solid was added to a mixture of 1200 g of ice and 100 mL of concentrated hydrochloric acid. A vigorous reaction took place which formed a gummy white solid. The reaction flask was rinsed with 400 mL of methylene chloride which was added to the ice mixture. The phases were separated and the aqueous phase was extracted with two 150 mL portions of methylene chloride. The methylene chloride solutions were combined and washed with one 200 mL portion of water, separated and dried over magnesium sulfate. After filtration and removal of methylene chloride under reduced pressure, a solid residue of 24.5 g was obtained. A melting point of 110-113°C was obtained and  $^{13}\text{C}$  and  $^1\text{H}$  NMR were taken. The spectra obtained were identical with the spectra of acetanilide.

Additional attempts employing 1,1,2,2-tetrachloroethane and nitrobenzene as solvents with dichlorophenylphosphine failed to yield the intended product. All three solvent systems with iron trichloride also failed to yield product, yielding acetanilide starting material only. Additional attempts to utilize dichlorophenylphosphine sulfide with aluminum chloride and the above solvents produced the starting material, acetanilide, in yields of 30% to 80%. This synthetic approach was abandoned.

### 5.3 RESULTS AND DISCUSSION

The exploration of the use of the Friedel-Crafts reaction for the direct attachment of phosphorus to an aromatic ring has been under investigation for many years. The

difficulties and limited success associated with the classical approaches have been reviewed extensively (245). The Friedel-Crafts reaction continues to be quite attractive as an industrially significant approach to the preparation of aryl phosphine oxide derivatives for several reasons. The classic Grignard approach normally requires expensive halogen substituted aromatic systems as feedstocks and the use of metallic magnesium and ether solvents. This reaction is quite often difficult to initiate and the hazard associated with peroxide formation in ethereal solvents and the inherent fire hazard limit the industrial acceptance of Grignard chemistry. The choice of substrates available for the production of aryl phosphine oxides by Friedel-Crafts approaches is quite large. Three starting materials for the preparation of disubstituted phenylphosphine systems are commercially available. The reactivity of these three starting materials increases from dichlorophosphine oxide to dichlorophosphine, to dichlorophosphine sulfide (233,237,245). The reactivity of dichlorophosphine oxide is quite low and it is suitable for Friedel-Crafts reactions only when a highly active substrate such as diphenyl ether or 4,4'-diphenoxydiphenyl sulfide is used (237). For reactions with less active substrates, such as fluorobenzene and chlorobenzene, dichlorophosphine and dichlorophosphine sulfide are more suitable intermediates (245).

To explore the feasibility and ease of preparation, the synthesis of bis(4-carboxyphenyl) phenylphosphine oxide by a Friedel-Crafts mediated routes was carried out. A direct comparison was made with the published procedure of Morgan and Herr (202) which utilized the classic Grignard route. As discussed previously, the Morgan route utilized the formation of a Grignard intermediate from p-bromotoluene and magnesium in ether and subsequent reaction with dichlorophenylphosphine oxide. The crude product bis(4-methylphenyl)phenylphosphine oxide was obtained contaminated with bromotoluene and bitolyl which required a difficult separation and purification prior to

oxidation to the intended bis(4-carboxyphenyl)phenylphosphine oxide. An overall yield of less than 50% was obtained based on the consumption of dichlorophenylphosphine oxide. By comparison, the reaction of toluene with dichlorophosphine sulfide in the presence of aluminum chloride gave a yield of 62% of bis(4-methylphenyl)phenylphosphine sulfide. Figure 110 represents a complete comparison of the two routes. By use of the Friedel-Crafts route, a step is saved and toluene is used as the solvent as well as the reactant in the single step preparation of the key intermediate, bis(4-methylphenyl)phenylphosphine sulfide. Using the Grignard route, two steps are needed to get to bis(4-methylphenyl)phenylphosphine oxide and the use of the more expensive p-bromotoluene is required. The cost and availability of the starting phosphine intermediates are approximately equal.

As indicated in the introduction to this section, the preparation and use of bis(4-hydroxyphenyl) phenylphosphine oxide for the production of a wide variety of phosphorous containing polymers continues to be of interest. Polyarylates, polycarbonates, and poly(arylene ethers) with flame retarding properties as well as potential use for high temperature resistant applications may be prepared with this useful intermediate.

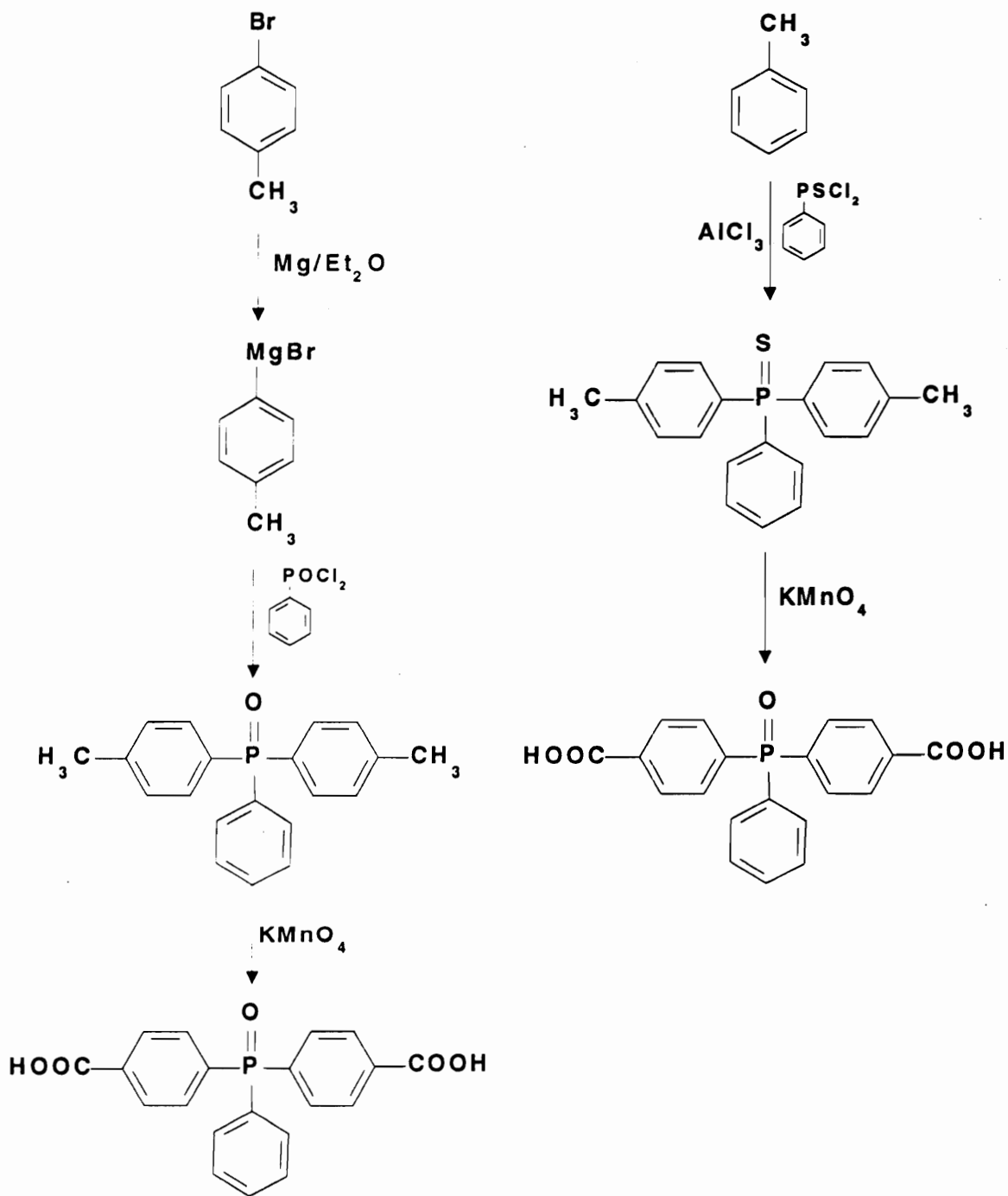


Figure 110. Preparation of bis(4-carboxyphenyl)phenylphosphine oxide by Grignard and Friedel-Crafts routes.

To date, the only published route to this intermediate has been that of Senear, Valient, and Wirth (213) utilizing a Grignard intermediate (Figure 111). As seen in Figure 111, p-bromoanisole is reacted with magnesium in tetrahydrofuran solvent to yield the Grignard intermediate which is subsequently reacted with dichlorophenylphosphine to yield bis(4-methylphenyl)phenylphosphine. The phosphine is then oxidized to the phosphine oxide and subsequently treated with aqueous hydrobromic acid to cleave the methoxy function to yield the free phenol. This four step process proceeds in an overall yield of approximately 46% and requires the use of an expensive p-bromoanisole intermediate. An alternative process based on a Friedel-Crafts process has been demonstrated in this investigation. In the teachings and examples of Ude *et al.* (237, U.S. Patent 4,698,448), the preparation of bis(4-phenoxyphenyl) phenylphosphine sulfide is disclosed. A Friedel-Crafts reaction of diphenyl ether and dichlorophenylphosphine sulfide in the presence of aluminum chloride is used to produce the phosphine derivative in yields that are greater than 90%. Diphenyl ether is used in excess as both the reactant and the solvent. The reaction proceeds very readily and allows the recovery of excess diphenyl ether.

Several attempts were made to facilitate nucleophilic substitution at the phenoxy linkage. Strong aqueous sodium hydroxide at elevated temperature produced no reaction. Sodium hydroxide in polar aprotic solvents also failed to react. The use of neat sodium hydroxide fused at 310°C in excess, in the presence of air did lead to nucleophilic substitution and simultaneous conversion of the phosphine sulfide moiety to the phosphine oxide moiety (Figure 112).



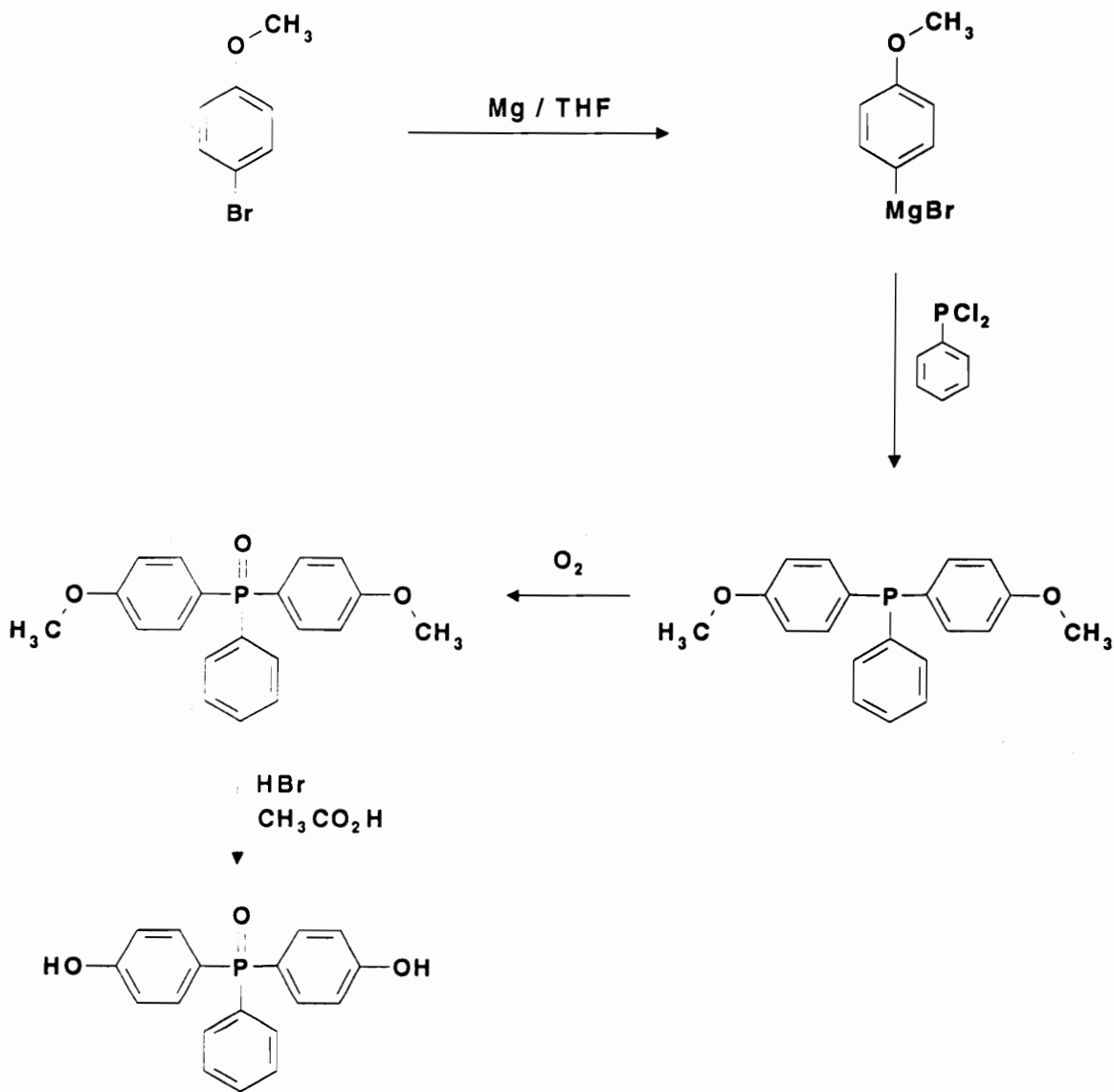


Figure 111. Grignard mediated preparation of bis(4-hydroxyphenyl)phenylphosphine oxide.

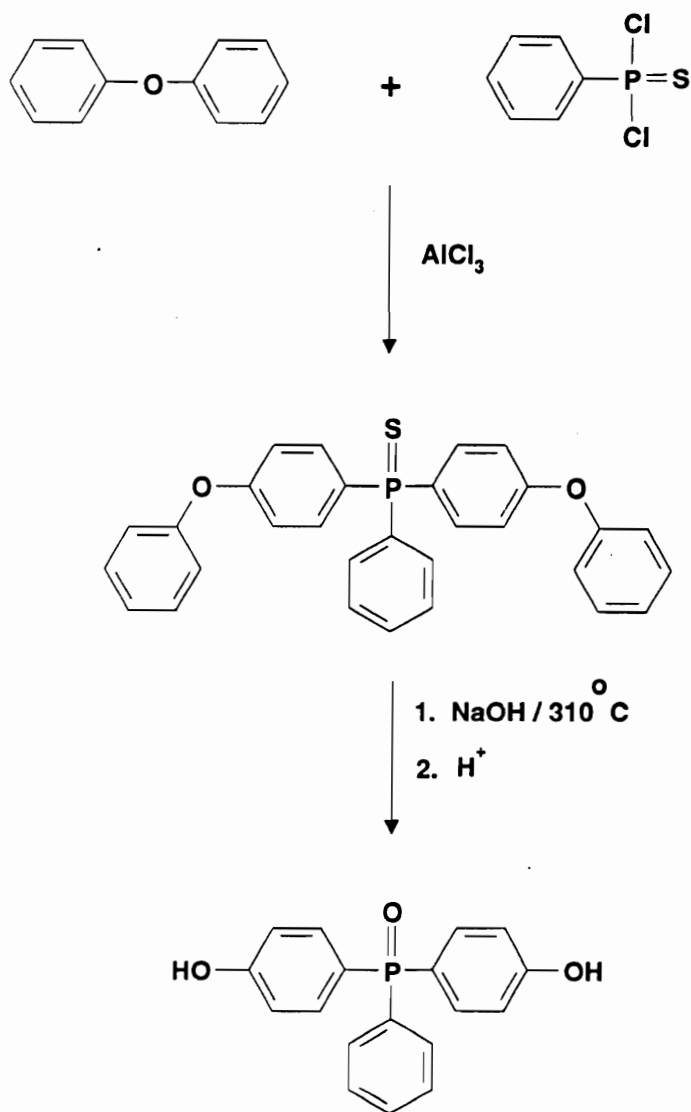


Figure 112. Friedel-Crafts mediated preparation of bis(4-hydroxyphenyl)phenylphosphine oxide.

The yield based on consumption of dichlorophosphine sulfide was 72%. The yield using the Grignard-based procedure was 46%.

A final example of a successful Friedel-Crafts preparation of an aryl substituted phosphine is the preparation of bis(4-isopropylphenyl) phenylphosphine sulfide. In this example, cumene is reacted with dichlorophenylphosphine sulfide in the presence of aluminum chloride to yield the isopropyl substituted phosphine product in 73% isolated yield. As proposed in Figure 113, this intermediate may prove useful as an alternative preparation of bis(4-hydroxyphenyl)phenylphosphine oxide via a modified cumene hydroperoxide route. Investigations of this route are currently in progress in our research group.

The preparation of bis(4-aminophenyl)phenylphosphine oxide was reported by Androva *et al.* (220) in 1971 and has not been reported in the open literature since. Their preparation was carried out by workers in our group (225) and could not be reproduced.

Based on the known efficiency of the addition of Grignard reagents to dichlorophenylphosphine oxide, the starting material selected was p-bromoaniline. As shown in Scheme 15, p-bromoaniline was reacted with N,N-diethyl trimethylsilylamine in the presence of a catalytic amount of ammonium sulfate (246) to yield N,N-bis(trimethylsilyl)-4-bromoaniline. The protected aniline was reacted with magnesium to yield a Grignard (Scheme 16) reagent which in turn was reacted with dichlorophenylphosphine oxide. The fully silylated diamine was not isolated but was subjected to acid hydrolysis and neutralization with base. A 30% yield of monomer grade diamine was obtained.

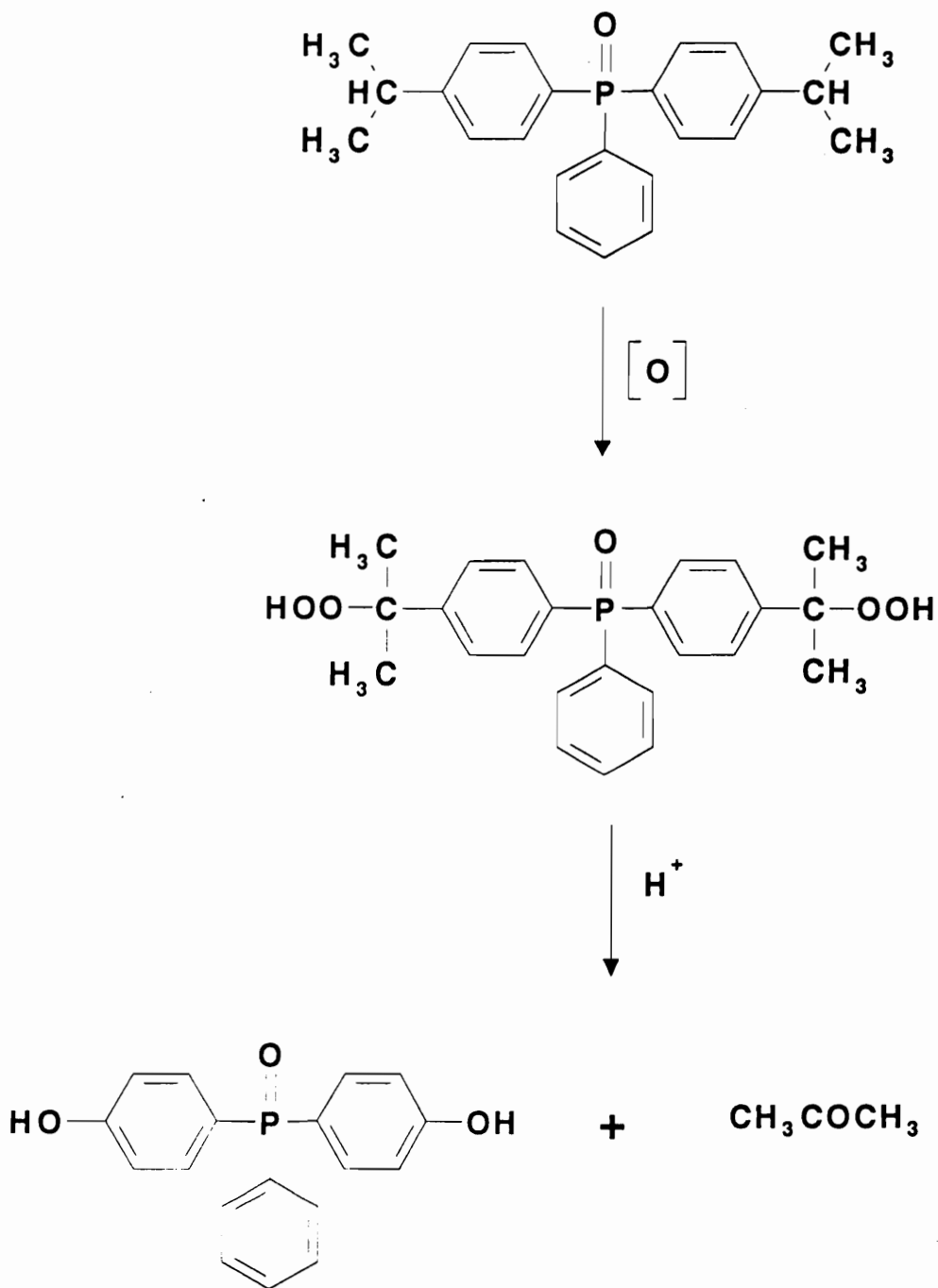
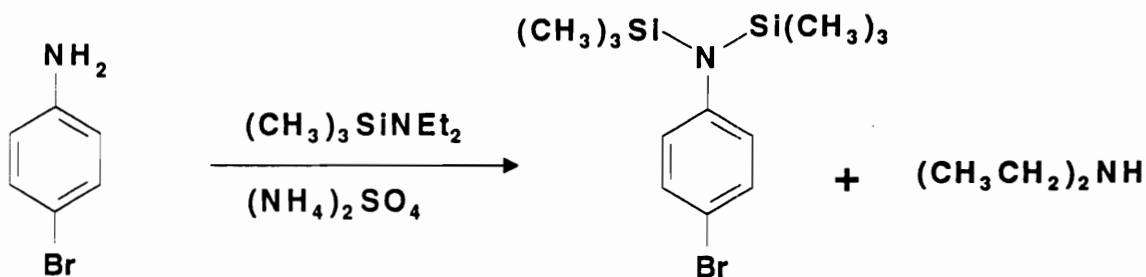
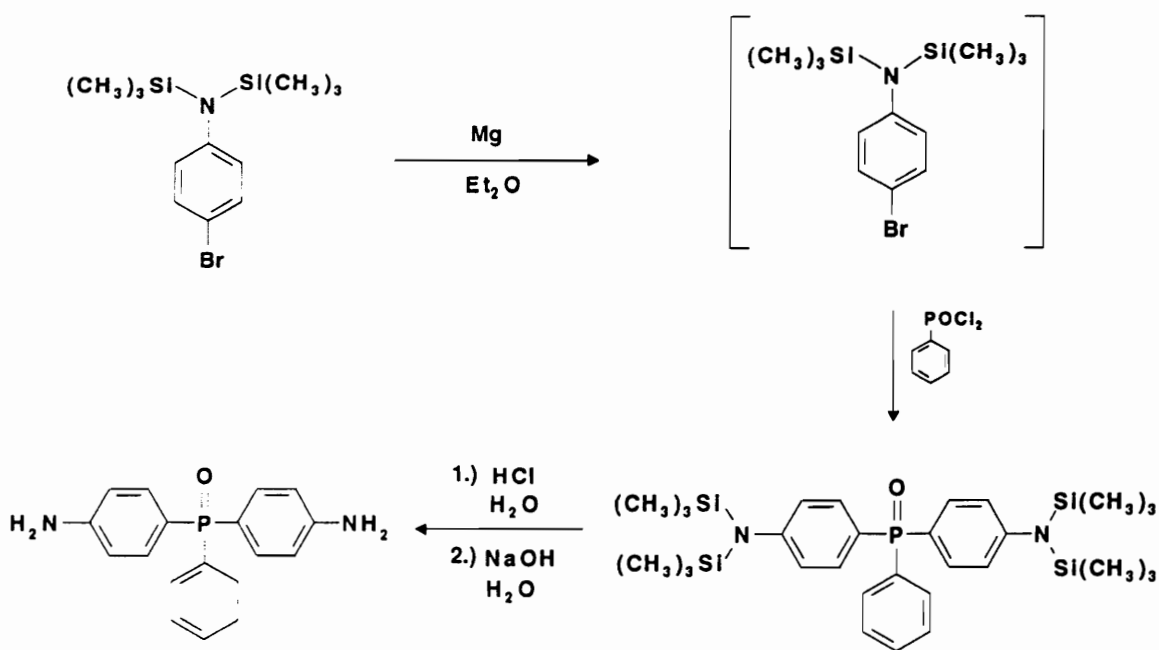


Figure 113. Proposed alternate synthesis of bis(4-hydroxyphenyl)phenylphosphine oxide.



Scheme 15. Preparation of N,N-bis(trimethylsilyl)-4-bromoaniline.



Scheme 16. Preparation of bis(4-aminophenyl)phenylphosphine oxide.

### 5.3.1 Liquid Chromatographic - Mass Spectrometric Investigations

An alternative route based on the direct amination of bis(4-fluorophenyl)phenylphosphine oxide was also explored. Bis(4-fluorophenyl)phenylphosphine oxide was prepared by the Grignard route previously discussed (225). Using a small scale Parr pressure reactor, bis(4-fluorophenyl) phenylphosphine oxide was subjected to direct ammonolysis in DMSO. Samples were removed from the reactor for analysis by TLC and the product bis(4-aminophenyl)phenylphosphine oxide and an unknown spot were observed. No starting material was observed. To corroborate this observation, an LC-MS analysis was performed. Separation by HPLC was accomplished with a Waters 600-MS solvent delivery system using a Waters Nova-Pak 3.9 x 75 mm phenyl column. A methanol/water linear gradient was employed with initial conditions of 30% methanol and programming to 80% methanol in 30 minutes. A step gradient to 100% methanol was performed at 31 minutes and held at 100% methanol for 10 minutes before returning to the initial conditions. Detection was at 260 nm and the flow rate was 0.5 ml/min. MS analysis of the sample mixtures was accomplished using a JEOL SX 102/SX 102 four-sector tandem mass spectrometer. The resolution obtained was approximately 1000, accelerating potential was 10 kV, and a scan slope of 0-2400 amu was used. Fast atom bombardment (FAB) ionization was employed using Xe atoms at 6 KeV energy as the ionizing particles. The interface chosen was the "frit-FAB" stainless steel frit. The FAB matrix, which was added to the mobile phase of the LC system forms a thin film on the distal surface of the frit. The analyte is suspended in this matrix, and the impact of the 6 KeV beam on the matrix covered frit surface serves to desorb and ionize the analyte. Ionization by this method results in very little fragmentation, usually producing "pseudo-molecular" ions  $[(M+H^+), (M^+ + \text{matrix}), (M-H^-)]$  and radical cations ( $M^+$ ) and anions ( $M^-$ ), depending upon the compound and conditions employed. Some limited fragmen-

tation does occur, and relatively more fragmentation is seen in "frit-FAB" than in static FAB because the higher source pressure occurring in the former technique leads to some collisional dissociation within the ion source.

Figure 114 is the FAB mass spectrum of the first eluted component at a retention time of approximately 13 minutes. This component is the product bis(4-aminophenyl)phenylphosphine oxide. This assignment is supported by the strong  $[M+H]^+$  ion at  $m/z$  309 and the ion  $m/z$  of 216 which corresponds to a fragment ion resulting from the loss of aniline. The retention time and the spectrum are also identical to those of a known reference sample.

Figure 115 is the FAB mass spectrum of the second unknown component observed by TLC. This component exhibits a very intense ion at  $m/z$  of 311, corresponding to the radical cation of the monofluoro mono-amino analog of the diamines. The signal at  $m/z$  of 312 may be the  $^{13}C$  peak of  $m/z$  of 311, or it may also represent a contribution by the  $[M+H]^+$  of the 311 species. The ion at  $m/z$  of 219 represents a fragment resulting from loss of aniline from the 311 ion. The ion at  $m/z$  of 294 represents loss of ammonia from the 311 ion. A proton-bound dimer is observed at  $m/z$  of 623 amu. No starting material could be detected.

As was previously discussed in the experimental section, this method of preparation appears quite promising. Further exploration and optimization of this process will continue in our laboratories.

In 1985, Schiemenz (227) reported a route to bis(4-nitrophenyl)phenylphosphine oxide (Scheme 17) based on the aromatic nucleophilic substitution of bis(4-fluorophenyl)phenylphosphine oxide using lithium nitrite in HMPT. Hydrogenation of this dinitro compound would lead directly to the target monomer bis(4-aminophenyl)phenylphosphine oxide. The Schiemenz article documented the production of a difficult to

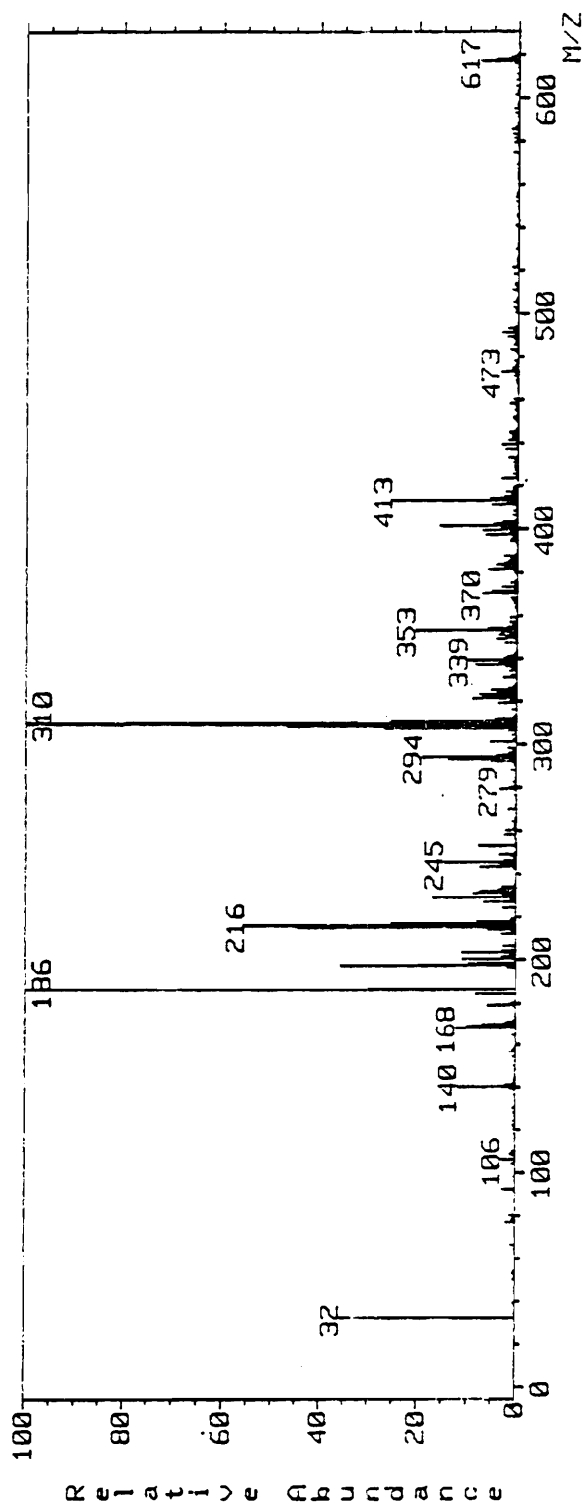


Figure 114. FAB mass spectrum of component 1 from the direct ammonolysis of bis(4-fluorophenyl)phenylphosphine oxide.



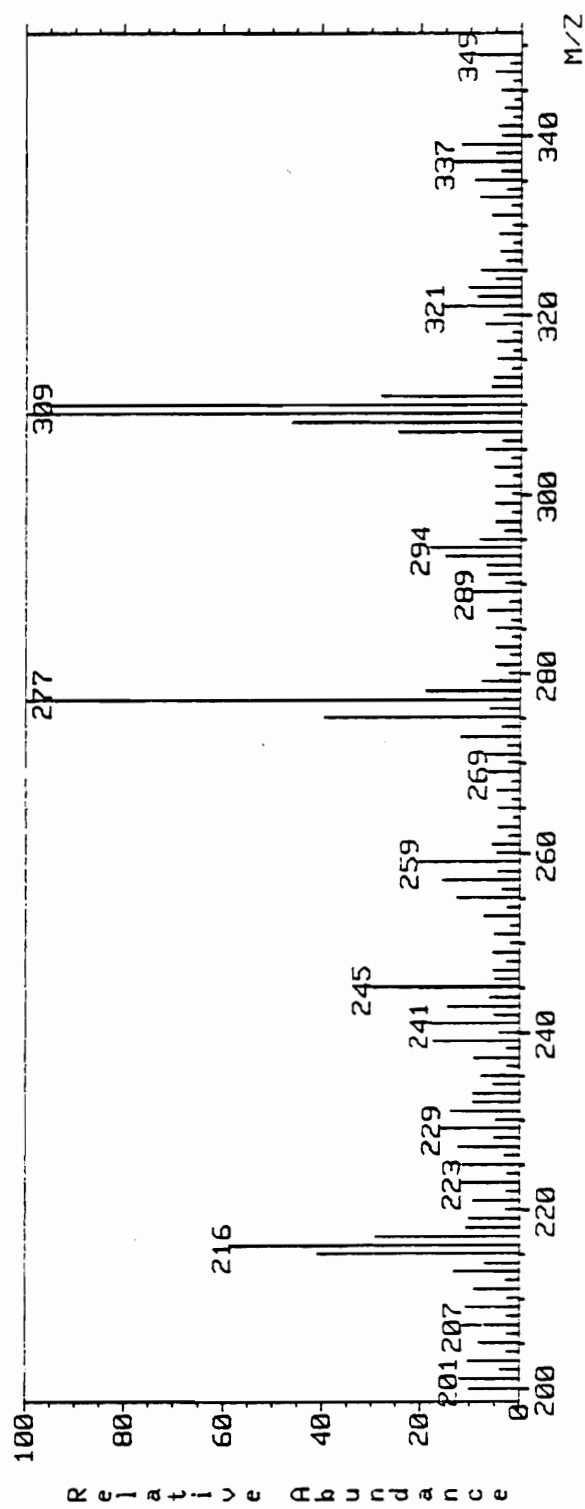
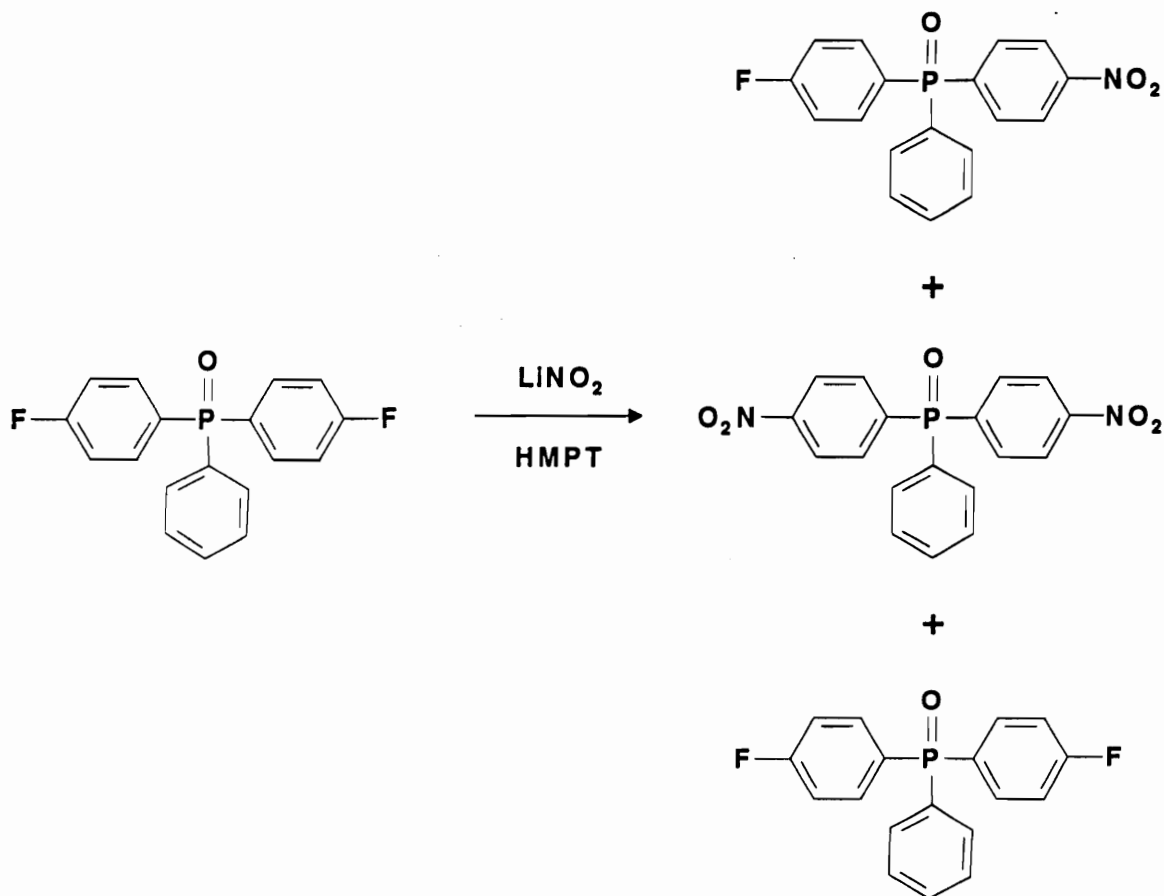


Figure 115. FAB mass spectrum of component 2 from the direct ammonolysis of bis(4-fluorophenyl)phenylphosphine oxide.

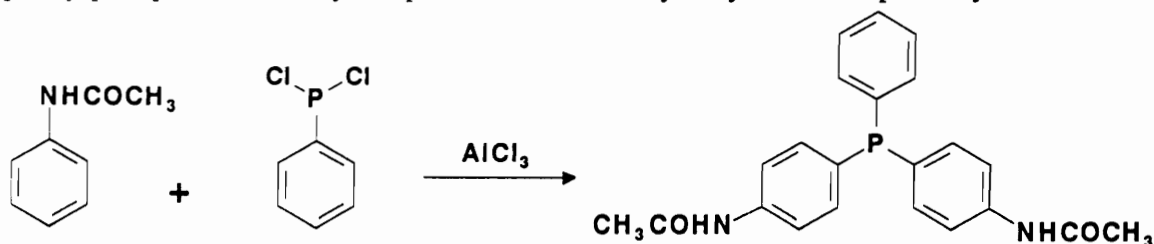


Scheme 17. Preparation of bis(4-nitrophenyl)phenylphosphine oxide.

separate mixture of the starting material and the mono-nitro and dinitro phosphine oxide products. Several experiments were carried out as described in the experimental section using a larger excess of lithium nitrite and various polar aprotic solvents. In all cases, mixtures of starting material, (4-fluorophenyl) (4-nitrophenyl) phenylphosphine oxide, and bis(4-nitrophenyl) phenylphosphine oxide were obtained with the desired bis(4-nitrophenyl)phenylphosphine oxide present as a minor component. Due to the low conversion and difficult-to-separate product distribution, further work with this system was abandoned.

The final area of exploration for the preparation of bis(4-aminophenyl) phenylphosphine oxide was the Friedel-Crafts reaction of dichlorophenylphosphine with acetanilide. There are numerous examples of the use of acetanilide in Friedel-Crafts reactions.

The proposed reaction as seen in Scheme 18 would employ conditions which were successful in the preparation of bis(4-methylphenyl)phenylphosphine and bis(4-phenoxyphenyl)phenylphosphine sulfide. The desired bis(4-acetamidophenyl)phenylphosphine could in turn be converted to the desired bis(4-aminophenyl)phenylphosphine oxide by simple oxidation and hydrolysis. Unexpectedly, the Friedel-



Scheme 18. Attempted preparation of bis(4-acetamidophenyl)phenylphosphine.

Crafts reaction in all cases examined would yield unreacted starting material as the only isolated product in quantity. Reaction solvents utilized were 1,1,2,2-tetrachloroethane, carbon disulfide, and nitrobenzene. In each case, reaction temperature was set at gentle reflux. With nitrobenzene as solvent, iron trichloride was also utilized. In each case, acetanilide was recovered in yields from 30% to 80% and tar-like complex mixtures which could not be characterized were obtained. A similar result was obtained with the use of dichlorophenylphosphine sulfide. All three previously mentioned solvent systems were employed with both aluminum chloride and iron trichloride. The yield of recovered

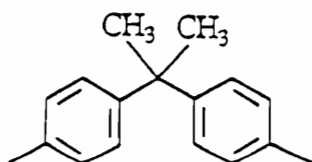
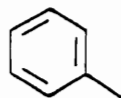
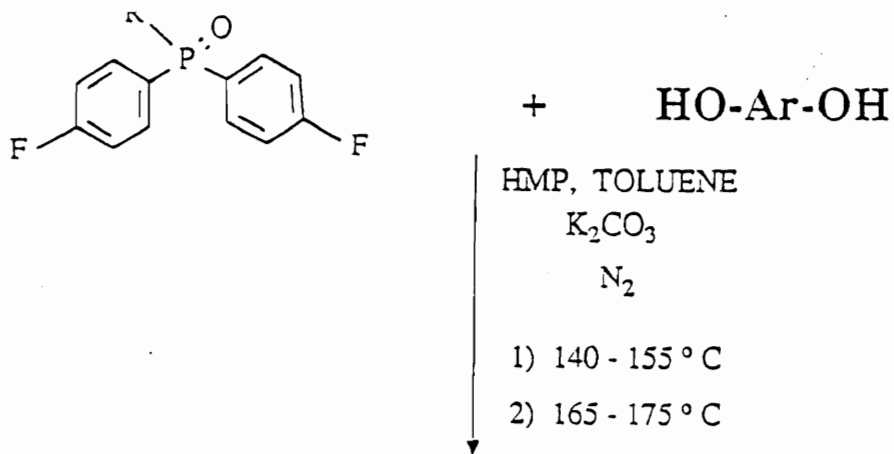
starting material acetanilide ranged from 60% to 90% with a black, complex tar-like mixture as a minor product . No further work in this system was carried out.

## **6.0 PYROLYSIS OF POLY(ARYLENE ETHER)**

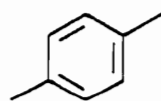
### **6.1 INTRODUCTION AND BACKGROUND**

Poly(arylene ether)s (PAE) are known to be engineering thermoplastics with excellent hydrolytic, thermal and dimensional stability. This class of polymers offers a range of thermal use temperatures depending on the choice of a wide variety of structurally different backbones (247,248). Such systems as poly(arylene ether sulfone)s and poly(arylene ether ketone)s have long been the standards of many PAE materials (249,250). Recently, our laboratories have reported on the synthesis and characterization of poly(arylene ether phosphine oxide) (PEPO) thermoplastic materials as homopolymers, copolymers and blends (251-252). An example of PEPO structure and synthesis is outlined in Scheme 19.

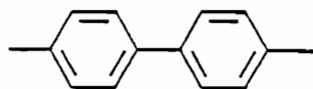
For the most part, these amorphous PEPO macromolecular systems acted similar to their polysulfone counterparts, in terms of synthesis, glass transition temperature, mechanical and dimensional behavior. Also examined recently, phosphorous containing polyimides containing the phosphine oxide unit (253) have shown highly desirable properties.



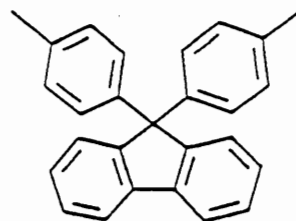
**BIS A**



**HQ**



**BP**



**FL**

Scheme 19. PEPO synthetic scheme.

In addition to the properties just described, the phosphorous containing engineering thermoplastics are superior to any other PAE's in fire resistance and aggressive oxygen plasma etch resistance due to the presence of the unique phosphine oxide moiety in the backbone (254-256).

There are two basic approaches for the production of fire resistant polymeric systems. The older of the two approaches is the blending of fire resistant materials with a combustible polymer substrate. The second approach is the addition of a monomeric material which, when incorporated in the polymer chain, will confer fire resistant properties to the macromolecular materials obtained. To better understand this latter technique, a brief review of polymer combustion will be discussed.

A number of workers have presented reviews on flammability features of polymeric materials (61,66,67,257-262) with a limited number of reviews specific to high performance polymers (263-265). As shown in Figure 116, several mechanisms must be in operation to sustain polymer combustion. The substrate must first obtain enough thermal energy to pyrolyze. The pyrolysis process decomposition will generate three basic types of products: carbonaceous char, flammable gases, and non-flammable gases. This process requires thermal input -  $Q_1$ . Of the three types of products obtained, only the flammable gases are capable of combustion and supplying additional thermal input ( $+Q_2$ ) which is then available for further pyrolysis decomposition.

Flame retardant additives or fire resistant materials are best understood in light of these mechanisms. Fire resistant materials must require a very high  $Q_1$  and a very low  $Q_2$  value. This would require large amounts of energy for bond breaking and simultaneously produce minimum amounts of flammable gases to fuel pyrolysis degradation.

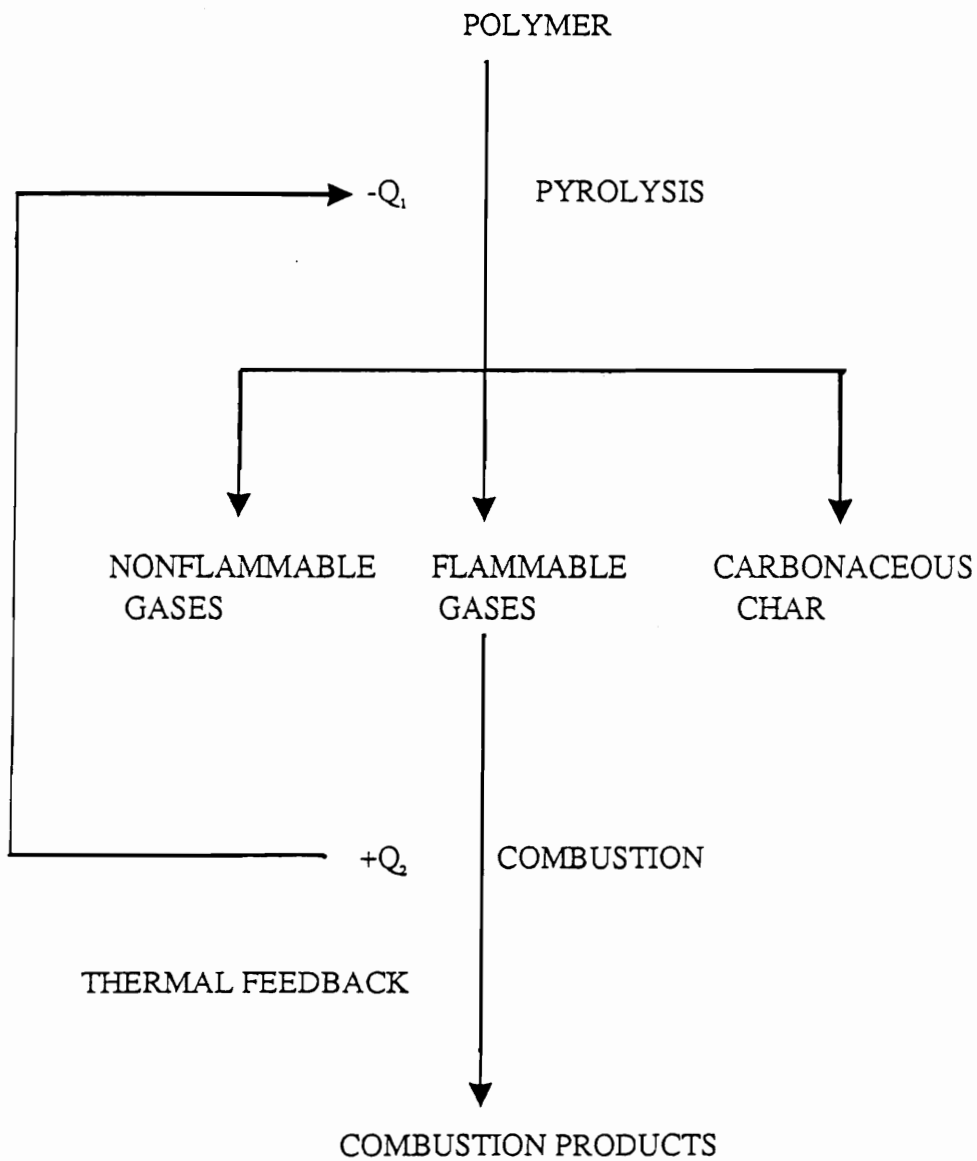


Figure 116. Polymer burning mechanism.

Polymeric systems with strong main chain chemical bonds are resistant to free radical chain scission and require high  $Q_1$  values. This system will produce larger amounts of carbonaceous char and/or gases which are non-flammable thus greatly reducing  $Q_2$  values. This is the basic mechanism by which flame retardant additives function. They volatilize to produce non-flammable gases to dilute fuel gases formed, or they scavenge free radicals to inhibit chain degradation to fuel gas materials.

A large number of both inorganic and organic additives are known. The requirements for these materials are quite difficult to meet. The additives should not decompose to generate toxic fumes as many fire fatalities are the result of smoke inhalation. They must be compatible with a polymer system such that valuable properties of the resin are not lost. They must be stable at temperatures at which the polymeric system is fabricated and must retain fire resistant properties for the service life of the article. Halogenated organic compounds (61), metal oxides and phosphorous ester materials (266) have been patented and reviewed in detail.

Polymeric systems which are inherently fire resistant would eliminate many of the challenges in selecting fire retardant additives for physical inclusion.

An example of a currently available inherently fire resistant polymer is the halogenated polysulfone system. These patented systems (267) have very high  $Q_1$  values and are recognized as high thermal stability polymers. Degradation of these materials generates large amount of toxic gases which limits utility of these systems.

The fire resistant nature of polysulfones led to their study relative to other engineering thermoplastics (263,264,268,269). The limiting oxygen index (LOI) of approximately 30-40 of the neat resins defined these systems as non-flammable. The LOI is measured as the percent oxygen in a continuously changing oxygen/nitrogen environment which will allow candle-like burning of the specimen being evaluated



(270,271). All materials with a LOI value of greater than 26 are defined as non-flammable (66). Bis-A based PSF of the Udel type had lower LOI values due to the partial aliphatic character when compared to Victrex PES. Studies have also correlated high char yields with high LOI values (66,263,264,271-273) as a consequence of the lower  $Q_2$  values.

PES degradation routes have been studied to determine the mechanisms by which the polymer chain degrades. Pyrolysis/gas chromatography/mass spectrometry is a powerful tool to probe the formation of low molecular weight compounds produced (275,276). In inert atmosphere (nitrogen) two assumptions may be made. The first is that thermal degradation mechanisms were the only mode of decomposition and that free radical reactions produced small volatile components. It is evident that many products can be obtained by more than one route. Some of the volatile products obtained include benzene, biphenyls, methane, sulfur dioxide, toluene and phenols. Pyrolysis products were less numerous when all aromatic PES samples were pyrolyzed (275). The product distribution, as well as quantities of pyrolyzate, were temperature dependent. When poly(arylene ether ketone)s were studied, similar results were obtained (277).

The use of phosphorous containing additives and the mechanisms of operation for imparting fire resistant properties has been well-documented (278-283). The data on phosphorous containing polymers is much more limited (284). To date, only the polymer systems with phosphorous-oxygen bonded chain structure have been studied. There is no available literature on the fire retardancy properties of phosphorous-carbon bonded systems. To study the mechanism of flame retardancy of phosphorous-carbon macromolecular systems, the PEPO series of engineering thermoplastics were chosen for study.

## 6.2. EXPERIMENTAL

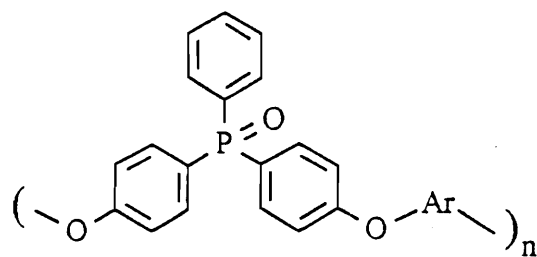
### 6.2.1 Pyrolysis Unit Construction

Details of the PEPO synthesis have been disclosed in the literature (254). Figure 117 illustrates the chemical structures of the polymers which were studied and the acronyms used in the discussion of results. All samples were pyrolyzed in air at 600°C with a quartz tube/furnace pyrolysis unit as shown in Figure 118. For gas chromatography/mass spectrometry analysis, volatile pyrolyzates were condensed at -100°C at the front of a thirty meter DB-5 fused silica capillary column. The oven temperature, initially at -100°C for three minutes, was programmed at 20°C per minute to 0°C and then 7°C per minute to 300°C. Three minutes after the onset of pyrolysis, spectra covering a range of  $m/z$  33 to 650 were obtained by scanning every second.

### 6.2.2 Neutron Activation Analysis

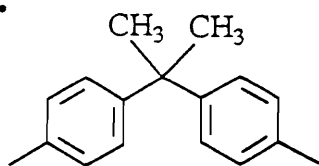
All samples were either in sheet or powder form with activation times of two minutes. Counting times ranged from two to five minutes depending on activity of the sample; a minimum of 5000 counts in the photo peak was the determining factor.

As a general procedure, a polymer sample was weighed into a tared polyethylene container. The polyethylene vial with sample was then placed in a water-tight Teflon capsule. The Teflon container was the transfer vehicle to and from the reactor core for the activation process. After irradiation at the reactor core, the activated material was retrieved and transferred to a previously tared counting vial. The weighed sample was then transferred to a gamma counting system for evaluation.

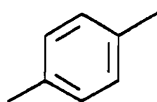


**PEPO**

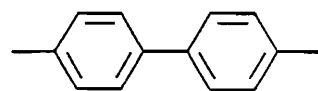
Ar:



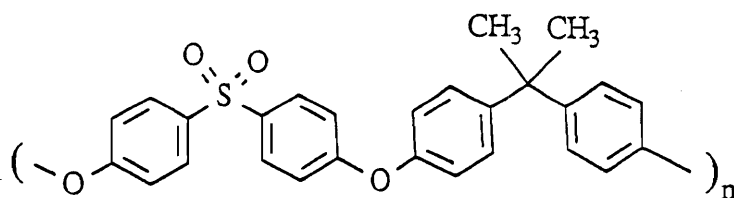
**BIS A**



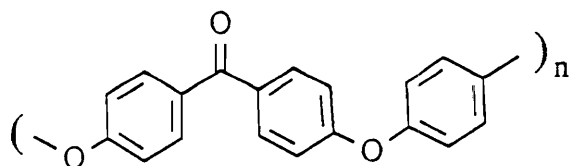
**HQ**



**BP**



**UDEL POLYSULFONE**



**PEEK**

Figure 117. Chemical structures of pyrolyzed engineering thermoplastics.

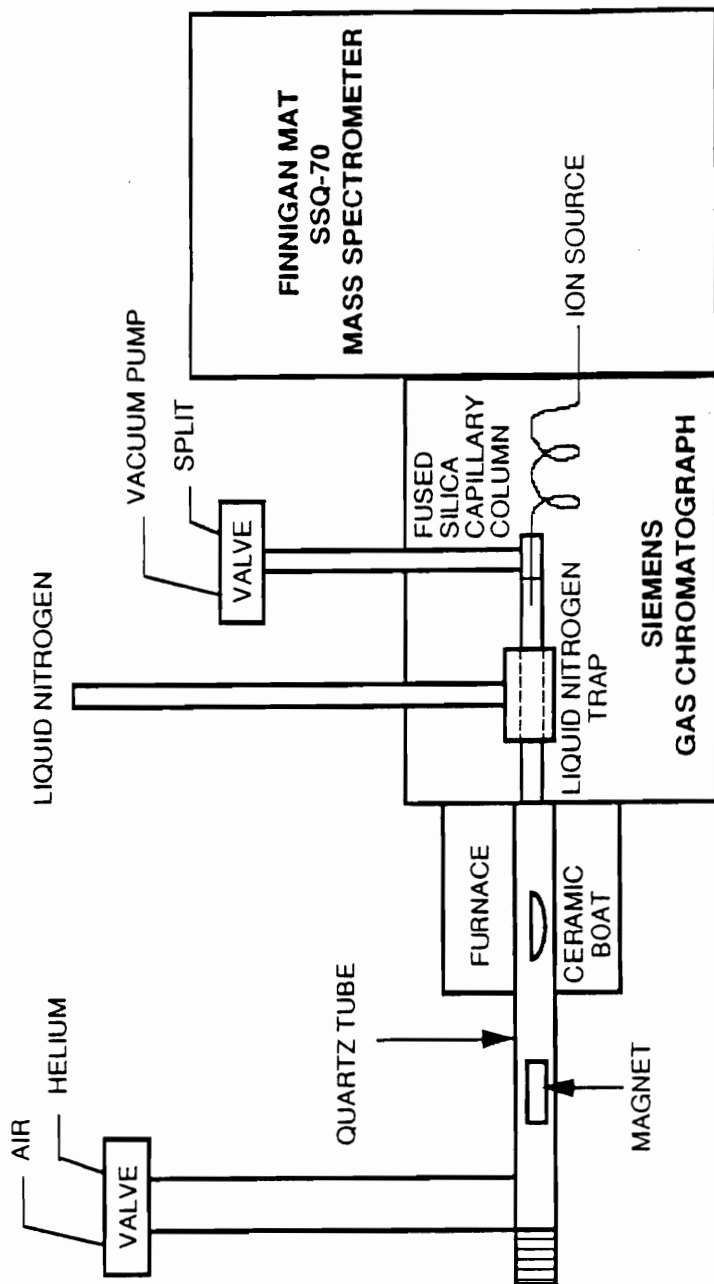


Figure 118. Pyrolysis unit construction.

The counting equipment used in this study consisted of a Princeton Gamma-Tech germanium detector with a 15.6% efficiency, with a source to detector distance of 25 centimeters. The counting geometry was made reproducible by employing a permanent shelf above the detector and a fixed source to detector distance. A Nuclear Data 66 multichannel pulse height analyzer (PHA) was used for data analysis. The PHA was coupled to a Nuclear Data 680 computer system with required application software to produce the analysis of the spectrum data.

The detector was calibrated using a mixed gamma standard of known activity for both energy and photo peak efficiency. Standard materials were provided by the National Bureau of Standards.

In order to provide accurate results over an extended time period, certified chemical standards were purchased from Aldrich Chemical Company. These standards, aluminum powder of 99.95% purity and red phosphorous of 99.999% purity, were run each time a series of polymers were subjected to activation analysis techniques. All samples were transferred using Teflon-coated spatula and tweezers to avoid cross-contamination of materials. Typical sample sizes for the standards were 10-20 mgs for aluminum and about 200 mg for phosphorous.

The pairing of standards with each set of polymers during activation analysis eliminates the need to know the counting efficiency, the gamma intensity, the cross section, and the reactor flux. By knowing the purity of the standard and by processing or irradiating it under the identical conditions as the sample, it is possible to ratio the counts from the standard and the counts from the sample to obtain the amount of phosphorus in the sample. This form of evaluation using neutron activation is termed the "comparator method". All data for polymer and pyrolyzate was generated using this technique.

### 6.2.3 Polymer Pyrolysis

To establish the level of phosphorus transfer under pyrolysis conditions and to determine char residue, an off-line pyrolysis experimental design was utilized.

Figure 119 is a block diagram of the experimental apparatus. The furnace, a Thermocraft Model 118-12-1-2V was coupled to an Omega Temperature Controller Model 1612 to maintain set temperatures. A sample boat made of glazed porcelain (Coors #07-660A), was introduced in the heated space of the furnace by magnet. Air flow to this system was maintained at 75 ml per minute with the collection tube trap cooled with liquid nitrogen. Pyrolysis time varied between three and five minutes or until vapor evolution ceased. Upon introduction of the sample into the furnace the temperature of the system dropped approximately 10°C with full recovery to set temperature in less than 10 seconds.

The condensed gas phase was collected as an oil and to facilitate transfer to the vial for irradiation it was necessary to use an organic solvent. The residue from pyrolysis of phosphorus containing polymers was a solid in each case examined. Quantitative transfer of the solid was easily accomplished for further irradiation.

Benzene was chosen to transfer the condensed volatile from the pyrolysis studies. Once the transfer was complete the benzene was permitted to evaporate, prior to sealing the vial and subjecting the sample to the activation process. Upon recovery of the sample from the reactor core, fresh benzene was added to the vial to solubilize the material for final transfer to a quartz container used for counting. The volume of benzene was 1.5 ml and the quartz container was tared prior to introduction of the solution containing the activated sample. Once the counting process completed, the solvent was allowed to evaporate and a second weight was obtained to establish the sample weight.

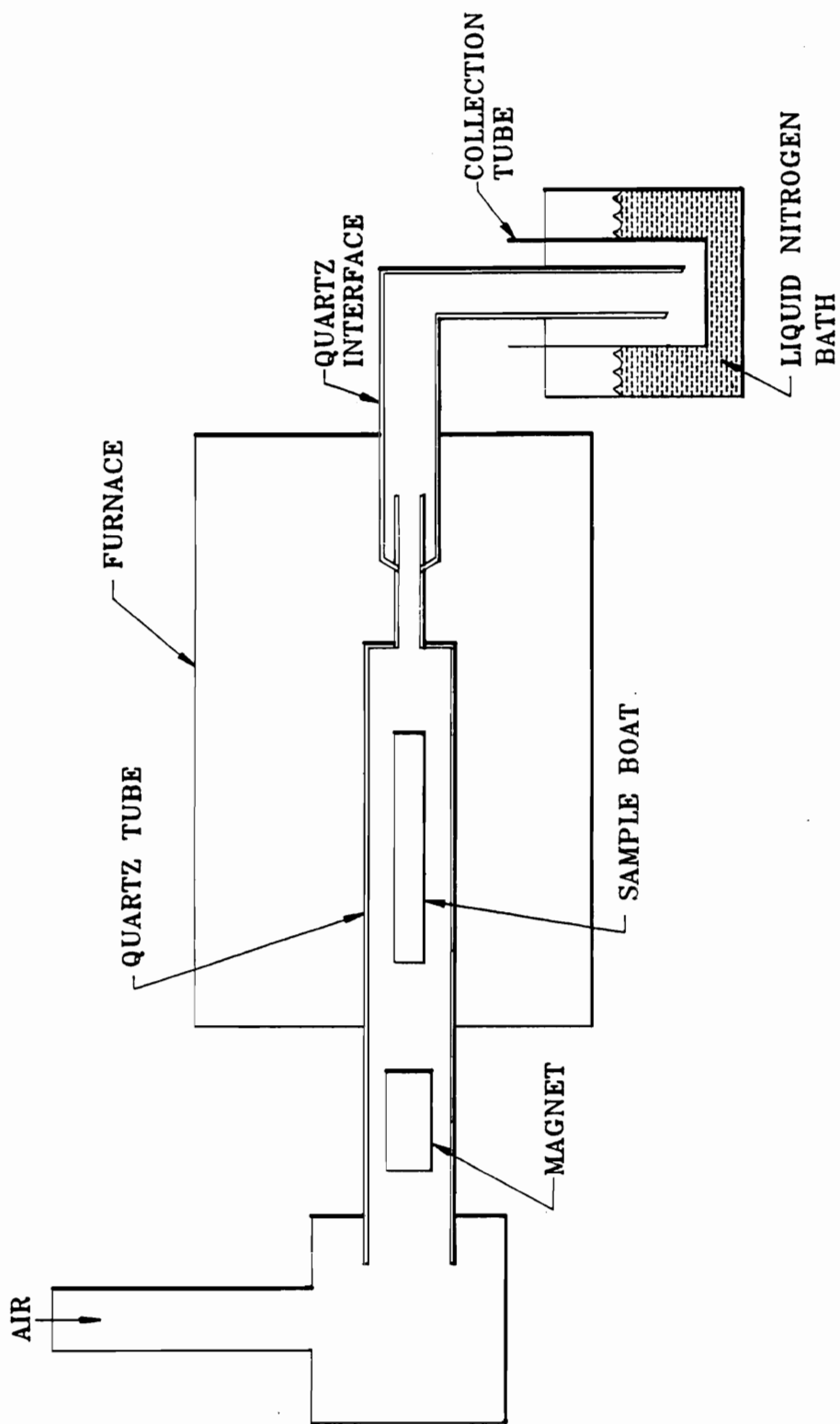


*Figure 119. OFF-LINE PYROLYSIS UNIT.*

### 6.3 Results and Discussion

Dynamic thermogravimetric analysis in air of the PEPO amorphous thermoplastics show these materials possess excellent thermal stability, losing 5% of their weight typically around 500°C (253,285). One of the immediate observations which was made on the TGA thermograms of all PEPO materials was the high degree of char yield between 600-800°C. Figure 120 illustrates the large difference in TGA thermograms between commercially available engineering thermoplastics, PEEK and UDEL PSF, and a phosphorus containing engineering thermoplastic, BP PEPO. The non-phosphorus containing polymers were completely volatilized by 700°C, but the PEPO systems typically show between 20-40% char yield.

Formation of char appears to play an important role in the self-extinguishing properties of engineering thermoplastics and char yields have previously been correlated with the LOI of many polymers. The LOI has been the most quoted measure of polymers' resistance to flame environments, but it seems to be dependent on such a long list of variables that it appears a single number cannot possibly describe the behavior of a polymer when burned. A qualitative test has been developed in these laboratories in which films on the order of 0.5-1 mm thick were exposed to a Bunsen burner flame in air for constant amounts of time, then removed after a predetermined period in the flame. In all cases, non-phosphorus containing engineering thermoplastics (PEEK, UDEL, ULTEM, polyimide, etc.) with very high literature LOI values appeared to completely volatilize; on the other hand, all phosphorus containing PEPO systems immediately extinguished upon removal of the flame. This test could be repeated several times for any single PEPO sample. As a consequence of these qualitative results, an effort was made to examine both the volatile and non-volatile portions of several engineering thermoplastics compared with the same for PEPO.



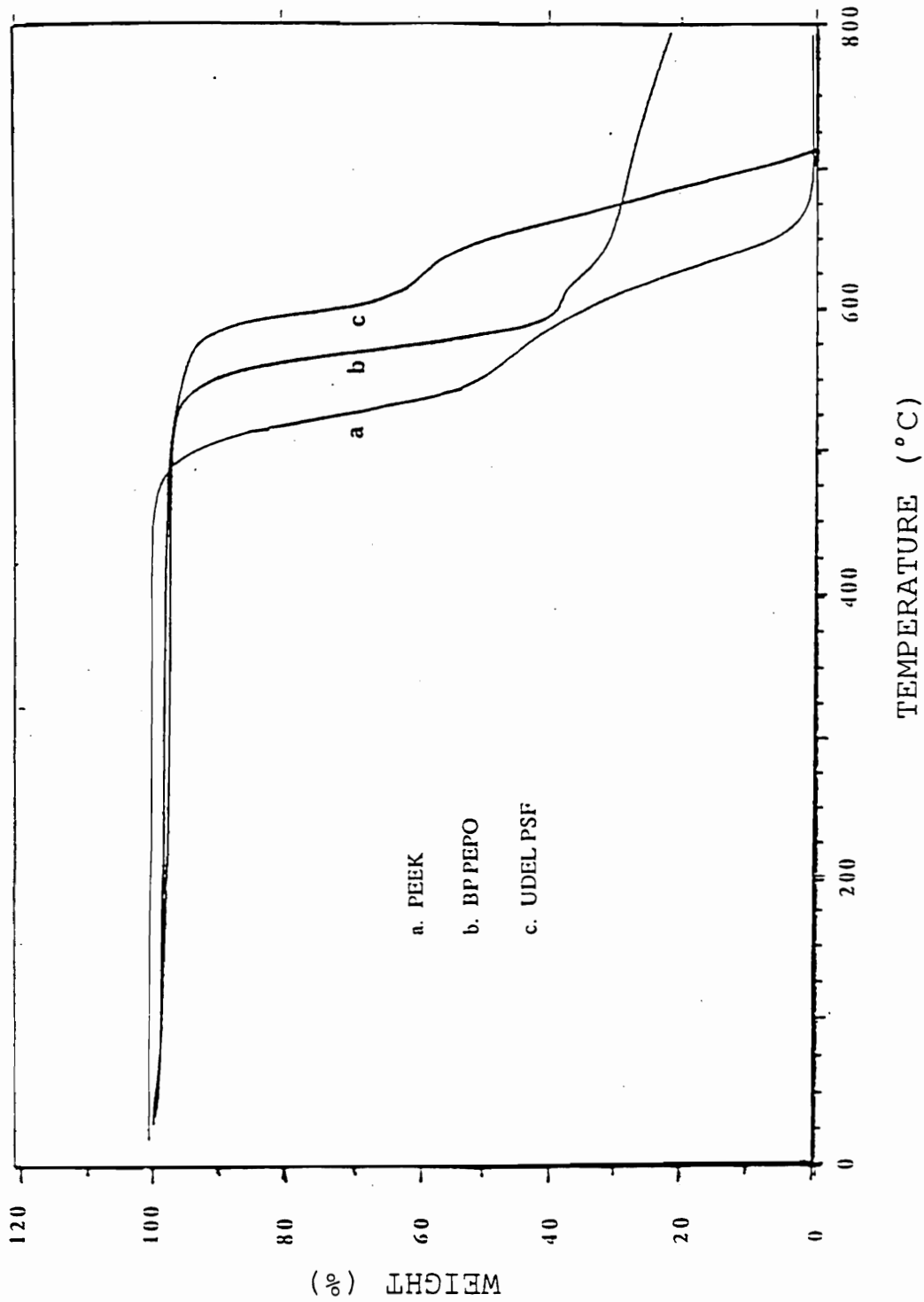


Figure 120. TGA thermogram of PEEK, UDEL PSF, and BP PEPO.

The presence of phosphorus in polymeric systems has been known for some time to generically impart flame retardance to materials. Indeed, molecules such as triphenyl phosphine oxide have been known to be thermally stable at temperatures of 700°C. However, the study of polymeric materials containing the triphenyl phosphine oxide moiety chemically bound within the polymer chain as flame retardant polymers has been limited. On the other hand, poly(arylene ether sulfone)s and poly(arylene ether ketone)s have been explored in terms of thermogravimetry or pyrolysis in order to obtain a more detailed analysis of the degradation process (286-291). Typically, these materials begin to degrade by chain scission at the sulfone or ketone group to give sulfur dioxide or carbon monoxide, respectively. The radicals formed from this initial reaction go on to initiate further chemistry, finally totally volatilizing the polymer at sufficiently high temperatures. Using pyrolysis-gas chromatography-mass spectrometry techniques, along with neutron activation analysis, it is possible to determine the fate of phosphorus in the burning process, as well as observing the degradation products of PEPO compared to other engineering thermoplastics.

Typical pyrograms of PEPO's and their PAE analogs (i.e., BIS A PEPO vs. UDEL and HQ PEPO vs. PEEK) are illustrated in Figures 121-126 along with compound identifications obtained from extensive model compound studies. One note should accompany discussions regarding decomposition, this being that any volatile formed which boiled lower than -100°C would not be trapped and therefore not identified.

The first striking difference between the pyrograms of PEPO and the other PAE was the lack of initial gas formation in the vapor. For UDEL polysulfone, sulfur dioxide was clearly formed during the decomposition process, and presumably carbon monoxide

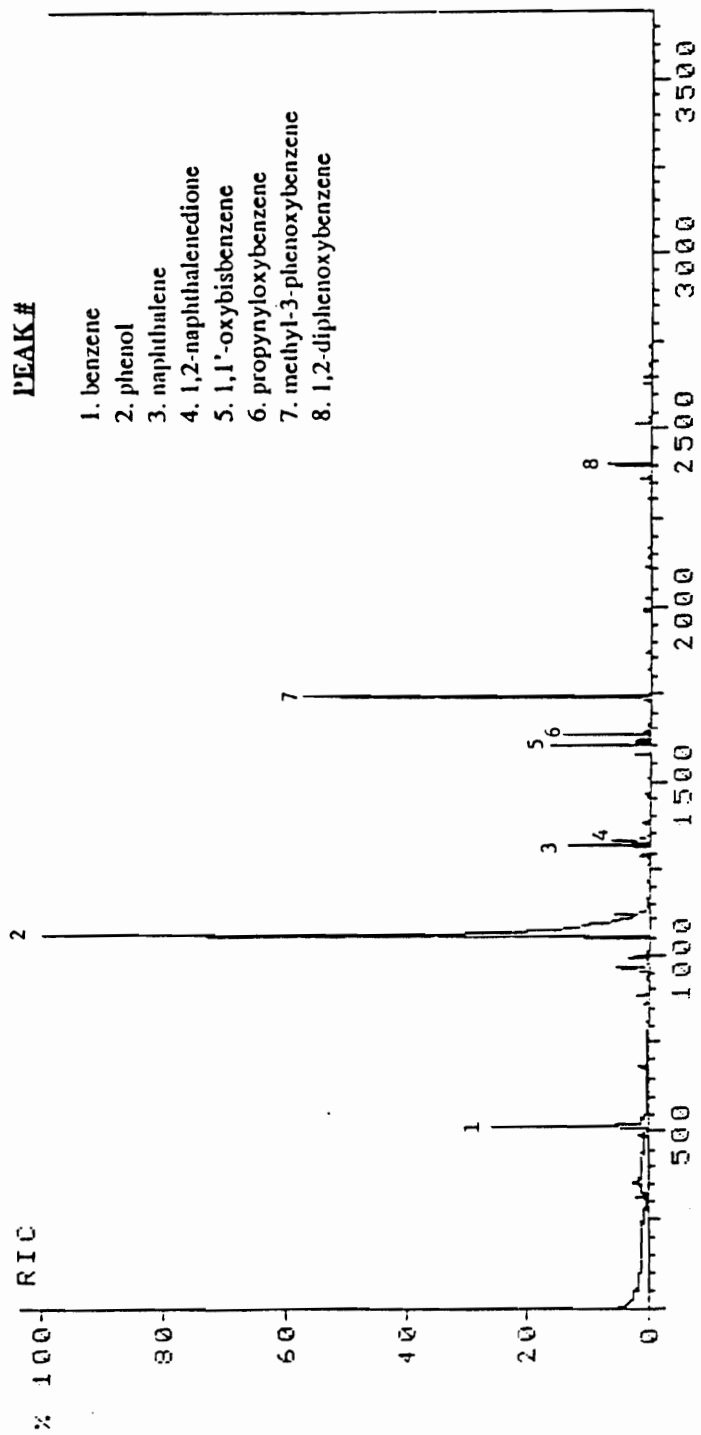


Figure 121. 600°C pyrogram of PEEK

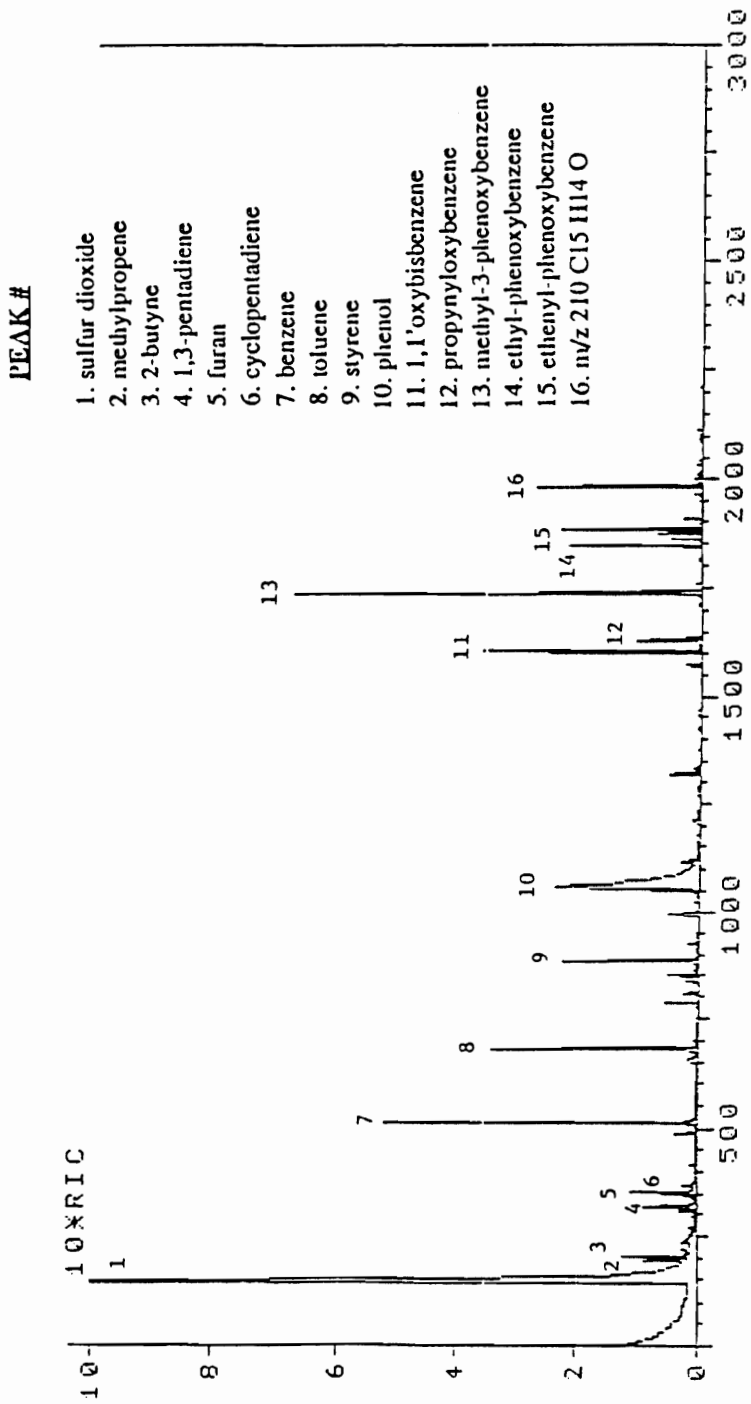


Figure 122. 600°C Pyrogram of UDEL

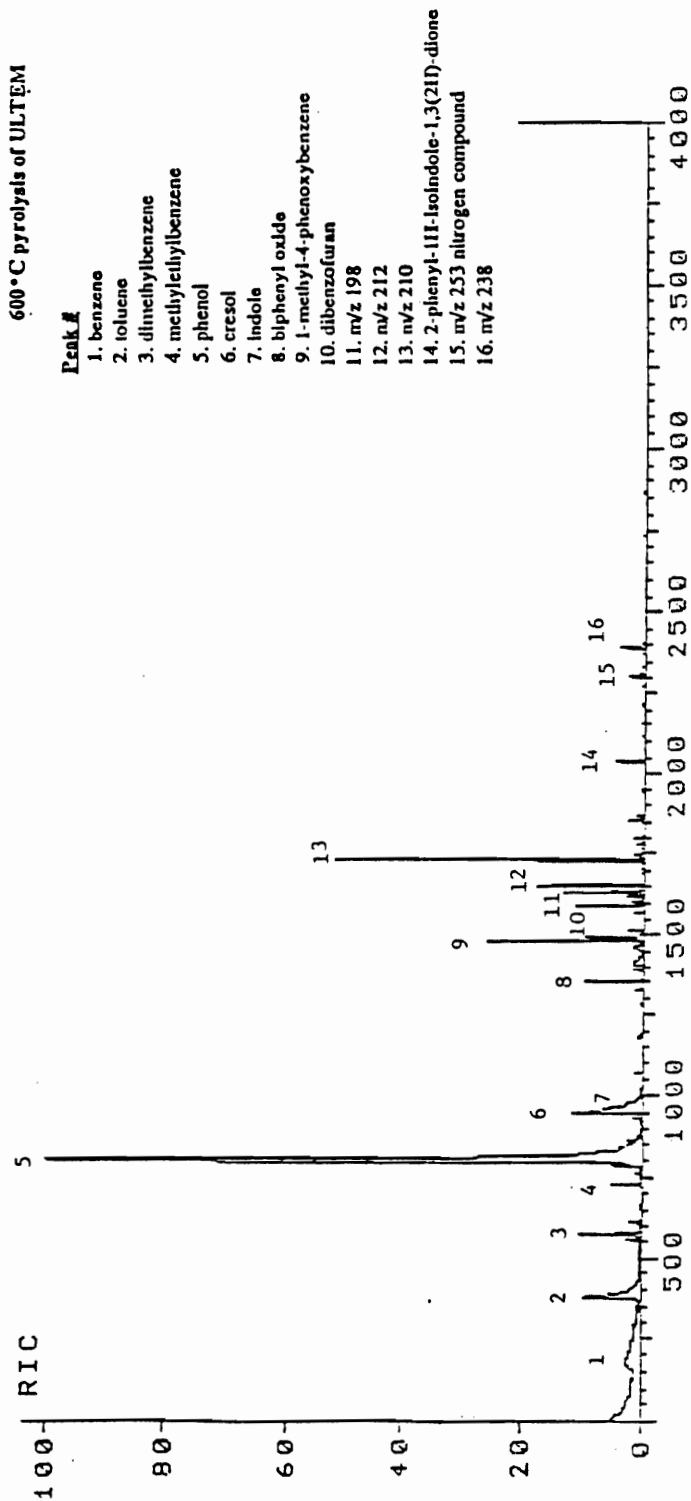


Figure 123. 600°C Pyrogram of ULTEM

**PEAK#**

1. methylpropene
2. 2-butyne
3. 1,3-pentadiene
4. cyclopentadiene
5. benzene
6. toluene
7. phenol
8. naphthalene
9. 1,1'-biphenyl
10. 1,1'-oxybisbenzene
11. propynyloxybenzene
12. methyl-biphenyl
13. dibenzofuran
14. ethyl-phenoxybenzene
15. ethenyl-phenoxybenzene
16. diphenoxybenzene
17. methyl-benz[*A*]anthracene
18. phenoxy-1,1'-biphenyl
19. m/z 260
20. m/z 272
21. m/z 288 possibly C<sub>16</sub>H<sub>17</sub>O<sub>3</sub>P

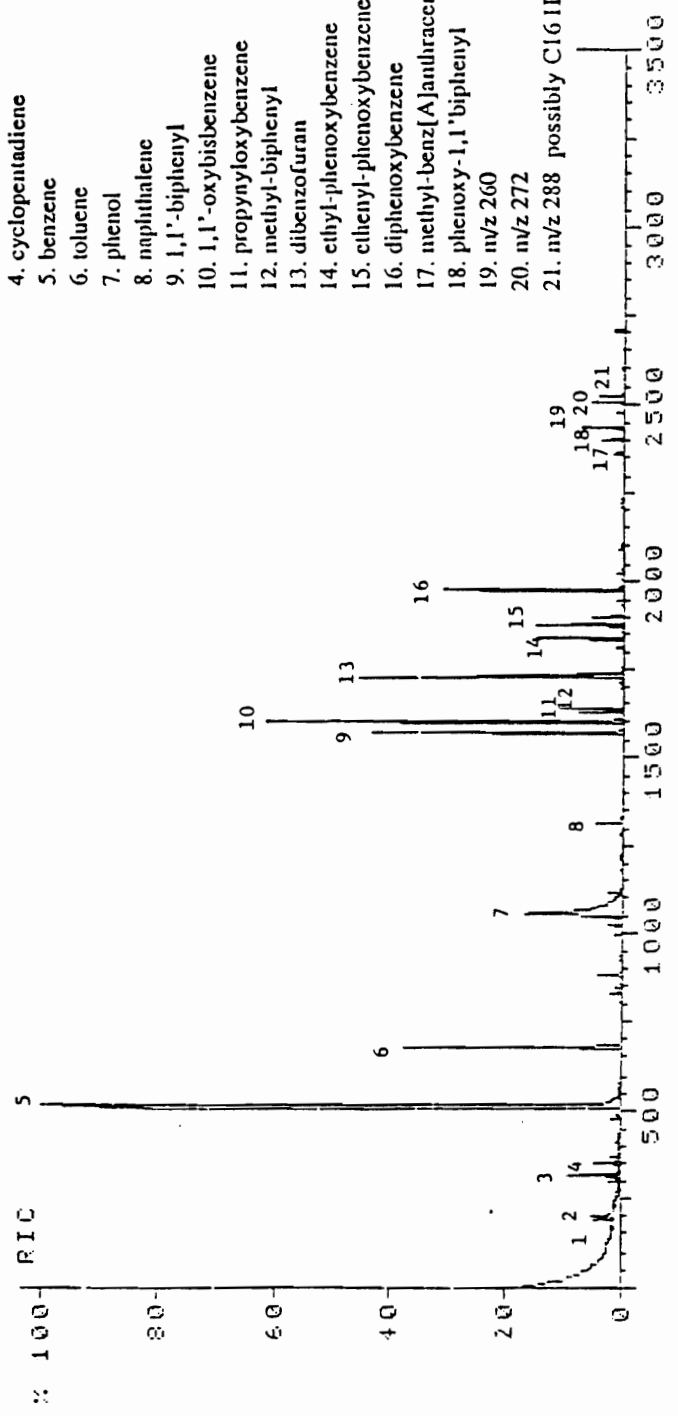


Figure 124. 600°C pyrogram of Bis A PEPO

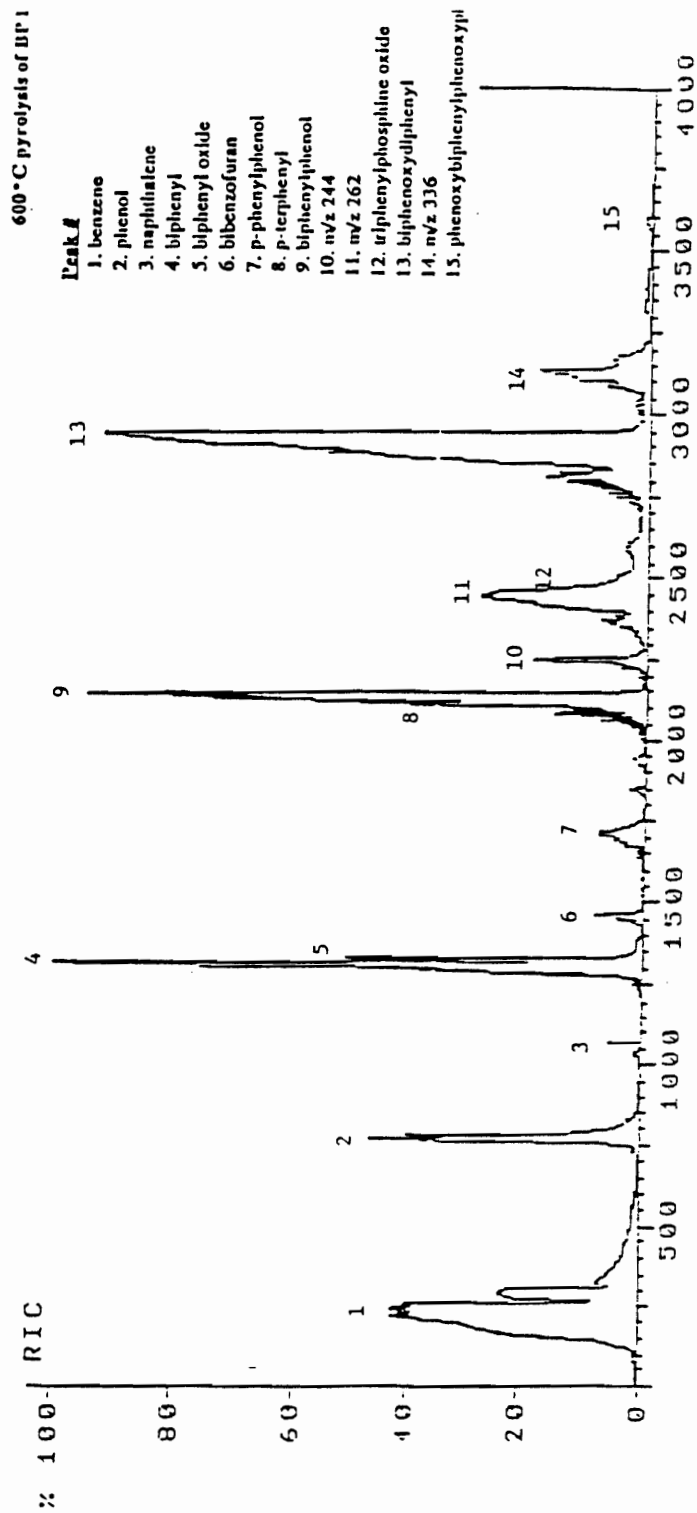


Figure 125. 600°C pyrogram of BP-PEPO

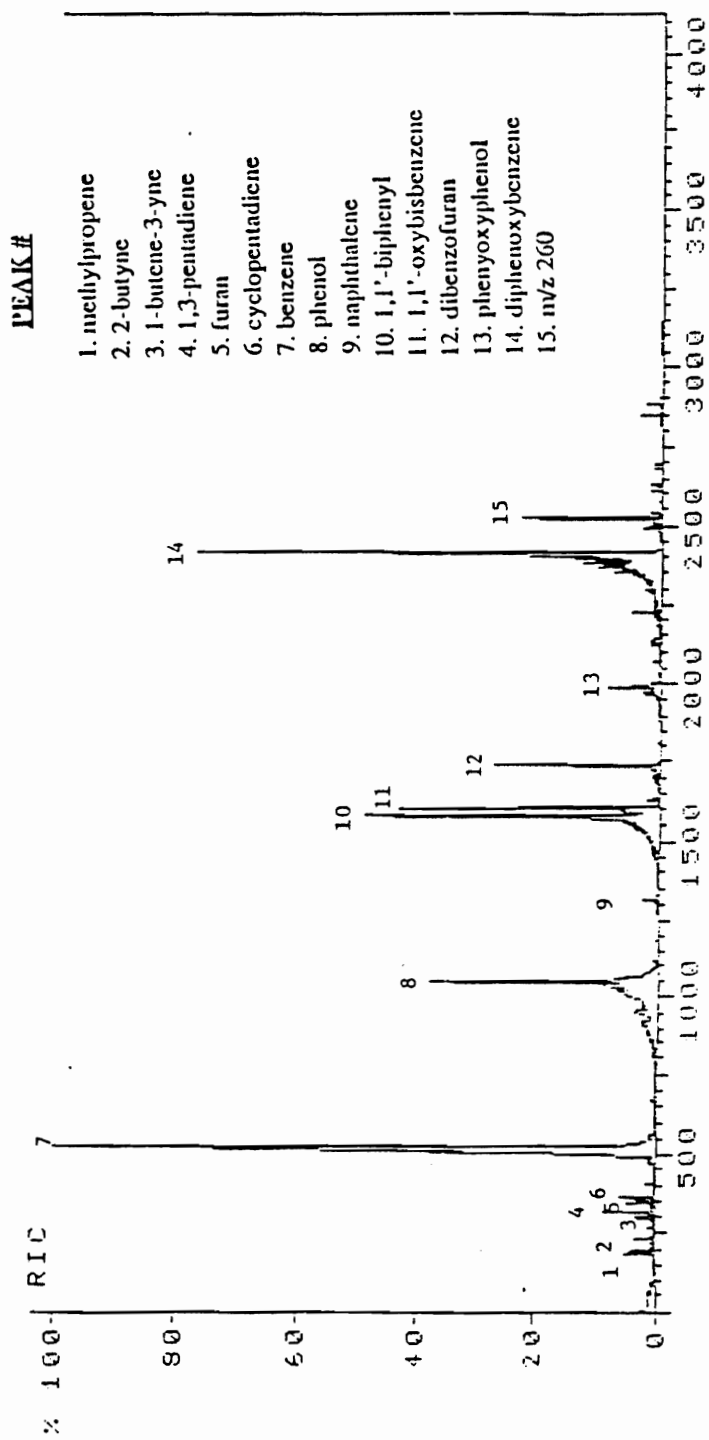
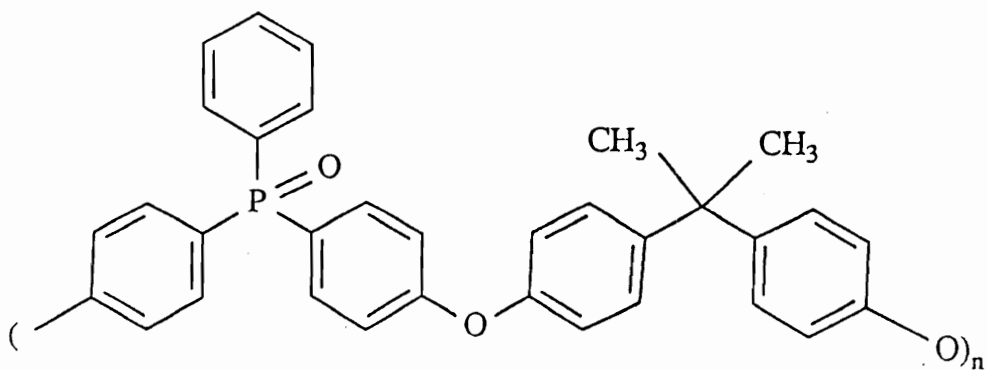


Figure 126. 600°C pyrogram of HQ PEPO



was a primary product for PEEK degradation. Typically, other than the lack of SO<sub>2</sub> or CO formation, degradation products were similar for PEPO's and their PAE counterparts (i.e., UDEL vs. Bis A PEPO and PEEK vs. HQ PEPO). In the case of the Bis A based polymers, the pyrograms were more complicated than the hydroquinone based polymer pyrograms due to the presence of isopropylidene linkages along the backbones, giving various degradation products characteristics of this type of moiety (291).

Pyrolysis of a triphenyl phosphine oxide standard at 600°C gave a single peak in the pyrogram corresponding to the starting model compound, indicating the surprising high thermal stability of this molecule. However, a very important variable in the pyrolysis of the PEPO samples was that the triphenyl phosphine oxide group was chemically linked in the polymer backbone; moreover, the carbon to phosphorus bond is the weakest in the chain, and is probably one of the first sites of scission. However, since no simple substituted phosphine oxide is formed, further reactions to carbonaceous char probably occurred. The large amounts of char formed in all cases with PEPO (Figures 124-126), along with the fact that very few phosphorus containing volatiles were identified, also pointed to the presence of phosphorus in the char. In order to confirm the presence of phosphorus in either the char or volatile fractions of the decomposition products, neutron activation analysis (NAA) was employed. This technique allows one to analytically determine atomic percents of constituents either in the volatile or solid phases. From NAA, it was confirmed that phosphorus containing degradation products were for the most part nonvolatile. Again, it should be noted that other poly(arylene ether)s gave essentially no char to analyze at 600°C in air, while PEPO materials all gave substantial amounts of char at 600°C in air. From the data in Figures 127-129, it is obvious that the char is much richer in phosphorus than the initial polymer. In all cases, the char is approximately double the content of phosphorus compared to the undegraded PEPO



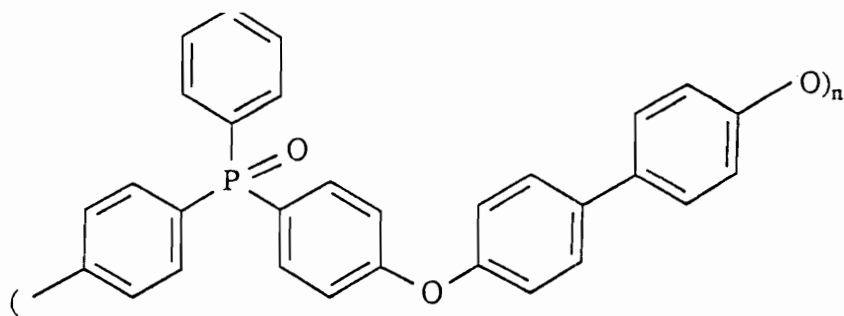
## Bis A PEPO

PEPO-BIS-A	<u>Weight (mg)</u>	<u>% Yield</u>
Initial	158.0	-
Residue	49.0	31.0
Pyrolysate	104.0	65.8
Total Recovery	153.0	96.8

### Phosphorus Content - Weight Percent

	<u>Calculated</u>	<u>NAA</u>
Initial	6.2	6.4
Residue	-	12.0
Pyrolysate	-	2.20

Figure 127. NAA phosphorus determination.



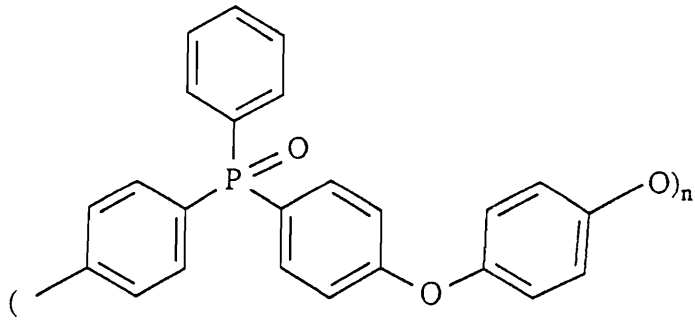
## BP PEPO

PEPO-BP	<u>Weight (mg)</u>	<u>% Yield</u>
Initial	85.1	-
Residue	36.9	43.4
Pyrolysate	26.9	31.6
Total Recovery	63.8	75.0

### Phosphorus Content - Weight Percent

	<u>Calculated</u>	<u>NAA</u>
Initial	6.6	6.8
Residue	-	12.6
Pyrolysate	-	1.7

Figure 128. NAA phosphorus determination.



## HQ PEPO

PEPO-HQ	<u>Weight (mg)</u>	<u>% Yield</u>
Initial	153.0	-
Residue	76.0	49.7
Pyrolysate	81.7	53.4
Total Recovery	157.7	103.1

### Phosphorus Content - Weight Percent

	<u>Calculated</u>	<u>NAA</u>
Initial	8.1	9.0
Residue	-	15.6
Pyrolysate	-	0.9

Figure 129. NAA phosphorus determination.

formation upon pyrolysis, while chemistry in the gas phase probably plays only a minor role in the self-extinguishing behavior.

## 7.0 SUMMARY

Polyimides and polybenzoxazoles have frequently been referenced in the literature as materials which show excellent thermooxidative and environmental stability. Many of these materials show superior mechanical properties at ambient and at elevated temperatures. A limitation which has continued to diminish widespread use of these materials is their intractability in the fully cyclized state. To obtain the goal of processable, thermally stable, solvent resistant polymers, much of the work to date has centered on the investigation of the incorporation of processable monomers containing the hexafluoroisopropylidene linkage, use of molecular weight control, and solution cyclization methods. This investigation has centered on the production of monomers from two relatively less explored monomer systems based on trifluoroacetophenone and the phenylphosphine oxide systems. The preparation of monomer grade bis(4-aminophenyl)-1-phenyl-2,2,2-trifluoroethane (3F-diamine) and bis(4-hydroxyphenyl)-1-phenyl-2,2,2-trifluoroethane (3F bis-phenol) was successfully developed based on the hydroxyalkylation reaction of trifluoroacetophenone. Bis(4-aminophenyl)phenylphosphine oxide and bis(4-hydroxyphenyl)phenylphosphine oxide were prepared in monomer purity also. Current investigations in the preparation and characterization of polyimides and polybenzoxazoles based on these materials have demonstrated exceptional thermal and mechanical properties and thus are candidates for high performance resin and structural adhesive applications. The benefits obtained by incorporation of these monomers into polymer backbones include chain rigidity, polarity, flame resistance, and outstanding thermal stability. The use of these high performance

monomers allows preparation of amorphous polymers with excellent thermooxidative stability and extremely high glass transition temperature values.

The synthesis and characterization of polymer systems containing the phosphine oxide unit along the backbone continue to be an area of active research. To date, the majority of research activity has centered on the synthesis and features of poly(arylene ether phosphine oxide)s (PEPO). All PEPO gave significant amounts of phosphorous containing char at temperatures where other engineering polymers are completely volatilized. A detailed pyrolysis degradation of the phosphorous containing PEPO system has been investigated. This has included the application of analytical techniques including pyrolysis-gas chromatography-mass spectrometry and neutron activation analysis.

## 8.0 REFERENCES

1. T. M. Bogert and R. R. Renshaw, *J. Am. Chem. Soc.*, **30**, 1135 (1908).
2. R. W. Thomas, T. M. Amirrab-Lavi and P. E. Cassidy, "Polyimides - A New Class of Polymers", in *New Monomers and Polymers*, ed. by B. M. Culbertson and A. Pittman, Jr., Plenum Press, New York, **1** (1984).
3. A. Walch, H. Lukas, A. Kimner and W. Pusch, *J. Polym. Sci.: Lett. Ed.* **12**, 697 (1974).
4. M. P. Stevens, *Polymer Chemistry, An Introduction*, Oxford University Press, New York (1990).
5. P. M. Hergenrother and N. J. Johnston, *Resins for Aerospace*, ed. by C. A. May, *Am. Chem. Soc.*, Supp. Symp. Ser. **3**, 132 (1980).
6. P. M. Hergenrother, *Encyclopedia of Polymer Science and Engineering*, ed. by J. I. Kroschwitz, Wiley-Interscience, **7**, 639 (1984).
7. J. P. Critchley, G. J. Knight and W. W. Wright, *Heat-Resistant Polymers*, Plenum Press, New York (1983).

8. J. Preston, *Kirk-Othmer Encyclopedia of Chemical Technology*, Wiley Interscience, New York, 3rd Ed., **12**, 203 (1978).
9. J. I. Jones, *J. Macromol. Sci.: Revs. Macromol. Chem.*, **C**, **2(2)**, 303 (1968).
10. P. W. Atkins, *Physical Chemistry*, W. H. Freeman and Company, San Francisco, 2nd Ed., **111** (1978).
11. T. L. Cothrell, *The Strength of Chemical Bonds*, Butterworths, London, 2nd Ed. (1958).
12. C. S. Marrel, *Soc. Plast. Eng. J.*, **20**, 220 (1964).
13. A. H. Frayer, *High Temperature Resistant Polymers*, John Wiley and sons - Interscience, New York (1968).
14. C. Arnold, Jr., *J. Polym. Sci.: Macromol. Revs.* **14**, 265 (1979).
15. C. J. Lee, *J. Macromol. Chem. Phys.*, **C**, **29(4)** 431 (1989).
16. G. H. Moelter, R. F. Tetrault and M. J. Hefferon, *Poly. News* **9**, 134 (1983).
17. W. J. Bailey, in "*Encyclopedia of Polymer Science and Engineering*," Editor in Chief, J. I. Kroschwitz, Wiley-Interscience, New York, Index Vol. **158** (1984).
18. J. Preston, "*Kirt-Othmer Encyclopedia of Chemical Technology*", Wiley Interscience, New York, 3rd Ed., **12**, 215 (1978).
19. Paul A. Wood, III, "Ph.D. Thesis", V.P.I. & S.U., 1993.
20. L. K. McCune, *Text. Res. H.* **32(9)**, 762 (1962); J. H. Ross, *Text. Res. J.* **32(9)**, 768 (1962).
21. J. Economy, R. S. Storm, V. I. Matkovich, S. G. Cottis and B. E. Nowak, *J. Polym. Sci.: Polym. Chem. Ed.* **14**, 2207 (1976).
22. G. Montaudo, P. Finocchiaro and S. Caccamese, *J. Polym. Sci. A-1*, **9**, 3627 (1971).
23. P. W. Morgan, *J. Polym. Sci.: Polym. Symp. No. 65*, **1** (1978).
24. J. G. Speight, P. Kovacic and F. W. Koch, *J. Macromol. Sci.: Rev. Macromol. Chem.*, **C**, **5(2)**, 295 (1971).

25. J. L. Hedrick, "Synthesis, Properties and Modifications of Engineering Polymers", Ph.D. Dissertation, Virginia Polytechnic Institute and State University, Blacksburg, Virginia (1985).
26. J. B. Rose, *Polymer* **15**, 456 (1974).
27. W. H. Bonner (DuPont), "Aromatic Polyketone and Preparation Thereof," U.S. Patent 3,065,205 (1962).
28. H. L. Finkbeiner, A. S. Hay and D. M. White, in "Polymerization Process," ed. by C. E. Schildknecht, Wiley-Interscience, Chp. 15, 537 (1977); J. T. Edmonds and H. W. Hill, "Production of Polymers from Aromatic Compounds," U.S. Patent 3,354,129 (1967).
29. "Polyimides: Materials, Chemistry, and Characterization," ed. by C. Feger, M. M. Khojaster and J. E. McGrath, Elsevier Science Publisher, Amsterdam (1989); "Polyimides," ed. by D. Wilson, H. S. Stenzenberger and P. M. Hergenrother, Blackie, New York (1990).
30. T. Shono, M. Hachihama and K. Shinra, *J. Polym. Sci., Polym. Lett.*, **B, 5**, 1001 (1967).
31. G. F. D'Alelio, D. M. Feigl, T. Ostdick, M. Saha and A. Chang, *J. Macromol. Sci. Chem.*, **A, 6(1)**, 1 (1972).
32. G. P. de Gaudemaris and B. J. Sillion, *J. Polym. Sci., Polym. Lett.*, **B, 2**, 203 (1964).
33. K. C. Brinker, D. D. Kameron and I. M. Robinson (DuPont), "Polybenzoxazoles," U.S. Patent 2,904,537 (1959).
34. H. Vogel and C. S. Marvel, *J. Polym. Sci.* **50**, 511 (1961).
35. C. J. Abshire and C. S. Marvel, *Makromol. Chem.* **44-46**, 388 (1961).
36. C. G. Overberger and S. Fujimoto, *J. Polym. Sci.*, **B, 3**, 735 (1965).
37. W. Bracke, *J. Polym. Sci. A-1*, **10(4)**, 975 (1972).
38. P. E. Cassidy, "Thermally Stable Polymers, Synthesis and Properties", Marcel Dekker, Inc., New York (1980).



39. D. F. Loncrini, W. L. Walton and R. B. Hughes, *J. Polym. Sci. A-1*, **4**, 440 (1966).
40. G. M. Bower and L. W. Frost, "Aromatic Polyimides," *J. Polym. Sci. A-1*, **1**, 3135 (1963); "Polyimides," ed. by D. Wilson, H. S. Stenzenberger and P. M. Hergenrother, Blackie, New York (1990).
41. B. C. Johnson, "High Performance Polyimide Copolymers: Synthesis and Characteristics," Ph.D. Dissertation, Virginia Polytechnic Institute and State University, Blacksburg, Virginia (1984).
42. C. A. Arnold, J. D. Summers, Y. P. Chen, T. H. Yoon, B. E. McGrath, D. Chen and J. E. McGrath, "Soluble Polyimide Homopolymers and Poly(Siloxane Imide) Segmented Copolymers with Improved Dielectric Behavior," in "*Polyimides: Materials, Chemistry and Characterization*," ed. by C. Feger, M. M. Khojasteh and J. E. McGrath, Elsevier Sci. Publishers, Amsterdam, **69** (1989).
43. B. Culbertson and R. Murphy, *J. Polym. Sci., Polym. Lett. B*, **4**, 249 (1966).
44. T. V. Sheremeteva, B. N. Larina, M. G. Zhenevskaya and V. A. Gusinskaya, *J. Polym. Sci., Part C*, **16**, 1631 (1967).
45. J. E. White. *Ind. Eng. Chem. Prod. Res. Dev.* **25**, 395 (1986).
46. D. H. Marrian, *J. Chem. Soc., Part 2*, **1515** (1949).
47. H. M. Relles and R. W. Schlunz, *J. Org. Chem.* **37(23)**, 3637 (1972).
48. T. Hagiwara, J. Mizota, H. Hamama and T. Narita, *Makromol. Chem., Rapid Commun.* **6**, 169 (1985).
49. V. Percec and B. C. Auman, in "*Reactive Oligomers*," ed. by F. W. Harris and H. J. Spinelli, Am. Chem. Soc., Washington, DC, ACS Symp. Ser. 282, Chp. 8, **91** (1985).
50. F. W. harris and K. Sridhar, in "*Reactive Oligomers*," ed. by F. W. Harris and H. J. Spinelli, Am. Chem. Soc., Washington, DC, ACS Symp. Ser. 282, Chp. 7, **81** (1985).
51. L. C. Hsu and W. Philips, "*Cyclopolymerization and Polymers with Chain-Ring Structures*," ed. by G. B. Butler and J. E. Kresta, Am. Chem. Soc., Washington, DC, ACS Symp. Ser. **195**, 285 (1982).

52. P. M. Hergenrother, in "*Reactive Oligomers*", ed. by F. W. Harris and H. J. Spinelli, Am. Chem. Soc., Washington, DC, ACS Symp. Ser. 282, Chp. 1, 1 (1985).
53. R. J. Kray, "*The NCNS Resins for Potential Applications and Advanced Composites*," 20th National SAMPE Symp. and Exhibit. 20, 227 (1975).
54. S. C. Lin, in "*Reactive Oligomers*," ed. F. W. Harris and H. J. Spinelli, Am. Chem. Soc., Washington, DC, ACS Symp. Ser. 282, Chp. 9, 105 (1985).
55. F. W. Harris, *J. Macromol. Sci.-Chem.*, A, 21(8 & 9), 1117 (1984).
56. B. Sillion, in "Recent Advances in Mechanistic and Synthetic Aspects of Polymerization," ed. by M. Fontanille and A. Guyot, D. Reidel Publishing Co., Dordrecht, Holland, 237 (1987).
57. L. S. Tan and F. E. Arnold, *Polym. Prepr., Am. Chem. Soc., Div. Polym. Chem.* 26(2), 176 (1985).
58. J. P. Droske and J. K. Stille, *Macromol.* 17(1), 1 (1984).
59. N. E. Searle (DuPont), "Synthesis of N-Aryl-Maleimides", U.S. Patent 2,444,536 (1948).
60. H. D. Stenyenberger, "Chemistry and Properties of Addition Polyimides", in "*Polyimides*", ed. by D. Wilson, H. D. Stenyenberger and P. M. Hergenrother, Blakie & Son Ltd., New York, Chp. 4, 79 (1990).
61. C. Gann, R. A. Dipert and M. J. Drews, *Encyclopedia of Polymer Science and Engineering*, ed. by J. I. Kroschwitz, Wiley-Interscience, New York, 7, 639 (1984).
62. H. L. Kaplan, A. I. Grand and G. E. Hartzell, *Combustion Toxicology Principles and Test Methods*, Technomic, Lancaster, PA (1983).
63. H. K. Limsisch, H. W. M. Hollander, and J. Thyssen, *J. Combust. Toxicol.*, 7, 243 (1980).
64. C. J. Hilado and J. E. Schneider, *J. Combust. Toxicol.* 6, 91 (1979).
65. C. J. Hilado, *Flammability Handbook for Plastics*, Technomic, Stamford, Conn. (1969).

66. D. W. van Krevden, *Polymer*, **16**, 615 (1975).
67. R. G. Bauer, *J. Fire Retard. Chem.* **5**, 200 (1978).
68. M. Lewin, S. M. Atlas, E. M. Pearce eds., *Flame-Retardant Polymeric Materials*, Vol. 2, Plenum Press, New York (1975).
69. V. M. Bhatnager ed. *Advances in Fire Retardants*, Technomic, Westport, Conn. (1987).
70. A. R. Hovrocks, D. Price, and M. Tune, *J. Appl. Polym. Sci.*, **34**, 1901 (1987).
71. H. Sivnier, G. Borissor, L. Labski, and Z. Jedlinski, *Eur. Polym. J.*, **23**, 891 (1987).
72. M. S. Chondhary, J. K. Fink, K. Lederer, and H. A. Krassig, *J. Appl. Polym. Sci.*, **34**, 863 (1987).
73. P. A. Fairhall and S. M. Spivak, *J. Fri. Sci.* **189** (1984).
74. P. J. Fasdell and C. Lukas, *Chem. Bro.* **23**, 221 (1987).
75. E. D. Weil, *Kirk-Othmer Encyclopedia of Chemical Technology*, Wiley-Interscience, New York, 3rd ed., **10**, 396, 1978.
76. W. W. Wendlandt and J. A. Brakson, *Anal. Chem.* **33**, 61 (1958).
77. D. A. Anderson and E. S. Freeman, *J. Appl. Poly. Sci.* **1**, 192 (1959).
78. J. Chin, *Thermoanalysis of Fiber and Fiber-Forming Polymers*, Interscience, New York, **25** (1966).
79. C. B. Murphy, *Anal. Chem.*, **52(5)**, 106 (1980).
80. J. G. Cobler, *Anal. Chem.*, **53(5)**, 273 (1981).
81. M. J. Emmet, J. F. Johnson, and P. S. Gill, *CRC Crit. Rev. Anal. Chem.*, **2**, 339 (1981).
82. W. J. Irwin, *J. Anal. Appl. Pyrol.* **1**, 3-122 (1979).
83. C. J. Wolf, M. A. Grayson and D. L. Fanler, *Anal. Chem.* **52** (missing).

84. W. J. Irwin, *Analytical Pyrolysis: A Comprehensive Guide*, Marcel-Dekker: New York (1982).
85. H. Meuyelaar, P. G. Kistemaker, *Biomed. Mass. Spectrom.*, **1**, 312 (1974).
86. H. Menyelarr, I. Haverkamp, F. D. Hileman, *Pyrolysis Mass Spectrometry of Recent and Fossil Biomaterials: Compendium and Atlas*, Elsevier, New York, 1982.
87. S. Tsuge and T. Takeuchi, *Anal. Chem.* **49**, 348 (1977).
88. P. G. Kistemaker, J. H. Baerhorm and H. L. C. Meuzelaar, *Dynamic Mass Spectrom.*, **4**, 139 (1976).
89. M. Seeger and R. Gritter, *J. Poly Sci. Polym. Chem. Ed.*, **15**, 1393 (1977).
90. D. O. Hummel, *Polymer Spectroscopy*, ed. by D. O. Hummel, Verlag Chemie: Weinheim, **355** (1974).
91. K. J. Voorhees, *J. Polym. Sci. Polym. Chem. Ed.*, **16**, 213 (1978).
92. K. J. Voorhees, R. P. Lattimer, *J. Polym. Sci. Polym. Chem. Ed.* **20**, 1457 (1982).
93. R. Holm and S. Storp, *Surface Interface Anal.* **2**, 96 (1980).
94. A. Ballistrei, S. Foti, P. Maravinga, G. Montando, and E. Scamporrino, *E. Polymer* **22**, 131 (1981).
95. R. P. Lattimer and W. Kroenke, *J. Appl. Polym. Sci.*, **25**, 101 (1980).
96. M. M. O'Mara, *Pure Appl. Chem.* **49**, 549 (1977).
97. W. H. Starnes and D. Edelson, *Macromolecules* **12**, 797 (1979).
98. R. P. Lattimer and W. J. Kroenke, *J. Appl. Polym. Sci.* **27**, 1355 (1982).
99. R. P. Lattimer, W. J. Kroenke and R. A. Buckderf, *J. Appl. Polym. Sci.*, **27**, 3633 (1982).
100. W. H. Starnes, *J. Org. Coatings Plast. Chem.* **46**, 556 (1982).
101. R. J. Gritter, M. Seeger and D. E. Johnson, *J. Polym. Sci. Polym. Chem. Ed.* **16**, 169 (1978).

102. J. L. Wuepper, *Anal. Chem.* **51**, 997 (1979).
103. G. J. Mol, R. J. Gritter and G. E. Adams, *Applications of Polymer Spectroscopy*, E. G. Brame ed. Academic, New York, **257** (1978).
104. D. L. Evans, J. Weaver, A. K. Mukherji, and C. Beatty, *Anal. Chem.* **50**, 857 (1978).
105. T. Nagaya, Y. Sugimura, and S. Tsuge, *Macromolecules*, **13**, 353 (1980).
106. S. Tsuge, T. Kobayashi, and T. Takeuchi, *J. Anal. Appl. Pyrol.*, **1**, 133 (1979).
107. S. Tsuge, T. Kobayashi, Y. Sugimura, T. Nagaya, and T. Takeuchi, *Macromolecules*, **12**, 988 (1979).
108. F. E. Rogers (E.I. du Pont de Nemours & Co.), U.S. Patent 3,356,648 (December 1967); *Chem. Abstr.*, 30429q (1968).
109. F. E. Rogers (E.I. du Pont de Nemours & Co.), Belgian Patent 649,336 (December 1964); *Chem. Abstr.*, **45**, 12837d (1966).
110. P. E. Cassidy, T. M. Aminabhavi, and J. M. Farley, *Rev. Macromol. Chem. Phys.*, **C29 (2&3)**, 365-429 (1989).
111. Paul M. Hergenrother, *Recueil des Travaux des Pays - Bas*, **110**, 481 (1991).
112. "Polyimides: Materials, Chemistry and Characterization," ed. by C. Feger, M. M. Khojasteh and J. E. McGrath, *Elsevier Sci. Pub. B. V.*, Amsterdam, 1989.
113. T. Matsuura, S. Nishi, M. Ishiyawa, Y. Yamada, and S. Hasuda, *Pacific Polym. Prepr.* **1**, 87 (1989).
114. F. W. Harris, S.L.C. Hsu, and C.C. Tso, *Polym. Prepr.* **31(1)**, 342 (1990).
115. A. J. Beuhler, M. J. Burgess, D. E. Fjare, J. M. Gaudette and R. T. Roginsk , *Matl. Res. Soc. Proc.* **154**, 73 (1989).
116. M. K. Gerber, J. R. Pratt, A. K. St. Clair and T. L. St. Clair, *Polym. Prepr.* **31(1)**, 340 (1990).
117. D. M. Stoakley, A. K. St. Clair, R. M. Baucom, 3rd International SAMPE Electronics Conference June 20-22, 1989, p. 224.

118. L. M. Ruiz, 3rd International SAMPE Electronics Conference, June 20-22, 1989, p. 209.
119. T. Ichino, S. Sasaki, T. Matsuura, Y. Hasuda, *Polym. Sci. Polym. Chem. Ed.*, **28**, 323 (1990).
120. T. Matsuura, Y. Hasuda, S. Nishi, and N. Yamada, *Macromolecules*, **24**, 5001-5005 (1991).
121. H. Gibbs, *J. Appl. Poly. Sci. Appl. Poly. Sym.* **35**, 207 (1979).
122. W. D. Kray and R. W. Rosser, *J. Org. Chem.* **42**, 1186-1189 (1977).
123. W. B. Alston, in "High Temperature Polymer Matrix Composites," NASA CP-2385, **187-205** (1985).
124. W. B. Alston and R. F. Gratz, in "Recent Advances in Polyimide Science and Technology," Society of Plastics Engineers: Poughkeepsie, NY, 1987, pp. 1-15.
125. W. B. Alston and R. F. Gratz, in "Symposium on Recent Advances in Polyimides and Other High Performance Polymers," American Chemical Society: Reno, Nevada, July 13-16, 1987. (Also NASA TM-89875 and U.S. Army AVSCOM-TR87-C-7).
126. K. A. McGrady and R. F. Gratz, *Virginia Journal of Science*, **39**, 140 (1988).
127. R. F. Gratz, NASA Grant Number NAG3-794, June 1, 1987,.
128. L. Crews and R. F. Gratz, *Virginia Journal of Science*, **40**, Number 2 (1989).
129. J. Pfeifer and O. Rhode, in "Recent Advances in Polyimide Science and Technology," Society of Plastics Engineers: Poughkeepsie, NY, 1987, pp. 336-350.
130. W. G. Alston and R. F. Gratz, U.S. Patent, 4,758,380, July 19, 1988.
131. W. G. Alston and R. F. Gratz, U.S. Patent, 4,845,167, July 4, 1989.
132. W. G. Alston and R. F. Gratz, U.S. Patent, 4,758,380, July 19, 1988.
133. D. A. Scola, U.S. Patent 4,742,152, May 3, 1988.

134. D. A. Scola, U.S. Patent 4,801,682, January 31, 1989.
135. W. B. Alston and R. F. Gratz, *Pacifica Polymer Preprints*, **1**, 313 (1989).
136. M. E. Rogers, H. Grubbs, A. Breenan, D. Rodriques, T. Lin, H. Marand, G. L. Wilkes, and J. E. McGrath, 37th International SAMPE Symposium and Exhibition, March 9-12, 1992.
137. W. D. Joseph, R. Mercier, A. Prasad, H. Marand, A. Brennan, and J. E. McGrath, 37th International SAMPE Symposium and Exhibition, March 9-12, 1992.
138. H. Schell and H. Drim, *Angew. Chem. Int. Ed. English*, **2**, 373 (1963).
139. B. S. Farah, E. E. Gilbert and J. P. Sibilias, *J. Org. Chem.*, **30**, 998 (1965).
140. E. E. Gilbert, E. S. Jones, and J. P. Sibilias, *J. Org. Chem.*, **30**, 1001 (1965).
141. I. L. Knunyants, C. Ching-Yun, N. P. Gambayan, and E. M. Roklilen, *Zh. Vses. Khim. O.va.*, **114** (1960).
142. B. S. Farah, E. E. Gilbert, M. Litt, J. A. Otto, and J. P. Sibilias, *J. Org. Chem.*, **30**, 1003 (1965).
143. D. S. England, French Patent 1 325 204 (1963).
144. S. Patai and S. Dayagi, *J. Chem. Soc.*, **3058** (1958).
145. A. Baeyer and V. Villiger, *Ber.* **37**, 2848 (1904).
146. J. H. Simons and E. P. Ramler, *J. Am. Chem. Soc.* **65**, 389 (1943).
147. M. Langsam, W. F. Burgoyne, J. P. Casey, and M. E. Ford, U.S. Patent 4,952,220, August 28, 1990.
148. R. A. Frosh, W. D. Kray, and R. W. Rosser, U.S. Patent 4,307,024, December 22, 1981.
149. S.V. Vinogradova, U.S.S.R. Patent 154,288, July 24, 1963.
150. A. K. Barbour, M. W. Buxton, P. L. Coe, R. Stephens, and J. C. Tatlow, *J. Chem. Soc.*, **808** (1961).

151. H. P. Braendlin, E. T. McBee, in "Advances in Fluorine Chemistry," M. Stacey, J. P. Tatlow, and A. G. Sharpe Edit., 1963, Vol. 3, Butterworths London, p. 1.
152. C. E. Doiran, T. B. McMahon, *Can. J. Chem.* **59**, 2689 (1981).
153. R. L. Salvador, M. Saucier, *Tetrahedron*, **27**, 1211 (1971).
154. J. P. Guthrie, *Can. J. Chem.*, **53**, 898 (1975).
155. W. J. Scott, P. Zuman, *J. Chem. Soc. Faraday Trans. I*, **72**, 1192 (1976).
156. A. Syekacs, P. O. Halarankar, M. M. Olmstead, K. A. Prag, B. D. Hammock, *Chem. Res. Toxicol.*, **17**, 76 (1982).
157. T. C. Liang and R. H. Abeles, *Biochemistry*, **26**, 7603 (1987).
158. L. H. Takahashi, R. Radhakrishnan, R. E. Rosenfield, E. F. Meyer, D. A. Trainor, and J. M. Stein, *Mol. Biol.*, **201**, 423 (1988).
159. L. S. Chen, G. J. Chen, C. Tamborski, *J. Fluorine Chem.*, **18**, 117 (1981).
160. T. F. McGrath, R. Levine, *J. Amer. Chem. Soc.*, **77**, 3634 (1955).
161. E. T. McBee, O. R. Pierce, and D. D. Meyer, *J. Amer. Chem. Soc.*, **77**, 83 (1955).
162. R. J. Jones, *J. Amer. Chem. Soc.*, **70**, 143 (1948).
163. T. F. McGrath and R. Levine, *J. Amer. Chem. Soc.*, **77**, 3656 (1955).
164. K. T. Dishart and R. Levine, *J. Amer. Chem. Soc.*, **78**, 2268 (1956).
165. A. Sykes, J. C. Tatlow and C. R. Thomas, *J. Chem. Soc.* **835** (1956).
166. D. A. Rausch, A. M. Lovelace, and L. E. Coleman, *J. Org. Chem.* **21**, 1328 (1956).
167. X. Creary, *J. Org. Chem.* **52**, 5026 (1987).
168. R. Stewart, K. C. Teo and L. K. Ng, *Can. J. Chem.*, **58**, 2497 (1980).
169. S. G. Cohen, H. T. Wolosinski, and P. J. Scheuer, *J. Am. Chem. Soc.*, **71**, 3439 (1949).



170. E. J. P. Fear, J. Thrower, and J. Veitch, *J. Chem. Soc.*, 3199 (1956).
171. G. Holan, W. M. P. Johnson, K. Riha, and C. T. Virgona, *Pestic. Sci.* **15**, 361 (1984).
172. G. Holymann, G. Kossmehl, and R. Nuck, *Makromol. Chem.*, **183**, 1711 (1982).
173. C. H. Cheng and E. M. Pearce, *J. Polym. Sci. Polym. Chem. Ed.*, **18**, 1883 (1980).
174. D. Bonnet-Delpon and M. Charpentier-Moriye, *Bull. Soc. Chim. Fr.* **933** (1986).
175. R. K. Mackie, S. Mhatre and J. M. Tedder, *J. Fluorine Chem.*, **10**, 437 (1972).
176. W. D. Cooper, *J. Org. Chem.*, **23**, 1382 (1958).
177. S. Clementi, F. Genel, and G. Marino, *J. Chem. Soc. Chem. Comm.*, **498** (1967).
178. S. Clementi and G. Marino, *Tetrahedron*, **25**, 4599 (1969).
179. V. G. Glukhovtsev, Y. V. Il'in, A. V. Ignatenko, and L. Y. Breyhnev, *Ivy. Akad. Nauk. SSSR, Ser. Khim*, **2631** (1988).
180. A. G. Anderson and R. G. Anderson, *J. Org. Chem.* **27**, 3578 (1962).
181. M. Hojo, R. Masuda, and E. Okada, *Tetrahedron Lett.*, **28**, 6199 (1987).
182. J. Taimr, J. Benes, and J. Krepelka, Czech CS 262,581 patent.
183. T. Keumi, M. Shimada, M. Takahashi, and H. Kitajima, *Chem. Letters*, **783** (1990).
184. W. E. Hull, K. Seeholyer, M. Baumeister and I. Ugi, *Tetrahedron* **42**, 547 (1986).
185. V. U. Korshak, I. F. Manucharova, S. V. Vinogradora, and V. A. Pankraton, *Vysokomolekulyarnye Soedineniya*, **7**, 1813 (1965).
186. M. Sander, "Phosphorus - Containing Polymers" in *Encyclopedia of Polymer Science and Technology*, N. M. Bikales, Ed. John Wiley and Sons, New York, 1969, vol. 10, pp. 123.

187. M. Sander and E. Steininger, *J. Macromol. Sci. Rev. Macromol. Chem. Phys.*, **1**, 7 (1967).
188. S. V. Shulyndin, Y. A. Levin and B. E. Ivanov, *Russ. Chem. Rev.*, **50**, 865 (1981).
189. M. Sander and E. Steininger, *J. Macromol. Sci. Rev. Macromol. Chem. Phys.*, **1**, 91 (1967).
190. Eastman Kodak, U.S. Patent 2,743,258 (4/24/56).
191. H. W. Coover, Jr., R. L. McConnell, and M. A. McCall, *Ind. Eng. Chem.*, **52**, 409-11 (1960).
192. Eastman Kodak, U.S. Patent 3,378,523 (4/16/68).
193. Farbwerke Hoechst, Brit. Patent 883,754 (12/6/61).
194. Gavaert Photoproducten, Bel. Patent. 610,953 (3/16/62).
195. A. Natansohn, *J. Appl. Polym. Sci.*, **32**, 2961 (1986).
196. K. S. Kim, *J. Appl. Polym. Sci.*, **28**, 1119 (1983).
197. F. Millich and L. L. Lambing, *J. Polym. Sci., Polym. Ed.*, **18**, 2155 (1980).
198. Y. Imai, N. Sato and M. Ueda, *Makromol. Chem., Rapid Commun.*, **1**, 419 (1980).
199. Y. Imai, H. Kamata and M. Kakimoto, *J. Polym. Sci., Polym. Chem. Ed.*, **22**, 1259 (1984).
200. E. D. Weil, "Phosphorus - Containing Polymers" in Encyclopedia of Polymer Science and Engineering, H. F. Mark, N. M. Bikales, C. G. Overberger and G. Menges, Eds. John Wiley and Sons, New York, 1986, vol. 11, pp. 98.
201. W. J. Bailey, W. M. Muir and F. Markscheffel, *J. Org. Chem.*, **27**, 4404 (1962).
202. P. W. Morgan and B. C. Herr, *J. Amer. Chem. Soc.*, **74**, 4526 (1952).
203. P. W. Morgan, U.S. Patent 264,620 (1953).
204. V. V. Korshak, *J. Polym. Sci.*, **31**, 319 (1958).

205. T. Y. Medved, T. M. Frunge, K. C. Mei, V. V. Kurashev, V. V. Korshak and M. I. Kabachnik, *Polym. Sci. USSR*, **5**, 386 (1964).
206. M. H. Bride, W. A. Cummings and W. G. Pickles, *J. Appl. Chem.*, **11**, 352 (1961).
207. T. M. Frunge, V. V. Korshak and V. V. Kurashev, *Polym. Sci. USSR*, **1**, 239 (1960).
208. S. V. Vinogravada, V. V. Korshak, G. S. Kolesnikor and B. A. Zhubanov, *Polym. Sci. USSR*, **1**, 125 (1960).
209. Y. W. Hsu, T. K. Yeh, Y. Y. Huang, I. K. Lin, S. C. Fang and Y. K. Chang, *Chem. Abstr.*, **64**, 11329 (1966).
210. T. M. Frunge, V. V. Korshak, A. A. Iyneer and V. V. Kusashec, *Polym. Sci. USSR*, **7**, 313 (1966).
211. V. V. Korshak, T. M. Frunge, V. V. Kurashev and G. S. Lopatina, *Poly. Sci. USSR*, **6**, 1379 (1964).
212. J. Kennedy, E. S. Lane and J. L. Williams, *J. Chem. Soc.*, 4670 (1956).
213. A. E. Senear, W. Valient and J. Wirth, *J. Org. Chem.*, **25**, 2001 (1960).
214. S. Hashimoto, I. Furukawa and T. Kondo, *J. Polym. Sci., Polym. Chem. Ed.*, **12**, 2357 (1974).
215. V. V. Korshak, T. M. Frunge, V. V. Kurashev, T. Y. Medred, Y. M. Polikarpov, C. M. Hsu and M. I. Kabachnik, *Chem. Abstr.*, **62**, 6507 (1965).
216. I. K. Varma and B. S. Rao, *J. Appl. Polym. Sci.*, **28**, 2805 (1983).
217. G. M. Kosalopoff and L. Maier, *Organic Phosphorus Compounds*, John Wiley and Sons, New York, 1972, vol. 1.
218. G. P. Pavlov, V. A. Kukhtin, W. A. Golynina and V. V. Kosmahev, *Chem. Abstr.*, **94**, 15816 (1981).
219. G. P. Pavlor, V. A. Kukhtin, N. A. Golynina and V. V. Kormachev, *Zh. Obshch. Khim.*, **50**, 1902 (1980).

220. N. A. Androva, M. M. Koton and L. K. Prokhosova, *Vysokomol. Soedin., Ser. B*, **13**, 235 (1971).
221. N. A. Androva, M. M. Koton and L. K. Prokhosova, *Chem. Abstr.*, **75**, 21174 (1971).
222. V. M. Svetlichnyi, V. V. Kudryavtsen, N. A. Androva and M. M. Koton, *Chem. Abstr.*, **81**, 151307 (1974).
223. V. M. Svetichnyi, V. V. Kudryabtsen, N. A. Androva and M. M. Koton, *Zh. Org. Khim.*, **10**, 1896 (1974).
224. M. M. Koton and Y. N. Sayanor, *Polym. Sci. USSR*, **15**, 1857 (1973).
225. Carrington C. Smith, *Ph.D. Thesis*, V.P.I. & S.U., 1991.
226. Cutmann, P. E. Hagen and K. Utvary, *Monats. Chem.*, **91**, 836 (1960).
227. G. P. Schiemenz and P. Nielsen, *Phos. Sulf.*, **21**, 259 (1985).
228. A. P. Melissaries and J. A. Mikroyannidis, *Eur. Polym. J.*, **25**, 275 (1989).
229. I. K. Varma, G. M. Fohlen and J. A. Parker, *J. Polym. Sci., Polym. Chem. Ed.*, **21**, 2017 (1983).
230. I. K. Varma, G. M. Fohlen and J. A. Parker, *J. Macromol. Sci., Chem.*, **A19**, 209 (1983).
231. I. K. Varma and H. P. Mittal, *J. Macromol. Sci., Chem.*, **A26**, 937 (1989).
232. S. Hashimoto, I. Furukawa and K. Ueyama, *J. Macromol. Sci., Chem.*, **A11**, 2167 (1977).
233. H. J. Kleiner and E. Weiss, US 4816605, to Hoechst Aktiengesellschaft (1989).
234. J. W. Rakshys, R. W. Taft and W. A. Sheppard, *J. Amer. Chem. Soc.*, **90**, 5236 (1968).
235. H. Schindlbauer, *Chem. Ber.*, **100**, 3432 (1967).
236. G. P. Schiemenz and M. Finzenhagen, *Liebigs Ann. Chem.*, **2126** (1976).

237. W. Ude, S. Besecke, A. Riemann and G. Schroeder, US 4698448, Rohm GmbH (1987).
238. E. Weiss and H. J. Kleiner, *Phos. Sulf.*, **34**, 39 (1987).
239. E. Bay, US 4760191, to Akzo America Inc. (1988).
240. W. Ude, J. Knebel and G. Schroeder, US 4696993, to Rohm GmbH (1987).
241. W. Ude and J. Knebel, US 4745225, to Rohm GmbH (1988).
242. S. Besecke, G. Schroeder, W. Ude and W. Wunderlich, US 4492805, to Rohm GmbH (1985).
243. S. Hirose, K. Nakamura, T. Hatakeyama and H. Natakeyama, *Sen-I Gakkaishi*, **43**, 595 (1987).
244. S. Hirose, K. Nakamura, T. Hatakeyama and H. Hatakeyama, *Sen-I Gakkaishi*, **44**, 563 (1988).
245. M. Fild and R. Schmutyler, Halo and pseudohalophosphines, in *Organic Phosphorus Compounds*, Vol. 4, G. Kosolapoff and L. Maier, Eds., Wiley-Interscience, 1972, 79.
246. F. D. King and R. M. Walton, *Synthesis*, **40**, 1976.
247. D. C. Clagett, "Engineering Plastics," in *Encycl. Polym. Sci. Tech.* (H. F. Mark, et al., eds.), Vol. 6, Wiley-Interscience, New York 1986, pp. 94-131.
248. S. Maiti and B. K. Mandal, *Prog. Polym. Sci.*, **12**, 111 (1986).
249. R. N. Johnson, A. G. Farnham, R. A. Clendinning, W. F. Hale and C. N. Merriam, *J. Polym. Sci., Pt A-1*, **5**, 2375 (1967).
250. P. M. Hergenrother, H. J. Tansen and S. J. Havens, *Polymer*, **29**, 358 (1988).
251. C. D. Smith, D. K. Mohanty and J. E. McGrath, *Int. SAMPE Symp. Exhib.*, **35**, 108 (1990).
252. C. D. Smith, A. Gungor, K. M. Keister, H. A. Marand and J. E. McGrath, *Amer. Chem. Soc., Div. Polym. Chem., Prepr.*, **32(1)**, 93 (1991).

253. A. Gungor, C. D. Smith, J. Wescott, S. Srinivasan and J. E. McGrath, *Amer. Chem. Soc., Div., Polym. Chem., Prepr.*, **32(1)**, 172 (1991).
254. "Poly (Arylene Ether Phosphine Oxide)s I. Overview of Chemistry, Thermal Stability and Oxygen Plasma Resistance," C. D. Smith, H. Grubbs, H. F. Webster, J. P. Wightman, and J. E. McGrath, *Amer. Chem. Soc., Div. Polym. Mater. Sci. Eng., Prepr.* **65**, 108 (1991).
255. "Poly (Arylene Ether Phosphine Oxide)s II. Pyrolysis Studies," H. Grubbs, C. D. Smith and J. E. McGrath, *Amer. Chem. Soc., Div. Polym. Mater. Sci. Eng., Prepr.*, **65**, 111 (1991).
256. "Poly (Arylene Ether Phosphine Oxide)s III. Investigations of Surface Modification by Oxygen Plasma Treatment," H. F. Webster, C. D. Smith, J. E. McGrath and J. P. Wightman, *Amer. Chem. Soc., Div. Polymer. Mater. Sci., Eng., Prepr.* **65**, 113 (1991).
257. W. C. Kuryla and A. J. Papa, Eds., *Fire Retardancy of Polymeric Materials*, vol. 1-5, Marcel Dekker, Inc., New York, 1979.
258. T. M. Aminabhavi and P. E. Cassidy, *Polym. -Plast. Technol. Eng.*, **28**, 717 (1989).
259. H. W. Emmons, *Combust. Sci. Tech.*, **40**, 167 (1984).
260. C. F. Cullis, *Br. Polym. J.*, **16**, 253 (1984).
261. A. Factor, *J. Chem. Ed.*, **51**, 453 (1974).
262. M. Lewin, S. M. Atlas and E. M. Pearce, *Flame-Retardant Polymeric Materials*, Vol. 1 and 2, Plenum Press, New York, 1975.
263. D. A. Kourtides and J. A. Parker, *Polym. Eng. Sci.*, **18**, 855 (1978).
264. D. A. Kourtides and J. A. Parker, *SAMPE Q.*, **36**, (1978).
265. S. Kuroda, K. Terauchi, K. Nogami and I. Mita, *Eur. Polym. J.*, **25**, 1 (1989).
266. A. Yehaskel, *Fire and Flame Retardant Polymers: Recent Developments*, Noyes Data Corp., Park Ridge, NJ, 1979.
267. S. Kurosawa and T. Ueshima, US 4533721, to Showa Denko Kabushiki Kaisha (1985).

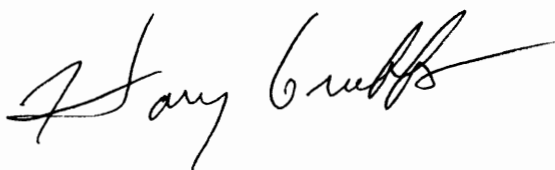
268. D. G. Chasin, *Natl. SAMPE Tech. Conf.*, **8**, 59 (1976).
269. N. W. Johnston and B. L. Joesten, *J. Fire Flamm.*, **3**, 274 (1972).
270. J. L. Isaacs, *J. Fire Flamm.*, **1**, 36 (1970).
271. K. Kishore and K. Mohandas, *J. Macromol. Sci., Chem.*, **A18** (1982).
272. D. W. Van Krevelen, *Chimia*, **28**, 504 (1974).
273. S. K. Brauman, *J. Fire Retard. Chem.*, **6**, 266 (1979).
274. S. K. Brauman, *J. Fire Retard. Chem.*, **6**, 249 (1979).
275. B. Crossland, G. J. Knight and W.W. Weight, *Br. Polym. J.*, **18**, 156 (1986).
276. W. F. Hale, A. G. Farnham, R. N. Johnson and R. A. Clendinning, *J. Polym. Sci., A-1*, **5**, 2399 (1969).
277. J. N. Hay and D. J. Kemmish, *Polymer*, **28**, 2047 (1987).
278. J. E. Bostic, Jr. and R. H. Barker, *J. Fire Retard. Chem.*, **4**, 165 (1977).
279. S. K. Brauman, *J. Fire Retard. Chem.*, **4**, 38 (1977).
280. S. K. Brauman, *J. Fire Retard. Chem.*, **4**, 18 (1977).
281. S. K. Brauman, and N. Fishman, *J. Fire Retard. Chem.*, **4**, 93 (1977).
282. S. K. Brauman, *J. Fire Retard. Chem.*, **7**, 61 (1980).
283. G. Avondo, C. Vovelle and R. Delbourgo, *Combustion and Flame*, **31**, 7 (1978).
284. E. D. Weil, R. B. Fearing and F. Jaffe, *J. Fire Retard. Chem.*, **9**, 39 (1982).
285. C. D. Smith, D. K. Mohanty and J. E. McGrath, *Int. SAMPE Symp. Exhib.*, **35** 108 (1990).
286. D. A. Kourtides and J. A. Parker, *Polym. Eng. Sci.*, **18(11)**, 855 (1978).
287. W. J. Bailey, W. M. Muir and F. Marktscheffel, *J. Org. Chem.*, **27**, 4404 (1962).

288. N. W. Johnston and B. L. Joesten, *Fire Flamm.*, **3**, 274 (1972).
289. B. Crossland, G. J. Knight and W. W. Wright, *Br. Polym. J.*, **18(3)**, 156 (1986).
290. J. N. Hay and D. J. Kemmish, *Polymer*, **28**, 2047 (1987).
291. S. I. Kuroda, K. Terauchi, K. Nogami and I. Mita, *Eur. Polym. J.*, **25(1)**, 1 (1989).



## VITA

Harvey Joseph Grubbs was born in Richmond, Virginia on September 27, 1948. He entered University of Richmond in September, 1966 and graduated with honors with a B.S. in Chemistry in June, 1970. The author entered the graduate program in chemistry at Virginia Polytechnic Institute and State University in August, 1989. Under the direction of Dr. James E. McGrath, Mr. Grubbs began his thesis research centered on the synthesis and characterization of fluorine and phosphorus containing monomers for the preparation of high performance polymeric systems. The author received his Ph.D. in Chemistry with an emphasis in polymer science in July, 1992, and is currently employed by Philip Morris U.S.A.

A handwritten signature in black ink, reading "Harvey Grubbs". The signature is written in a cursive style with a long, sweeping horizontal line extending to the right from the end of the name.